

RELATING VEHICLE GENERATED POLLUTANTS TO URBAN STORMWATER QUALITY

Janaka M.A. Gunawardena

B.Sc. (Civil Engineering, Honours)

M.Eng. (Environmental Engineering)

A THESIS SUBMITTED
IN PARTIAL FULFILLMENT OF THE REQUIREMENTS OF
THE DEGREE OF DOCTOR OF PHILOSOPHY

SCIENCE AND ENGINEERING FACULTY
QUEENSLAND UNIVERSITY OF TECHNOLOGY

April -2012

KEYWORDS

Atmospheric deposition, heavy metals, polycyclic aromatic hydrocarbons, air sampling, stormwater quality modelling, pollutant build-up, pollutant wash-off

ABSTRACT

Rapid urbanisation and resulting continuous increase in traffic has been recognised as key factors in the contribution of increased pollutant loads to urban stormwater and in turn to receiving waters. Urbanisation primarily increases anthropogenic activities and the percentage of impervious surfaces in urban areas. These processes are collectively responsible for urban stormwater pollution. In this regard, urban traffic and land use related activities have been recognised as the primary pollutant sources. This is primarily due to the generation of a range of key pollutants such as solids, heavy metals and PAHs.

Appropriate treatment system design is the most viable approach to mitigate stormwater pollution. However, limited understanding of the pollutant process and transport pathways constrains effective treatment design. This highlights necessity for the detailed understanding of traffic and other land use related pollutants processes and pathways in relation to urban stormwater pollution.

This study has created new knowledge in relation to pollutant processes and transport pathways encompassing atmospheric pollutants, atmospheric deposition and build-up on ground surfaces of traffic generated key pollutants. The research study was primarily based on in-depth experimental investigations. This thesis describes the extensive knowledge created relating to the processes of atmospheric pollutant build-up, atmospheric deposition and road surface build-up and establishing their relationships as a chain of processes.

The analysis of atmospheric deposition revealed that both traffic and land use related sources contribute total suspended particulate matter (TSP) to the atmosphere. Traffic sources become dominant during weekdays whereas land use related sources become dominant during weekends due to the reduction in traffic sources. The analysis further concluded that atmospheric TSP, polycyclic aromatic hydrocarbons (PAHs) and heavy metals (HMs) concentrations are highly influenced by total average daily heavy duty traffic, traffic congestion and the fraction of commercial and industrial land uses. A set of mathematical equation were developed to predict

TSP, PAHs and HMs concentrations in the atmosphere based on the influential traffic and land use related parameters.

Dry deposition samples were collected for different antecedent dry days and wet deposition samples were collected immediately after rainfall events. The dry deposition was found to increase with the antecedent dry days and consisted of relatively coarser particles (greater than 1.4 μm) when compared to wet deposition. The wet deposition showed a strong affinity to rainfall depth, but was not related to the antecedent dry period. It was also found that smaller size particles (less than 1.4 μm) travel much longer distances from the source and deposit mainly with the wet deposition. Pollutants in wet deposition are less sensitive to the source characteristics compared to dry deposition. Atmospheric deposition of HMs is not directly influenced by land use but rather by proximity to high emission sources such as highways. Therefore, it is important to consider atmospheric deposition as a key pollutant source to urban stormwater in the vicinity of these types of sources.

Build-up was analysed for five different particle size fractions, namely, <1 μm , 1-75 μm , 75-150 μm , 150-300 μm and >300 μm for solids, PAHs and HMs. The outcomes of the study indicated that PAHs and HMs in the <75 μm size fraction are generated mainly by traffic related activities whereas the > 150 μm size fraction is generated by both traffic and land use related sources. Atmospheric deposition is an important source for HMs build-up on roads, whereas the contribution of PAHs from atmospheric sources is limited.

A comprehensive approach was developed to predict traffic and other land use related pollutants in urban stormwater based on traffic and other land use characteristics. This approach primarily included the development of a set of mathematical equations to predict traffic generated pollutants by linking traffic and land use characteristics to stormwater quality through mathematical modelling. The outcomes of this research will contribute to the design of appropriate treatment systems to safeguard urban receiving water quality for future traffic growth scenarios. The 'real world' application of knowledge generated was demonstrated through mathematical modelling of solids in urban stormwater, accounting for the variability in traffic and land use characteristics.

LIST OF PUBLICATIONS

Book Chapters

1. **Gunawardena, J.**, Goonetilleke, A., Egodawatta, P. Ayoko, G. and Kerr, J. (2010). Urban traffic characteristics and urban stormwater quality: A methodology to measure traffic generated water pollutants, in Rethinking sustainable development. Yigitcanlar, T. (ed.), Engineering Science Reference, Hershey, New York, 168-184.

Journal Publications

1. **Gunawardena, J.**, Egodawatta, P., Ayoko, G. A., and Goonetilleke, A. (2012). Role of traffic in atmospheric accumulation of heavy metals and polycyclic aromatic hydrocarbons. *Atmospheric Environment*, 54, 502-510.

Conference Publications

1. **Gunawardena, J.**, Egodawatta, P. K., Ayoko, G. A., and Goonetilleke, A. (2012). Exploratory investigation of atmospheric total suspended particulate matter and heavy metals in urban air. In Proceedings of the Annual International Conference on Sustainable Energy and Environmental Sciences, Hotel Fort Canning, Singapore.
2. **Gunawardena, J.**, Egodawatta, P., Ayoko, G. A., and Goonetilleke, A. (2011). Atmospheric Deposition as a Source of Stormwater Pollution in Gold Coast, Australia 34th IAHR Biennial World Congress, Brisbane, CD-ROM (No: 1849).
3. **Gunawardena, M. J. A.**, Goonetilleke, A., Egodawatta, P (2009). Relating Vehicle Generated Pollutants to Urban Stormwater Quality. Proceedings of the Infrastructure Theme Postgraduate Conference 2009, QUT Gardens Point Campus.

TABLE OF CONTENTS

Chapter 1 - Introduction	1
1.1 Background	1
1.2 Research problem	2
1.3 Project aims	3
1.4 Objectives	3
1.5 Research hypothesis	3
1.6 Scope	4
1.7 Innovation and contribution to knowledge	4
1.8 Significance and justification for the research	5
1.9 Outline of the report	7
Chapter 2 - Urban Water Quality	9
2.1 Background	9
2.2 Urban stormwater pollutants	11
2.3 Stormwater pollutant sources	13
2.4 Impacts of vehicle generated pollutants	14
2.4.1 Air pollution	15
2.4.2 Water pollution	15
2.5 Traffic related pollutants in urban stormwater	17
2.5.1 Sediments and suspended solids	18
2.5.2 Hydrocarbons	20
2.5.3 Heavy metals	21
2.5.4 Airborne particulate matter	23
2.6 Atmospheric pollutant build-up	24
2.6.1 Rainfall and antecedent dry period	25
2.6.2 Urban traffic	25
2.7 Atmospheric deposition	27
2.7.1 General concepts	27
2.8 Pollutant build-up on road surfaces	28
2.9 Pollutant wash-off processes	31
2.10 Conclusions	34

Chapter 3 -Research Design and Methods	37
3.1 Background	37
3.2 Research Methodology	37
3.2.1 Literature review	38
3.2.2 Selection of key pollutants	38
3.2.3 Selection of influential variables	39
3.2.4 Site selection criteria	40
3.2.5 Analytical test method selection	40
3.2.6 Sampling equipment selection	41
3.2.7 Sample collection and testing	41
3.2.8 Data Analysis	41
3.2.9 Mathematical modelling	41
3.3 Sampling equipment	42
3.3.1 Air sampling	42
3.3.2 Atmospheric deposition sampling	44
3.3.3 Build-up sampling	47
3.4 Statistical and multivariate analytical tools	49
3.4.1 Principal component analysis (PCA)	50
3.4.2 Multiple linear regression (MLR)	51
3.4.3 Multicriteria decision making methods (MCDMs)	52
3.5 Stormwater models	55
3.5.1 EPA SWMM	55
3.5.2 MIKE URBAN	57
3.5.3 MUSIC	58
3.5.4 Model selection	59
3.6 Quality control and quality assurance	60
3.6.1 Quality control procedures for PAHs sampling and testing	60
3.6.2 Quality control for heavy metal sampling and testing	61
3.6.3 Quality control for particulate matter sampling and testing	63
3.7 Summary	63
Chapter 4 - Study Sites	65
4.1 Background	65
4.2 Study site selection	65

4.3	Summary	69
Chapter 5 - Sample Collection and Testing		71
5.1	Background	71
5.2	Air Sampling	72
5.3	Build-up sampling	75
5.4	Atmospheric deposition sampling	76
5.4.1	Dry deposition sampling	78
5.4.2	Bulk deposition sampling	78
5.5	Sample Preservation and Transport	79
5.5.1	Air sample preservation and transport	80
5.5.2	Atmospheric deposition sample preservation and transport	80
5.5.3	Build-up sample preservation and transport	81
5.6	Laboratory Testing	81
5.7.1	TSP testing	82
5.7.2	HMs testing	82
5.7.3	PAHs testing	84
5.7.4	pH and EC testing	88
5.7.5	Particle size distribution (PSD)	88
5.7.6	Organic carbon	89
5.7.7	Total suspended solids and total dissolved solids	90
5.7	Summary	90
Chapter 6 - Analysis of Air Samples		93
6.1	Background	93
6.2	Air sampling sites	93
6.3	Preliminary data analysis	95
6.3.1	Data pre-processing	95
6.3.2	Analysis of TSP	96
6.3.3	Heavy metals (HMs)	99
6.3.4	Polycyclic aromatic hydrocarbons (PAHs)	102
6.4	Multivariate analysis	105
6.4.1	Heavy metals	105
6.5	Multivariate analysis of PAHs	113

6.6	Development of predictive models	126
6.6.1	Heavy metals	126
6.6.2	Polycyclic aromatic hydrocarbons (PAHs)	130
6.6.3	Prediction of overall air quality	134
6.7	Conclusions	137
Chapter 7 - Analysis of Atmospheric Deposition		139
7.1	Background	139
7.2	Field investigations	140
7.2.1	Study sites	140
7.2.2	Field sampling and testing	141
7.3	Physical characteristics of atmospheric deposition	142
7.3.1	Data pre-treatment	142
7.3.2	Data analysis	143
7.3.3	Dry deposition	143
7.3.4	Bulk deposition	146
7.3.5	Physical characteristics of atmospheric deposition	147
7.4	Heavy metals in atmospheric deposition	150
7.4.1	Analysis of heavy metals	150
7.4.2	Influence of traffic on atmospheric deposition	152
7.4.3	Variation of atmospheric deposition with land use characteristics	156
7.5	Ranking of sites	160
7.6	Conclusions	163
Chapter 8 - Analysis of Pollutant Build-up Data		165
8.1	Background	165
8.2	Field investigations	165
8.3	Analysis	166
8.3.1	Pre-treatment	166
8.3.2	Univariate analysis	167
8.3.3	Multivariate Analysis of Heavy Metals and Solids	174
8.3.4	Analysis of polycyclic aromatic hydrocarbons (PAHs)	187
8.4	Traffic generated pollutant transport pathways	201
8.5	Conclusions	205

Chapter 9 - Mathematical Modelling	207
9.1 Background	207
9.2 Computer modelling	207
9.2.1 Model selection	207
9.2.2 Modelling approach	208
9.2.3 Model schematisation	208
9.2.4 Boundary conditions	210
9.2.5 Replication of pollutant build-up and wash-off	212
9.3 Model simulation and results	218
9.3.1 Results for heavy metals	219
9.3.2 Results for PAHs	220
9.3.3 Development of predictive equations	222
9.4 Conclusions	224
Chapter 10 - Conclusions and Recommendations	227
10.1 Conclusions	227
10.1.1 Atmosphere pollutant build-up	228
10.1.2 Atmospheric pollutant deposition	229
10.1.3 Pollutant build-up	230
10.1.4 Mathematical modelling	232
10.1.5 Practical applications of knowledge generated	233
10.2 Recommendations for further research	234
References	237

LIST OF FIGURES

Figure 2-1: Changes in stream hydrology as a result of urbanisation	10
Figure 2-2 : Comparison of TSP concentration before and during rainfall in Dehli, India	25
Figure 2-3: VOC emissions as a function of volume capacity ratio	26
Figure 2-4 : Mass of pollutant present in the air as a function of dry and wet deposition	28
Figure 2-5 : Accumulation of pollutants on urban surfaces	30
Figure 2-6 : Hypothetical representations of surface pollutant load over time.	32
Figure 3-1 High volume air sampler	44
Figure 3-2: Wet and Dry atmospheric deposition collector	46
Figure 3-3: Delonghi Aqualand water filter system	48
Figure 3-4: Build-up sample collection (wet and dry vacuuming)	49
Figure 4-1: Location of study sites in the Gold Coast	68
Figure 5-1: Calibration set up	73
Figure 5-2: Air sampling, (a): placement of the sampler, (b): key components, (c): placement of generator with reference to sampler	75
Figure 5-3: Fixing arrangement-a	77
Figure 5-4: Fixing arrangement-b	78
Figure 5-5: Hot block digester	83
Figure 5-6: ICP-MS	84
Figure 5-7: Apparatus used for extraction	86
Figure 5-8: GC-MS	86
Figure 5-9: Malvern Mastersizer S	89
Figure 5-10: Shimadzu TOC-VCSH Total Organic Carbon Analyser	90
Figure 6-1: TSP concentrations at the study sites	97
Figure 6-2: Variation of TSP concentration with traffic, (a): for weekend sampling, (b): weekday sampling	98
Figure 6-3: Atmospheric heavy metal concentration during weekdays and weekends	101

Figure 6-4: GAIA biplot of heavy metals against the first two principal components for weekdays, (a): for “Set 3” sites, (b): for “Set 3” and “Set 1” sites	107
Figure 6-5: GAIA biplot of heavy metals against the first two principal components for weekends, (a): for “Set 3” sites, (b): for “Set 3” and “Set 1” sites	110
Figure 6-6: GAIA biplot of heavy metals against the first two principal components for “Set 3” sites	112
Figure 6-7: GAIA biplot of gas phase PAHs against the first two principal components for “Set 3” sites	114
Figure 6-8 GAIA biplot of gas phase PAHs against the first two principal components for weekday sampling, (a): for “Set 3” sites, (b): for “Set 3” and “Set 1” sites	116
Figure 6-9: GAIA biplot of gas phase PAHs against the first two principal components for weekend sampling, (a): for “Set 3” sites, (b): for “Set 3” and “Set 1” sites	119
Figure 6-10: GAIA biplot of gas phase PAHs against the first two principal components for weekend sampling	121
Figure 6-11: GAIA biplot of particulate phase PAHs against the first two principal components for weekday sampling, (a): for “Set 3” sites, (b): for “Set 3” and “Set 1” sites	123
Figure 6-12: GAIA biplot of particulate phase PAHs against the first two principal components for weekend sampling, (a): for “Set 3” sites, (b): for “Set 3” and “Set 1” sites	125
Figure 7-1: Variation of dry deposition with antecedent dry days	144
Figure 7-2: Variation of bulk deposition with rainfall depth for set 1 sites and set 2 sites	146
Figure 7-3: Cumulative average particle size distribution	148
Figure 7-4: Variation of average particle size distribution for different study sites for dry and bulk deposition	149
Figure 7-5: Average deposition rates of heavy metals: (a) dry deposition, (b) bulk deposition	151
Figure 7-6: GAIA biplot of dry deposition for “Set 2” sites	153
Figure 7-7: GAIA biplot of bulk deposition for “Set 2” sites	155
Figure 7-8: GAIA biplot of dry deposition for “Set 1” and “Set 2” sites	157
Figure 7-9: GAIA biplot of bulk deposition for “Set 1” sites	159

Figure 7-10: GAIA biplot of dry deposition for “Set 1” and “Set 2” sites	162
Figure 8-1: Variation solids with average daily traffic, (a): dissolve solids, (b): total solids	168
Figure 8-2: Variation of particle distribution among selected road sites	170
Figure 8-3: Comparison of heavy metal concentrations with particle size	172
Figure 8-4: Variation PAHs in build-up for study sites	173
Figure 8-5: GAIA biplot of PSD based on 11 sites	175
Figure 8-6: PCA biplot of HMs with the first two principal components for <1 μ m fraction	177
Figure 8-7: PCA biplot of HMs with the first two principal components for 1-75 μ m fraction, (a): for actions, (b): for criteria	179
Figure 8-8: PCA biplot of HMs with the first two principal components for 75-150 μ m fraction	181
Figure 8-9: PCA biplot of HMs with the first two principal components for 150-300 μ m and >300 μ m fractions, (a): for actions, (b): for criteria	183
Figure 8-10: PCA biplot of HMs with the first two principal components for all size fractions, (a): for actions, (b): for criteria	186
Figure 8-11: GAIA biplot of PAHs for the first two principal components for <1 μ m fraction, (a): for actions, (b): for criteria	188
Figure 8-12: GAIA biplot of PAHs for the first two principal components for 1-75 μ m fraction, (a): for actions, (b): for criteria	191
Figure 8-13: GAIA biplot of PAHs for the first two principal components for 75-150 μ m fraction, (a): for actions, (b): for criteria	193
Figure 8-14: GAIA biplot of PAHs for the first two principal components for 150-300 μ m fraction, (a): for actions, (b): for criteria	195
Figure 8-15: GAIA biplot of PAHs against the first two principal components for >300 μ m fraction, (a): for actions, (b): for criteria	197
Figure 8-16: GAIA biplot of HMs against the first two principal components for all size fractions, (a): for actions, (b): for criteria	200
Figure 8-17: GAIA biplot of HMs for the first two principal components for all three phases	202
Figure 8- 18: GAIA biplot of particulate bound PAHs for the first two principal components for build-up and air, (a): for actions, (b): for criteria	204

Figure 9-1: Schematisation of road cross section	209
Figure 9-2: Schematisation of catchment area	210
Figure 9-3: Variation of total rainfall over the last 10 years at Gold Coast Seaway	211
Figure 9-4: Exponential solid build-up curves	214
Figure 9-5: Variation of fraction wash-off with the Runoff rate for solids	215
Figure 9-6: Variation of co-fractions with duration	216
Figure 9-7: Variation of co-fractions with duration	218

LIST OF TABLES

Table 2-1: Sources of pollutants in roadway runoff	18
Table 2-2: Source of heavy metals in urban pavement runoff	22
Table 3-1: Comparison of air sampling equipment	42
Table 3-2: Comparison of atmospheric deposition sampling techniques	45
Table 3-3: Comparison of build-up sampling techniques	47
Table 3-4: List of preference functions in Decision Lab software	54
Table 4-1: Predicted traffic characteristics for the selected roads	66
Table 5-1: Data required for calibration	73
Table 5-2: Selected roads for atmospheric deposition sampling	77
Table 5-3: Total number of samples collected	79
Table 5-4: Methods adopted for sample testing	80
Table 5-5: Target polycyclic aromatic hydrocarbons	85
Table 6-1: “Set 1” sites	94
Table 6-2: “Set 3” sites	94
Table 6-3: Comparison of airborne heavy metal concentrations	100
Table 6-4: Average airborne PAHs concentrations	103
Table 6-5: Atmospheric gas phase PAHs concentrations	104
Table 6-6: Atmospheric particulate phase PAHs concentrations	105
Table 6-7: Correlation matrix for Figure 6-4(a)	108
Table 6-8: Equations derived for HMs for weekdays and weekends	129
Table 6-9: Equations derived for weekday PAHs	131
Table 6-10: Equations derived for weekend PAHs	133
Table 6-11: Ranking of influential parameters	136
Table 6-12: Variability of HMs and PAHs	137
Table 7-1: The selected “Set 1” sites	140
Table 7-2: The selected “Set 2” sites	141
Table 7-3: Comparison of metrological condition on dry deposition	145
Table 7-4: PROMETHEE 2 complete ranking of dry deposition sampling sites	161
Table 8-1: Classification of particle size distribution (PSD)	169
Table 8-2: Heavy metals build-up on roads	171

Table 8-3: PAHs build-up on roads	172
Table 9-1: Coefficients for power function	213
Table 9-2: Heavy metal co-fractions based on TSS	217
Table 9-3: Co-fraction coefficients used for modelling	218
Table 9-4: Annual heavy metal load from 100 m long road section	219
Table 9-5: PROMETHEE 2 ranking of sites based on year 2004 HMs loading	220
Table 9-6: Annual PAHs load from 100 m long road section	221
Table 9-7: PROMETHEE 2 ranking of sites based on year 2004 PAHs loading	222
Table 9-8: A summary of equations developed for solids	223

LIST OF APPENDICES

Appendix A: Supporting Data for Air sample Analysis.....	261
Appendix B: Supporting Data for Atmospheric Deposition Analysis.....	277
Appendix C: Supporting Data for Build up Analysis.....	281
Appendix D: Validation Plots.....	289

ABBREVIATIONS

ADT	- Average Daily Traffic
ADT_to	- Total Average Daily Traffic
ADT_hv	- Total Average Daily Heavy Duty Traffic
AS/NZS	- Australian and New Zealand Standards
ACE	- Acenaphthene
ACY	- Acenaphthylene
ANT	- Anthracene
BaA	- Benzo[a]anthracene
BeP	- Benzo[e] pyrene
BaP	- Benzo[a]pyrene
BgP	- Benzo[ghi]perylene
Cd	- Cadmium
Cr	- Chromium
Cu	- Copper
CHR	- Chrysene
C	- Percentage Commercial
CRM	- Certified Reference Materials
DbA	- Dibenzo[a,h]anthracene
EC	- Electrical Conductivity
EPA SWMM	- United State Environmental Protection Agency-Stormwater Management Model
FLU	- Flourene
FLA	- Fluoranthene
GCCC	- Gold Coast City Council
GIS	- Geographic Information System
HM	- Heavy Metal
HNO ₃	- Nitric Acid
HDPE	- High Density Polyethylene
ICP-MS	- Inductively Coupled Plasma – Mass Spectrometer
I	- Percentage Industrial
IND	- Indeno[1,2,3-cd]pyrene

Mn	- Manganese
MMT	- Methylcyclopentadienyl Manganese Tricarbonyl
MLR	- Multiple Linear Regressions
MCDM	- Multi Criteria Decision making Methods
Ni	- Nickel
PHE	- Phenanthrene
PYR	- Pyrene
ppm	- Parts per million
PAH	- Polycyclic Aromatic Hydrocarbon
Pb	- Lead
PCA	- Principal Component Analysis
PM _{2.5}	- Particulate Matter that is 2.5 micrometers in diameter and smaller
PUF	-Polyurethane Foam
POT	- Power of the Test
PC	- Principal Components
P	- Preference threshold
Q	- Indifference threshold
RSD	- Residual Standard Deviation
R	-Precentage Residential
S	- Gaussian threshold
TOC	- Total Organic Carbon
TSP	-Total Suspended Particulate Matter
TSS	- Total Suspended Solids
TN	-Total Nitrogen
TP	-Total Phosphorus
USEPA	- United States Environmental Protection Agency
USA	- United States of America
V/C	- Traffic Congestion
we	- Weekend
wk	- Weekday
Zn	- Zinc
RG1	- Rain gauge

STATEMENT OF ORIGINAL AUTHORSHIP

The work contained in this thesis has not been previously submitted for a degree or diploma from any other higher education institution to the best of my knowledge and belief. The thesis contains no material previously published or written by another person except where due reference is made.

Janaka M.A. Gunawardena

Date:

ACKNOWLEDGEMENTS

I wish to express my profound gratitude to my principal supervisor Dr. Prasanna Egodawatta for his guidance, support and professional advice during the research. I extremely appreciate my associate supervisors Prof. Ashantha Goonetilleke and Prof. Godwin Ayoko for their invaluable support, guidance throughout the completion of this research. I would like to acknowledge the Science and Engineering Faculty, Queensland University of Technology for financial support during my candidature.

I would like to express my appreciation to QUT technical staff for their generous support given to me during my field work and laboratory testing. In particular, I wish to thank to Mr. Nathaniel Raup, Mr. Matthew Mackay, Mr. Chris Carvalho, Ms. Leonora Newby, Mr. Glenn Geary, Mr. Jim Hazelman, Mr. Scott Allbery and Mr. Colin Phipps for their patience and endless support in carrying out the field work and laboratory testing. My thanks are also extended to Mr. Shane Russell for providing me necessary laboratory facilities and invaluable technical support in my laboratory testing. I am also grateful to Dr. Jason Kerr for supporting me during my field sampling activities.

I would also like to acknowledge my fellow researchers and friends, Dr. Anjana Singh, Mr. Praveen Moragaspitiya and Ms. An Liu for their valuable support in my research. My acknowledgement is further extended to Ms. Elaine Reyes for organising language development classes for improving my writing skills.

This research would not have been possible without the support received from Gold Coast City Council and Queensland Department of Transport and Main Roads under the Australian Research Council (ARC) Linkage project (LP0882637). The support received from Gold Coast City Council in providing essential data and permitting me to conduct investigations within council property is gratefully acknowledged.

Finally, I would like to express my gratitude to all my relatives and friends for the encouragement during this work.

DEDICATION

I wish to dedicate this thesis to my wife, Mrs. Thanuja Dilhani Muthumala and to my two daughters Tharusha D. A. Gunawardena and Hirunima D. A. Gunawardena. Their love, morale support and motivation throughout the completion of this doctoral research are gratefully appreciated.

Chapter 1 - Introduction

1.1 Background

Urban stormwater pollution leading to the reduction of key environmental values in urban receiving water is of serious concern (Ghafouri and Swain 2005; Pavoni 1977). Urban stormwater pollutants are generated by traffic and other land use related activities. Emissions from these sources either deposit directly on land surfaces such as roads, roofs and parking areas or initially contributed to atmospheric pollutant loads and subsequently deposit on land surfaces (Sartor and Boyd 1972; Schauer et al. 1996). During storm events, these pollutants wash-off contributing pollutant loads to receiving waters. Pollutant contributions from impervious surfaces are particularly critical due to their rapid runoff response and being active even for small rainfall events. For example, Davis and Birch (2010a) noted that in a highly urban catchment, road surfaces can contribute up to 26% of the total runoff volume and 19 to 40 % of the total heavy metal load.

In order to mitigate the adverse impacts of stormwater pollution, a detailed understanding of pollutant processes and pathways are needed. Stormwater pollutants are subjected to a range of processes such as build-up and wash-off and transport to receiving waters. These processes are associated with a range of pathways such as atmospheric build-up and deposition. Pollutant generation processes are highly influenced by the dynamic scenarios of urban population growth, traffic growth and resulting spread of urbanisation. Urban traffic has been identified as the primary source responsible for generating a range of critical pollutants to urban stormwater (Egodawatta 2007; Sartor and Boyd 1972; Hengren 2005). Accordingly, appropriate mitigation strategies need to be implemented to minimise stormwater pollution. A key factor in the development of stormwater quality mitigation strategies is efficient treatment designs based on a sound theoretical understanding of pollutants generation and transport, and their associated processes. Therefore, the development of stormwater quality mitigation strategies depends on the accurate estimation of pollutant loads generated by traffic and other land use related sources. Unfortunately, currently there is no reliable approach to

estimate critical pollutant contributions to urban stormwater based on traffic and land use characteristics. This constrains the development of scientifically robust management strategies for the protection of urban receiving waters.

1.2 Research problem

There is continuous traffic growth throughout Australia for the transportation of passengers and goods. For example, the Australian Bureau of Statistics (ABS 2008) reported that there has been a 3% average annual traffic growth over the last five years (from year 2003 to 2008). Accordingly, the pollutant loads in the atmosphere and on road surfaces are also rapidly increasing as a consequence (AATSE 1997; Lim et al. 2005). This is compounded by the rapid spread of urbanisation and the resulting increase in land use related emissions. These increases are especially significant during the antecedent dry period with the wash-off of increasingly higher pollutant loads with rainfall causing significant degradation of urban receiving waters. Over the years, many studies have been conducted to understand the characteristics and composition of traffic related pollutants on road surfaces (Boddy et al. 2005). However, it is difficult to find a comprehensive approach focusing on defining pollutant pathways.

The effective management of stormwater pollution is dependent on the accurate estimation of critical pollutant loads and their concentrations in urban stormwater. Therefore, there is a need for approaches for the accurate prediction of urban stormwater quality due to wash-off of road surface accumulated pollutants, based on traffic and land use characteristics. However, the current understanding of direct and indirect deposition of pollutants generated by traffic and land use activities on urban road surfaces is limited. Consequently, this constrains the accurate prediction of pollutant loads to urban receiving waters, especially for future scenarios due to changes in urban traffic and land use characteristics.

The research problem can be primarily described as the lack of understanding of the linkages between traffic and land use related emissions and urban stormwater quality. These linkages are related to a range of processes such as atmospheric pollutant build-up, atmospheric deposition and build-up on road surfaces through

direct and indirect pathways and pollutants wash-off. This underlines the importance of the research focus on developing a comprehensive approach to estimate stormwater quality based on traffic and land use related parameters. In this regard, the three important processes which need to be understood in-depth include, atmospheric pollutant build-up, atmospheric pollutant deposition and direct pollutant build-up on road surfaces. Additionally, the research study developed a robust approach to predict urban stormwater quality due to wash-off of road deposited pollutants.

1.3 Project aims

- Identification of key traffic related pollutants and their deposition pathways on catchment surfaces
- Quantification of key traffic related pollutants based on influential traffic and land use characteristics:
 - in atmospheric build-up
 - in deposition on catchment surfaces
 - in stormwater

1.4 Objectives

Establish linkages between traffic related atmospheric pollutants, pollutant build-up on catchment surfaces and stormwater quality based on influential traffic and land use parameters.

1.5 Research hypothesis

- Urban stormwater quality is directly influenced by urban traffic and land use. Therefore, stormwater quality can be related mathematically to traffic and land use factors.
- Atmospheric deposition of traffic related pollutants is the major source of road surface pollutant build-up.
- Pollutants in the atmospheric phase and build-up on roads can be predicted based on traffic and land use characteristics.

1.6 Scope

The research study developed a detailed understanding of atmospheric pollutant build-up, atmospheric deposition and pollutant build-up on roads. The scope of the research study were:

- The research focused on pollutants generated by traffic and other land use related sources in selected urban study sites in the Gold Coast area.
- The research encompassed three processes, namely, atmospheric build-up, atmospheric deposition and road surface build-up. Wash-off from road surfaces was not specifically investigated in this study.
- Sample analysis specifically focused on polycyclic aromatic hydrocarbons (PAHs), heavy metals (HMs), total suspended particulate matter (TSP) and solids. These pollutants are predominantly generated by traffic activities. However, as various land use related activities too can generate these pollutants, this factor was also taken into consideration in the research investigations undertaken. Consequently, the study areas included residential, commercial and industrial land uses.
- Possible seasonal variations in air quality, deposition and pollutants build-up were not taken into consideration.
- The sample collection was undertaken at 11 road sites and 4 sites with high traffic activities to cover typical variability in traffic and land use characteristics in the Gold Coast area.
- A commercially available model was used for mathematical modelling to predict stormwater quality due to pollutant wash-off from urban roads.

1.7 Innovation and contribution to knowledge

Pollutant processes and transport pathways from generation to receiving waters are not defined comprehensively. A fraction of traffic generated pollutants can deposit directly on road surfaces and the remainder can suspend in air and subsequently deposit on roads via wet or dry deposition.

Understanding the processes and pathways of traffic generated pollutants plays a vital role in mitigating urban stormwater pollution. Based on the sound understanding of these processes and pathways, mathematical relationships can be established leading to better pollutant estimation models. Consequently, these mathematical relationships can be further extended to estimate pollutant loads in urban stormwater under variable traffic and land use scenarios. Hence, the degradation of receiving water quality can be mitigated not only for the present but also for future scenarios. At present, there is only a limited understanding of traffic and other land use related pollutant build-up. Formulation of appropriate mitigation strategies depends on the accurate estimation of pollutant build-up and resulting stormwater quality.

An important outcome arising from this research project is the development of a detailed understanding of processes and pathways of traffic and other land use related pollutant deposition and thereby the development of an innovative approach to estimate urban stormwater quality based on traffic and land use characteristics. The contribution to knowledge can be summarised as follows:

- Definition of the processes and pathways of traffic generated stormwater pollutants; and
- Development of linkages between atmospheric and catchment surface build-up of pollutants.

1.8 Significance and justification for the research

It is widely accepted that traffic sources generate an array of pollutants which are deposited on urban road surfaces (Herngren 2005; Lim et al. 2005). These pollutants include polycyclic aromatic hydrocarbons (PAHs) and heavy metals (HMs) and could be directly deposited on road surfaces or initially emitted to atmosphere and undergo deposition via dry and wet deposition. PAHs and HMs are particularly important in the context of stormwater pollution due to their toxic nature (WDT, 2007; EPASGV, 1999). PAHs and HMs are directly related to human health effects including asthma, lung cancer and other respiratory illnesses (Lim et al. 2005) and ecosystem degradation (Balestrini and Tagliaferri 2001).

Stormwater pollutants originate not only from land based activities but also from atmospheric deposition. During rainfall events, stormwater transports these pollutants to receiving waters causing adverse water quality impacts. Moreover, surface water and ground water can mix during this process. Therefore, stormwater quality is important to minimise the receiving water and ground water quality impacts. However, the formulation of effective mitigation measures strongly depends on the accuracy and reliability of stormwater quality estimation. In this regards, there has been only limited research undertaken to link atmospheric pollutants and pollutant build-up on catchment surfaces based on influential traffic and other land use parameters. This has primarily been attributed to the limited understanding of pollutant pathways and the interaction of traffic generated pollutants present in atmospheric and ground phases.

There are two widely accepted ways of improving urban stormwater quality. They are: (1) control of pollutant generation using appropriate urban planning approaches; and (2) improvement of stormwater quality using treatment structures. The first method is commonly used to manage stormwater pollution as it is the more sustainable approach. However, important traffic characteristics in the context of stormwater pollutant generation need to be taken into consideration. Accordingly, appropriate traffic planning can be implemented to minimise traffic generated pollutant loads to urban stormwater. This justifies research focus on identifying important traffic characteristics in relation to traffic generated stormwater pollutants.

This research extends the understanding of traffic and other land use related pollutant accumulation processes in the urban atmosphere and road surfaces and mathematical relationships have been developed accordingly. The knowledge generated through this research will help in predicting contributions of traffic and other land use related key pollutants to urban road surfaces due to traffic growth and changes in land use in future scenarios.

The research study was formulated to create an integrated methodology to estimate urban stormwater quality based on traffic characteristics such as traffic volume and traffic congestion and land use characteristics. The study specifically targeted

pollutants which are primarily generated by traffic sources as they are the important stormwater pollutants in terms of their impacts on receiving waters. As traffic growth can be estimated and predicted for future scenarios, the resulting pollutant loads in turn can be predicted using the developed methodology. Hence, stormwater management measures can be implemented well in advance to mitigate the impacts of these pollutants on receiving waters.

1.9 Outline of the report

This report consists of ten chapters. Chapter 1 presents the introduction to the research project, its aims and objectives and justification for the research along with its significance. Chapter 2 presents the “state-of-the-art” literature review undertaken and based on which this research project was formulated. Publications relating to the accumulation of traffic and other land use related pollutants both in the atmospheric and ground phases was reviewed and the accumulation of these pollutants in receiving waters were investigated. Pollutant build-up and wash-off was also reviewed specifically relating to urban road surfaces.

Chapter 3 presents the research methodology formulated for the study and the conceptual research framework. Chapter 4 discusses the study tools, test methods and quality control and quality assurance procedures adopted. Chapter 5 presents the sampling and testing procedures undertaken.

Data analysis is discussed in Chapters 6, 7, and 8. Chapter 6 presents the analytical outcomes in relation to traffic and other land use related pollutant build-up processes in the atmospheric phase. Chapter 7 presents the outcomes of the analysis undertaken on atmospheric deposition and linkages to atmospheric build-up. Chapters 6 and 7 generated the essential fundamental knowledge required for the analysis presented in Chapter 8. Analysis of build-up data and the investigation of pollutant transport pathways are presented in Chapter 8. Chapter 9 discusses the ‘real world’ application of the study outcomes. The chapter discusses the mathematical modelling undertaken to predict stormwater quality due to traffic and other land use related pollutants and the development of mathematical equations to predict these pollutants in urban stormwater generated from road surfaces. Chapter 10 summarises the outcome of the

research study and provide conclusions and recommendations for further research. This chapter presents further applications of the knowledge generated. References cited throughout the thesis and appendices containing background information such as processed data matrices and supporting data are provided at the end.

Chapter 2 - Urban Water Quality

2.1 Background

Urbanisation is a common phenomenon witnessed in most parts of the world. It transforms natural and rural lands into residential, commercial and industrial development. This transformation leads to clearing of vegetated lands and replacing them with impervious surfaces such as roads, buildings and paved areas. Although urbanisation is an integral part of development, rapid development of infrastructure and increase in anthropogenic activities can cause irreversible impacts. The impacts are particularly significant on the receiving water environment (Shuster et al. 2005).

During rainfall events, stormwater runoff originating from impervious surfaces carries an array of pollutants and transports them to receiving waters creating significant quality impacts (Barry et al. 2004). Qualitative impacts of urban stormwater are greatly enhanced by quantitative changes in runoff due to urbanisation. Shuster et al. (2005) noted that the higher runoff velocities and relatively smoother surfaces in urban catchments enhances the wash-off of pollutants and their transport to receiving waters.

The quantitative changes to stormwater runoff resulting from urbanisation are primarily due to the presence of impervious surfaces such as roads, roofs and paved areas. As the percentage of impervious surfaces increase, the local hydrological cycle is substantially altered from its rural state. The primary quantitative changes can be listed as follows:

- Increase in runoff volume;
- Increase in peak runoff;
- Decrease in infiltration;
- Reduced time of concentration and decreased time to peak flow;
- Increase in runoff velocity; and
- Decreased base flow.

These changes can be best illustrated in graphical form as shown in Figure 2-1 (Scheuler 1994).

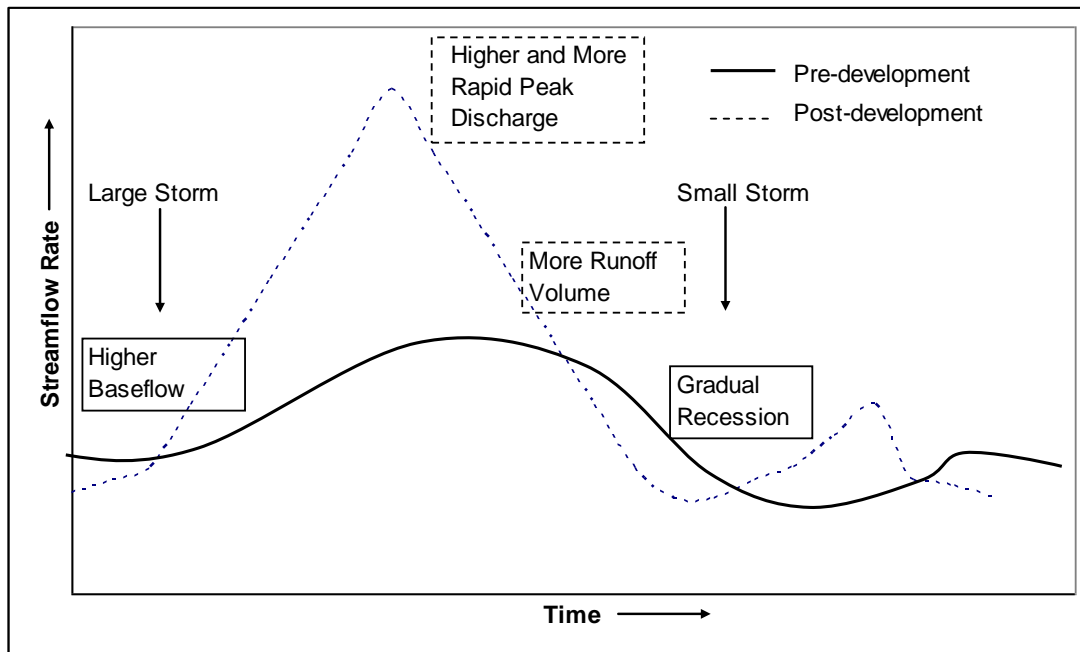


**Figure 2-1: Changes in stream hydrology as a result of urbanisation
(Adapted from Scheuler 1994)**

Quantitative changes to runoff due to urbanisation can be visible not only on a single event basis, but also in long term hydrologic characteristics. Urban catchments typically produce runoff even for small storm events (Delleur 1982; Imhof and Annable 1993). The primary reason being reduced infiltration caused by the presence of impervious surfaces. This increases the frequency of runoff events originating from urban catchments. Creation of frequent runoff from urban catchments increases the frequency of pollutant wash-off events thereby increasing the quality impacts (Karr 1991). Natural catchments retain considerable amounts of rainwater in the form of infiltration and depression storage. It has been estimated that the depression storage volume in natural areas is at least four times that of impervious surfaces (Novotny and Chesters 1981).

From the above discussion, it is clear that hydrologic changes created by the increase in the percentage of impervious surfaces have a significant influence on urban receiving water quality. Additionally, the increase in the number of pollutant sources as a result of increased anthropogenic activities is one of the main reasons for urban

stormwater pollution (Wei et al. 2009). These pollutant generation activities include traffic related emissions, industrial emissions and domestic emissions.

USEPA (1997) has classified sources of stormwater pollutants according to the way they enter the receiving waters as point sources and non-point sources. The point sources are the sources where pollutants discharge from a traceable outlet. For example, effluent from a culvert outlet in an industrial area can be treated as a point source of pollution. Non-point source pollution cannot be traced to a specific source of origin. For example, stormwater runoff is in the non-point source pollutant category and stormwater pollutants can only be traced to a general area. Non-point source pollution normally occurs during rain events where runoff picks up an array of pollutants deposited on the ground and transports to receiving waters (NRDC 1999). As stormwater runoff belongs to non-point source category, it is difficult to control stormwater pollutants using conventional treatment techniques (USEPA 1997).

2.2 Urban stormwater pollutants

Stormwater pollutants have been broadly classified as follows:

- Litter;
- Pathogens;
- Toxicants (trace metals, hydrocarbons);
- Nutrients; and
- Solids.

(USEPA 2007)

Litter

This category of pollutants is readily recognised as it is the visible solid matter such as rubbish from road traffic, from household bins and shops and plant debris. Sartor and Boyd (1972) suggested that litter is not a major category of water pollutants and they can be readily removed through conventional road cleaning practices. However, litter can clog catch basins and gradually decomposing oxygen demanding matter will increase oxygen demand, suspended solids and turbidity.

Pathogens

USEPA (2007) described pathogens as organisms that cause disease under appropriate conditions and include bacteria, protozoans, oomycetes, fungi, worms and arthropods. They noted that pathogens can enter receiving waters from farms and urban areas. Concentration of pathogens are measured in terms of “indicators” that may not be disease-causing themselves but are intended to indicate the presence of fellow pathogens.

Toxicants

Toxicants are compounds that are poisonous at certain concentrations. They primarily include hydrocarbons such as oil, petrol, heavy metals and other compounds such as pesticides and herbicides (USEPA 2007). The toxicants accumulate on road surfaces during the dry period and wash-off into receiving waters during storm events. Toxicants such as pesticides and herbicides can also originate from agricultural lands but their concentration is very small in urban areas as not many agricultural activities take place. Hydrocarbons and heavy metals are discussed in detail under Section 2.5.2 and 2.5.3.

As Pitt and Lalor (2000) noted, organic and metallic toxicants in urban stormwater runoff can contribute to receiving water quality degradation. Therefore, toxicants are a very important group of pollutants. Additionally, they are of concern because of their high potential toxicity to various biological forms. USEPA (2007) has noted that the accumulation of toxicants in fish could threaten commercial and recreational fishing through impacts on human health. Some toxicants can accumulate in very high concentrations in fish and then in turn can accumulate in the human body through bioaccumulation as people consume fish.

Nutrients

Nutrients (primarily nitrogen and phosphorous) are essential elements for all living organisms. However, when nutrients are present at excessive levels, they can have a negative impact on receiving waters and can lead to the degradation of stormwater quality (Barrett et al. 1995). For example, nutrients can be absorbed by plants living in the water column. The bottom deposited nutrients can be absorbed by bottom living plants. As a result, they can stimulate excessive growth of aquatic plants

(Drewry et al. 2006). With the subsequent death and decomposition of aquatic plants, dissolved oxygen concentration in the receiving waters are depleted (Beman et al. 2005).

Since the most common environmental impact on receiving waters is the over stimulation of aquatic plants, nutrients are of great significance. Researchers agree that nutrients (primarily various forms of nitrogen and phosphorus) are a concern because of the long-term potential for eutrophication of water bodies (Barrett et al 1995).

Solids

APHA (2004) defines total solids (TS) as the material residue left after evaporation of a water sample. Solids are separated into dissolved solids, suspended solids and sediments depending on their particle sizes and how they behave in the water column. Total dissolved solids (TDS) include the portion of total solids passing through a filter (smaller 0.45 micron). Suspended solids refer to small solid particles which remain in suspension in water as a colloid. Sediment is any particulate matter which is transported by water or wind and is eventually deposited. Although sediments transported with stormwater runoff settles quickly as velocity reduces, suspended particles do not settle quickly. They can remain in suspension in a receiving water column for a long period of time even in calm conditions.

As stormwater flows over the impervious surfaces, pollutants can wash-off in dissolved or suspended particulate forms. Sediments and suspended solids are discussed in detail in Section 2.5.1.

2.3 Stormwater pollutant sources

Researchers have identified seven primary pollutant sources as noted below:

- Traffic related activities;
- Atmospheric depositions (wet and dry);
- Spills;
- Soil erosion;
- Corrosion of surfaces;

- Construction and demolition activities; and
- Industrial and commercial activities.

(Sartor and Boyd 1972; Pitt 1979).

As this research is focused on vehicle generated pollutants, traffic related pollutant sources such as exhaust emissions, abrasion products and road surfaces are reviewed in detail.

Brinkmann et al. (1985) have noted that atmospheric deposition is a significant pollutant source for urban catchments where pollutant generation processes such as vehicular traffic and construction and demolition activities are predominant. Vehicular traffic contributes a significant amount of pollutants not only to urban catchment surfaces but also to the urban atmosphere in the form of solids, liquid, vapour and gases. These pollutants are generated in the form of exhaust, leakage and abrasion (Brinkmann et al. 1985).

Atmospheric deposition is the process by which airborne pollutants are deposited either on land or water surfaces. This occurs either as wet deposition or dry deposition. Polycyclic aromatic hydrocarbons, heavy metals and particulate matter are important atmospheric pollutants (Kalantari et al. 2006). Traffic related pollution generation processes are discussed in detail in Section 2.5.

2.4 Impacts of vehicle generated pollutants

The environmental pollution caused by vehicle generated pollutants can be primarily classified into water and air pollution. It is widely accepted that pollutants present in these two phases are highly dependent on traffic volume. The air pollution caused by traffic is an important environmental issue (Lim et al. 2005; Mage et al. 1996; Fenger 1999; Faiz and Sturm 2002). Vehicle generated pollutants present in the atmospheric phase can be mainly categorised as gases and particulate matter (Chu et al. 2008). Whilst the heavier particulate fraction is directly deposited on roads and nearby surfaces rapidly, the lighter fraction and gases accumulate in the atmosphere during the antecedent dry period.

2.4.1 Air pollution

Major air pollutants generated by vehicle emissions has been identified as airborne total suspended particulate matter (TSP), sulfur dioxide (SO₂), carbon monoxide (CO), ozone (O₃), nitrogen oxides (NO_x), heavy metals (HMs) and hydrocarbons (HC) (Delfino 2002). Researchers have noted the significance of these pollutants in terms of associated health risks (Brook et al. 1997; Ghose et al. 2005). For example, exposure to airborne TSP leads to illnesses such as cancer and cardiovascular disease (Pope et al. 2002; Zuraimi 2007). Additionally, Kermine et al. (1997) found that diesel-powered vehicle emissions in particular, are the main source of ultra fine particles in urban cities and are responsible for lung disease. Past studies have linked the elevated levels of air pollution to health problems such as low birth weight and birth defects, infant mortality, child asthma, increased hospital admittance, increase allergy cases, respiratory and cardiovascular disease and mortality (Kunzli et al. 2000). Moreover, Stayner et al. (1998) concluded that exposure to polluted air can aggravate existing illnesses.

Garivait et al. (2001) reported that 70% of airborne hydrocarbons are associated with smaller particles (<2.1 µm). Hence, a key issue that needs to be noted is the possibility of inhaling these substances leading to their deposition in the respiratory system. As past studies have indicated, the predominant occurrence is the respiratory fraction of particles (<5 µm) and as such, the risk of human exposure to these substances could be very high (Stayner et al. 1998; Solomon and Balmes 2003; Ravindra et al. 2006).

2.4.2 Water pollution

Traffic related water pollution starts from the accumulation of pollutants on road surfaces. Traffic related pollutants on road surfaces are generated primarily from the following processes:

- Leakage of fuel, lubricants and coolants;
- Fine particles worn-off from tyres, clutch and brake lining;
- Exhaust emissions;
- Dirt, rust and decomposed coatings which drop off undercarriages;
- Vehicle components broken by vibration or impact; and

- Atmospheric deposition.

(Sartor and Boyd 1972).

Water pollution from diffuse sources, including urban stormwater runoff is considered to be the most important source of pollutants to receiving waters (USEPA 1997; Barrios 2000). Additionally, some substances such as fuel, lubricants and hydraulic fluids float on water surfaces causing an unhealthy film (Sartor and Boyd 1972). Moreover, runoff from car washing contributes oil, grease and detergents to the stormwater runoff. In addition, gas vapour emitted when re-fuelling vehicles can subsequently mix with rain, contributing pollutants to stormwater runoff (NAC 1985).

Toxicants such as Hydrocarbons and HMs have received considerable attention due to associated adverse impacts. Water quality degradation due to toxicants, causes direct and indirect health impacts on humans. The main direct impact is health problems due to ingesting polluted water. Indirect impacts are not readily identifiable and take a long time for the consequences to appear. USEPA (2007) noted that toxicants such as Hydrocarbons and HMs can affect the life-cycle of animals or weaken an animal's ability to fight off predators. Toxicants can also build-up in plants and aquatic animals, potentially killing them or animals that consume them.

Some aquatic plants not only take up nutrients, but are also able to absorb and accumulate heavy metals (Petrovic et al. 1999). As fish consume these aquatic plants as their food and as humans consume fish, these toxic heavy metals could finally enter the human body (Negrel and Roy 2002). Also, it has been identified that an increased risk of tuberculosis, silicosis and lung cancer can be related to accumulation of lead and zinc in the human body (Sullivan and Krieger 2001). One of the major problems associated with heavy metals is that they cannot be chemically transformed or destroyed, as other compounds such as organic matter (Davis et al. 2001).

2.5 Traffic related pollutants in urban stormwater

Kalaiarasan et al. (2009) noted that the heavier fraction of vehicle generated pollutants deposit either on roads or nearby areas within a very short time, whilst fine particulate matter (particles $<2.5 \mu\text{m}$) and gases will remain in the atmosphere for a long time.

Following are the primary constituents of vehicle generated pollutants which contribute to stormwater pollution:

- Sediments and suspended solids;
- Hydrocarbons;
- Heavy metals; and
- Airborne particulate matter.

(Truc and Oanh 2007).

Sartor and Boyd (1972) concluded that although the above are the major pollutants generated by traffic related activities, there are also many other pollutants generated by road traffic. Their study further showed that vehicle generated pollutants are not uniformly distributed along the length of the road and high pollutant loads can be observed at intersections, vehicle stops and special turning lanes. Furthermore, they found that traffic lanes are less heavily loaded with pollutants than the space between traffic lanes. This is due to the tendency to blow pollutants out of the traffic lane by traffic generated wind turbulence and the space between traffic lanes is a relatively quiet area. Also, it was found that around 70% of particulate matter is deposited within 150 mm of the road kerb. The common sources of pollutants in road runoff are given in Table 2-1.

**Table 2-1: Sources of pollutants in roadway runoff
(Adapted from WDT 2007)**

Pollutants	Sources
Particulates (solids)	Pavement wear, vehicles, atmospheric deposition, maintenance activities, sediment disturbance
Rubber	Tyre wear
Asbestos	Clutch and brake lining
Lead	Tyre wear, atmospheric deposition, bearing wear
Zinc	Motor oil and grease, tyre wear
Iron	Auto body rust, road structures (bridges, guardrails), moving engine parts
Copper	Engine wear, brake lining wear, metal plating, insecticides and fungicides
Cadmium	Tyre wear, lubricants
Chromium	Metal plating, brake lining wear, moving engine parts
Nickel	Lubrication oil, diesel fuel and gasoline, metal plating, asphalt paving, brake lining wear
Manganese	Moving engine parts
Nitrogen and phosphorous	Atmospheric deposition, fertilizer applications, dead plant material, road-kill, sediments, exhaust
Sulfates	Fuel
Petroleum	Spills, leaks, hydraulic fluids, asphalt surfaces
PAHs	Exhaust
Pesticides, Herbicides	Atmospheric deposition, spraying of rights-of-way, soils
PCBs	Atmospheric deposition
Bacteria	Soil litter, wildlife waste, road-kill,

PAHs=Polycyclic aromatic hydrocarbons (a specific family of hydrocarbons considered to be highly toxic).

PCBs=Polychlorinated biphenyls hydrocarbons (a specific family of hydrocarbons considered to be highly toxic).

2.5.1 Sediments and suspended solids

Sartor et al. (1974) identified that important factors affecting sediment yield are the vehicle condition, topography, type of fuel used and driving style. In addition, sediment generation from road surfaces is highly dependent on road usage, with heavily used roads generating substantially more sediments than lesser used roads. For example, Kaarle (2007) found that in a forested catchment in New South Wales sediment runoff was five to eight times higher in well used roads than abandoned roads. A high level of traffic increases sediment production because the vehicle passage generates loose material, which can be carried away with each rain event. The loose material is then replenished after each rainfall by continued vehicle use. Particles deposited on or in the vicinity of the roads may be re-entrained, or re-

suspended into the air through vehicle-induced turbulence and shearing stress of the tyres (Sartor et al. 1974). However, the generation processes affecting road dust emissions are complex and currently not well known.

Another important phenomenon relating to solids wash-off from impervious surfaces is the first flush behaviour. CSIRO (1999) has defined first flush as the high concentration of pollutants, especially solids, which often occur in the early part of a runoff event. Wong et al. (2000) confirmed that over 60% of the runoff events exhibit first flush behaviour. Moreover, Gnecco et al. (2005) noted that first flush of suspended solids can occur in more than 70% of rainfall events. Barco et al. (2008) and Wong et al. (2000) also noted that as the concentration of suspended solids and other pollutants is high in the first flush, treatment of first flush is becoming increasingly popular in stormwater treatment practices.

Barry et al. (2004) and Brodie and Porter (2006) noted that road runoff is one of the major contributors of suspended particle loads generated from urban catchments. Egodawatta (2007) noted that higher fraction of fine particles, which are less than 100 μm remains in suspension for longer time. Therefore, these suspended solids particles are most likely to reach receiving waters. Sediments and suspended solids loading causes significant water quality impacts on receiving waters. These impacts are, reduced water transparency preventing photosynthesis and dying of bottom living plants and animals (Goonetilleke and Thomas 2003).

Additionally, suspended solids (SS) have the ability to absorb other pollutants in stormwater such as heavy metals and hydrocarbons (Hamilton et al. 1984; WDT 2007; Barrett et al 1995). As fine particles have a relatively larger surface area, they are able to absorb a relatively larger amount of pollutants. Herngren et al. (2005a) noted that heavy metals and organic carbon are strongly correlated with suspended solids in stormwater. This behaviour is due to the fact that pollutants such as heavy metals are adsorbed to clay and organic matter in suspended solids by electrostatic attraction (Sheoran and Sheoran 2006; Warren et al. 2003).

2.5.2 Hydrocarbons

A broad family of several hundred chemical compounds that originate from crude oil are commonly referred to as total petroleum hydrocarbons (TPHs) (Sadler and Connell 2003). TPHs are expressed as the measurable gross quantity of petroleum-based hydrocarbons without identifying its constituents in the environment (Okonkwo et al. 2006). TPHs can be subdivided into volatile organic compounds (VOCs) and semi volatile organic compounds (SVOCs) depending on their volatility. Common VOCs are collectively referred to as BTEXs which include benzene, toluene, ethylbenzene, and xylenes.

Polycyclic aromatic hydrocarbons (PAHs) are semi volatile organic compounds and are an important pollutant group because they are toxic organic compounds commonly found in the urban environment (Herngren 2005b). Although there are more than hundred different PAHs in the environment, USEPA (1999) found that 16 PAHs are particularly toxic to aquatic flora and fauna. These 16 PAHs include low molecular weight compounds such as Acenaphthene (3-4 rings) as well as higher molecular weight compounds such as Benzo(a)pyrene (4-6 rings). While the presence of high concentrations of low molecular weight (LMW) hydrocarbons would be more indicative of crude and refined oils as the primary source (Brown and Maher 1992; Schauer et al. 1996; Watson et al. 1998; Fraser et al. 2003), the presence of high molecular weight (HMW) PAHs tends to indicate combustion processes as the source (Boehm and Farrington 1984; Brown and Maher 1992).

Majority of hydrocarbons are generated from anthropogenic activities including traffic related activities such as the release of petroleum products and combustion of fossil fuel (Soclo et al. 2002; Brcic and Skender 2003; Kucklick et al. 1997; Van Metre et al. 2000). Sorensen (1994) and Nam et al. (2003) noted that incomplete combustion of petroleum products as a primary source of hydrocarbons on urban roads. Other sources of hydrocarbons in urban road runoff include asphalt leaching, particles from tyre wear and spilling of lubricants (Latimer et al. 1990; Takada et al. 1991). Bhargava et al. (2004) found that household cooking also generates PAHs due to burning of firewood and liquid petroleum gas. Natural sources such as forest fires and volcanoes also contribute hydrocarbons, but are not very significant (Stenstrom et al. 1984).

As road vehicles use many petroleum-based products such as gasoline, diesel and oil, stormwater pollution due to these hydrocarbons is widespread. Stein et al. (2006) found that mobile sources contribute exceedingly high level of PAHs to the urban atmosphere during antecedent dry periods and then, with time, they deposit on roads and other surfaces as atmospheric deposition. Consequently, these PAHs are transported to receiving water with stormwater runoff during rainfall events. While lighter PAHs are somewhat soluble in water, heavier compounds are not (Herngren 2005b; Schirmer et al. 1998). As the water solubility of the majority of PAHs is very low, most of their mass in the aquatic environment is bound to solid particulates and can endanger the food chain when they are ingested by various organisms (Jane et al. 2005). A study by Sanger et al. (1999) found that sediments in waterways in industrial areas in South Carolina had significantly higher concentrations of PAHs and other organic pollutants compared to waterways in suburban and forested catchments.

2.5.3 Heavy metals

Klein et al. (1974) noted that the primary loading of heavy metals to receiving waters can be attributed to urban stormwater runoff and a relatively larger portion originates from traffic sources. As heavy metals mainly belong to the toxic stormwater pollutant group, they have received considerable attention from researchers (Rocher et al. 2004). The primary factor affecting the toxicity of heavy metals is pH (Hall and Anderson 1998). Low pH enhances the solubility of heavy metals and converts them into dissolved form. Moreover, as degradation of organic materials produce humic acids, it generates the required acids for this conversion (Petrovic et al. 1999). Consequently, as bioavailability of heavy metals is promoted, it will increase the impacts on receiving waters.

It has been reported that copper (Cu), lead (Pb), and zinc (Zn), are among the most prevalent heavy metals in urban stormwater runoff (Marsalek et al. 1999; Roesner 1999; Brown et al. 2000a, b). However, Sartor and Boyd (1972) found that Mercury (Hg), chromium (Cr), nickel (Ni) and cadmium (Cd) are also present in urban stormwater runoff, but to a lesser extent. It can be seen from Table 2-2 that vehicles

contribute an array of heavy metals to urban road surfaces and tyre wear is the dominant source. This was also confirmed by Pitt (1979). He further noted that about 50% of the tyre wear particles settle on roads and the majority of the particulates settle within about 6 meters of the roadway.

**Table 2-2: Source of heavy metals in urban pavement runoff
(Adapted from Sansalone 1997)**

	Brakes	Tyres	Frame and Body	Fuels and oils	De-icing salts	Litter
Cadmium						
Chromium						
Copper						
Iron						
Lead						
Nickel						
Zinc						

Primary source



Secondary source



Sartor and Boyd (1972) determined that the fine sediment fraction in urban roads (<43 µm) is only about 5.9% of the total sediment mass, but contain over 50% of the heavy metals. This clearly indicates that heavy metals are mainly associated with the fine fraction of particles present on road surfaces. This was further supported by Hamilton et al. (1984) as they found that fine particles play an important role in transporting heavy metals with urban runoff. It has been found that there is a strong correlation between total suspended solids (TSS) concentrations and metals present in urban stormwater (Chui 1981; Preciado and Li 2005).

Heavy metals in stormwater runoff can exist either in dissolved form or particulate form (Herngren 2005a). The impact on organisms may vary depending on the concentration of dissolved heavy metals as particulate bound heavy metals are deposited at the bottom of the receiving waters and cannot be absorbed readily by plants and animals (Janssen et al. 2003). Furthermore, Herngren (2005a) concluded

that dissolved organic carbon (DOC) plays an important role in partitioning of metals between dissolved and particulate fractions.

Sansalone and Buchberger (1997) observed that low intensity rainfall events exhibits first flush behaviour for particulate bound heavy metals such as cadmium, copper, zinc and lead. Whilst cadmium had the highest first-flush behaviour, zinc displayed the lowest first flush behaviour for low intensity rainfall events. According to Sansalone and Buchberger (1997), first flush behaviour is not significant for dissolved cadmium, copper, zinc and lead during low intensity rainfall events. They further noted that for high intensity rainfall events, copper and zinc exhibit first flush behaviour for both dissolved and particulate bound fractions.

2.5.4 Airborne particulate matter

Carter (2007) reported that there is no significant contribution to road surface pollutants from vehicle emitted gases as they do not accumulate on ground surfaces, but rather in the atmosphere. However, there is a significant contribution to pollutant accumulation on road surfaces from vehicle generated particulate matter (Querol et al. 2004). Hence, it is important to focus on particulate matter associated pollutants as a primary air pollutant relevant to water quality studies.

Fine et al. (2004) found that vehicular emissions is one of the most prominent sources of ultrafine particles ($<2.5 \mu\text{m}$) to the urban atmosphere. For example, source apportionment studies suggest that motor vehicle emissions contribute from 25% to 35% of $\text{PM}_{2.5}$ (particulate matter with diameter $<2.5 \mu\text{m}$) to the atmosphere (Chow et al.1996; Japar 1995).

Samara and Voutsas (2005) noted that most of the airborne particulate matter mass (52%) is associated with $<0.8 \mu\text{m}$ size fraction. They also reported that traffic generated metals are strongly associated with the fine particulate fraction. Additionally, Querol et al. (2004) noted that vehicle generated particulate matter is also one of the main sources of coarse particles to the urban atmosphere (diameter between 2.5 and $10 \mu\text{m}$). Therefore, it can be concluded that vehicle emissions is a dominant source of particular matter to the urban atmosphere (diameter $<10 \mu\text{m}$).

Chang et al. (2005) have defined atmospheric particulate matter as material below 297 μm . However, commonly accepted upper limit for airborne particulate matter is 10 μm (Chow et al. 1996).

Zhang and Wexler (2004) reported that most of the vehicle generated particles are due to incomplete combustion (combustion particles) and wear particles from vehicles (non-combustion particles). However, the generation of combustion particles are highly dependent on the vehicle type and the operating conditions. Operating conditions are a significant factor as vehicle emissions are dependent on fuel consumption which in turn is dependent on the vehicle speed. Additionally, vehicle engines burn more fuel when travelling at high speed than at average speed. McGaughey et al. (2004) noted that while carbon emission rates for light duty vehicles (cars, four-wheel drive vehicles) were 42 and 65 g per vehicle kilometre for downhill and uphill traffic respectively, the rates for heavy duty vehicles (heavy duty trucks) were 154 and 327 g, respectively.

Above discussion highlight the importance of vehicle generated pollutants in the atmospheric phase. The discussion primarily focused on identifying traffic related emissions and understanding their physical and chemical characteristics. There have been limited attempts to relate atmospheric pollution to traffic related parameters. Furthermore, the spatial and temporal distribution of atmospheric particulate matter has not been clearly explained.

2.6 Atmospheric pollutant build-up

Atmospheric pollutant accumulation due to vehicle generated emissions is a major concern not only in relation to air pollution but also for urban stormwater pollution (Sabin et al. 2006). It has been noted from the research literature that atmospheric pollutant build-up primarily depends on the following factors:

- Rainfall and antecedent dry period; and
- Urban traffic.

(Gnecco et al. 2005; Davis and Birch 2010b; Ravindra et al. 2003; Sabin et al. 2005).

2.6.1 Rainfall and antecedent dry period

Airborne particulate mass is influenced by rainfall as particulates are absorbed by raindrops and removed during rainfall events (see Figure 2-2) (Ravindra et al. 2003). In other words, this process reduces the atmospheric particulate matter concentration. Ravindra et al. (2003) further noted that the atmospheric concentration of NO_2 , SO_2 also follow similar trends. Additionally, Sabin et al. (2005) noted that dry deposition is directly proportional to the atmospheric pollutant concentration and higher dry deposition could be expected from highly polluted urbanised areas. Therefore, it can be concluded that dry deposition is minimal after a rainfall event as the concentration of atmospheric particulate matter is low. Hence, it can be further concluded that not only atmospheric pollutant concentration, but also dry deposition depends on the dry period between rainfall events.

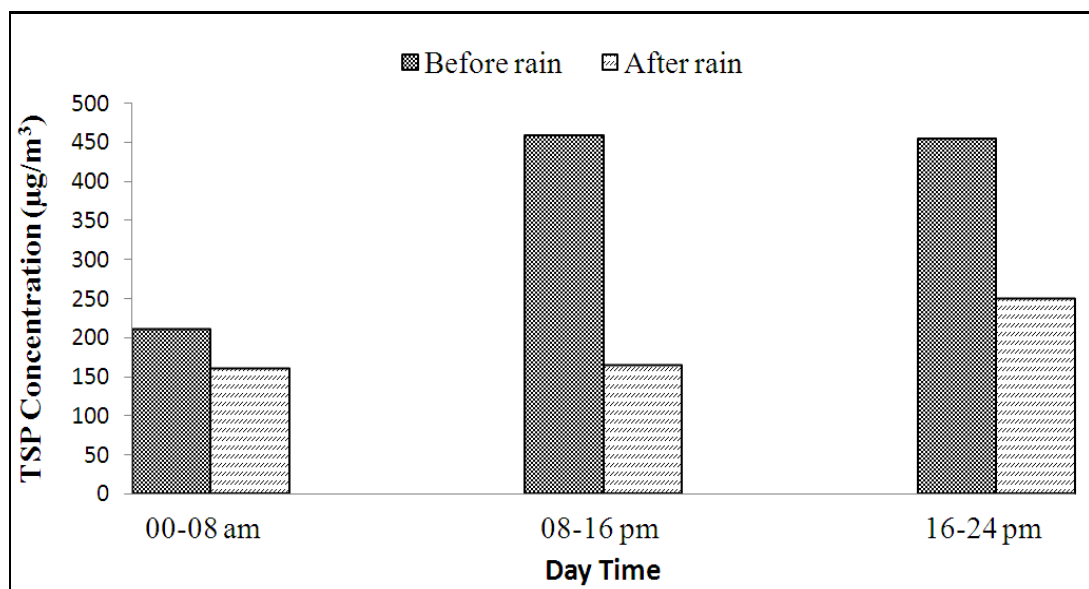


Figure 2-2 : Comparison of TSP concentration before and during rainfall in Dehli, India
(Adapted from Ravindra et al. 2003)
(Where TSP is the total suspended particulate in the air)

2.6.2 Urban traffic

It has been already identified under Section 1.2 that vehicle usage is growing at a very high rate in Queensland, Australia. This increase contributes to increasing pollutant loads to the urban atmosphere and in turn to the receiving waters (Colville et al. 2001). Emissions are linked to a given vehicle along with the fuel consumption, vehicle class, vehicle age, traffic flow and grade of road and traffic congestion

(EPASGV 1999). AATSE (1997) has developed a relationship between volatile organic compounds (VOCs) emissions and congestion for a dual carriageway arterial road (see Figure 2-3) where volume capacity ratio (V/C) is the actual volume of traffic to the theoretical traffic capacity. A V/C ratio over 1.0 indicates the road capacity is being exceeded. Therefore, traffic volume capacity ratio is an important traffic parameter for vehicle emission studies. Additionally, AATSE (1997) has concluded that the deterioration over the life of a vehicle can result in emissions from individual vehicles being up to 10 times higher than a typical new vehicle.

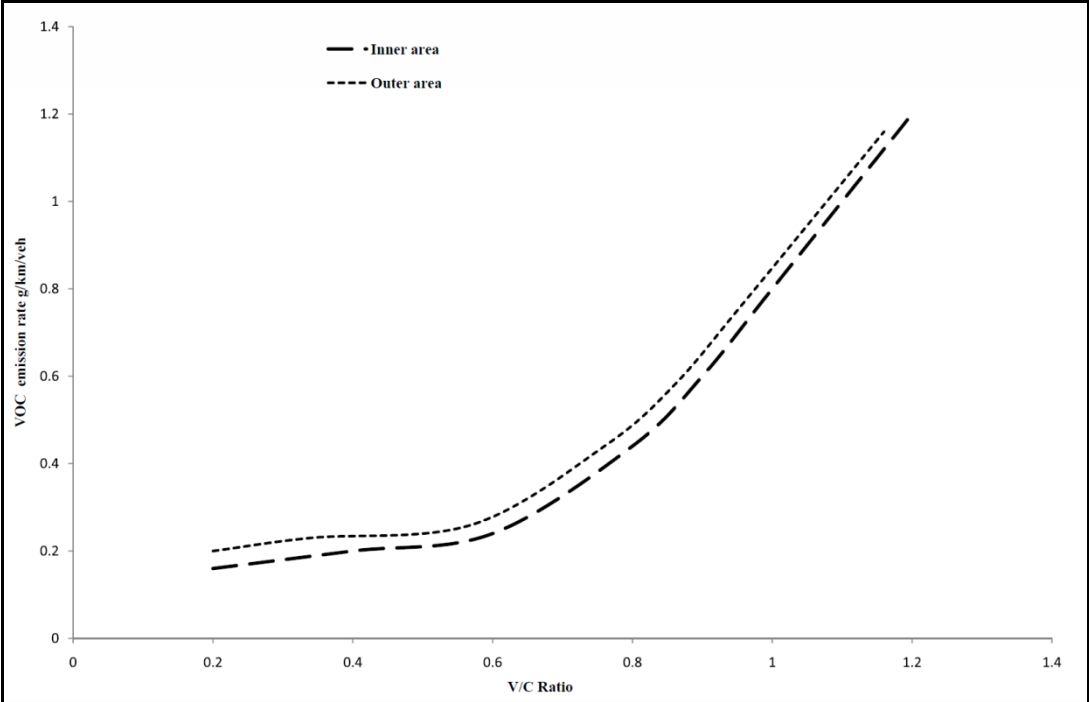


Figure 2-3: VOC emissions as a function of volume capacity ratio (Adapted from AATSE 1997)
 (Where inner and outer areas refer to the city and outside areas)

Pohjola et al. (2002) studied the seasonal variation of vehicle induced atmospheric particulate matter and observed them in high concentration during spring. This indicates that particulate matter accumulation depends on climatic factors. Also, road sweeping can contribute particulate matter PM10 (< 10 μm) to the atmosphere (Chow et al. 1996). Furthermore, Motallebi et al. (2003) noted that heavy duty traffic is a major source of suspended particulate matter to the atmosphere. Also, Karar et al. (2006) reported that the majority of pollutants in atmospheric deposition are generated by traffic sources (Karar et al. 2006). Therefore, both total traffic volume and heavy duty traffic volume are important pollutant sources.

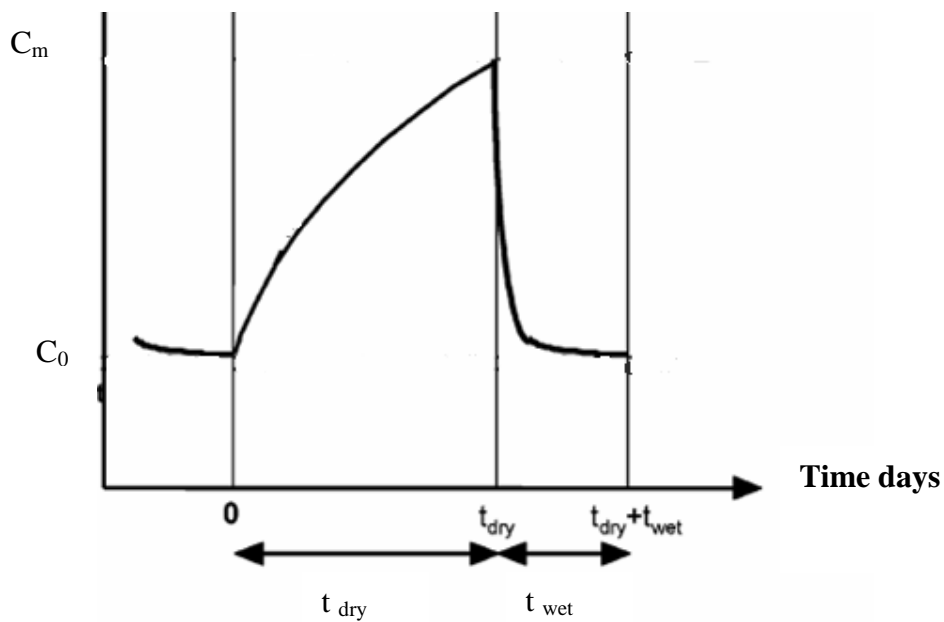
2.7 Atmospheric deposition

2.7.1 General concepts

Atmospheric deposition is a process by which atmospheric pollutants are transferred back to ground surfaces. Atmospheric deposition takes place in two different forms referred to as wet deposition and dry deposition (Ravindra et al. 2003). While wet deposition takes place with rainfall, dry deposition occurs during the antecedent dry period. Sabin et al. (2005) noted that there are relatively few studies which have specifically investigated pollutant contribution by atmospheric deposition to urban stormwater runoff. Additionally, until recently, research on atmospheric deposition was primarily focused on wet deposition (Chu et al. 2008). However, Morselli et al. (2003) found that dry deposition fluxes are almost always predominant for heavy metals compared to wet deposition. This indicates that dry deposition can contribute significant pollutants loads to urban stormwater.

Sabin et al. (2005) found that dry deposition is directly proportional to pollutant concentration in the atmosphere. Furthermore, they concluded that higher deposition fluxes and subsequent higher loading from atmospheric deposition could be expected in highly urbanised areas which has a higher concentration of atmospheric pollutants. They further noted that atmospheric deposition potentially account for as much as 57-100% of the total trace metal loads in Los Angeles stormwater based on the assumption that almost all the atmospheric deposition is dissolved and washed-off with stormwater.

Wet deposition depends on the rainfall intensity and duration (Luo 2001; Huston et al. 2009). For example, Shannon and Voldner (1982) found that maximum wet deposition of 80% of airborne mass occur during a 6 hr rainfall event. Furthermore, Huston et al. (2009) noted that wet deposition dominates over dry deposition in terms of solids mass. Traffic is a primary pollutants contributor to the atmosphere. Dry deposition depends on atmospheric pollutant load, antecedent dry period and physical parameters such as temperature and relative humidity (Luo 2001). The conceptual model proposed by Jolliet et al (2005) shown in Figure 2-4 illustrates that pollutants build-up during the dry period and deposition with rainfall.



Where:

C_0 = background atmospheric pollutant concentration

C_m = maximum atmospheric pollutant concentration for t_{dry} dry period

t_{dry} = antecedent dry period

t_{wet} = rainfall duration

**Figure 2-4 : Mass of pollutant present in the air as a function of dry and wet deposition
(Adapted from Jolliet et al. 2005)**

It is clear from the review of research literature that there is no experimental approach available to link air quality and atmospheric deposition. Furthermore, effects of antecedent dry period on wet and dry deposition have not been investigated in detail. Also, there is only limited research studies which have focused on both, wet and dry depositions simultaneously.

2.8 Pollutant build-up on road surfaces

Sartor et al. (1974) defined pollutant build-up as the process of accumulating pollutants on impervious surfaces during dry periods. They found that road surface pollutant build-up depends on a large number of factors such as traffic volume, climatic conditions, type of fossil fuel used, antecedent dry period, condition of the vehicles and road cleaning frequency. Antecedent dry period (ADP) is an important

governing factor in determining pollutant build-up (Shaheen 1975). Sartor and Boyd (1972) found a weak exponential relationship between antecedent dry period and mass of solids accumulated on asphalt road surfaces. Pitt (1979) concluded that though road cleaning can remove appreciable quantities of sediments and debris (70%) present as road surface pollutants, but not the most critical pollutants such as HMs and PAHs which are attached to the finer fraction (<43 μ m). Additionally, street sweeping can generate fine materials on road surfaces due to abrasion caused by cleaning in addition to the loosening of particulates which are strongly bound to the surface.

Since the detailed experiments of Sartor and Boyd in 1972, a number of other studies have been conducted to understand pollutant build-up processes on roads (for example, Deletic et al. 1998; Deletic and Orr 2005; Vaze and Chiew 2002). Vaze and Chiew (2002) concluded that road surface pollutants accumulate quickly after a rainfall event, but slow down after several days due to re-distribution. They also noted that the surface pollutants become finer over the dry days due to traffic and traffic related turbulence and due to the abrasion of particles themselves in the process. Sartor and Boyd (1972) concluded that particle size distribution is a very important characteristic of road surface pollutants as it can be applied to identify transport mechanisms depending on the size ranges.

Sartor and Boyd (1972) found that different land uses can contribute different pollutant loads to urban road surfaces and they further noted that industrial areas had much higher pollutant loads than residential areas (see Figure 2-5). Sartor and Boyd (1972) assumed that initial street solids loading is zero after a major rain or street cleaning in developing Figure 2-5. Figure 2-5 shows very rapid pollutant build-up at the beginning and the build-up rate reduces quite significantly with time. Also, Egodawatta (2007) reported the same observation and further suggested that pollutant build-up rate after 7 days is much reduced. Furthermore, Egodawatta (2007) also found that pollutant build-up asymptotes to an almost constant value after 21 dry days.

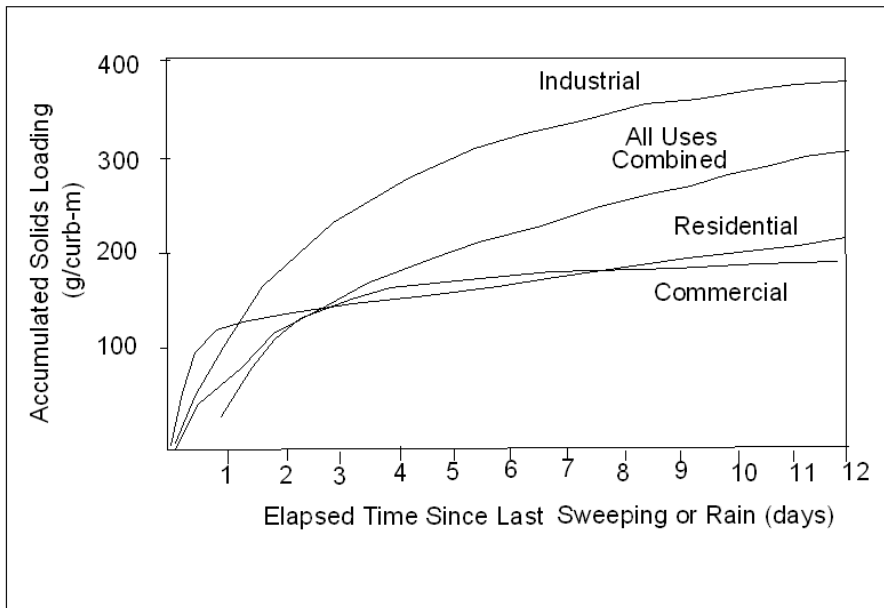


Figure 2-5 : Accumulation of pollutants on urban surfaces (Adapted from Sartor and Boyd, 1972)

A number of previous studies have hypothesised that the accumulation of pollutants on road surfaces is directly related to the density of traffic on a particular section of a road. For example, Tsihrintzis and Hermid (1997) and Shaheen (1975) noted that pollutant accumulation on a road section and wash-off by stormwater are proportional to traffic volume. USEPA (1977) reported that approximately 0.7 g/axle-km of solids are directly generated from traffic and direct tyre wear generated 0.2 g/axle-km of solids. Also, a majority of studies have reported a weak relationship between average daily traffic (ADT) and pollutants in road runoff (Opher and Friedler 2010).

Egodawatta (2007) recommended a power function to replicate pollutant build-up on road surfaces as shown in Equation 2.1. He also noted that the coefficient (*a*) is dependent on the site-specific parameters such as population density and time exponent (*b*) depends only on the road surface type.

$$B = aD^b \dots \dots \dots \text{Equation 2.1}$$

Where:

B = Build-up load on road surface (g/m²);

D = Antecedent dry days; and

a and *b* = Build-up coefficients.

(Egodawatta 2007)

It is clear from the above review that pollutant build-up on road surfaces have been investigated by many researchers (for example Egodawatta (2007); Hengren 2005; Sartor and Boyd 1972). Consequently, pollutant build up processes have been understood in greater detail when compared to other processes such as atmospheric build-up and depositions. However, as Duong and Lee (2011) and Opher and Friedler (2010) have noted that there is no widely accepted relationships available for describing pollutant build-up with traffic and land use characteristics.

2.9 Pollutant wash-off processes

Wash-off is the term used to describe the series of sub-processes, which are collectively responsible for pollutants removal during runoff events. Wash-off depends on several factors which include rainfall pattern, intensity and urban drainage system configuration (Chui et al. 1981). The initial process is the dissolution and detachment of pollutants from catchment surfaces by utilising the kinetic energy of the raindrops (Egodawatta and Goonetilleke 2008a). Then, the detached pollutants are kept in suspension. The final process is the transportation of these pollutants into receiving waters. This overall process is accelerated due to the impervious and relatively smooth nature of urban catchment surfaces. Vaze and Chiew (2002) defined two terms referred to as ‘free load’ and ‘fixed load’ to explain pollutant wash-off characteristics. According to their definition, free load is the readily removable fraction that can be removed by vacuuming without brushing and the fixed load fraction can only be removed by brushing and vacuuming. They concluded that although a small rain event can remove only the ‘free load’, bigger events can remove the ‘fixed load’ as well. Hence, pollutants wash-off is influenced by the pollutant attachment characteristics and rainfall intensity and duration.

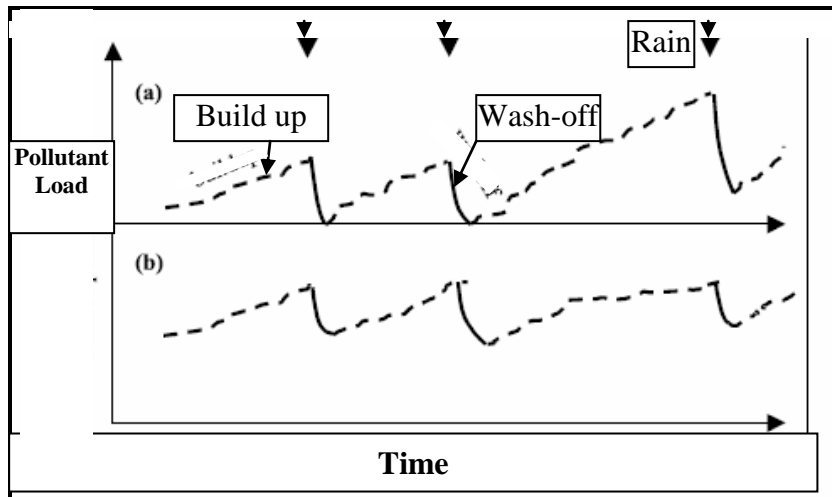


**Figure 2-6 : Hypothetical representations of surface pollutant load over time.
(Adapted from Vaze and Chiew 2002)**

Vaze and Chiew (2002) proposed two possible alternative pollutant wash-off processes as illustrated in Figure 2-6. These processes have been named as source limiting (Figure 2-6a) and transport limiting (Figure 2-6b). In the source limiting process, road surface pollutant load builds-up from zero during the antecedent dry period. A storm event washes-off almost all the available load. In the transport limiting process, only part of the pollutant build-up load is removed by a storm event and quickly returns back to the original pollutant build-up load within several days (Vaze and Chiew 2002).

Boyd and Gardner (1990) have identified two primary pollutant wash-off processes. They named them as “transport and transformation”. They further noted that both processes of surface pollutant wash-off and pollutant deposition are jointly related to the transport and transformation processes, which are responsible for the distribution of pollutants in the aquatic environment. The transport process moves pollutants from one location to another and the transformation process alters pollutant characteristics as a result of physical, chemical and biological processes. Typical transport processes include wash-off with stormwater and typical transformation processes include biodegradation (Senyah 2005).

Pollutant wash-off starts with a rainfall event. From the time rain falls on the ground to the time it reaches the receiving waters, it encounters several pollutant sources. An understanding of the pollutant wash-off processes in urban catchments is essential to

develop appropriate pollutant removal measures (Tsihrintzis and Hamid 1997). One such pollutant removal measure is the treatment of urban stormwater runoff which is steadily becoming common practice (Deletic 1998; Anderson 1996). In this context, the identification of first flush is very important in receiving water quality management as stormwater runoff during the initial period of a rainfall event carries a higher pollutant concentration (Barco et al. 2008). However, there is no clear agreement among researchers as to how the first flush should be defined (Gupta and Saul 1996; Ashley et Al. 1992).

With reference to first flush, estimation of stormwater quality variation with the storm duration is important for effective treatment design. This variation can be predicted using mathematical modelling. Mathematical modelling is a commonly used approach to estimate pollutant wash-off (Egodawatta and Goonetilleke 2008b). Currently, there are a large number of mathematical models to estimate pollutant wash-off (Obropta and Kardos 2007). However, the prediction accuracy of these models depends on the accuracy of the replication equations used in the model. Therefore, formulation of accurate mathematical equation to replicate pollutants wash-off is very important (Egodawatta 2007). In this regard, Sartor and Boyd (1972) proposed an exponential equation to predict pollutant wash-off as given below:

$$N = N_0(e^{-kIt}) \dots \dots \dots \text{Equation 2.2}$$

where:

- N = residual road pollutant load (after a rainfall event);
- N₀ = initial road pollutant load;
- t = rainfall duration;
- I = rainfall intensity; and
- k = constant.

(Sartor and Boyd 1972)

Due to decreasing particulate supplies, the exponential wash-off curve predicts decreasing concentration of particulates with time from the start of a rainfall event (Sartor and Boyd 1972). The proportionality constant, k in Equation 2.2 was found by Sartor and Boyd (1972) to be slightly dependent on road texture and condition, but was independent of rainfall intensity and particle size. However, Vaze and Chiew

(2002) has pointed out that there are many significant problems in using the exponential form for pollutant wash-off. For example, an exponential wash-off function cannot simulate an increase in concentration at any time during the storm. Egodawatta and Goonetilleke (2008b) proposed a modified exponential equation with the introduction of capacity factor (C_F) which varies with rainfall intensity (See Equation 2.3) that could be used to replicate solids wash-off.

$$F_w = \frac{W}{W_0} = C_F(1 - e^{-kIt}) \dots\dots\dots \text{Equation 2.3}$$

Where:

- W = Weight of the material mobilised after time t ;
- W_0 = Initial weight of the material on the surface;
- F_w = Fraction wash-off;
- C_F = Capacity factor;
- I = Rainfall intensity; and
- k = Wash-off coefficient

(Egodawatta and Goonetilleke 2008b).

2.10 Conclusions

This section summarises the important findings drawn from the state-of-the-art literature review carried out primarily to understand the influence of urban traffic and impervious surfaces on stormwater quality. The review was mainly focused on traffic generated pollutants in urban stormwater and their transport pathways.

Urban traffic has been identified as one of the primary sources of key pollutants to urban stormwater. While traffic generated pollutants associated with larger particles deposit on the ground very rapidly, others stay in the atmosphere for longer periods of time and deposit on the ground either as dry deposition or wet deposition with rainfall. Consequently, stormwater runoff transports these pollutants to receiving waters creating significant quality impacts. Quality impacts are greatly enhanced by the increased and faster flowing runoff generated mainly by impervious surfaces.

Until recently, research on atmospheric deposition was primarily associated with rainfall events or wet deposition. However, recent studies indicate that dry deposition

fluxes are an important heavy metals source to urban stormwater. Atmospheric dry deposition processes are currently not very well understood. Recent studies indicate that atmospheric dry deposition is directly proportional to pollutant concentration in the atmosphere. However, there is no commonly accepted mathematical relationship to describe this phenomenon.

Pollutants on road surfaces originate from vehicular sources as well as other non-vehicular sources. Vehicular sources can generate a significant amount of pollutants to the urban atmosphere and road surfaces. The main types of vehicle generated pollutants are total suspended particulate matter (TSP), suspended solids, heavy metals and hydrocarbons. Heavy metals and polycyclic aromatic hydrocarbons have received considerable attention from researchers due to their potential toxicity. It has been found that TSP or solids is one of the most important pollutants present in both air and build-up because other pollutants such as polycyclic aromatic hydrocarbons and heavy metals are associated mainly with particulates. The accumulation processes of these pollutants are complex due to the dynamic interaction between the atmosphere and road surfaces. The complexity in accumulation processes explains lack of knowledge linking the interaction between atmospheric and ground based phases of pollutants.

From the review of research literature on pollutant build-up and wash-off, it was found that these two processes are collectively responsible for receiving water pollution. The identification of possible mitigation actions is strongly related to the understanding of pollutant generation, accumulation and transport processes. Therefore, researchers have undertaken in-depth investigations into these processes especially with reference to solids. As a result, well developed mathematical equations are available to replicate build-up and wash-off of solids from urban roads.

Chapter 3 -Research Design and Methods

3.1 Background

Stormwater pollution due to traffic generated pollutants is complex due to the involvement of many interlinked processes and influential factors. Vehicle emissions typically contain an array of critical pollutants, a portion of which will accumulate in the atmosphere and the remainder will deposit directly on the ground surfaces. Pollutants emitted to the atmosphere will eventually deposit on the ground as wet and dry deposition. Wet deposition is the deposition of atmospheric pollutants during rainfall events and dry deposition is the deposition of atmospheric pollutants during dry weather. Wet and dry deposition and the pollutants directly deposited on ground surfaces forms the pollutant build-up. Pollutant build-up is a dynamic process due to re-suspension potential of pollutants.

Chapter 2 discussed in detail the complexity associated with pollutant processes such as atmospheric build-up, wet and dry deposition and build-up on ground surfaces. Chapter 2 also highlighted the lack of approaches for describing the linkages between these pollutant processes. In order to develop an understanding of the linkages between of traffic generated pollutant processes, a comprehensive research program was needed. This Chapter presents the formulation of research methodology and the program of research to support this comprehensive research study. This Chapter further discusses the selection of sampling equipment for air sampling, wet and dry deposition sampling and build-up sampling, laboratory testing of key pollutants and data analysis tools. This Chapter also discusses the selection of the stormwater quality modelling tool that formed an essential component of this research project.

3.2 Research Methodology

The research methodology consisted of the integration of a series of activities to achieve the research aims and objectives. The research methodology is discussed under the following key activities:

- Literature review;
- Selection of key pollutants;
- Selection of influential variables;
- Site selection criteria;
- Analytical test method selection;
- Sampling equipment selection;
- Sample collection and testing
- Data analysis; and
- Mathematical modelling.

3.2.1 Literature review

A state-of-the-art literature review was conducted to gain in-depth knowledge on urban stormwater pollutant sources, processes and pathways. The literature review provided knowledge primarily in the following areas:

- Traffic and other land use related pollutants, pollutant processes and pathways;
- Current knowledge in relation to traffic and other land use related pollutants in the atmosphere and deposition on the ground; and
- Current state of knowledge in relation to the replication of pollutant build-up.

3.2.2 Selection of key pollutants

Test parameters were selected based on the outcomes of the detailed literature review discussed in Chapter 2. As noted in Chapter 2, pollutants on road surfaces primarily originate from traffic sources and land use related anthropogenic activities. Generally, traffic related pollutant sources dominate. Pollutants from traffic sources can either directly deposit on ground surfaces or contribute to atmospheric pollutant load. The primary pollutants generated from traffic sources are atmospheric total suspended particulate matter (TSP), solids, heavy metals and hydrocarbons (WDT 2007; EPASGV 1999; Truc and Oanh 2007). Heavy metals and polycyclic aromatic hydrocarbons have received considerable attention from stormwater researchers due to their potential toxicity (Rocher et al. 2004; Hengren 2005). Similarly, TSP in air and solids in the ground phase are important pollutants due to their physical presence

and capability to associate with other pollutants such as polycyclic aromatic hydrocarbons and heavy metals.

TSP was considered only specific to air whereas solids replace TSP in build-up and atmospheric deposition. Heavy metals (HMs), polycyclic aromatic hydrocarbons (PAHs) and total suspended particulate matter (TSP) are significant because of their adverse impacts on humans and the environment. Hence, they were selected as the target pollutants to understand the impacts of traffic generated pollutants on urban stormwater quality.

3.2.3 Selection of influential variables

The literature review discussed in Chapter 2 highlighted the fact that traffic generated pollutants in the atmosphere and on ground surfaces are dependent on many factors such as driving habits, fuel used, road geometry, traffic volume, traffic congestion and antecedent dry period. Among these factors, traffic volume and traffic congestion are reported as the most dominant traffic related influential parameters (Lim et al. 2005). Other parameters are subjected to less variability within a specific region and it was therefore decided to standardise within site selection and experimental processes. The influence of driving habit was taken into account by using traffic congestion as an independent variable. It was assumed that the traffic mix is typical to the region. It was decided to ensure uniform road geometry in site selection to avoid the influence of this factor. Additionally, dominant land use type in the vicinity of each study site was incorporated as an independent variable. Land use can influence pollutant generation indirectly in altering the traffic mix as well as by specific pollutant generation processes (Singh et al. 2008; Ötvös et al. 2003). Therefore, the parameters which were selected as independent variables for the study were:

- Antecedent dry period;
- Indicator for traffic congestion (V/C) which is the ratio of the actual traffic volume to theoretical capacity of a road section;
- Dominant land use type in each study site; and
- Indicator for traffic volume—average daily traffic (ADT).

The target dependent variables for the research study were:

- Pollutants in the air;
- Pollutants in atmospheric deposition;
- Pollutants in build-up on road surfaces; and
- Stormwater quality.

3.2.4 Site selection criteria

The following criteria were adopted for study sites selection:

- Sites should represent the land uses within the study region;
- Traffic volume at selected sites should encompass the range typical to the study region;
- Uniform topography and road geometry at all selected sites;
- Convenient accessibility;
- Minimum disturbance to road users including cyclists and pedestrians; and
- Availability of traffic data.

Details of the selected sites and their characteristic are discussed in Chapter 4.

3.2.5 Analytical test method selection

The selection of analytical methods was underpinned by the literature review discussed in Chapter 2. The test methods were selected after a detailed study of available methods. The United States National Institute for Occupational Health and Safety (USNIOH) has developed test methods to measure traffic generated key air pollutants such as PAHs and HMs. However, the selected United States Environmental Protection Program (USEPA) test methods are much more relevant for this study as they are specially designed for environmental sampling and testing. Therefore, USEPA test methods were adapted for this study. Additionally, it was found that USEPA test methods have been commonly used in Australia for a long time (Berko 1999). A summary of selected methods are given in Table 5-3 of Chapter 5.

3.2.6 Sampling equipment selection

As air, atmospheric deposition and build-up samplings had to be carried out covering atmospheric and ground phases, the following criteria were adapted for the selection of sampling equipment:

- Suitability to collect target pollutants;
- Portability of the equipment;
- Sampling efficiency;
- Ability to ensure consistency in sampling; and
- Ease of use.

The specific sampling equipment selection is discussed in Section 3.3.

3.2.7 Sample collection and testing

Field sampling was conducted to collect air, atmospheric deposition and build-up samples from the selected study sites. Initially, trial samples were collected and laboratory analysis were undertaken to ensure the adequacy of sampling time to collect all the target pollutant, especially for air and atmospheric deposition.

Samples were tested for selected key pollutants according to the selected test methods discussed in Section 3.2.5. In this regard, the trial samples were tested to validate the accuracy of each analytical method adapted prior to actual sampling. Additionally, each analytical method was validated against certified reference material before and during actual sampling and testing.

3.2.8 Data Analysis

The data analysis methods adopted were selected taking into consideration the involvement of multiple pollutant species and influencing variables. Accordingly, appropriate multivariate analytical techniques were used. A detailed discussion of the multivariate analytical techniques is given in Section 3.4.

3.2.9 Mathematical modelling

Mathematical modelling was conducted to demonstrate the ‘real-world’ applicability of knowledge developed in this research study. After detailed evaluation of

commonly used mathematical models, a suitable model was selected as discussed in Section 3.5.

3.3 Sampling equipment

Three sets of sampling equipment were selected for this research. They are discussed in following sections.

3.3.1 Air sampling

Two types of sampling equipment have been commonly used for air sampling. They are Low-volume sampler and High volume sampler. A detailed review of advantages and limitations of these two were undertaken to select the most appropriate equipment (Berko 1999; Peltonen and Kuljukka 1995). The criteria discussed in Section 3.2.6 was used as the basis in selection. After evaluating the advantages and limitations as listed in Table 3-1, it was decided to use the High volume air sampling equipment for this study.

Table 3-1: Comparison of air sampling equipment

Techniques	Advantages	Limitations
Low-volume sampler	<ul style="list-style-type: none"> 1) Battery operated 2) Recommended for occupational environments 3) Handling of sampling is easy (Peltonen and Kuljukka 1995) 	<ul style="list-style-type: none"> 1) PAHs samples are not widely available 2) loss of target PAHs due to longer sampling time
High volume sampler	<ul style="list-style-type: none"> 1) High flow rate reduces sampling time (generally 24 hr) 2) No sample loss due to reduced sampling time 3) Commonly used in Australia for outdoor sampling 	<ul style="list-style-type: none"> 1) Main power supply or generator supply required 2) Handling requires at least two people

High volume air sampling equipment is also recommended by the USEPA (1999) for investigations similar to this study. Reduced sampling time was considered as an important advantage in using a High volume air sampler. As noted by Berko (1999), most Australian studies have sampled PAHs over a period of 24 hour using High volume air samplers. In the case of a Low volume sampler, 2 to 9 days sampling is required to collect sufficient sample. Use of shorter sampling times is preferred to minimise loss of PAHs during sampling (Berko 1999).

High volume air sampling equipment has been widely used to sample traffic generated critical pollutants (PAHs and HMs) in the atmosphere (Kalantari et al. 2006). However, some modifications were incorporated to the sampling methodology by considering the requirements of USEPA Method IP-7 (USEPA 1989), USEPA Method IO-2.1 and Method IO-3.1 (USEPA 1999). The Method IP-7 is for the determination of pollutants in indoor air. Method IO-2.1 is for the sampling of ambient air for total suspended particulate matter and Method IO-3.1 is for the sampling of inorganic pollutant in ambient air.

As atmospheric concentrations of PAHs, HMs and TSP are highly dependent on the temperature, relative humidity, wind and other atmospheric disturbances, it was decided to undertake sampling of PAHs, HMs and TSP concurrently.

High volume polyurethane foam (PUF) air sampling system which is illustrated in Figure 3-1 is designed to simultaneously collect airborne pollutants both in vapour and particulate phases at the same time including PAHs and HMs. This instrument is capable of drawing ambient air through a quartz filter paper and the PUF sorbent cartridge at a flow rate of 15m³/hr. As air is drawn through the filter and PUF sorbent, the particulate bound PAHs, HMs and PM are trapped in the filter paper and gas phase PAHs are trapped in the PUF sorbent.

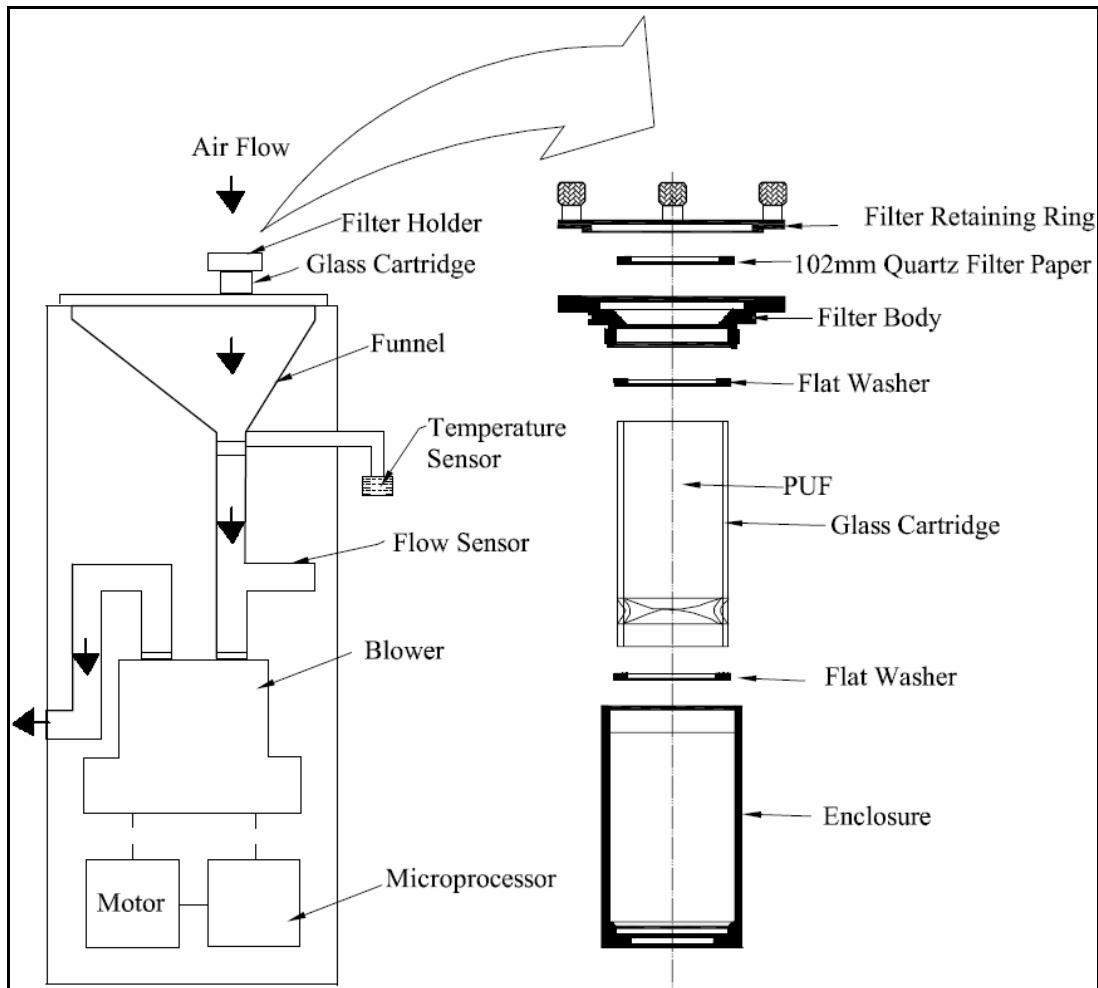


Figure 3-1 High volume air sampler

3.3.2 Atmospheric deposition sampling

It was found that there is no commonly accepted sampling method available to collect atmospheric deposition. Therefore, researchers have used a range of different sampling methods (Huston et al. 2009; Pekey et al. 2007). For example, Hill and Caritat (2002) used plastic funnels and 500 mL high density polyethylene (HDPE) narrow-neck bottles (called wet and dry atmospheric deposition collector) whereas Davis and Birch (2010) conducted sampling using cylindrical high-density polyethylene tanks with opening diameter of 33 cm. In both cases, samplers were mounted 2.0 m above the ground level to minimise the deposition of re-suspended particles. Azimi et al. (2005) used an automatic sampler called ARS 1000 (MTX-Italia SPA, Modane, Italy) collector which can collect both wet and dry deposition separately. Huston et al. (2009) used 4 L amber glass bottles and 15-18 cm diameter clear glass funnels to collect bulk deposition samples.

The sampling equipment required for this study was selected by considering criteria given in Section 3.2.6 and advantages and limitations reported in Table 3-2. Table 3-2 provides a comparison of advantages and limitations of techniques used for wet and dry deposition sampling.

Table 3-2: Comparison of atmospheric deposition sampling techniques

Techniques	Advantages	Limitations
Wet and dry atmospheric deposition collector designed by Hill and Caritat (2002)	1) Simple and easy to construct and transport 2) Easy to install (Hill and Caritat 2002)	1) Cannot collect wet and dry deposition separately
High-density polyethylene tanks	1) Simple and easy to construct (Davis and Birch 2010)	1) Handling of sampling apparatus is difficult as its diameter is 33 cm 2) Cannot collect wet and dry deposition separately 3) Wind effect is high due to its size 4) Sample collection requires much deionised water
ARS 1000	1) Can collect wet and dry deposition separately as it automatically regulates sampling (Azimi et al. 2005)	1) Expensive 2) Not readily available in Australia
4 L amber glass bottles and clear glass funnels (15–18 cm diameter) (Huston et al. 2009)	1) Simple and easy to construct (Huston et al. 2009)	1) Cannot collect wet and dry deposition separately 2) Bottles and funnels need to be transported carefully 2) Separate arrangement required for mounting

After evaluating the advantages and limitations, wet and dry atmospheric deposition collection apparatus developed by Hill and Caritat (2002) was selected to collect dry and bulk deposition samples for this study.

The equipment suggested by Hill and Caritat (2002) has been successfully used to sample atmospheric deposition in Australia. However, the apparatus was modified to suit the proposed sampling programme for this study (see Figure 3-2). Instead of one sampling head, two sampling heads were incorporated to accommodate wet and dry sampling. One head was used for total deposition sampling and the other for dry deposition sampling.

The sampler needed to be installed in such a way that the sampling funnels are 2.0 m above the ground level. The 2.0 m height above ground was aimed at preventing contamination from re-suspended particles generated by traffic induced turbulence

and natural wind (Rocher et al. 2004). The collection vessel for the unit consisted of a 500 mL high density polyethylene (HDPE) narrow-neck bottle (167 mm high x 73 mm outside diameter) with a 100 mm inner diameter plastic funnel. As it was found after initial studies that the concentration of target pollutants such as HMs and PAHs were below the method detection limit, the size of the funnel was increased from 100 mm to 190 mm to collect sufficient sample volume.

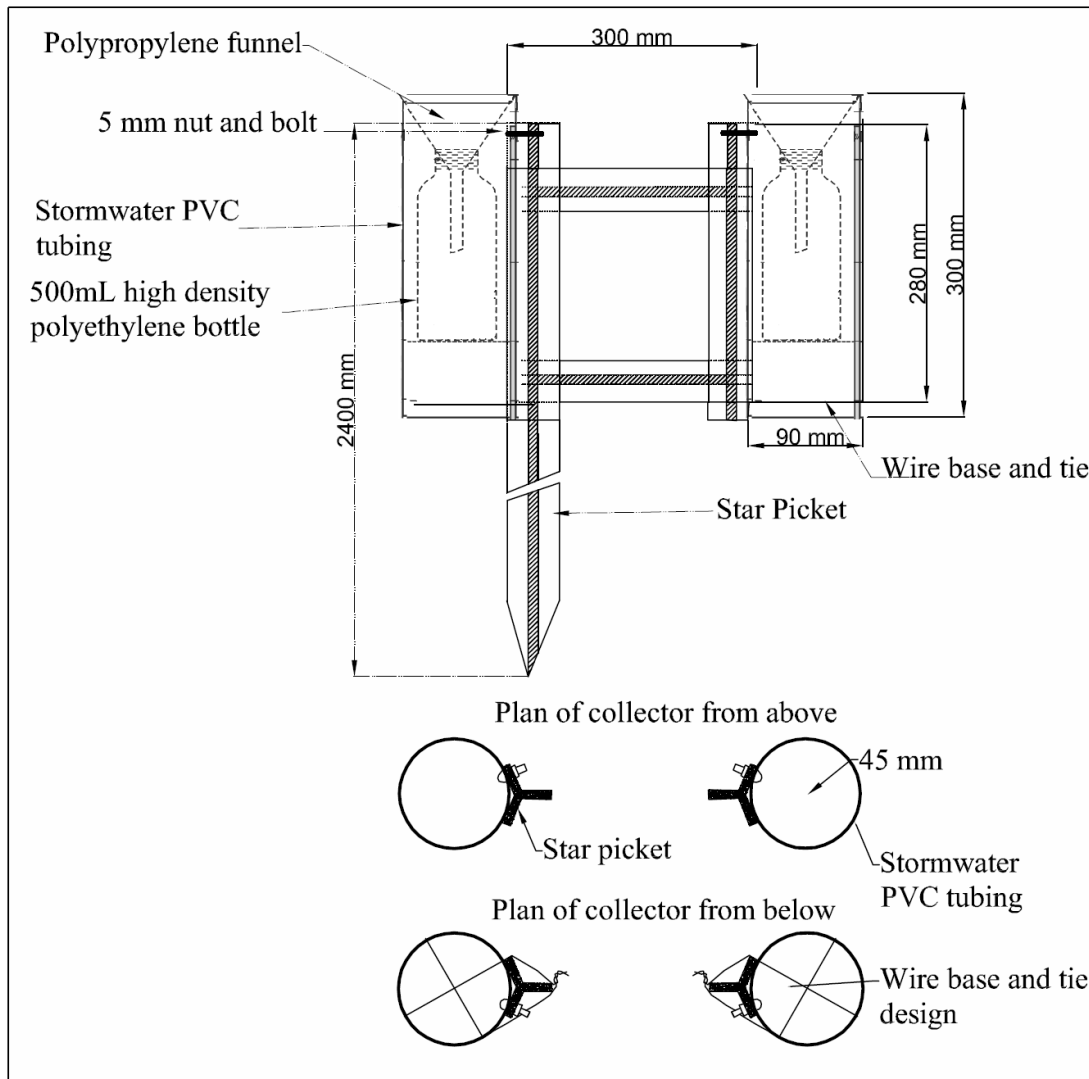


**Figure 3-2: Wet and Dry atmospheric deposition collector
(Adapted from Hill and Caritat 2002)**

3.3.3 Build-up sampling

As reported in research literature, different techniques have been used by researchers to collect build-up samples (Egodawatta 2007; Deletic and Orr 2005; Vaze and Chiew 2002). Deletic and Orr (2005) reported that the sampling method used influences the results. Therefore, it was important to select the most suitable sample collection system for the study. Following methods have been used in the past:

- (1) Brushing and sweeping;
- (2) Dry vacuuming;
- (3) Wet vacuuming; and
- (4) Wet and dry vacuuming.

Each method described above has its own advantages and limitations. The most suitable technique was selected by considering the criteria given in Section 3.2.6 and evaluating advantages and limitations of these techniques as listed in Table 3-3.

Table 3-3: Comparison of build-up sampling techniques

Techniques	Advantages	Limitations
Brushing and sweeping	(1) Fine pollutants attached to the surface are released (Vaze and Chiew 2002)	(1) The method itself is not capable of collecting solids into a container
Dry vacuuming	(1) Capable of collecting over 80% of particles below 75 μm (Deletic and Orr 2005)	(1) Only 50% collection efficiency for particles <43 mm (Deletic and Orr 2005)
Wet vacuuming	(1) Capable of collecting small particles (Deletic and Orr 2005)	(1) Wetting procedure need to be consistent. (2) Pollutants can be washed out of the sampling area due to excessive wetting.
Wet and dry vacuuming	(1) Capable of collecting small particles (2) Optimum wetting can be achieved using a sprayer (Mahbub 2009)	(1) Additional sprayer is required to wet the surface (2) Sampling takes a longer time compared to dry or wet method

As evident from Table 3-3, wet and dry vacuuming is the most efficient method to collect road deposited pollutants. Therefore, this method was selected for this study. Wet and dry sampling was carried out using a sprayer and a vacuum collection system. The selected vacuum system has a water filtration system to ensure minimal escape of fine particles through the exhaust.

Vacuum systems have been used by previous researchers to collect road surface build-up samples (for example Herngren 2005; Egodawatta 2007). Also, Herngren (2005) found that the vacuum system he used was capable of collecting 96.4 % of road dust <75 μm . Therefore, it was decided to use the same vacuum system to collect build-up samples for this project. Additionally, its simplicity and portability was also considered when selecting this equipment.

The vacuum system is a Delonghi Aqualand (see Figure 3-3) model. It consists of a 1500 W motor and efficient water filtration system which prevents the escape of fine particles. A commercially available sprayer was used to wet the surface for wet sample collection. Mahbub (2011) achieved an optimum total collection efficiency of 93.3 % for wet and dry collection for a 1 m x 1 m test plot spraying water at 3 bar pressure for 3 minutes. The same sprayer and specification was used to wet the surface. Both wet and dry sampling was carried out using the same vacuum system.

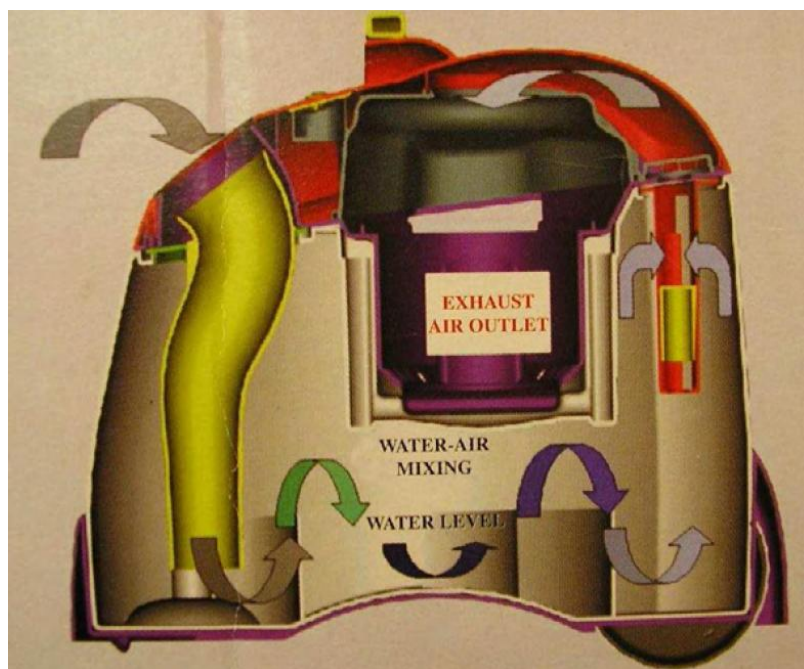


Figure 3-3: Delonghi Aqualand water filter system

The equipment was tested for sample collection efficiency before it was used for the field sample collection. For this, 1 m x 1 m bituminous surface area was selected. The area was cleaned by applying water. After allowing for an hour to dry the plot, 100 g of uniformly graded fine material was spread uniformly. Initially, dry sampling was carried out using the vacuum system. Then, water was sprayed on the plot at 3

bar pressure for 3 minutes and wet sampling was carried out. Finally the sample was carefully transferred to a crucible and oven dried. The total recovered weight was 97.4 g giving a sample collection efficiency of 97.4 %. This was considered adequate for the field investigations.

The field sampling undertaken can be described in four steps. Firstly, the selected sampling plots of 2 m x 1.5 m (3 m²) were cleaned and demarcated for later identification. Secondly, a dry sample was collected from the selected plot after 7 antecedent dry days. A small plot of 3 m² was selected to ensure homogeneity of the sampling area (Herngren 2005). After that, the same area was moistened using a sprayer at 3 bar pressure for 3 minutes. Then, that area was sampled again using the same vacuum system. Finally, the vacuum system was washed with deionised water and the sample was transferred to a 25 L polyethylene container. Figure 3-4 illustrates the build-up sample collection on actual road surfaces.

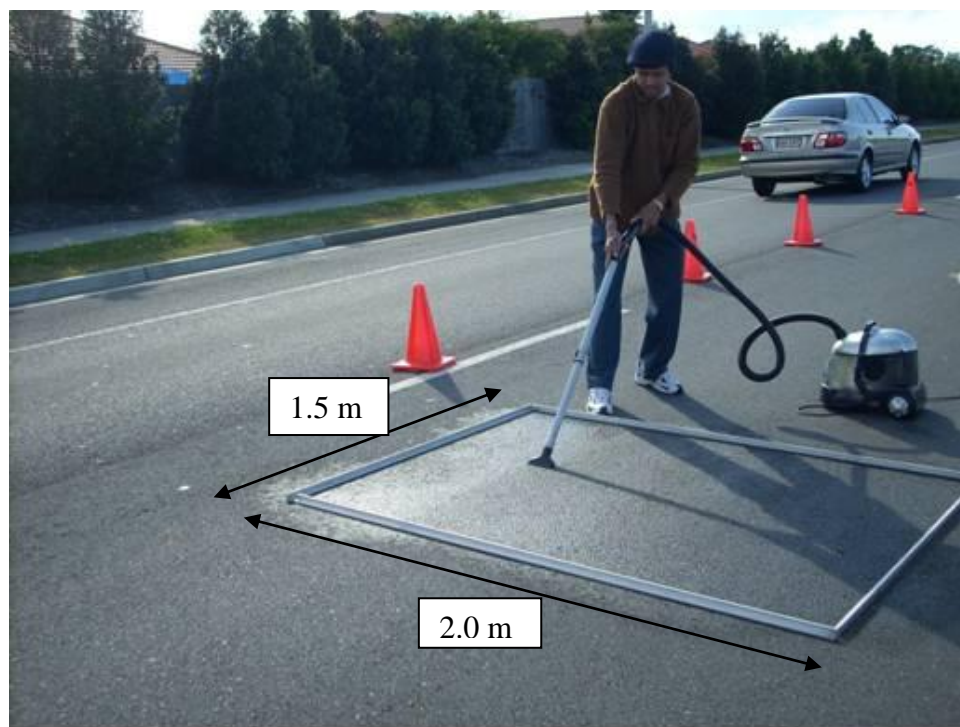


Figure 3-4: Build-up sample collection (wet and dry vacuuming)

3.4 Statistical and multivariate analytical tools

For the data analysis, statistical and multivariate analytical tools were selected by carefully considering the type of analysis to be carried out and capabilities of the available analytical tools.

The primary objective of using analytical tools was to recognise the patterns of variability observed in the data sets. This was carried out firstly by plotting the measured data in x-y plane. Multivariate statistical tools were then used for detailed pattern recognition. The following multivariate tools were used for the study:

- Principal component analysis (PCA);
- Multiple linear regression (MLR); and
- Multicriteria decision making methods (MCDM).

3.4.1 Principal component analysis (PCA)

PCA was selected for this research as it is one of the most important multivariate analytical tools. PCA is a pattern recognition technique that reduces data dimensionality by performing a covariance analysis between factors. It is a widely used analytical tool in water quality research studies to extract meaningful information from multivariate databases (Massart et al. 1997).

Herngren et al. (2006) have used this technique to identify the pattern in heavy metals associated with different particle size fractions of road dust. Also, this technique has been used as a pattern recognition technique in many environmental studies (for example Goonetilleke et al. 2005; Kokot et al. 1998). Ong et al. (2007) found that PCA analysis coupled with multiple linear regression becomes a powerful tool for source identification of polycyclic aromatic hydrocarbons in house dust samples. Moreover, PCA technique has widely been used to evaluate the impacts of human activities on the quality of surface water (Topalian et al. 1999; Carroll et al. 2006).

One of the main advantages of PCA is that the technique can be used to reduce a set of raw data to a number of independent principal components while retaining most of the variance in the original data set (Goonetilleke et al. 2005; Mahmud et al. 2007). However, PCA assumes that the observed data set to be a linear combination of optimally-weighted observed variables. This assumption limits the applicability of the method to data which satisfies this requirement (Shlens 2003).

As the contribution of original variables to a principal component can be expressed as a linear combination of original variables, these contributions are called “Factor Loading”. When several variables have large loading on a principal component, they can be interpreted as being significantly associated with that principal component (Mahmud et al. 2007). Furthermore, Massart et al. (1997) explained that the loading of each variable can be graphically displayed in principal component space. These loading plots can be used to identify relationships between different variables and are called a biplot. In this plot, selected variables and objects are displayed in two-dimensional PCA space (for example PC1 and PC2). Relationships between objects and variables can be investigated using biplots. For example, if the angle between two variables in the biplot is acute, then the two variables are correlated. Variables are independent if the angle between two variables is close to 90 degrees and variables are inversely related if the angle between variables is obtuse (Massart et al. 1997).

However, it is required to select suitable principal components (PCs) to draw a biplot. Scree plot method is one of the most commonly used techniques to select the number of PCs to represent the data structure without losing much of the important information (Dong et al. 2007). Scree plot is a simple plot that shows the fraction of total variance in the data as explained by each PC.

3.4.2 Multiple linear regression (MLR)

Development of mathematical equations to predict the variability of dependent variables based on observed independent variables was one of the primary requirements in this research. Hence, multivariate linear regression techniques were selected based on the following criteria:

- Ability to remove redundant variables efficiently;
- Regression is simplified;
- Accuracy of predictions; and
- Ability to use independent variables efficiently.

(Tranmer and Elliot 2008).

Multivariate linear regression was carried out using SigmaPlot 11 software (SigmaPlot 2008).

3.4.3 Multicriteria decision making methods (MCDMs)

MCDMs were selected by considering following criteria:

- Ability to select the optimum solution in multi criteria problems;
- Ability to rank objects according to user preference; and
- Accepted largely by the research community.

According to research literature, there are numerous multicriteria decision making methods available (Miguntanna et al. 2009). However, PROMETHEE (Preference Ranking Organisation METHod for Enrichment Evaluations) and GAIA (Graphical Analysis for Interactive Assistance) are commonly used methods in research studies (Ayoko et al. 2003; Herngren et al. 2006). PROMETHEE is a well established decision support system which deals with the appraisal and selection of a set of options on the basis of several criteria, with the objective of identifying the advantages and limitation of the alternatives. For example, Herngren et al. (2006) applied this method to identify heavy metals associated with different particle size fractions on road surface pollutant build-up. Also, they were able to predict the affinity of heavy metals to specific particle size ranges.

PROMETHEE and GAIA can be applied to analyse a data matrix containing only two objects unlike PCA which requires a large data set for obtaining reliable outcomes (Miguntanna 2009). Therefore, this method has been widely used to analyse environmental data in research studies (for example, Ayoko et al. 2007; Ayoko et al. 2003; Herngren et al. 2006). In this research study, PROMETHEE and GAIA methods were applied to analyse air, atmospheric deposition and build-up samples as the data matrices did not have a large number of objects.

Lim et al. (2005) applied PROMETHEE and GAIA to identify the most polluted site in terms of PAHs and HMs in an air pollution study. Herngren et al. (2006) used PROMETHEE and GAIA to identify the most polluted particle size fraction in terms

of heavy metals in build-up solids on road surfaces. For example, they used GAIA visualisation plot to investigate the correlation of heavy metals with organic carbon.

Chapter 6 discusses the use of PROMETHEE and GAIA methods to investigate the atmospheric PAH and HM build-up processes. These methods were used for data analysis with the help of Decision Lab software (DL 2000b). Theory relating to these methods are available in research literature (Lim et al. 2005; Keller et al. 1991). However, a short description of these methods is given below.

(a) PROMETHEE

PROMETHEE is a non-parametric method and it ranks a number of objects or actions based on a range of variables or criteria (PAHs and HMs concentration in air, atmospheric deposition and build-up) in a data matrix. In this analysis, ranking order, weighting, preference function and a threshold value must be defined for each variable.

In the PROMETHEE analysis, the user needs to select the ranking order according to the objective of the analysis. The user can select to either maximise (higher value of a variable) or minimise (lower value of a variable) each criteria to define the preference ranking order. As a result, actions are ranked in ascending order (smaller to larger) or descending order (larger to smaller).

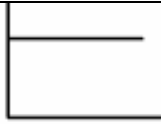
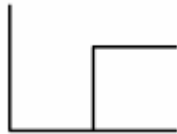
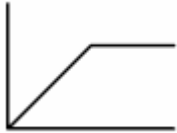
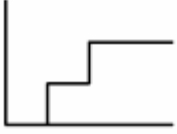


Weightings are used in the PROMETHEE analysis to reflect the importance of one criterion over the other. For example, a larger weighting indicates the importance of that criterion over the other. By default, Decision Lab software assigns 1 as the criterion weight for all the criteria (DL 2000a). However, the user can change the weighting as required to suit the analysis.

Preference functions in PROMETHEE are applied to decide how much one outcome is preferred over the other and to translate the deviation between the evaluations of two actions on a single criterion into a preference degree. Preference degree defines an increasing function of the deviation. A larger deviation will contribute a high degree of preference whereas a smaller deviation will contribute to a weaker degree

of preference (DL 2000b). There are six preference functions within the Decision Lab software used, as shown in Table 3-4.

The shape of the preference function is dependent on the preference threshold (P) and indifference threshold (Q) where Q cannot be greater than P. P is the smallest deviation that is considered as decisive. Q is the largest deviation that is considered negligible. Gaussian threshold, S, is a middle value that is used only with the Gaussian preference function (Herngren et al. 2006; Keller et al. 1991; Visual Decision Inc. 2000).

Table 3-4: List of preference functions in Decision Lab software

Function	Shape	Threshold
Usual		No threshold
U-shape		Q threshold
V-shape		P threshold
Level		Q and P thresholds
Linear		Q and P thresholds
Gaussian		S threshold

(b) GAIA

GAIA is a visualisation technique which is used to visualise PROMETHEE results as a simple principal component biplot in PC1 and PC2 space. A typical GAIA plot can be used to explore the relationships among objects and variables. The decision axis, π_i , points towards the direction of compromised solution proposed by PROMETHEE (Lim et al. 2005).

GAIA results can be explained according to guidelines presented by Espinasse et al. (1997) and summarised as follows:

- 1) Longer projected vector contains more variance while shorter projected vector contains less variance.
- 2) Independent variables are represented by almost orthogonal vectors.
- 3) Variable vectors pointing towards the same direction are correlated while those oriented in opposite directions are conflicting.
- 4) Objects pointing in the direction of a particular variable are correlated to that variable whereas opposite objects are weakly correlated to that variable.
- 5) Dissimilar objects have significant different PC coordinates whereas similar objects show as clusters.
- 6) If the decision vector, π_i , is long, then the decision power of the plan is strong and the best choices are those closest possible to the decision axis and vice versa.

3.5 Stormwater models

Three commonly used industry standard urban stormwater models were evaluated to select the most suitable model for the study. They are:

- EPA SWMM (Storm Water Management Model)
- MIKE URBAN
- MUSIC (Model for Urban Stormwater Improvement Conceptualization)

3.5.1 EPA SWMM

EPA SWMM is a fully dynamic stormwater and wastewater modelling package developed by the United State Environmental Protection Agency (USEPA 2010a). It is a physically based, discrete-time simulation model that employs the principles of

conservation of mass, energy and momentum. As it is a comprehensive modelling package for hydrologic, hydraulic and water quality simulation, the model can be used for both planning and design and overall assessment of urban runoff issues (USEPA 2004). It can simulate up to ten pollutants without pollutant interactions. As it can simulate suspended solids, heavy metals and other toxicants, this model is suitable for modelling the wash-off of critical pollutants (USEPA 2004; USEPA 2010a). Additionally, it is capable of modelling stormwater treatment processes. Obropta and Kardos (2007) noted that the software can model urban stormwater quantity and quality from natural and artificial drainage systems. Furthermore, it can simulate pollutant loads due to atmospheric deposition as well. For example, it can simulate pollutant concentrations in rainfall, but the concentrations must be held constant and cannot vary with time (Obropta and Kardos 2007).

EPA SWMM can estimate not only the generation of surface runoff, but also the production of pollutant loads due to key catchment processes. These processes are modelled for any number of user-defined water quality parameters (USEPA 2004; USEPA 2010b). They are:

- Dry-weather pollutant build-up over different land uses;
- Pollutant wash-off from specific land uses during storm events;
- Routing of water quality constituents through the drainage system;
- Reduction in constituent concentrations through treatment in storage units.

As this model is incorporated with three different pollutant build-up and wash-off functions, the user can select the most appropriate one for a particular catchment by considering the behaviour of the actual pollutant build-up and wash-off processes. Also, EPA SWMM is provided with upper and lower limits of event mean concentration of key pollutants such as TSS, Cu, Zn and Pb. Hence, the user can ensure the accuracy of field data before inserting data for key pollutants into the model (USEPA 2004; USEPA 2010b).

The model takes into account spatial and temporal variation of rainfall and land use characteristics. Variation of spatial rainfall is handled by setting a series of rain gauges for each sub-catchment. Infiltration related processes are simulated by the

groundwater component of the model. In the case of high imperviousness, when groundwater processes are not important, there is an option to remove this component making the modelling fast and easy (USEPA 2004). One of the key advantages of EPA SWMM is that it simulates the generation, inflow and transport of any number of user-defined pollutants. Lockie (2007) noted that the spatial variation of pollutant build-up and wash-off can be handled by defining small sub-catchments with homogeneous properties. He further noted that it simulates user-defined treatment functions to model treatment techniques.

EPA SWMM is USEPA open source freeware and has been improved significantly from its origins in year 1971 (USEPA 2004). Since it is open source software, the user can customise and incorporate necessary improvements. Also, the user can check the source code to see exactly how the software simulates a certain process. Additionally, this model simulates not only simple steady flow routing, but also complex kinematic flow routing as well (USEPA 2004; USEPA 2010a).

However, this model has a number of limitations. These include: GIS based data is not supported; the hydraulic engine is slower than other common hydraulic engines; and there is no formal support offered by USEPA (Lockie 2007). In addition, a maximum of 100 sub-catchments and 200 inlets and channels are allowed (USEPA 2004; USEPA 2010a).

3.5.2 MIKE URBAN

MIKE URBAN is a GIS based integrated urban modelling system developed by the Danish Hydraulic Institute (DHI). This model includes the collection system (CS) and water distribution (WD) system, data management, stormwater modelling, wastewater modelling and water distribution network modelling (DHI 2007). As it is GIS based, data can be imported conveniently from other sources into the model. As this model incorporates the latest version of EPA SWMM for hydrologic, hydraulic and water quality modelling of urban stormwater, it has all the capabilities of EPA SWMM (DHI 2007). As the catchment element is divided into a number of different contaminant-generating surfaces, it is easy to simulate different land uses with

different properties (Elliott and Trowsdale 2007). Furthermore, this model and EPA SWMM can be used for detailed design of stormwater drainage systems (DHI 2007).

MIKE URBAN can simulate both the dissolved phase and particulate phase pollutants and uses an advection-dispersion equation to simulate pollutant transport (DHI 2007). Elliott and Trowsdale (2007) noted that model calibration can be performed much quicker as the software is incorporated with automatic calibration capability. Moreover, as this software is capable of simulating both kinematic-wave routing and dynamic-wave hydraulic routing, the backwater effect can be taken into account (DHI 2007).

The model has been implemented with both linear and exponential pollutant build-up functions and the user has to select the most appropriate function based on experimental results (DHI 2007). The model replicates pollutant wash-off processes in greater detail as pollutant wash-off is assumed to vary with rainfall intensity and pollutant detachment rate. Despite the model using many parameters to replicate wash-off processes in great detail, only the key parameters are required to set up the model and default values are assigned for others. Hence, a comprehensive data collection programme is not required to calibrate the model (DHI 2007).

Despite having several benefits, the MIKE URBAN model also has limitations. They are; high degree of model complexity and calibration difficulties due to many model parameters (Obropta and Kardos 2007). Additionally, despite the fact that wash-off of sediment is influenced by both rain drop and overland flow erosion, only the rain drop erosion is taken into account in the model (DHI 2007). Furthermore, Elliott and Trowsdale (2007) noted that MIKE URBAN is too complex to be used by an inexperienced person and significant time and effort is required to become fully familiar with the model.

3.5.3 MUSIC

This software was developed by the Cooperative Research Centre (CRC) for Catchment Hydrology in Australia. It simulates both stormwater quantity and quality and has been developed to undertake simulation on an event or continuous basis.

Hence, the effectiveness of treatment devices such as buffer strips and wetlands can be evaluated to ensure both short term and long term goals (MUSIC 2005; MUSIC 2009). Another advantage of this model is that it can simulate a range of stormwater devices including ponds, infiltration buffer strips, sedimentation basins, pollutant traps, wetlands and swales (Elliott and Trowsdale 2007). This model was primarily designed to simulate the generation and transport of total suspended solids (TSS), total nitrogen (TN) and total phosphorus (TP) from Australian urban catchments (MUSIC 2009). Additionally, it simulates gross pollutant load together with runoff. As MUSIC is relatively simple and easy to use, it is a popular modelling tool.

As this model simulates a minimum time step of 6 min, its applicability is limited for predicting runoff from catchments smaller than about 0.01 km². Also, it is very difficult to model more than 100 catchment elements, as catchment elements have to be inserted manually (Elliott and Trowsdale 2007). The model can simulate treatment processes as a first order pollutant decay process towards an equilibrium value. First order kinetics is applicable only for physical pollutant processes and not for chemical and biochemical pollutant processes (MUSIC 2005). Hence, MUSIC is suitable for conceptual design and is not a detailed design tool. Additionally, it cannot be applied to simulate wash-off of toxicants such as HMs and PAHs directly (Elliott and Trowsdale 2007). However, this can be carried out by relating them to total suspended solids (TSS) as they are dependent on TSS wash-off.

3.5.4 Model selection

In summary, either MIKE URBAN or EPA SWMM mathematical models would be appropriate for predicting road generated stormwater quality. As MIKE URBAN is integrated with GIS software to provide additional spatial modelling and data handling capabilities, export and import of spatial data is convenient. MIKE URBAN software incorporates the EPA SWMM's modelling engine. While MIKE URBAN is a commercial software package and EPA SWMM is a free software tool, capabilities and limitations needed to be evaluated against cost and benefits. MUSIC is suitable for conceptual modelling applications but not for detailed design applications as only the first order process kinetics is implemented in the model. In MUSIC, the only way to simulate toxicants is to consider them as co-pollutants of TSS.

As EPA SWMM is a free software tool, source code is available only for this model. This is one of the most important features as the user should be able to improve the software by incorporating newly generated knowledge into the model such as the variation of atmospheric deposition with the antecedent dry period. Therefore, EPA SWMM model was selected as the most suitable modelling tool for this study.

3.6 Quality control and quality assurance

Quality control and quality assurance are activities that are required to ensure accuracy (nearness to truth) and precision (the reproducibility of a result) of all testing starting from sampling to final testing and interpretation of results. Quality control refers to the overall plan for maintaining quality in all aspects of sampling and testing. Quality assurance refers to the steps that are undertaken to determine the validity of sampling and analytical testing procedures. Following sections discuss the quality control measures undertaken for sampling and testing of key test parameters. For some parameters, the quality control and quality assurance procedures given in the relevant test methods were followed.

3.6.1 Quality control procedures for PAHs sampling and testing

As a part of the quality assurance procedure, analytical reagent grade organic solvents were used for all the extractions. Prior to sampling, glass filters were baked at 250 °C for 12 hours to remove traces of organic compounds. Before the actual sampling, polyurethane foam (PUF) sorbents were extracted using soxhlet extraction apparatus for 6 hours to remove any organic impurities left. Then, they were dried in a vacuum desiccator followed by wrapping in aluminium foil and preserved in clean zipped polyethylene bags. Clean glass filters were wrapped in aluminium foil that had been rinsed with hexane and sealed in zipped polyethylene bags for cold storage until required. All the glassware was acid washed and then rinsed with deionised water followed by storing in plastic boxes to prevent contamination in the laboratory environment.

The following standards were used for quality control and quality assurance:

Calibration standards: 2000 µg/mL each component in methylene chloride, prepared by Sigma Aldrich.

Internal standards: Following standards were obtained from Sigma Aldrich

- i. Perylene-D12, 2000µg/mL in methylene chloride.
- ii. Chrysene-D12, 2000 µg/mL in methylene chloride.
- iii. Acenaphthene-D10, 2000 µg/mL in methylene chloride.
- iv. Phenanthrene-D10, 2000 µg/mL in methylene chloride.

Field surrogate: Fluoranthene-d10, 1000 µg/mL in methylene chloride prepared by Absolute standards

Laboratory surrogate: Fluorene-d10, 1000 µg/mL in methylene chloride prepared by Absolute standards

Certified reference material: Standard reference material 1649b urban dust prepared by National Institute of Standards & Technology, USA.

As specified in the Method TO-13A (USEPA 1999), method blanks, reagent blanks and field blanks were used. Method blank is a sample containing all components except the analyte and it was taken through all steps of the analytical procedure. Response of the method blank was subtracted from the response of a real sample prior to calculating the quantity of analyte in the sample. Reagent blank is similar to a method blank, but it had not been subjected to all sample preparation procedures. The method blank is a more complete estimate of the blank contribution to the analytical response. Field blank is similar to a method blank, but has been taken to the actual study sites.

Surrogate standards are chemical compounds not expected to occur in an environmental sample and mainly used to identify the recovery of target analyte. Surrogate standards are also referred to as spike recovery, are a known quantity of analyte added to a sample to test the sample recovery errors (Harris 2007).

3.6.2 Quality control for heavy metal sampling and testing

All the quality control and quality assurance samples were prepared and tested as specified in Method 200.8 (USEPA 1991). The method recommends testing of calibration blanks, laboratory reagent blanks, laboratory fortified blanks, field

reagent blanks, calibration standards, internal standards and certified reference materials (CRMs) as part of the quality assurance measures. Additionally, all the sampling and testing equipments were acid washed and then rinsed with deionised water followed by storage in plastic boxes to prevent contamination in the laboratory environment. As a part of the quality assurance procedure, analytical grade stock solutions were used for the preparation of samples and standards as recommended in Method 200.8 (USEPA 1991).

As the test results are highly dependent on the accuracy of calibration, special attention was paid during the preparation of calibration standards. Sometimes, these standards had to be prepared several times by eliminating possible measurement errors and blank interferences until an acceptable calibration curve was obtained ($R^2 > 0.98$). Also, despite the fact that the number of calibration standards has to be greater than three, a minimum of five calibration standards were always used to obtain an accurate calibration curve. Complete test method was validated by using CRMs and ensured that its recovery was always within 85% and 115% as specified in the test method.

As recommended in Method 200.8 (USEPA 1991), following standards were used for quality control and quality assurance:

Internal standards (from Accustandard):

- i. Scandium ICP-MS standard 100 $\mu\text{g/mL}$ in 2% HNO_3 .
- ii. Bismuth ICP-MS Standard 100 $\mu\text{g/mL}$ in 2% HNO_3 .
- iii. Indium ICP-MS 100 $\mu\text{g/mL}$ in 2% HNO_3 .
- iv. Terbium ICP-MS 100 $\mu\text{g/mL}$ in 2% HNO_3 .
- v. Yttrium ICP-MS 100 $\mu\text{g/mL}$ in 2% HNO_3 .

External standards: ICP-MS quality control standard 100 $\mu\text{g/mL}$ in 5% HNO_3 prepared by Accustandard.

Certified reference material: Multi-element standard solution V for ICP-MS prepared by TraceCERT®

3.6.3 Quality control for particulate matter sampling and testing

As specified in Method IO-2.1 (USEPA 1999), all the quality control and quality assurance procedures were followed. Despite the fact that Method IO-2.1 suggests a number of possible different filter types for air sampling, quartz filters were selected by considering its particle sampling efficiency, chemical and physical stability and temperature stability. As specified in Method IO-2.1, as part of the quality control and quality assurance procedure, quartz filters were pre-weighed in the laboratory under prescribed climate control conditions of temperature and relative humidity. Additionally, filters were stored in zipped polyethylene bags so that they are not contaminated during storage in the laboratory and transported to the field. Also, blank filters were tested together with actual sampled filters to make blank corrections for both laboratory and field conditions. As specified in Method IO-2.1 (USEPA 1999), before handling filters, very clean gloves were worn and filters were handled extremely carefully to prevent possible wear.

3.7 Summary

This chapter has discussed the research methodology adopted, selection of sampling equipment, selection of data analysis tools, selection of stormwater quality modelling tool and quality control and quality assurance adopted in this study. Methodology was formulated to achieve research aims and objectives by sequentially undertaking the key activities.

In this Chapter, following key decisions were made:

- Heavy metals (HMs), polycyclic aromatic hydrocarbons (PAHs), total suspended particulate matter (TSP) and solids were selected as the key traffic generated pollutants to be investigated in this research study.
- Dependent and independent variables were selected based on the detailed understanding gained from the literature review.

- Analytical test methods selection, sample collection and testing, data analysis and mathematical model selection were selected based on the requirements of the study. The EPA SWMM model was selected as the most suitable mathematical model for this study.
- The selected sampling equipment included, high volume air sampling system, wet and dry deposition collection system, and vacuum collection system.
- Considering the nature of the data analysis to be undertaken, a series of multivariate data analysis methods were selected. The selected data analysis methods included, principal component analysis (PCA), multiple linear regression (MLR), and multi criteria decision making methods (MCDM).

Chapter 4 - Study Sites

4.1 Background

Site selection was undertaken to identify the most suitable sites for this study. As discussed in Chapter 2, traffic related pollutants in atmospheric and ground phases were of the primary focus of this study. Field investigations necessary for this study included the collection of samples from the atmosphere, wet and dry deposition and build up on road surfaces. The key traffic generated pollutants selected for this study were PAHs, HMs and solids or TSP.

As the focus was traffic generated pollutants, typical suburban road sites were selected. In order to account for emission characteristics specific to land use, representative sites from typical urban land uses, namely, residential, industrial and commercial were selected. This was based on the current land use classification adopted in the Gold Coast area. Gold Coast was considered as the regional laboratory for this study.

Based on the criteria established in Chapter 3, this Chapter presents the details of the selected study sites and their characteristics. Investigations such as wet and dry deposition and build-up were undertaken in selected clusters of sites.

4.2 Study site selection

Study sites were selected within the Gold Coast region, Queensland State, Australia based on the criteria established in Section 3.2.4. Gold Coast is among the cities with high population growth rates in Australia, in turn, resulting in high traffic growth (GCCC-WEB 2010). Due to residential nature of most Gold Coast suburbs, traffic emissions dominate over the other emissions. However, it was found that traffic growth is not uniform throughout the Gold Coast area (Cook 2008). Furthermore, Cook (2008) noted that there is considerable spatial distribution of traffic generated pollutants. This provided ideal characteristics to select Gold Coast as the study region.

As traffic emissions are higher in steep terrain, selecting sites with appropriate topography was important. Therefore, sites with steep slopes were avoided during the site selection process. Available traffic data was also closely examined during the site selection process. This was to select sites with representative mixture of traffic characteristics. The traffic data published by ABS (2008) was used to identify the distribution of different types of traffic in the Gold Coast area. Traffic data predicted by Gold Coast City Council was used as the primary basis for selecting sites. Attention was paid to select sites from industrial, commercial and residential land uses. Special attention was paid to avoid nearby construction or demolition activities. Eleven study sites were selected based on the pre-determined criteria discussed in Section 3.2.4. The selected sites are listed in Table 4-1. Figure 4-1 shows the selected road sites located in Helensvale and Coomera suburbs of Gold Coast. Details of the land use of selected sites are given in Table 6-2.

Table 4-1: Predicted traffic characteristics for the selected roads

No	Name	Predicted for year 2011		Predicted for year 2016		Predicted for year 2021	
		ADT	V/C	ADT	V/C	ADT	V/C
1	Abraham Road	8149	0.57	11414	0.86	10314	0.83
2	Reserve Road	8144	0.61	8733	0.62	10713	0.26
3	Peanba Park road	6420	0.76	8652	1.03	4423	0.6
4	Billinghurst Cres	628	0.14	1411	0.33	812	0.25
5	Beattie Road	3822	0.39	4117	0.55	2935	0.36
6	Shipper Drive	2501	0.39	4074	0.49	3765	0.57
7	Hope Island Road	26506	0.64	27619	0.71	29697	0.76
8	Lindfield Road	14091	1.21	14698	1.25	15175	1.28
9	Town Centre Drive	9860	0.31	15318	0.45	19023	0.43
10	Dalley Park Drive	2888	0.26	3080	0.27	3063	0.27
11	Discovery Drive	6856	0.46	6454	0.47	6334	0.45

(Where ADT is the average daily traffic, V/C indicator of traffic congestion, details in bold represents “Set 2” sites as shown in Figure 4-1)

Additional four sites were specifically selected for air and atmospheric deposition sampling. These were, Yatala, Southport Library, Highland Park and Miami Deport as shown in Figure 4-1. These sites are referred to as “Set 1”, and have intense anthropogenic activities compared to the selected eleven sites with typical urban characteristics. The four sites were selected to investigate the maximum PAHs and HMs levels in the atmosphere and atmospheric deposition within the study region. Considering the availability of actual surveyed traffic data and the representative

nature of dominant land use types, four sites (referred to as Set 2” sites) were selected for atmospheric deposition sampling. These four sites encompassed all three land uses, namely, commercial residential and industrial.

Air sampling was undertaken at fifteen sites (“Set 1” and “Set 3” sites) as shown in Figure 4-1. Atmospheric deposition sampling was carried out at eight sites (selected “Set 1” and Set 2” sites) as shown in Figure 4-1. Build-up sampling was carried out at “Set 3” sites and there are 11 sites in this set as shown in Table 4-1. The four “Set 2” sites were also included in the “Set 3” sites. Two air samples were collected at each sampling location covering weekdays and weekends. Multiple atmospheric deposition samples were collected at each site to cover the variability of deposition with antecedent dry period. Build-up samples were collected after 7 antecedent dry days at each site. Further details on the sampling are given in Chapter 5.

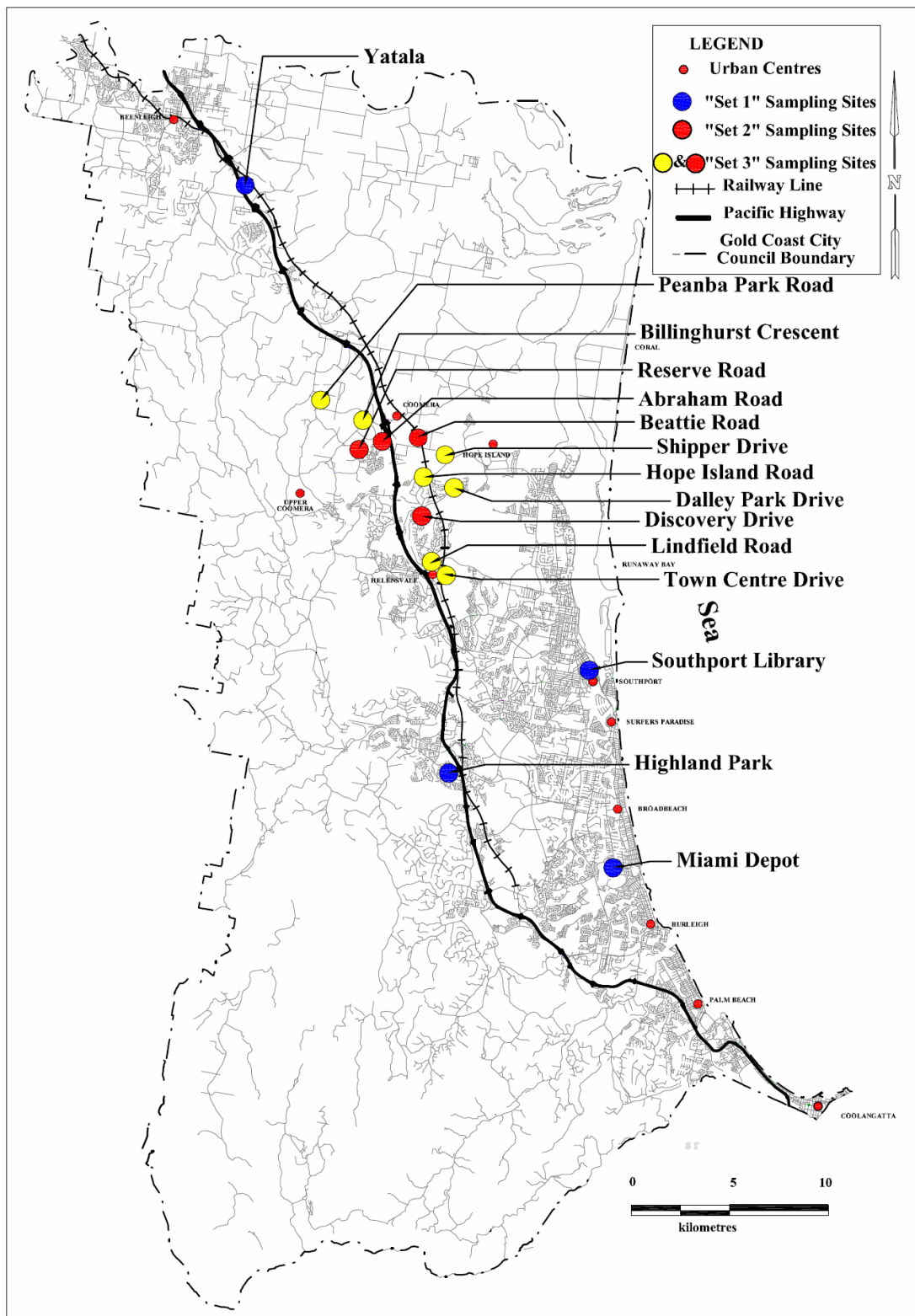


Figure 4-1: Location of study sites in the Gold Coast

4.3 Summary

This Chapter primarily discussed the details of the sites selected for field investigations and their characteristics. Study site were selected within the Gold Coast City Council area. Altogether 15 study sites were selected for investigations. Among the fifteen sites, eleven sites are typical urban road sites and four sites are in proximity to urban amenities where the intensity of anthropogenic activities is high. Road sites were selected so that they cover the typical spectrum of traffic data within Gold Coast area. The Chapter also presents the locations of the selected study sites along with clusters of sites used for specific field investigations.

Chapter 5 - Sample Collection and Testing

5.1 Background

Sample collection methodology was formulated to obtain the requisite data to undertake the envisaged program of research. Consequently, field investigations were carried out to collect target pollutants present in the atmospheric and the ground phases. The key traffic characteristics considered in this research were average annual daily traffic (AADT) and traffic volume (V) over capacity (C) factor, which is an indicator of traffic congestion. The target pollutants were polycyclic aromatic hydrocarbons (PAHs), heavy metals (HMs) and total suspended particulate matter (TSP) and solids. Primarily, US Environmental Protection Agency test methodologies were adopted for sample collection and testing, as they are specifically designed for sampling of PAHs, HMs and PM in outdoor conditions. Additionally, these methodologies are widely used for environmental sampling studies in Australia.

Sample collection and testing was one of the key steps in this research study as all the consequent steps depend entirely on the accuracy of these tasks. Therefore, in order to collect traffic generated pollutants in the atmospheric and ground phases, the field sampling programme was specifically designed to collect PAHs, HMs and PM present in these two phases. Sampling equipment selection is discussed in Chapter 4. Air sampling was undertaken to determine the instantaneous concentrations of PAHs, HMs and PM in the atmospheric phase. Build-up sampling was undertaken to collect solids accumulated over a period of 7 days. In addition, bulk and dry deposition sampling was undertaken to collect atmospheric deposition samples for 3, 4, 5, 6 and 7 antecedent dry days. This Chapter discusses, air sampling, build-up sampling, and atmospheric deposition sampling together with sample collection, preservation, preparation and analytical testing.

5.2 Air Sampling

As noted in Section 3.3.1, high volume air sampling equipment was used for air sampling. Atmospheric pollutant build-up is a dynamic process and influenced by a number of factors. The dominant factors are, temperature, wind, relative humidity, atmospheric pressure, sampling day and antecedent dry period (Violante et al. 2006). Based on the hypothesis that the day of the week influences atmospheric pollutant build-up, air sampling was carried out covering both weekdays and weekends. The relevant meteorological parameters were collected for the sampling period from the meteorological station located at Gold Coast seaway maintained by the Bureau of Meteorology.

Before field sampling, the air sampler was calibrated for ambient pressure and temperature. For the calibration, a 16 mm diameter calibrated orifice plate was placed on top of the instrument and then a U-tube manometer was fixed to the orifice plate (ECOTECH 2005). The calibration set up used is illustrated in Figure 5-1. The pressure drop across the orifice plate for any flow-rate within the range of the sampler is proportional to the square of volumetric flow rate and ambient pressure and inversely proportional to the ambient temperature as give in Equation (1).

$$(\Delta H) = \left(\frac{Q_{DISPLAY}}{C} \right)^2 \frac{P_a}{T_a} \dots\dots\dots(1)$$

Where

ΔH the difference in the water level in the two manometer tubes (mm of H₂O)

$Q_{DISPLAY}$ the volumetric flow-rate reading on the air sampler digital display (m³/hour)

P_a the ambient pressure (in kPa)

T_a the ambient temperature (in degrees Kelvin)

C orifice constant which is equal to 1.028 (for the orifice plate being used)

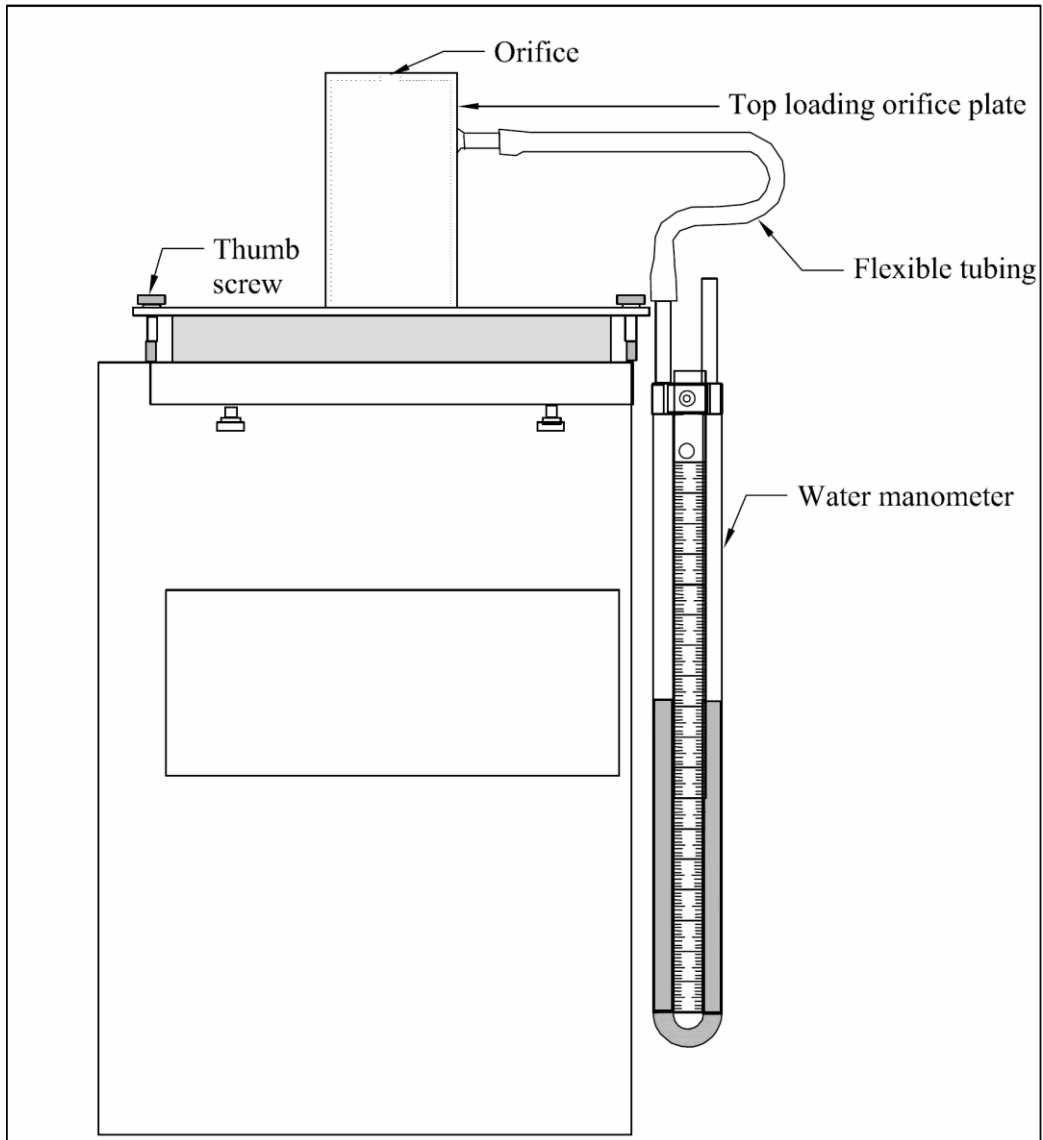


Figure 5-1: Calibration set up
(Adapted from ECOTECH 2005)

Table 5-1 shows the data required for the calibration of air sampler. Readings 1, 2, 3 and 4 need to be selected from the table provided with the instrument depending of the ambient temperature and pressure.

Table 5-1: Data required for calibration

Flow rate (m ³ /hr)	ΔH mm H ₂ O
5	reading 1
10	reading 2
15	reading 3
20	reading 4

The calibration procedure can be explained in five steps as follows:

1. Ambient temperature and barometric pressure was measured;
2. Sampler was fixed with calibrated standard orifice plate as shown in Figure; 5-1
3. The sampler was started and the flow rate set to 5 m³/hr;
4. The motor speed was adjusted until the manometer read the corresponding pressure drop (calculated as given in Table 5-1); and
5. Time was allowed for the signal to stabilise and “lock-in” the point.

The same procedure was followed for 10 m³/hr, 15 m³/hr and 20 m³/hr flow rates. Regular flow rate calibration was carried out in the field as part of the quality assurance procedure.

As atmospheric concentrations of PAHs, HMs and PM are highly dependent on the temperature, relative humidity, wind speed and other atmospheric disturbances, it was decided to undertake sampling for these three parameters concurrently. Also, as the concentration of PAHs and HMs are quite high in the urban atmosphere, it was decided to collect a lower volume than the 300 m³ specified in TO-13A (USEPA 1999). The sampling volume recommended by USEPA IP-7 (30 m³) was initially selected for the testing of all three parameters. However, target PAHs were below the detection limit. Therefore, the sampling volume was subsequently increased to 120 m³ which enabled almost all of the targets PAHs to be detected. As recommended by ECOTECH (2005), the sampling flow rate was set at 15 m³/hr, and 8 hr sampling was carried out covering morning and evening traffic emission peaks to collect 120 m³ air samples (see Figure 5-2).



Figure 5-2: Air sampling, (a): placement of the sampler, (b): key components, (c): placement of generator with reference to sampler

Oven dried quartz filter papers and pre-extracted PUFs were used for sample collection. Pre-extracted PUFs were spiked with field surrogate standards before being used for sample collection. This was to monitor unusual matrix effects and sample recovery. After setting up of PUF and filter paper in the sampling equipment, it was programmed for an 8 hr sampling period.

5.3 Build-up sampling

Road surface pollutant build-up is a dynamic process, which is influenced by a range of parameters (Egodawatta 2007; Sartor and Boyd 1972). Key parameters are traffic

volume, traffic congestion, antecedent dry period and dominant land use. However, a constant seven day antecedent dry period was adopted as Egodawatta (2007) noted that road surface pollutant build-up rate increases rapidly and then asymptotes to an almost constant value after seven days. The selected road sites consisted of typical bitumen surfaces.

Plots of size 2.0 m length x 1.5 m width was selected for build-up sampling at all the 11 study areas. A small plot was selected to minimise the spatial heterogeneity of pollutant build-up on the road surfaces (Herngren 2005). Firstly, the selected plots were cleaned by wet and dry vacuuming and clearly demarcated for later identification. Pollutants deposition was allowed to take place on the pre-cleaned plots over a dry period of seven days. In the event of rainfall during this period, the procedure was repeated until a seven day dry period was achieved. At the end of the seven day dry period, the boundary of the sampling plot was demarcated using an aluminium frame and the pollutant build-up samples were collected by wet and dry vacuuming technique discussed in Chapter 4.

The sample retained in the filtration compartment of vacuum system was transferred to a polyethylene container and all the hoses and the compartments of the vacuum system were completely washed with deionised water and transferred to the same container. Cleaning of the vacuum system and sample transport and storage was carried out as per quality control procedures outlined in AS/NZS 5667:1 (AS/NZS 1998).

5.4 Atmospheric deposition sampling

Atmospheric deposition sampling was carried out at the selected eight study areas as discussed in Section 3.3.2 of Chapter 3. Additionally, their spatial coordinates and corresponding suburbs are listed in Table 5-2. In order to minimise disturbance to traffic and pedestrians, sampling equipment were fixed to existing sign posts which were located in between the road edge and pedestrian path as shown in Figure 5-3 (arrangement-a). Where there was no suitable sign post to fix the samplers, the equipment was fixed to a star picket and installed as shown in Figure 5-4 (arrangement-b).

Table 5-2: Selected roads for atmospheric deposition sampling

No	Suburb	Site name
1	Helensvale	Discovery Drive
2	Coomera	Abraham Road
3	Coomera	Beattie Road
4	Coomera	Reserve Road
5	Beenleigh	Yatala (Department of main road office)
6	South Port	South Port Library
7	Miami	Miami GCCC Depot (No.80, Pacific Avenue)
8	Highland Park	Jabiluka Drive (No. 30)



Figure 5-3: Fixing arrangement-a



Figure 5-4: Fixing arrangement-b

5.4.1 Dry deposition sampling

Dry deposition sampling apparatus were installed in the field immediately after a rainfall event, as the atmospheric pollutant load is minimal at that stage (Ravindra et al. 2003). Samples were collected at close interval at the beginning to capture the variation in pollutant build-up in the atmosphere. The selected sampling periods were 3, 4, 5, 6, and 7 days after a rainfall event. The procedure was repeated if it rained in between sampling times. After collecting a sample, acid washed bottles and funnels were replaced in the apparatus to be used for the next sampling event.

5.4.2 Bulk deposition sampling

As it is not possible to measure only wet deposition, total deposition (bulk) was collected. The sampling apparatus were installed immediately after a rainfall event. Total deposition samples were collected immediately after the next rainfall event. Consequently, a rainfall event was sampled together with dry deposition for the intervening period. The total sampling period for each event was dependent on the time between two consecutive rainfall events. Three rainfall events were sampled at each location in order to calculate the average bulk deposition at each location.

Sample type and number of samples collected from each sampling episode is summarised in Table 5-3.

Table 5-3: Total number of samples collected

No	Site Name	Number of Samples Collected				
		Air		Deposition		Build up
		Weekdays	Weekends	Dry	Bulk	
1	Abraham Road	1	1	5	3	1
2	Reserve Road	1	1	5	3	1
3	Peanba Park road	1	1			1
4	Billinghurst Cres	1	1			1
5	Beattie Road	1	1	5	3	1
6	Shipper Drive	1	1			1
7	Hope Island Road	1	1			1
8	Lindfield Road	1	1			1
9	Town Centre Drive	1	1			1
10	Dalley Park Drive	1	1			1
11	Discovery Drive	1	1	5	3	1
12	Southport Library	1	1	5	3	
13	Miami Depot	1	1	5	3	
14	Highland Park	1	1	5	3	
15	Yatala	1	1	5	3	

5.5 Sample Preservation and Transport

Sample collection and testing was done according to the test methodologies listed in Table 5-4. Samples were transported to the laboratory and preserved as per quality control procedures outlined in AS/NZS 5667:1 (AS/NZS 1998).

Table 5-4: Methods adopted for sample testing

Parameters	Methods	References	Comments
PAHs in Air	USEPA TO-13A and USEPA IP-7	USEPA (1999), USEPA (1989)	16 USEPA priority PAH species (see Table 5-5). Analysis by Gas Chromatograph – Mass Spectrometer (GC-MS)
PAHs in Build-up	USEPA 610	USEPA (1991a)	As above
HMs in Air	USEPA IO-2.1, IO-3.1, and IO-3.5	USEPA (1999)	Zn, Cu, Pb, Mn, Cd, Cr, Ni. Analysis was conducted by Inductively Coupled Plasma-Mass Spectrometry (ICP-MS).
HMs in Build-up	USEPA 200.8	USEPA (1991b)	As above
PM in Air	USEPA IO-2.1	USEPA (1999)	Total suspended particulate matter (TSP).
TSS/TDS	APHA 2540C and 2540D	APHA (2004)	Build-up and atmospheric deposition sampling
TOC/DOC	APHA 5310C	APHA (2004)	As above
pH	APHA 4500-HB	APHA (2004)	For build-up samples
EC	APHA 2510B	APHA (2004)	For build-up samples

5.5.1 Air sample preservation and transport

After 8 hr sampling, the filter paper and polyurethane foam (PUF) were removed from the sampler and wrapped with an aluminium foil and placed in zipped polyethylene bags and sealed. PUF and filter paper were kept separate so that there was no contamination of samples during transport and handling. The samples were labelled including information regarding the date, location, sample number, sampling time, temperature. Immediately after transporting PUFs and filter papers to the laboratory, they were stored at 4 °C till they were analysed. Sample collection and handling was carried out as per procedures outlined in AS/NZS 5667:1 (AS/NZS 1998) and laboratory testing was carried out as per test Method TO-13A (USEPA 1999).

5.5.2 Atmospheric deposition sample preservation and transport

Atmospheric deposition samples were collected in acid washed 500 mL high-density polyethylene bottles. Prior to installation, bottles were labelled with information such as sampling site, sampling duration, date, time, type of sample (bulk or dry). The

funnels and bottles with the sample were washed with deionised water in order to transfer samples to polyethylene bottles (300 mL for dry deposition samples and 50 mL for bulk deposition). Samples were filtered with a plastic tea strainer to remove insects collected before being transferred into polyethylene bottles. The samples were transported to the laboratory and stored at 4 °C temperature until the analysis was carried out.

5.5.3 Build-up sample preservation and transport

After labelling the collected build-up samples, they were transported to the laboratory on the same day. Subsequently, wet sieving was carried out using a set of 300 µm, 150 µm, 75 µm sieves to prepare sub-samples for the laboratory analysis. The filtrate passing through 75 µm sieve was further filtered using a 1 µm glass microfibre filter paper to obtain the <1 µm fraction. The following particulate fractions were stored in a refrigerator at 4 °C until they were analysed:

- >300 µm;
- 150-300 µm;
- 75-150 µm;
- 1-75 µm; and
- <1 µm.

5.6 Laboratory Testing

As noted in Chapter 2, PAHs, HMs are mainly generated by traffic sources (Herngren 2005; Lim et al. 2005). Additionally, Lim et al. (2005) noted that PAHs and HMs are highly associated with total suspended particulate matter (TSP). Consequently, laboratory testing primarily focused on PAHs, HMs and PM. Additionally, physio-chemical parameters such as pH, PSD, TOC, DOC, TSS TDS were also tested as these parameters influence the adsorption of PAHs and HMs to particulates (Preciado and Li 2006; WDT 2007; Barrett et al. 1995). Laboratory testing was carried out as per procedures given in the relevant test methods listed in Table 5-4.

Appropriate quality control procedures were followed to verify the accuracy of testing as discussed under the Section 3.6. The samples were analysed within the possible maximum preservation time as specified in corresponding test methods. For example, PAHs were extracted within 7 days of sampling and analysed within 40 days of extraction as specified.

5.7.1 TSP testing

The test Method IO-2.1 (USEPA 1999) defines atmospheric total suspended particulate matter (TSP) as airborne solid particles with particle sizes ranging from 0.01 to 100 μm . Sampling and testing of TSP was carried out as per Method IO-2.1, IO-3.1, and IO-3.5 (USEPA 1999). Prior to sampling, quartz filter papers were pre-conditioned by baking and weighing at room temperature. This was to remove any traces of PAHs. Subsequently, quartz filter papers were set up in the high-volume sampler. Air sampling was conducted by drawing air through quartz filter paper. In this process, atmospheric particulates are collected on the filter paper surface. After the samples were collected, the filter papers were weighed again under the same conditions to determine the total suspended atmospheric particulate matter (TSP) load. As the instrument flow rate indicator was calibrated against a reference orifice plate, actual sampling volume was directly read from the machine. By using total sampling volume, concentration of atmospheric TSP load was calculated.

5.7.2 HMs testing

As per Method 200.8 (USEPA 1994), nitric and hydrochloric acid digestion was carried out to extract total recoverable heavy metals from the build-up, atmospheric deposition and air samples. Hot Block digester shown in Figure 5-5 was used for the digestion. Hot Block digester provides an efficient method for digesting water, wastewater, soil and sludge samples for metals analysis (Environmental Express 2005). This digestion system allows samples to be digested in a small area with minimum heat loss. Samples were digested at 95 °C for 2.5 hr without boiling, inside a fume cupboard. After allowing samples to reach room temperature, the samples were made up to the original volume. Subsequently, samples were filtered using 0.45-micron syringe filters followed by adding internal standards including the

blanks and certified reference material (CRM). Samples were analysed for the following heavy metals:

- Lead (Pb);
- Zinc (Zn);
- Cadmium (Cd);
- Chromium (Cr);
- Nickel(Ni);
- Manganese (Mn); and
- Copper (Cu).

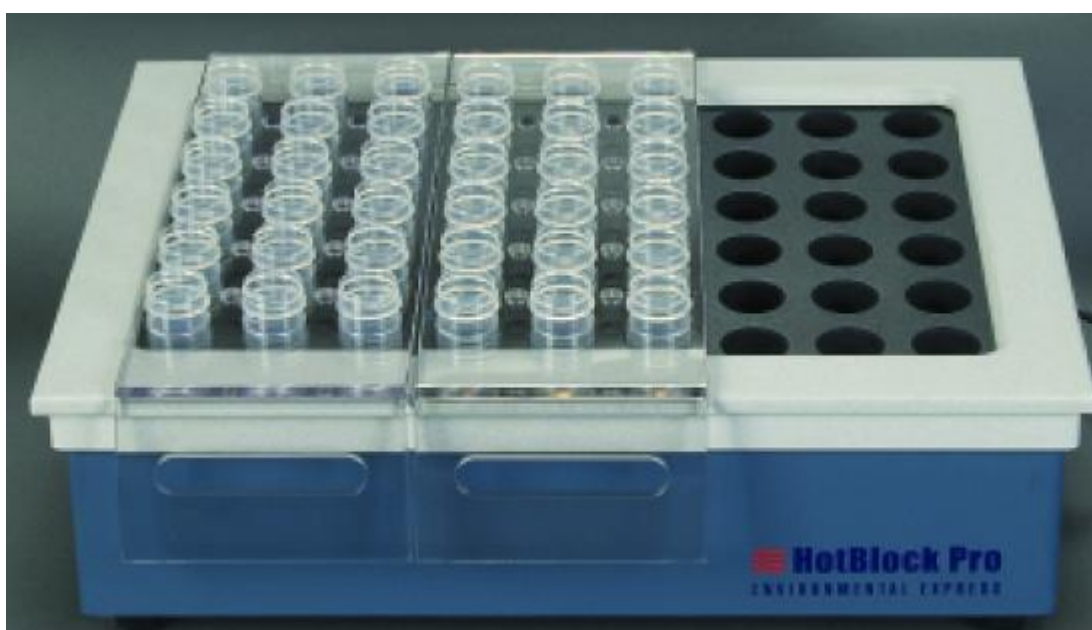


Figure 5-5: Hot block digester

Detection and determination of heavy metals were carried out by Inductively Coupled Plasma Mass Spectrometer (ICP-MS). The instrument is shown in Figure 5-6. ICP-MS was selected by considering its ability to detect heavy metals even at low concentrations (ranged from 0.001 to 0.005mg/L). Firstly, the instrument was tuned by testing a specially made solution prepared by mixing beryllium, magnesium, cobalt, indium and lead stock solutions in 1% nitric acid to produce a concentration of 100 µg/L of each element as per Method 200.8 (USEPA 1994). This solution is referred to as a tuning solution. Tuning solution was used to determine acceptable instrument performance prior to calibration and sample analysis. After satisfactory tuning, sample sequence including calibration standards were prepared.

Consequently, samples in the liquid matrix were introduced into the machine by pneumatic nebulization into radio frequency plasma where energy transfer processes cause atomization and ionization. The ions were extracted from the plasma through a differentially pumped vacuum interface and separated based on their mass to charge ratio by a quadrupole mass spectrometer. The ions transmitted through the quadrupole were detected by an electron multiplier.

After the sample sequence was tested along with calibration standards, calibration curves were set up and ensured that the residual mean square (R^2) was greater than or equal to 0.98. The concentration of the target heavy metals in actual samples were calculated using already established calibration curves. Consequently, certified reference material (CRM) recovery was compared against values given in standard certificate and was found to be within 85% to 115% which was considered acceptable. This was one of the most important quality assurance checks. For air samples, only half of the filter papers was analysed for heavy metals and the other half was analysed for PAHs.



Figure 5-6: ICP-MS

5.7.3 PAHs testing

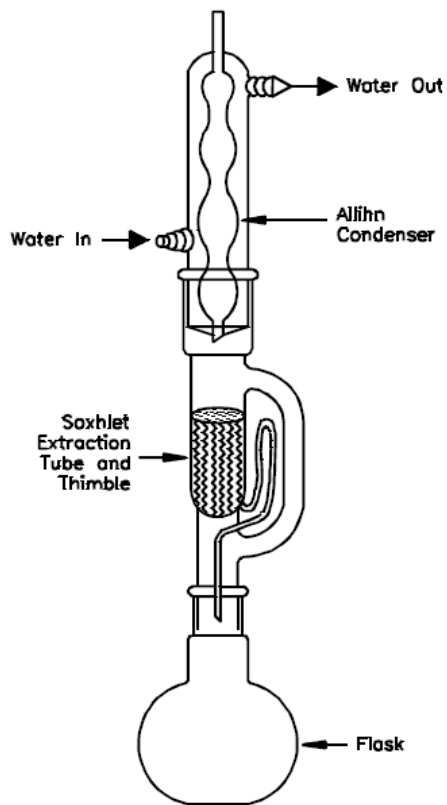
PAHs were also a primary group of pollutants investigated in this project. Both, air and build-up samples were tested for PAHs present. Analysis was carried out as per Method TO-13A and Method 610 (USEPA 1999). The target 16 priority PAHs identified by USEPA are given in Table 5-5.

**Table 5-5: Target polycyclic aromatic hydrocarbons
(Adapted from Herngren, 2005 and TO-13A of US EPA 1999)**

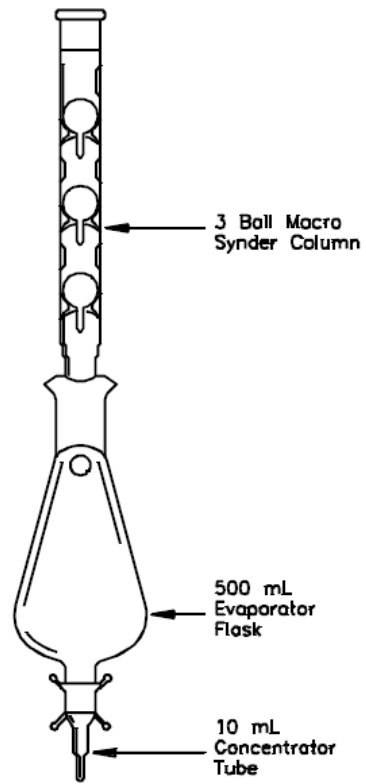
No	PAH compound	Formula	Molecular weight(g/mol)	Water Solubility (mg/L)	Boiling point °C
1	Naphthalene	$C_{10}H_8$	128.18	32	218
2	Acenaphthene	$C_{12}H_{10}$	154.20	3.4	278-279
3	Acenaphthylene	$C_{12}H_8$	152.20	3.93	265-280
4	Flourene,	$C_{13}H_{10}$	166.23	1.9	293-295
5	Anthracene	$C_{14}H_{10}$	178.24	0.05-0.07	340
6	Phenanthrene	$C_{14}H_{10}$	178.24	1.0-1.3	339-340
7	Fluoranthene	$C_{16}H_{10}$	202.26	0.26	375-393
8	Benzo(a)anthracene	$C_{18}H_{12}$	228.30	0.01	435
9	Benzo(b)fluoranthene	$C_{20}H_{12}$	252.32	-	481
10	Benzo(k)fluoranthene	$C_{20}H_{12}$	252.32	-	480-471
11	Chrysene	$C_{18}H_{12}$	228.30	0.002	441-448
12	Pyrene	$C_{16}H_{10}$	202.26	0.14	360-404
13	Benzo(a)pyrene	$C_{20}H_{12}$	252.32	0.0038	493-496
14	Dibenzo(a,h)anthracene	$C_{22}H_{14}$	278.35	0.0005	524
15	Benzo(ghi)perylene	$C_{22}H_{12}$	276.34	0.00026	525
16	Indeno(1,2,3-cd)pyrene	$C_{22}H_{12}$	276.34	-	536

a) Air sample testing

While particulate bound PAHs were collected using a filter paper, gas phase PAHs were collected using PUF sorbents. PUF sorbents and quartz filter papers were tested separately to determine the gas and particulate phase PAHs in the atmosphere as per TO-13A (USEPA 1999). The initial step was to extract from half of the filter paper and PUF sorbent by Soxhlet extraction with 10% diethyl ether in hexane solvent. Before extracting, laboratory surrogate standards were added. The extract was concentrated by Kuderna-Danish (K-D) evaporator (see Figure 5-7), followed by sodium sulphate cleanup using column chromatography to remove potential interferences prior to analysis by GC-MS. The sample was further concentrated by N₂ blow-down and then analysed by GC-MS (see Figure 5-8). Prior to testing, internal standards were added to the samples, blanks and CRM.



(a) Soxhlet Extraction Apparatus with Allihn Condenser



(b) Kuderna-Danish (K-D) Evaporator with Macro Synder Column

Figure 5-7: Apparatus used for extraction
(Adapted from USEPA 1999)

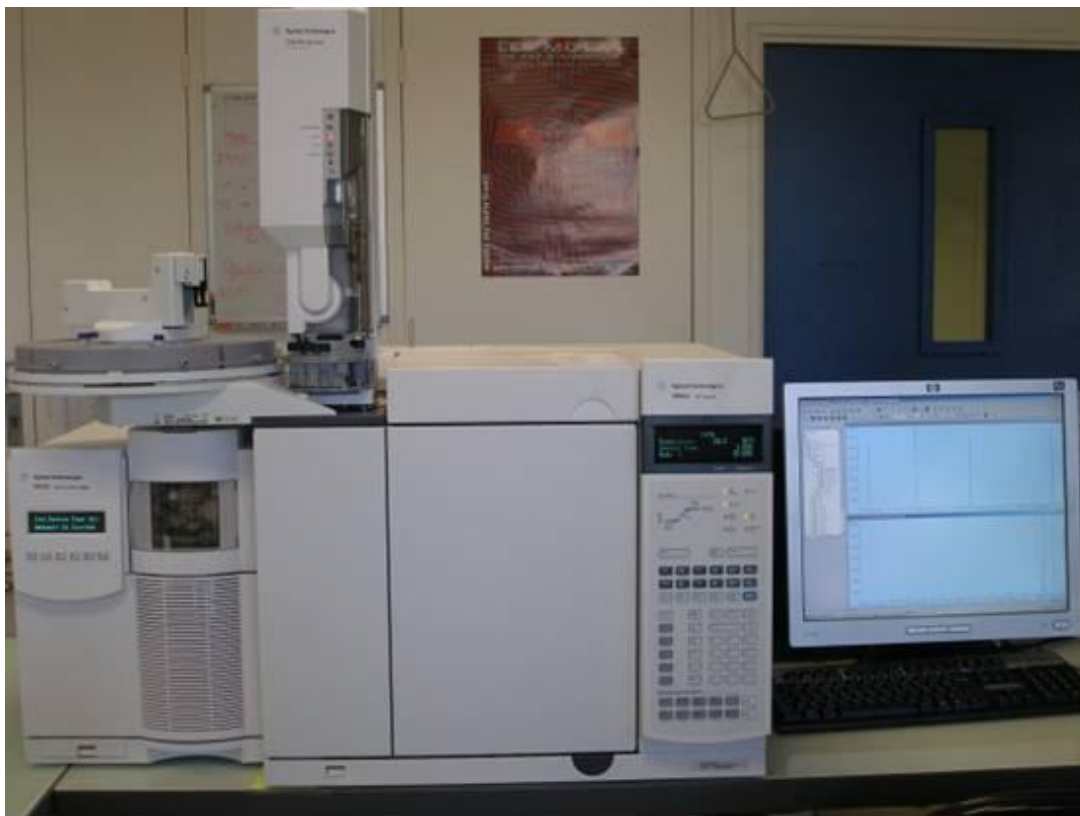


Figure 5-8: GC-MS

Method development was to detect all target PAHs with a uniquely identifiable peak in the chromatogram. It was found that temperature programming was one of the most important methods to achieve good separation of PAHs. Additionally, injection volume, flow rate of carrier gas, detection mode and its resolution were changed until optimum separation was achieved. The separation of 16 PAHs was a difficult exercise, as there are some PAHs, which has the same molecular weight but different configurations and almost the same boiling points. However, after a number of trial runs, the test method was developed to the required level of accuracy so that all the target PAH compounds were separated.

As solvents used had traces of Naphthalene, it was not analysed. Also, Benzo(b)fluoranthene was not analysed as it was not present in the standards used. Therefore, only 14 USEPA priority PAHs were detected and quantified. Calibration was carried out with five concentration levels by diluting external standards. As recommended by the GC-MS user manual, standards were tested initially. Then samples were tested using already developed and calibrated test method. Subsequently, sample concentrations were calculated using data analysis software available with the GC-MS. As a part of the quality assurance procedure, CRM recovery was compared against values given in standard certificate and found to be within 85% to 115% as specified.

b) Road surface build-up sample testing

Road surface build-up samples were tested to determine the PAHs present in the ground phase. The Method 610 (USEPA 1999) was adopted to test build-up samples for PAHs which is the method recommended for organic chemical analysis for municipal and industrial wastewaters. The testing procedure was similar to that of air sample testing. However, instead of Soxhlet extraction, liquid-liquid extraction technique was used to extract build-up samples as specified in the test Method 610 (USEPA 1999). Hengren (2005) found that this is an efficient technique to extract PAHs in the liquid matrix. All the other steps were the same as for testing of PAHs in air samples.

The extraction of PAHs was done using a 500 mL separatory funnel. As specified, a 100 mL aliquot from each sample was extracted with a 60 mL of extraction solvent. The sample aliquot was mixed with solvent in the separatory funnel for 2 minutes with periodic venting to release excess pressure. The separatory funnel was then kept for 10 minutes without disturbing so that the organic layer was separated. Subsequently, the organic layer was separated to a beaker by carefully regulating the bottom valve. The same sample was extracted three times with 60 mL of extraction solvent as described above.

5.7.4 pH and EC testing

Testing of pH and electrical conductivity (EC) was conducted as per procedures given in standard methods 4500-HB (APHA 2004) and 2510B (APHA 2004), respectively. Immediately after the sample was transported to the laboratory, build-up sample volume was corrected to 8 L and then pH and EC were analysed. Volume standardisation is to compare parameters such as pH and EC. Despite the fact that the initial pH and EC of deionised water have an influence on the measurements, the variation was not significant. The pH of deionised water range from 7.6 to 7.0 and EC varied from 2 to 10 μ S. Therefore, it was assumed that the measured values could be reasonably used as actual pH and EC of the samples.

5.7.5 Particle size distribution (PSD)

Malvern Mastersizer S instrument (see Figure 5-9) was selected for this analysis, based on ease of use and accuracy. This instrument is capable of analysing particles in the range of 0.05-900 μ m diameter range (Malvern-Instrument-Ltd 1997). The accuracy of the measurement is \pm 2% of the volume mean diameter.

The particle size distribution measured by Malvern Mastersizer S instrument is based on the Fraunhofer model (Malvern-Instrument-Ltd 1997). This model can predict the scatter pattern created when a solid opaque disc of a known size is passed through a laser beam. The laser beam creates a scatter pattern for a flow of particles. Then, it determines the size of particles using a Reverse Fourier lens from the scatter pattern of the laser beam.

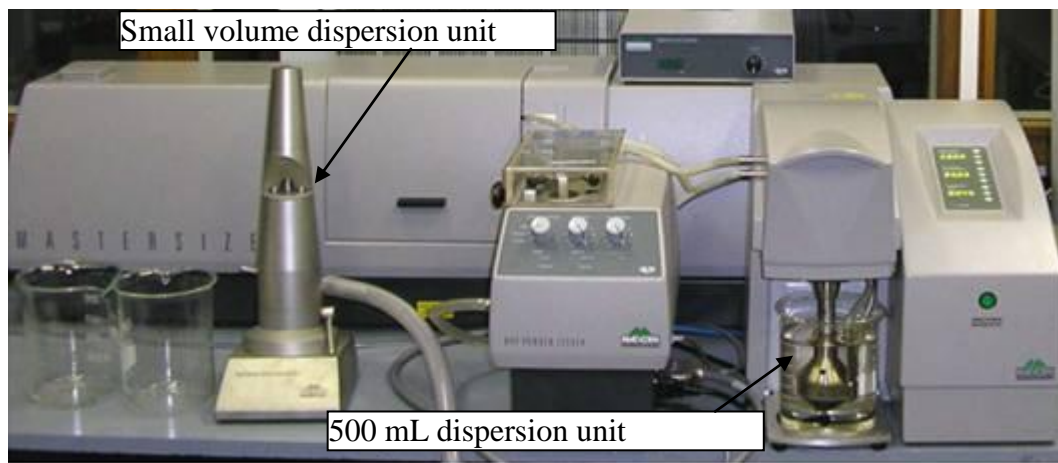


Figure 5-9: Malvern Mastersizer S

There are two sample dispersion units in Malvern Mastersizer S instrument as illustrated in Figure 5-9. While the small volume dispersion unit is recommended for 100 mL small samples, the other unit requires at least 500 mL to determine particle size distribution of a sample. In this study, build-up samples were analysed using 500 mL sample deposition unit whereas atmospheric deposition samples were analysed using the small volume dispersion unit. Specialised software provided with the instrument was used to convert the optical signal to percentage particle size distribution. There are two important concepts, which need to be understood to interpret the results. They are:

1. The results are volume based; and
2. The results are expressed in terms of equivalent spheres.

(Malvern-Instrument-Ltd 1997).

5.7.6 Organic carbon

Total organic carbon (TOC) is the total amount of carbon bound in an organic compound. Dissolved organic carbon (DOC) is the organic carbon remaining after filtering a sample using a 0.45 μm filter. TOC and DOC were measured using Shimadzu TOC-VCSH Total Organic Carbon Analyser (see Figure 5-10) according to method 5310C (APHA 2004). This instrument is capable of measuring organic carbon content in the range of 4 $\mu\text{g/L}$ - 25000 $\mu\text{g/L}$. As specified by APHA (2004), the original sample was analysed to determine TOC and, after filtering using a 0.45 μm syringe filter, the filtrate was tested to determine DOC.



Figure 5-10: Shimadzu TOC-VCSH Total Organic Carbon Analyser

5.7.7 Total suspended solids and total dissolved solids

Total suspended solids (TSS) concentration was analysed by measuring the dry weight retained on a 0.45 μm pore size nitrocellulose filter paper. The filter papers were pre-washed and oven dried to 103 $^{\circ}\text{C}$ -105 $^{\circ}\text{C}$ for 1 hr to remove any traces of solids present and then pre-weighed as specified in method 2540D (APHA 2004). A 100 mL volume was filtered and the filter paper with the residue was oven dried at 103 $^{\circ}\text{C}$ -105 $^{\circ}\text{C}$ for 1 hr and weighed. TSS was determined by subtracting the blank filter paper weight from the final weight with the residue.

Total dissolved solids (TDS) concentration was determined by measuring the dry weight after evaporating a 50 mL water sample. Pre-washed, pre-weighed Petri dishes were used to evaporate the filtrate. The filtrate was evaporated for 1 hr at 180 $^{\circ}\text{C}$ as specified in method 2540C (APHA 2004). Dry weight was determined by subtracting the empty Petri dish weight from the final weight.

5.7 Summary

Air, atmospheric deposition and build-up sampling were conducted at selected study sites. The Chapter discusses the procedures adopted for sample collection, preservation and testing together with the sampling apparatus used. Appropriate

analytical methods were adopted to test target pollutants such as PAHs, HMs and TSP and relevant water quality parameters such as pH, EC, PSD, TOC, DOC, TSS and TDS. Special attention was paid to incorporate quality control procedures specified in test methodologies.

Three types of sampling procedures were followed to collect air, atmospheric deposition and build-up samples. The important factors considered in sampling were antecedent dry period and sampling day of the week (weekday, weekend).

Chapter 6 - Analysis of Air Samples

6.1 Background

Stormwater pollution is a phenomenon, which occurs as a result of a range of pollutant processes and pathways. The pollutant processes and pathways include, atmospheric pollutant processes, atmospheric deposition, pollutant build-up on catchment surfaces and pollutant wash-off. Most of these processes and pathways are interrelated and interdependent. For example, Davis and Birch 2010 and Pereira et al. 2007) noted that a fraction of road deposited pollutants originate as atmospheric deposition. Also, it is commonly accepted that a majority of pollutants in atmospheric deposition are generated by traffic sources (Karar et al. 2006). As confirmed by the critical review of research literature presented in Chapter 2, polycyclic aromatic hydrocarbons (PAHs), heavy metals (HMs) and solids are among the most critical traffic generated pollutants in urban stormwater, which result from atmospheric accumulation and subsequent deposition. Therefore, a greater understanding of the accumulation and distribution patterns of these three groups of pollutants in the atmospheric phase is essential in order to minimise stormwater pollution.

Data required to develop a detailed understanding of atmospheric pollutant processes was obtained using the air sampling methodology outlined in Chapter 5. This Chapter details the outcomes of the air sample analysis. Analysis undertaken provides essential background information required for the investigation of wet and dry deposition and pollutant build-up. Analysis of atmospheric deposition and pollutant build-up are discussed in Chapter 7 and Chapter 8 respectively.

6.2 Air sampling sites

As detailed in Chapter 4, air sampling was conducted at two sets of study sites. The first set of sites were selected from areas where the intensity of anthropogenic activities is high (referred to as “Set 1”) and consisted of four locations. Locations of these sites and their dominant anthropogenic activities are listed in Table 6-1. The second set consisted of 11 typical suburban road sites (referred to as “Set 3”) selected

primarily based on their variability in traffic and land use characteristics. Locations of these sites and their traffic data are listed in Table 6-2. Further details of the study sites and sampling techniques are included in Chapter 4. The sample collection and testing was conducted as detailed in Chapter 5.

Table 6-1: “Set 1” sites

Site name	Anthropogenic activities
Southport Library (So)	Traffic, commercial, residential and industrial activities
Miami Depot (Mi)	Traffic, commercial, residential and industrial activities
Highland Park (Hi)	Traffic and residential activities
Yatala (Ya)	Traffic and industrial activities

Table 6-2: “Set 3” sites

No	Road	Land use	ADT_to		ADT_hv	
			Weekday	Weekend	Weekday	Weekend
1	Abraham Road (Ab)	Commercial	9976	6273	439	102
2	Beattie Road (Be)	Industrial	5988	1924	180	35
3	Billinghurst Crest (Bi)	Residential	2459	973	397	43
4	Dalley Park Drive (Da)	Residential	919	1152	376	248
5	Discovery Drive (Di)	Residential	10803	10463	126	55
6	Hope Island Road (Ho)	Commercial	26904	22925	242	113
7	Lindfield Road (Li)	Commercial	9123	7551	395	165
8	Peanba Park Drive (Pe)	Residential	35	22	6	1
9	Reserve Road (Re)	Residential	11311	7458	604	178
10	Shipper Drive (Sh)	Industrial	2836	1036	1503	775
11	Town Centre Drive (To)	Commercial	6701	4390	34	36

As discussed in Chapter 5, air samples were tested for the following parameters:

- 1) Total suspended particulate matter (TSP)
- 2) Heavy metals (Zn, Cd, Cr, Cu, Mn, Ni, Pb)
- 3) Polycyclic aromatic hydrocarbons (PAHs) (14 of the 16 USEPA identified critical PAHs for the gas and particulate phases)

Data generated from the laboratory analysis was arranged into two matrices based on weekday and weekend sampling. As air sampling was undertaken at 15 sites (“Set 1” plus “Set 3” sites), there are 15 objects in each data matrix. HMs were tested only in the particulate phase as they are not typically present in the gas phase.

6.3 Preliminary data analysis

The analysis detailed in this Chapter is organised in a logical order so that the physical and chemical characteristics of air quality and its variation with traffic and land use parameters can be understood. Firstly, data pre-processing was undertaken to eliminate possible biased outcomes and outliers. Secondly, a graphical analysis of the pre-processed data was undertaken to compare data trends. Additionally, the data set was compared with similar study outcomes given in the literature to ensure that the data set is in similar range as those observed by previous researchers. Thirdly, multivariate data analysis was undertaken to investigate possible relationships between heavy metals, PAHs, traffic and land use parameters included in the data set.

Initially, total suspended particulate matter was subjected to univariate analysis and the analysis was then extended to heavy metals and PAHs. This analysis was done based on the assumption that most of the other pollutant species are associated with total suspended particulate matter in the atmospheric phase. Subsequently, multivariate analysis was undertaken.

6.3.1 Data pre-processing

The dataset arranged in matrices were in the form of concentrations in mg/m^3 , $\mu\text{g/m}^3$ and ng/m^3 for TSP, HMs and PAHs, respectively. The data was pre-processed prior to the analysis. The data pre-processing was as follows:

- 1) Outliers were removed from the matrix prior to the analysis. Outliers were detected using the detection tool available in Sirius 8 software (PRS 2009). This tool isolates objects in one or several projections of score plots as potential outliers. These were then confirmed by checking residual standard deviation (RSD) and leverage. Low RSD and high leverage indicate possible outliers as explained in the software user manual.

- 2) Standardization was conducted by dividing the individual value in each cell by the standard deviation of that column and mean centering was carried out by subtracting the mean value of each column from the individual value in each cell

6.3.2 Analysis of TSP

In order to ensure that the TSP data set is in similar range as those observed by previous researchers, the concentrations detected in this study was compared with previous studies carried out by Mogo et al. (2006) and Pagano et al. (1996). These two studies were selected for comparison as they are among the most recent studies which investigated total atmospheric suspended particulate matter concentration. As TSP concentrations were measured for weekdays and weekends separately, the comparison was also undertaken accordingly.

The data analysis showed that atmospheric total suspended particulate matter concentration varies from $8 \mu\text{m}/\text{m}^3$ to $108 \mu\text{m}/\text{m}^3$ during weekends and $11 \mu\text{m}/\text{m}^3$ to $306 \mu\text{m}/\text{m}^3$ during weekdays. Pagano et al. (1996) noted in a similar study that total suspended particulate matter concentration varied from $35 \mu\text{m}/\text{m}^3$ to $127 \mu\text{m}/\text{m}^3$ in Bologna, Italy. Mogo et al. (2006) found that atmospheric total suspended particulate matter concentration was in the range of 39.86 - $184.88 \mu\text{g}/\text{m}^3$ in Valladolid, Spain. This confirms that TSP concentrations observed in this study is consistent with the previous observations.

In order to understand the variation of atmospheric TSP concentration with the sampling day, TSP concentrations determined for each sampling event were plotted as shown in Figure 6-1.

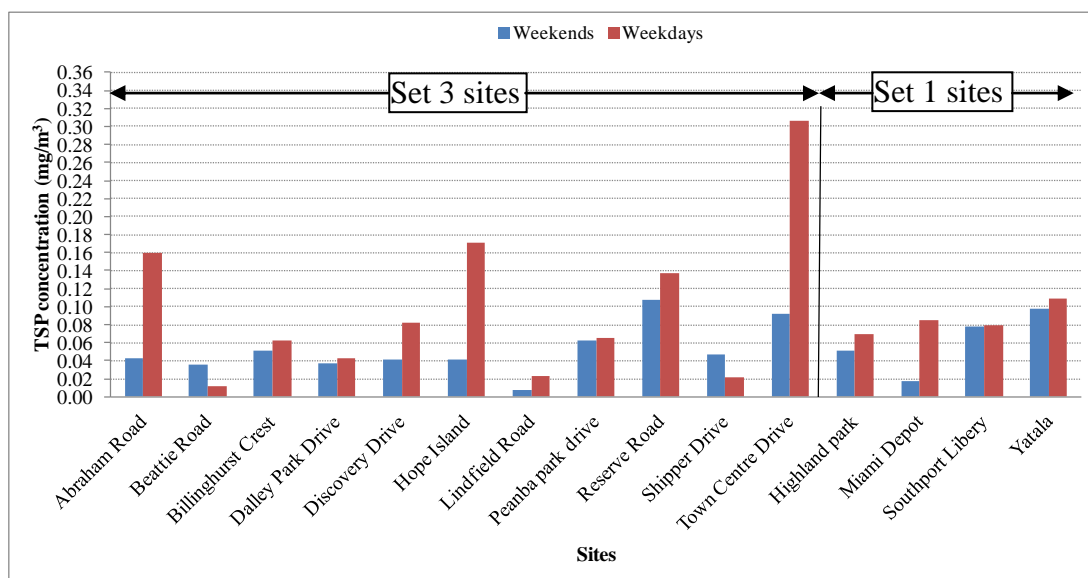


Figure 6-1: TSP concentrations at the study sites

Figure 6-1 shows high TSP concentrations consistently during weekdays compared to weekends, which relates to higher traffic emissions. The higher total suspended particulate matter concentrations detected during weekdays compared to weekends can be attributed to two main reasons: (1) traffic volumes are higher during weekdays compared to weekends resulting in higher emissions to the atmosphere; (2) as traffic volume increases, traffic induced wind can re-suspend already deposited particles (Lonati and Giugliano 2006).

It has been noted in the research literature that traffic is one of the main sources of atmospheric total suspended particulate matter (Lonati and Giugliano 2006; Sharma et al. 2010; Tasdemir and Esen 2007). Also, researchers have developed a conceptual pollutant build-up pattern for the atmosphere (Jolliet et al. 2005). This was explained in Section 2.7.1 However, there is no explicit mathematical relationship established to replicate atmospheric pollutant build-up. It was hypothesised that mathematical relationships can be developed to describe atmospheric build-up of traffic generated pollutants (PAHs, HMs and TSP).

In order to investigate the variation of atmospheric TSP concentration with traffic, TSP concentration determined from each sampling episode was plotted against traffic as shown in Figure 6-2. Weekday and weekend total suspended particulate matter concentrations were plotted separately as shown in Figure 6-2(a) and 6-2(b). It is evident that Town Centre Drive is an outlier for this analysis and it was removed

from the data matrix. TSP concentration at Town Centre Drive was significantly different compared to the rest of the sites especially during weekdays and was postulated to be due to the re-suspension of soil particles from the nearby unpaved car park.

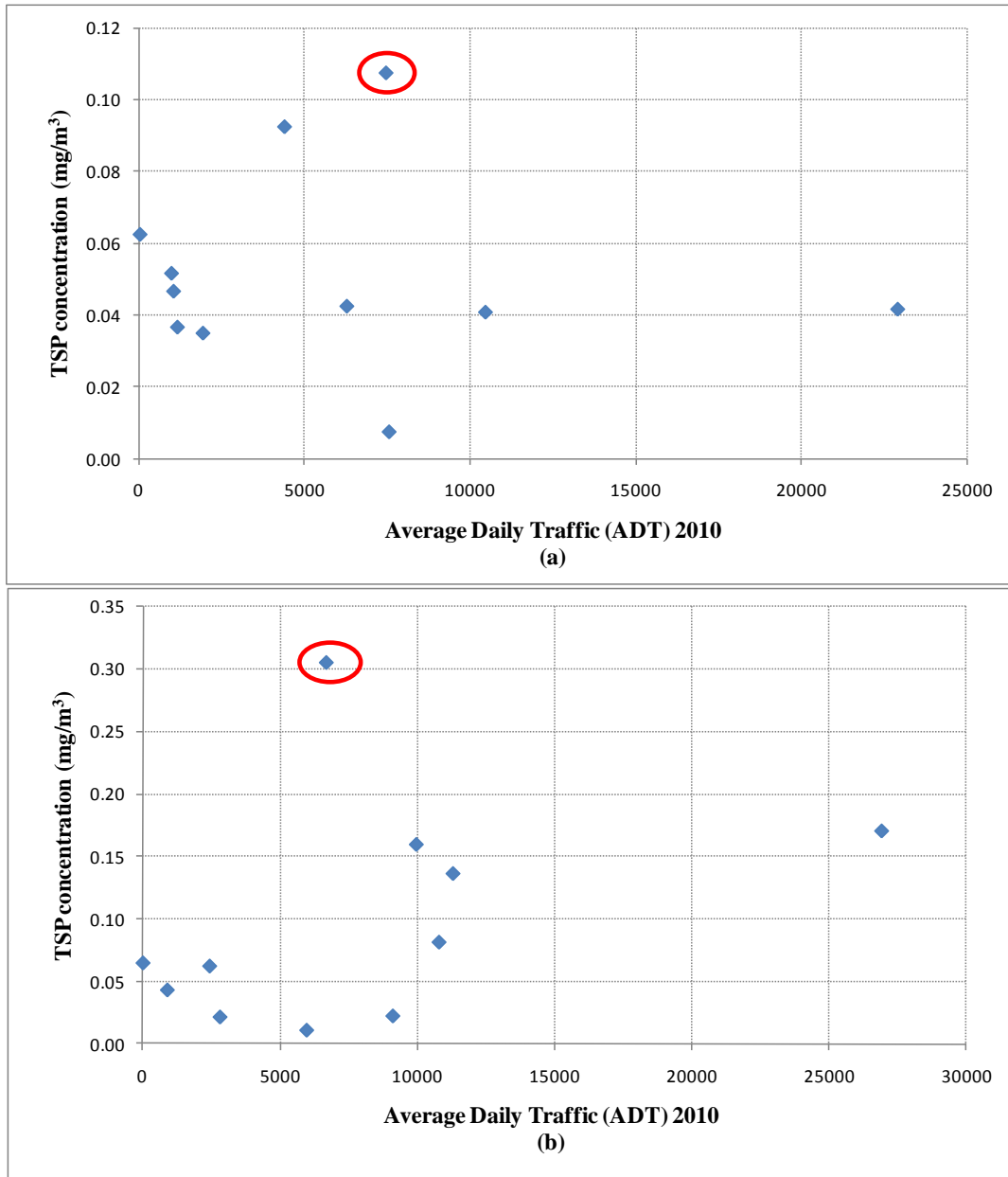


Figure 6-2: Variation of TSP concentration with traffic, (a): for weekend sampling, (b): weekday sampling

Figure 6-2(a) shows scattered data plot of TSP concentration whereas Figure 6-2(b) illustrates an increasing trend in TSP concentration with traffic (ADT). It was found from linear regression analysis that traffic and TSP correlated with regression coefficients (R) of 0.7 and 0.07 for weekdays and weekends, respectively. From this,

it can be concluded that weekday atmospheric TSP concentration is influenced by the traffic volume. This is attributed to the relatively high traffic volume during weekdays compared to weekends as shown in Table 6-2. Therefore, land use related emissions is an important source during weekends. Furthermore, traffic related emissions are influenced not only by traffic volume but also by traffic congestion (V/C) or speed (Tuntawiroon et al. 2006; Levy et al. 2010). Factors influencing TSP on weekends is discussed below.

Air pollutants at a road site can be due to traffic emissions from the road close to the site and pollutants transported from other sources including anthropogenic activities and surrounding roads. During weekdays, emissions close to the sampling sites become dominant. Consequently, a relationship becomes evident. During weekends, other sources become dominant. Hence, a clear relationship with traffic is not evident. Therefore, it can be hypothesised that there are pockets of concentrated total suspended particulate matter close to investigated roads during weekdays due to high traffic volume whereas air quality is more spatially uniform during weekends. Moreover, a majority of heavy duty vehicles, which are a major source of particulate matter, do not operate during weekends (Motallebi et al. 2003). For example, traffic data collected in year 2010 as part of the study indicates that the volumes of class 3 and 4 heavy duty vehicles are much higher during weekdays compared to weekends. Multivariate data analysis was subsequently conducted incorporating the volume of heavy duty traffic (ADT_hv) as a variable to investigate the influence of heavy duty traffic on atmospheric TSP concentration.

As both traffic volume and congestion influences atmospheric pollutant concentration, both parameters were incorporated into the multivariate analysis undertaken. Galindo et al. (2010) noted that wind is an influential factor in ambient TSP concentration as the atmospheric dispersion processes and removal mechanisms depend on wind speed. Consequently, wind speed was also incorporated as a variable in the multivariate data analysis undertaken.

6.3.3 Heavy metals (HMs)

In order to investigate the pathways of traffic generated heavy metals (HMs), seven heavy metal species consisting of Cr, Cd, Ni, Pb, Mn, Zn and Cu were investigated

as discussed in Chapter 4. However, Ni and Cd were not detected at almost all of the sampling sites. Hence, the remaining five elements were incorporated into the analysis. In order to ensure that the HM data set is in similar range as those observed by previous researches prior to analysis, heavy metal (HM) concentrations detected in this study were compared with the past research outcomes as shown in Table 6-3.

Table 6-3: Comparison of airborne heavy metal concentrations

HMs	Concentrations observed in current study		Adapted from Voutsas and Samara (2002)	
	Average (weekdays) (ng/m ³)	Average (weekends) (ng/m ³)	Industrial site Average (ng/m ³)	Urban site Average (ng/m ³)
Cr	24	13	NA	NA
Mn	57	28	100	33
Cu	12	7	70	118
Zn	150	100	750	127
Pb	57	41	62	77

Notes:

1. NA - Data is not available
2. For the comparison, the study conducted by Voutsas and Samara (2002) was selected, as this is the most recent study, which measured atmospheric heavy metal concentrations separately for different land uses.

Table 6-3 shows that the average heavy metal concentrations detected in this study are less than previously reported values by Voutsas and Samara (2002). One of the main reasons for this is that compared to this study, Voutsas and Samara (2002) conducted their study at a highly populated urban centre in Greece. High Mn concentration detected in this study is attributed to the introduction of methylcyclopentadienyl manganese tricarbonyl (MMT) into gasoline used in Australia since year 2000 (Cohen et al. 2005; Gulson et al. 2006). Despite the fact that Australia discontinued the usage of leaded fuel more than a decade ago, this study detected significant Pb concentrations. This is attributed to the presence of Pb in tyre and brake wear particles (Sansalone et al. 1996).

In order to evaluate the variation in HM concentrations among the investigated sites, the data values obtained were plotted as histograms as shown in Figure 6-3. As weekday traffic volumes are much higher compared to weekend traffic volumes (See Table 6-2), atmospheric HM concentrations are also correspondingly high during

weekdays. Consequently, HM concentrations were plotted separately for weekend and weekday sampling. As the sampling sites are spatially distributed, Figure 6-3 can be used to assess the spatial variability of heavy metals in the atmospheric phase. Spatial variability is important as atmospheric phase HMs are a major contributor to the HMs in stormwater runoff (Sabin et al. 2005; Melaku et al. 2008).

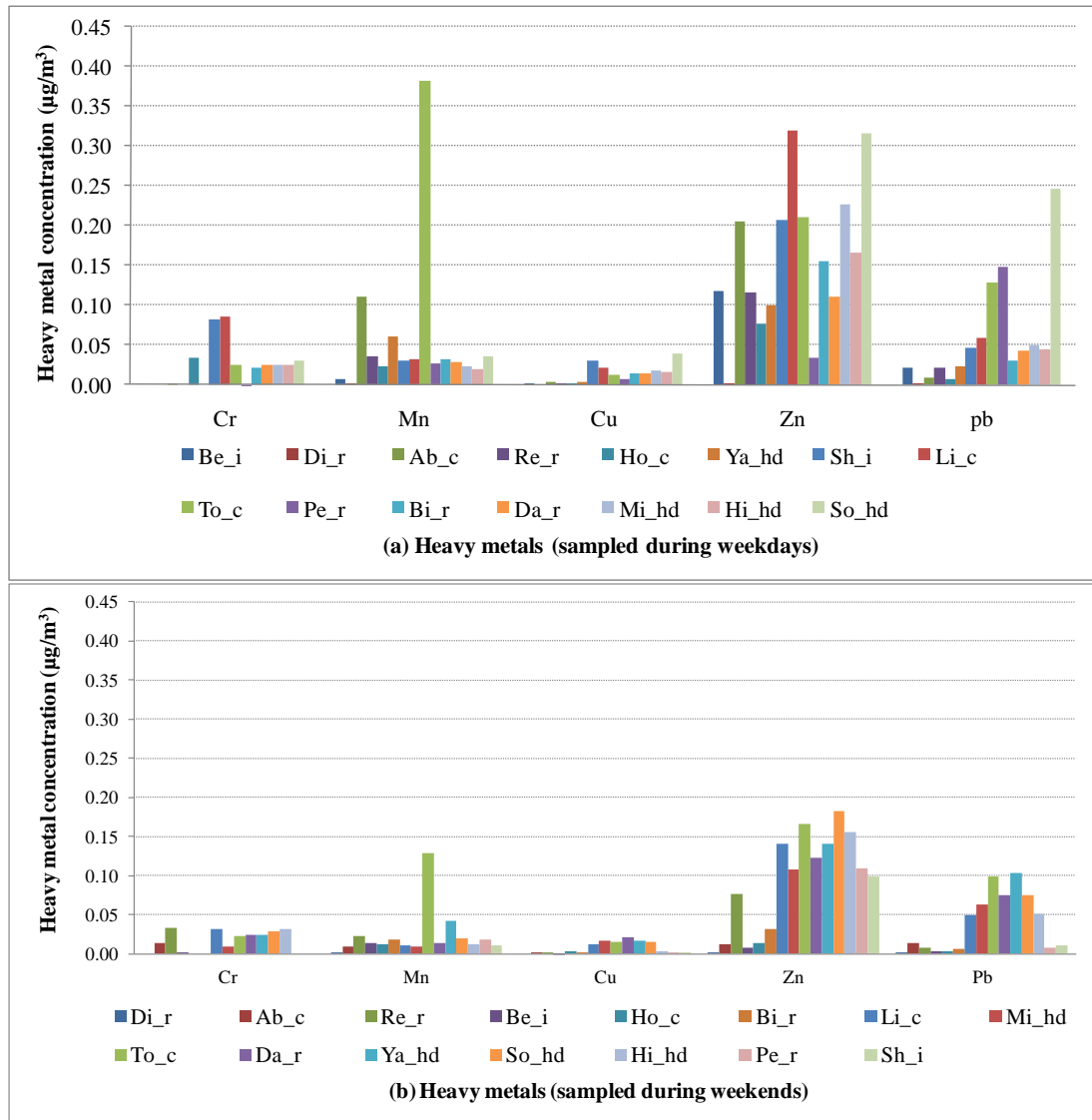


Figure 6-3: Atmospheric heavy metal concentration during weekdays and weekends

(Where; i = industrial, c = commercial, r = residential, hd = high anthropogenic activities, Abbreviations used for road names defined in Table 6-1 and 6-2)

Figure 6-3 shows that Zn is detected consistently in high concentration during weekdays as well as weekends at most of the sites. Therefore, Zn sources would be common to all the sites. One of the main Zn sources is vehicular traffic which is common for all sites (Kemp 2002). Xia and Gao (2011) and Councell et al. (2004)

noted that tyre wear particles were one of the primary sources of Zn in the urban atmosphere. However, there can be other sources of Zn emissions such as industrial and commercial activities (Tippayawong et al. 2006; Voutsas and Samara 2002). Therefore, land use related sources needed to be incorporated into the analysis undertaken.

Figure 6-3 shows that except at five sampling events, Pb is the second most commonly detected heavy metal. Tyre wear and brake pad wear is a source of Pb (Sansalone et al. 1996). Maher et al. (2008) noted that resuspended soil dust, enriched with lead from previous decades of leaded fuel usage can also be a major source of Pb at urban roadsides. This conclusion is further supported by the findings of Usman (2008) who noted that the adsorption of heavy metals to soil particles follow the order of $Pb > Cu > Zn > Ni > Cd$.

6.3.4 Polycyclic aromatic hydrocarbons (PAHs)

In order to ensure that the PAH data set is in similar range as those observed by previous researchers, concentrations detected in this study were compared with similar study outcomes conducted in Brisbane by Berko (1999) as shown in Table 6-4. Although Lim et al. (2005) have also measured atmospheric concentration in Brisbane, they have not provided PAHs concentration for gas and particulate phases separately. Therefore, PAHs concentrations recorded by Berko (1999) were compared with those recorded in this study. However, Berko (1999) has not mentioned whether the sampling was conducted during weekdays or weekends. It can be seen from Table 6-4 that PAH levels in the Gold Coast area (this study) are generally higher than those in Brisbane. However, investigations in Brisbane were undertaken in 1995-1998 period, whereas investigations in this study were undertaken in 2009-2010 in the Gold Coast area. Therefore, the difference can be a result of increased traffic and anthropogenic activities over the intervening period.

Table 6-4: Average airborne PAHs concentrations

PAHs	Brisbane ^a		Gold Coast ^b (ng/m ³)			
	(ng/m ³)		(2009-2010)			
	(1995-1998)		Vap.		Part.	
	Vap.	Part.	wk	we	wk	we
Acenaphthene (ACE)	5.86	Bdl	3.71	4.90	2.11	2.21
Acenaphthylene (ACY)	10.9	0.03	0.97	1.33	1.17	1.15
Anthracene (ANT)	1.6	0.04	8.92	4.85	2.00	2.20
Benz(a)anthracene (BaA)	0.09	0.21	0.84	0.55	0.52	0.31
Benzo(a)pyrene (BaP)	0.03	0.34	3.10	3.11	3.03	3.09
Benzo(e)pyrene (BeP)	0.03	0.35	3.10	3.12	3.07	2.88
Phenanthrene (PHE)	19.8	0.52	3.50	0.40	0.80	4.60
Chrysene (CHR)	0.26	0.43	1.00	0.50	0.50	1.40
Indeno(1,2,3-c,d)pyrene (IND)	Bdl	0.83	2.50	1.90	1.40	2.00
Benzo(g,h,i)perylene (BgP)	Bdl	1.39	4.50	3.00	3.10	4.10
Pyrene (PYR)	4.36	0.41	4.80	2.20	3.10	5.20
Fluorene (FLU)	11.4	0.04	6.70	2.70	2.2	6.40
Dibenz(a,h)anthracene (DbA)	0.01	0.02	2.10	1.80	1.70	2.00
Fluoranthene (FLA)	Na	Na	8.30	3.90	3.40	6.50

^a - Adapted from Berko (1999)^b - this study

(Where wk = weekdays, we = weekends, Vap.= vapour phase, Part.= particulate phase, Bdl = below detection limit, Na= data is not available)

In order to investigate the variation of PAH concentrations in the atmosphere, statistical parameters of mean, maximum, minimum and standard deviation were determined. These statistical parameters for gas and particulate phases are summarised in Table 6-5 and Table 6-6, respectively. As many physical properties such as volatility and water solubility depends on the number of benzene rings, PAHs with equal number of rings were grouped together as shown in Table 6-5 and Table 6-6. Additionally, Table A-1 of Appendix A presents the molecular weights and solubility's for the selected PAHs.

Table 6-5: Atmospheric gas phase PAHs concentrations
(a): Sampled during weekdays

PAHs	ACY	ACE	FLU	ANT	PHE	PYR	FLA	BaA	CHR	BaP	BeP	DbA	BgP	IND
Mean (ng/m ³)	1.0	3.7	6.7	8.9	3.5	4.8	8.3	0.8	1.0	3.1	3.1	2.1	4.5	2.5
Maximum (ng/m ³)	3.2	12.0	29.9	42.5	17.8	13.5	21.5	2.4	2.9	4.9	5.0	3.7	7.8	4.4
Minimum (ng/m ³)	0.5	0.7	0.5	0.4	0.0	0.0	0.6	0.0	0.0	0.7	0.8	1.1	1.1	1.0
Standard dev.	0.8	4.0	7.8	11.6	5.1	3.9	5.5	0.9	1.1	0.8	0.8	0.8	2.3	1.3
Number of rings	3 rings				4 rings				5 rings			6 rings		

(b): Sampled during weekends

PAHs	ACY	ACE	FLU	ANT	PHE	PYR	FLA	BaA	CHR	BaP	BeP	DbA	BgP	IND
Mean (ng/m ³)	1.3	4.9	6.4	4.9	4.6	5.2	6.5	0.5	1.4	3.1	3.1	2.0	4.1	2.0
Maximum (ng/m ³)	5.1	14.4	26.0	23.8	18.9	13.8	13.9	1.8	8.1	3.2	3.2	2.8	6.5	3.3
Minimum (ng/m ³)	0.5	1.3	0.5	0.3	0.0	0.0	0.1	0.0	0.0	3.1	3.1	1.3	1.4	0.9
Standard dev.	1.3	4.2	6.4	6.6	5.7	3.8	4.2	0.7	2.2	0.1	0.0	0.5	1.8	1.0
Number of rings	3 rings				4 rings				5 rings			6 rings		

Table 6-5 shows that three and four ring PAHs have been detected in high concentration in the gas phase. This is because they are able to generate high vapour pressure in the atmosphere (Kishida et al. 2008; Wey et al. 2000). Therefore, it is logical to detect three and four rings PAHs primarily in the gas phase.

As evident in Table 6-5, FLU, FLA and ANT have been detected in high concentration during weekdays compared to weekends (with a notable difference). This is attributed to the fact that vehicular traffic is one of the main sources of PAHs and weekday traffic volumes are relatively higher (Brachtel et al. 2009). The detection of traffic generated PAHs in high concentration suggests that traffic sources are important compared to the other sources for gas phase PAHs. However, land use related sources also generate PAHs to the atmosphere (Singh et al. 2008).

Table 6-6(a) and (b) shows that 4 and 5 ring particulate phase PAHs were detected in similar concentration ranges among all the sites. This is attributed to the fact that these compounds have relatively higher molecular weight and low volatility as they are associated primarily with total suspended particulate matter in the atmosphere (Han et al. 2009; Wu et al. 2006; Halek et al. 2008; Shimmo et al. 2004). As ABS (2010) have noted that 83.0% of the total vehicle fleet in Australia are run on gasoline, it is hypothesised that gasoline would be the main source of particulate bound PAHs. Furthermore, Velasco et al. (2004) noted that light gasoline engines are a principal source of particulate bound 4 and 5 ring PAHs. Additionally, Riddle et al.

(2007) noted that although diesel vehicles emit both lighter PAHs as well as heavier PAHs, emission of light 3 ring PAHs is high compared to gasoline vehicles at the optimum operating conditions. Therefore, it can be confirmed that the current observation are in agreement with the findings of past studies.

Table 6-6: Atmospheric particulate phase PAHs concentrations
(a): Sampled during weekdays

PAHs	ACY	ACE	FLU	ANT	PHE	PYR	FLA	BaA	CHR	BaP	BeP	DbA	BgP	IND
Mean (ng/m ³)	1.2	2.1	2.7	2.0	0.4	2.2	3.9	0.5	0.5	3.0	3.1	1.8	3.0	1.9
Maximum (ng/m ³)	2.6	4.8	15.6	6.0	1.6	5.7	7.6	1.3	1.4	3.3	5.7	2.9	3.2	5.6
Minimum (ng/m ³)	0.4	0.2	0.3	0.2	0.0	0.0	0.5	0.0	0.0	1.8	1.6	1.3	2.0	1.0
Standard dev.	0.9	1.2	4.0	1.9	0.5	1.3	2.2	0.3	0.6	0.4	1.3	0.4	0.3	1.2
Number of rings	3 rings					4 rings				5 rings			6 rings	

(b): Sampled during weekends

PAHs	ACY	ACE	FLU	ANT	PHE	PYR	FLA	BaA	CHR	BaP	BeP	DbA	BgP	IND
Mean (ng/m ³)	1.2	2.3	2.2	2.1	0.8	3.1	3.4	0.3	0.5	3.1	2.8	1.7	3.1	1.4
Maximum (ng/m ³)	3.3	9.0	6.5	8.8	5.6	14.6	10.5	1.0	2.9	3.3	5.4	2.6	3.2	3.0
Minimum (ng/m ³)	0.4	1.3	0.0	0.0	0.0	0.0	0.0	0.0	0.0	3.0	1.1	1.3	3.1	0.8
Standard dev.	1.0	2.0	2.1	2.7	1.4	3.7	3.2	0.4	0.8	0.1	1.6	0.4	0.0	0.7
Number of rings	3 rings					4 rings				5 rings			6 rings	

Urban traffic is one of the main sources of PAHs to the atmosphere as noted in Chapter 2. Primarily, there are three types of traffic related PAH emissions to the atmosphere, namely, exhaust emissions, abrasion products and re-suspension of road deposited particulate associated PAHs. These three processes determine traffic generated PAH concentrations and an in-depth understanding is required to identify the influence of vehicular traffic on these processes. Additionally, there are land use related PAH sources such as industrial and commercial activities (Hong et al. 2007; Amodio et al. 2009). Overall atmospheric PAH levels depend not only on different traffic parameters such as traffic volume and congestion (V/C), but also on land use related activities (Hoshiko et al. 2011).

6.4 Multivariate analysis

6.4.1 Heavy metals

As evident from the Figure 6-3, “Set 1” sites have generated heavy metals in relatively high concentrations. This is due to the fact that these sites are located close to high anthropogenic activities. Therefore, in order to investigate the influence of

anthropogenic activities on the generation of heavy metals, detailed analysis was undertaken incorporating important variables to represent these activities. There are three important traffic variables, which influence atmospheric phase heavy metal concentrations, namely, total average daily traffic volume (ADT_{to}), average daily heavy duty traffic volume (ADT_{hv}) and traffic congestion (V/C). Furthermore, atmospheric phase heavy metal concentrations also depend on land use characteristics (Ötvös et al. 2003). Therefore, in order to identify the effect of land use on atmospheric heavy metal concentrations, three types of land uses, namely, industrial, commercial and residential were investigated. Consequently, three traffic variables and three land use types were included in the multivariate analysis.

The Multi Criteria Decision making method, PROMETHEE 2 (Preference Ranking Organisation Method for Enrichment Evaluation) and GAIA were employed for the analysis. Despite the fact that principal component analysis (PCA) is a common multivariate method used in water quality research, its applicability is limited for this analysis due to the requirement of large number of objects in the data matrix (Miguntanna 2009). However, being a non-parametric method, there is no such limitation in the use of PROMETHEE 2 and GAIA. Detailed discussions of multivariate analytical methods are given in Section 3.4.3.

The variables used for the analysis were, Pb, Cr, Zn, Cu, Mn, wind, ADT_{to}, ADT_{hv}, V/C and TSP. There were fifteen objects in each data matrix corresponding to the fifteen sampling sites. The analysis was conducted with and without traffic data. Firstly, the analysis was conducted with the traffic data for “Set 3” sites to investigate the influence of traffic on the atmospheric heavy metal concentrations. Secondly, the analysis was conducted without traffic data to investigate the interrelationships among HMs and the influence of different land uses on atmospheric HM and TSP concentrations.

In the PROMETHEE 2 analysis, V-shape preference function was selected for all the variables. This function compares values based on one threshold value for each variable (Podvezko and Podvieszko 2010). In this analysis, variables are set as maximum so that the decision axis, π_i , pointed towards the most polluted site/s in

terms of heavy metals. The resulting biplot is shown in Figure 6-4 and PROMETHEE 2 complete rankings are given in Tables A-2 and A-3 of Appendix A.

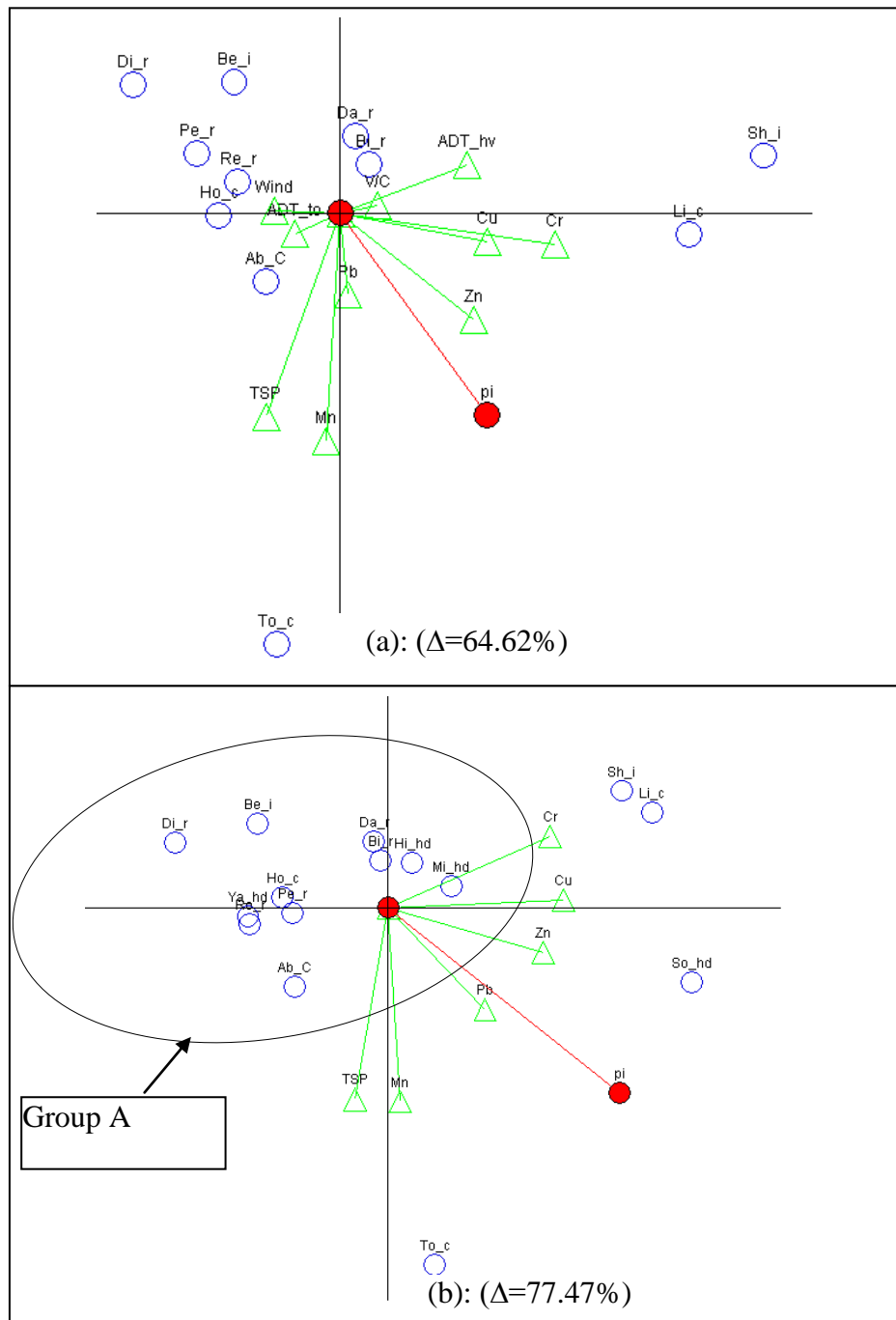


Figure 6-4: GAIA biplot of heavy metals against the first two principal components for weekdays, (a): for “Set 3” sites, (b): for “Set 3” and “Set 1” sites (Where; i = industrial, c = commercial, r = residential, hd = high anthropogenic activities, Abbreviations for road names given in Table 6-1 and 6-2, Δ = the percentage variance described by the GAIA biplot)

For further confirmation of the conclusions derived from Figure 6-4(a), a correlation matrix was generated. The correlation matrix is given in Table 6-7. As this matrix is symmetrical around one diagonal, only half of the data matrix is presented.

Table 6-7: Correlation matrix for Figure 6-4(a)

	Cr	Mn	Cu	Zn	Pb	TSP	ADT_to	V/C	ADT_hv	Wind
Cr	1.000									
Mn	-0.026	1.000								
Cu	0.861	0.097	1.000							
Zn	0.688	0.354	0.644	1.000						
Pb	0.075	0.518	0.317	0.104	1.000					
TSP	-0.263	0.830	-0.294	0.039	0.243	1.000				
ADT_to	0.004	-0.050	-0.459	-0.112	-0.483	0.399	1.000			
V/C	0.352	-0.210	0.053	0.308	0.138	-0.149	0.299	1.000		
ADT_hv	0.590	-0.234	0.657	0.377	-0.263	-0.337	-0.145	-0.092	1.000	
Wind	-0.427	-0.049	-0.554	-0.660	0.243	0.248	0.335	0.175	-0.732	1.000

Figure 6-4(a) and Table 6-7 confirm the strong correlation of ADT_hv, Cu and Cr with correlation coefficients of 0.657 and 0.590, respectively. This suggests that heavy duty traffic is one of the main sources of Cu and Cr in the atmosphere. Johansson et al. (2009) noted that vehicular traffic as one of the key sources of heavy metals in urban air. Kemp (2002) noted that Cu was mainly generated from the wear of brake pads. The findings from the current study are in agreement with past research study outcomes.

Although Figure 6-4(a) and Table 6-7 show correlation of TSP and Mn, they are not correlated to traffic parameters. This suggests that TSP and Mn are primarily generated from other sources such as surrounding soil (Moreno et al. 2006). Soil related Mn and TSP are contributed to the atmosphere by natural and traffic generated wind. Tippayawong et al. (2006) noted that there are three main sources of atmospheric particulate matter. They are: (1) long distance sources such as wind transported TSP; (2) short distance sources such as re-suspension of road deposited sediments; and (3) unknown sources with low influence of traffic emissions. The second source is the most important for this study. This could be the reason for not detecting a clear relationship with traffic and TSP. However, Patel et al. (2009) reported that vehicle emissions can be a dominant source of PM_{2.5} (particulate matter that is 2.5 micrometers in diameter and smaller) in the atmosphere. Although traffic

is a main contributor of $PM_{2.5}$, it is not the dominant source for total suspended particulate matter (TSP).

Figure 6-4(b) shows a close grouping of sites (Group A). This is due to the generation of similar heavy metals and TSP loadings to the atmosphere by these sites. There are four sites with different land uses within 'Group A'. Therefore, this suggests that heavy metals and TSP concentrations in the atmosphere have limited dependency on the surrounding land use activities. As noted in the paragraph above, there are three sources of atmospheric particulate matter. Although re-suspension is the main source, 'Group A' sites have similar emissions to the atmosphere due to different combinations of the three sources noted above. For example, for some sites, re-suspension related emission is very high whereas it is not high for others. However, the total emissions are still the same in 'Group A' sites. This is the reason for the grouping in Figure 6-4(b).

Subsequently, weekend samples were also analysed using PROMETHEE 2 and GAIA. Analysis was carried out with and without traffic data. Analysis of "Set 3" sites were conducted incorporating traffic data. "Set 1" and "Set 3" sites were analysed together without traffic data. V-shape preference function was selected for the analysis. Therefore, the decision axis, π_1 , points towards the most polluted site/s in terms of heavy metals. The resulting biplot is shown in Figure 6-5 and PROMETHEE 2 complete rankings are given in Tables A-4 and A-5 of Appendix A.

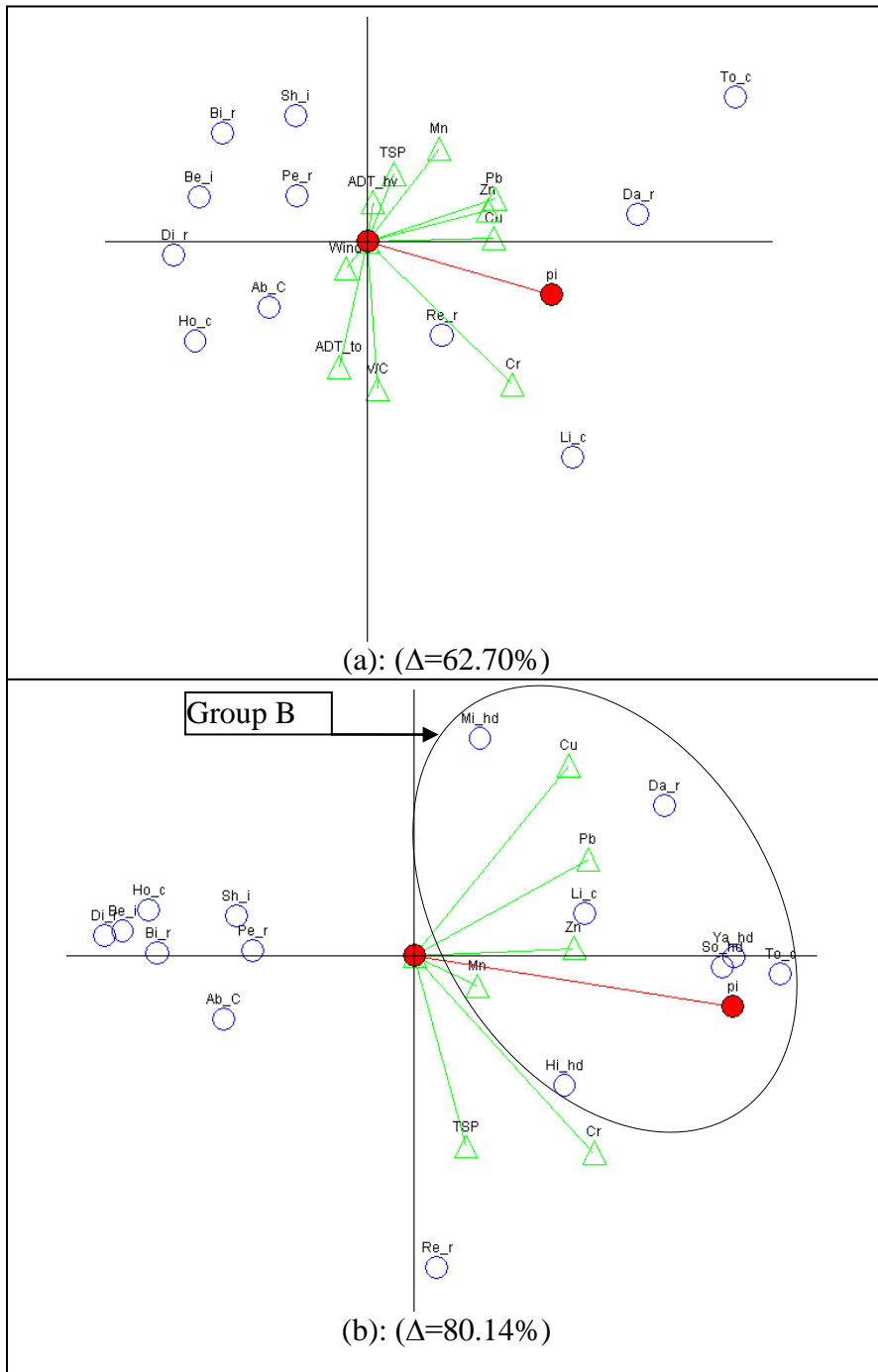


Figure 6-5: GAIA biplot of heavy metals against the first two principal components for weekends, (a): for “Set 3” sites, (b): for “Set 3” and “Set 1” sites Where; i = industrial, c = commercial, r = residential, hd = high anthropogenic activities, Abbreviations used for road names given in Table 6-1 and 6-2, Δ = the percentage variance described by the GAIA biplot)

Figure 6-5(a) shows that during weekends neither traffic related variables nor wind is correlated with any of the investigated heavy metals. This behaviour was further investigated by considering the sources of emissions. Air pollutants at a road site originate from traffic emissions from the sampled road and other sources including land use related activities and surrounding roads. Others sources can become dominant during weekends as traffic volume is low compared to weekdays. Therefore, atmospheric heavy metal concentrations are generally not highly influenced by traffic during the weekends. Furthermore, as emissions to the atmosphere are relatively low during the weekends, atmospheric heavy metal concentrations are relatively uniform and close to the background concentrations. Therefore, redistribution is not possible due to atmospheric disturbances such as the effects of wind.

Figure 6-5(b) shows a close grouping of “Set 1” sites, Li_c, Da_r and To_c (Group B). This is due to the fact that these sites contribute similar HMs and TSP loading to the atmosphere. Furthermore, Figure 6-5(a) shows that traffic characteristics are not correlated with most of the HMs even though vehicular traffic is one of the common sources of HMs to the atmosphere (Johansson et al. 2009; Onder and Dursun 2006). This behaviour is attributed to the fact that traffic volume is low during the weekends. Although traffic data is not available for “Set 1” sites, they are located close to urban amenities such as a public library and Gold Coast City Council office where the intensity of traffic activities can be relatively high even during weekends. Therefore, traffic related emissions are one of the main sources of HMs at “Set 1” sites. Also, traffic related emissions generated by surrounding roads are the main emission sources even at Li_c, Da_r and To_c sites during weekends. As Li_c and To_c sites are located close to a highway and an urban centre respectively, additional traffic generated emissions could be contributed to these sites. In addition, Da_r is located close to a marina where emissions coming from pleasure boats are a key source. Therefore, Li_c, Da_r and To_c sites receive contributions not only from the selected road, but also from the surrounding sources. This explains the grouping of Li_c, Da_r and To_c sites together with “Set 1” sites (Group B). Furthermore, all the heavy metals vectors point towards Group B. These sites generate the investigated metals in high concentrations.

Both weekend and weekday data was analysed together using PROMETHEE 2 after incorporating traffic data in order to investigate the influence of traffic on atmospheric heavy metal concentrations. “Set 1” sites were removed from the analysis, as traffic data was not available for these sites. Heavy metal concentrations were divided by corresponding total suspended particulate matter concentrations (TSP) prior to the analysis to remove any bias caused by different TSP loadings. Total average daily traffic (ADT_to), average daily heavy duty traffic (ADT_hv) and wind speed (wind) were also incorporated into the analysis. The resulting biplot is shown in Figure 6-6 and ranking is given in Table A-6 of Appendix A.

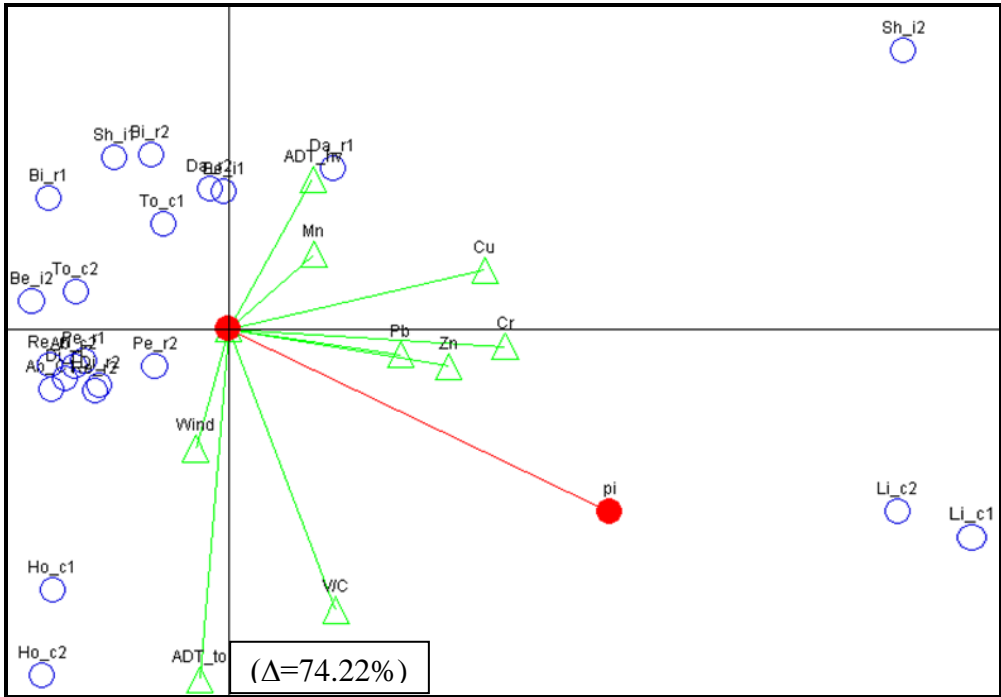


Figure 6-6: GAIA biplot of heavy metals against the first two principal components for “Set 3” sites

(Where; i = industrial, c = commercial, r = residential, hd = high anthropogenic activities, numeral 1 = weekend samples, numeral 2 = weekday samples, abbreviations used for road names given in Tables 6-1 and 6-2, Δ = the percentage variance described by the GAIA biplot)

Figure 6-6 shows that average daily traffic is not correlated with atmospheric heavy metals but average daily heavy duty traffic is correlated with Zn, Mn, Cu, Pb and Cr. This suggests that heavy duty traffic is one of the main sources of airborne heavy

metals. Additionally, traffic congestion is weakly correlated with the investigated heavy metals as evident in Figure 6-6. Two primary reasons can be attributed for this behaviour. Firstly, the increase in traffic congestion leads to high emissions at a given location on a road. Secondly, traffic induced wind speed reduces as the traffic congestion increases leading to reduced re-suspension and re-distribution. This analysis confirms the fact that heavy duty traffic and traffic congestion are the important traffic variables for heavy metal emissions to the atmosphere.

6.5 Multivariate analysis of PAHs

As noted in Section 6.3.3, generation of PAHs to the atmosphere depends on a number of parameters such as traffic volume, traffic congestion and land use characteristics. Furthermore, it was found that lighter PAHs (3 and 4 rings) are mainly present in the gas phase whereas heavier PAHs (5 and 6 rings) are mainly present in the particulate phase. However, univariate analysis failed to identify the variation of light and heavy PAHs in the atmosphere with traffic and land use characteristics. Consequently, multivariate analysis was undertaken to determine the variation of PAHs in the gas and particulate phases with traffic and land use characteristics. For this analysis, all the tested 14 USEPA priority PAHs were included.

The phases to which PAHs are linked determine their fate and transport mechanisms in the atmosphere (Vardar et al. 2008; Esen et al. (2008). Additionally, physical properties such as volatility determines the transport processes as more volatile PAHs disperse over a larger geographical area than less volatile compounds (Lang et al. 2008). Furthermore, more volatile PAHs are dominant in the gas phase whereas less volatile PAHs are mainly associated with the particulate phase (Lee et al. 1995). This highlights the fact that transport and distribution of PAHs in the atmosphere is highly dependent on the phase to which they are attached and their physical properties. Therefore, gas phase PAHs and particulate phase PAHs were analysed separately. As noted in Section 6.3.3, the highest PAH concentration was detected in the gas-phase. Therefore, gas phase PAHs were analysed first.

The analysis was conducted using PROMETHEE 2 and GAIA. Gas phase PAHs collected during weekdays and weekends were analysed together for “Set 3” sites. This was to investigate the influence of land use on gas phase PAHs. V-shape preference function was selected for all the variables in the analysis. Therefore, the decision axis π_i pointed towards the most polluted site/s in terms of PAHs. The GAIA biplot is shown in Figure 6-7 and the ranking is given in Table A-7 of Appendix A.

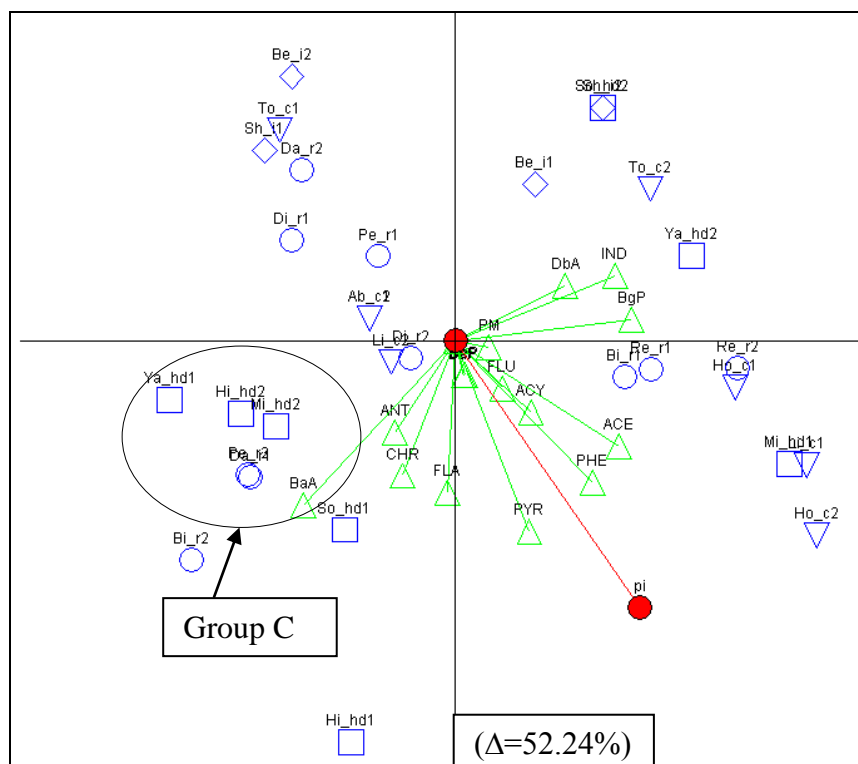


Figure 6-7: GAIA biplot of gas phase PAHs against the first two principal components for “Set 3” sites

[Where; i = industrial (Diamond), c = commercial (Triangle), r = residential (Circles), hd = high anthropogenic activities (Square), Δ = percentage of variance explained by the GAIA biplot, numeral 1 = weekend samples, numeral 2 = weekday samples, abbreviations used for road names are defined in Tables 6-1 and 6-2]

Figure 6-7 shows a grouping of sites based on their dominant land use (for example group C). This suggests that the emissions of PAHs to the atmosphere are influenced by the type of land use activities. However, as the groups are not clearly separated, it can be concluded that these activities are not unique to each land use. Therefore, even though similar land use activities generate similar PAH loadings to the

atmosphere, the distribution of emission sources in each land use type is different. There are two possible reasons for this behaviour. Firstly, there are site-specific sources of PAH emissions in each land use type. Secondly, there are common PAH sources in all three land uses such as traffic.

In order to investigate the variation of PAH concentrations with the sampling day, analysis was undertaken for weekday and weekend samples separately. Weekday sampling data was analysed first, with and without traffic data. Data matrix for “Set 3” sites were analysed with the traffic data to investigate the influence of traffic on atmospheric PAH concentrations. Then data matrices for “Set 1” and “Set 3” sites were analysed together without traffic data to investigate the influence of land use on atmospheric PAHs concentration. For this analysis, PROMETHEE 2 and GAIA were employed as the data matrices do not have a large number of objects (Miguntanna 2009). The V-shape preference function was selected for both analyses as discussed in Section 6.4. The GAIA biplot is given in Figure 6-8. The resulting PROMETHEE 2 complete rankings are given in Tables A-8 and A-9 of Appendix A.

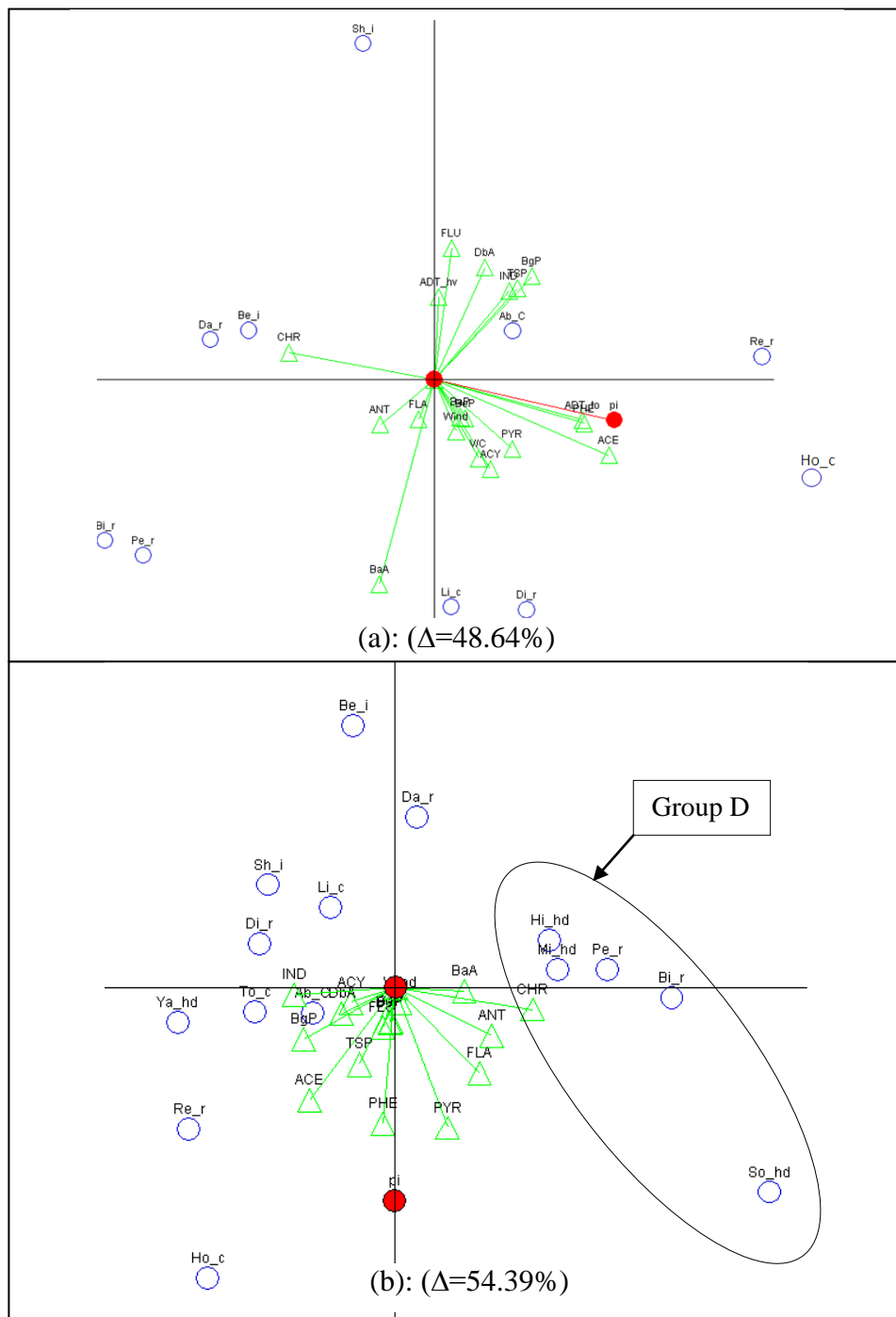


Figure 6-8 GAIA biplot of gas phase PAHs against the first two principal components for weekday sampling, (a): for “Set 3” sites, (b): for “Set 3” and “Set 1” sites

(Where i = industrial, c = commercial, r = residential, hd = high anthropogenic activities, ADT_to = ADT of total vehicles, ADT_hv = ADT of heavy duty vehicles, Δ = percentage of variance explained by the GAIA biplot, numeral 1 = weekend samples, numeral 2 = weekday samples, abbreviations used for road names are defined in Tables 6-1 and 6-2)

Figure 6-8(a) shows correlation of FLU, DbA, IND, BgP, TSP and ADT_hv indicating that these PAHs are generated mainly by heavy duty traffic sources. Among these four PAHs, three PAHs have 5 and 6 rings and these PAHs are correlated with TSP. This conclusion is supported by the findings of Stracquadiano and Trombini (2006). They noted that combustion processes emit both soot and particulate associated PAHs. Furthermore, heavy duty diesel vehicles emit light PAHs at optimum driving condition whereas they emit heavier PAHs when idling or running at low speeds (Riddle et al. 2007). Therefore, these findings suggest that heavy duty vehicles operating at low speed are among the primary contributors of PAHs at these sites.

Figure 6-8(a) shows close correlation of ADT_to, ACE, PHE, BaP, BeP, PYR, ACY, V/C and wind. Majority of these PAHs have three to five benzene rings. Gasoline vehicles are a major source of four and five ring PAHs (Hong et al. 2007). Furthermore, as diesel engines emit heavy PAHs (>4 rings) in idle or slow moving condition, they could contribute five ring PAHs. Also, as diesel vehicles generate three ring PAHs at optimum efficiency, they could contribute 3 ring PAHs. This suggests that diesel vehicles operate in a congested mode or slow moving mode as well as in a fast mode at the same sampling location during 8 hr sampling period. This is logical as vehicles move in a congested mode during morning and evening peak hours whereas they move in a fast mode during other times. Therefore, this confirms the correlation of these PAHs with traffic congestion. Even though wind shows correlation with these PAHs, the small wind vector in Figure 6-8(a) indicate that the effect of wind speed is minimal on these PAHs.

Figure 6-8(b) shows grouping of Hi_hd, Mi_hd and So_hd of three “Set 1” sites (Group D). This suggests that these sites generate similar PAHs loading to the atmosphere. As these sites are located in areas with high anthropogenic activities, it is presumed that these activities generate similar PAHs loading to the atmosphere. One of the common activities in all the sites is traffic. Additionally, there are commercial, industrial and residential activities in these sites. In other words, atmospheric PAH concentrations also depends on the type of land use related activities as well. However, Fon et al. (2007) noted that even though there are many

PAH emission sources in an urban area such as vehicular emissions and stationary emission sources, vehicular emissions generally tends to be the dominant PAHs source (Muendo et al. 2006). Therefore, traffic could be the main emission source even for these sites.

Gas phase PAHs data for weekends were analysed using PROMETHEE 2 and GAIA. Data matrix for “Set 3” sites was analysed after incorporating traffic data. Data matrices for “Set 1” and “Set 3” sites were analysed together without traffic data to investigate the influence of land use on PAHs concentration in the atmosphere. As variables were set to maximum, the decision axis π points towards most polluted site/s. The GAIA biplot derived is shown in Figure 6-9. The resulting PROMETHEE 2 complete rankings are given in Tables A-10 and A-11 of Appendix A.

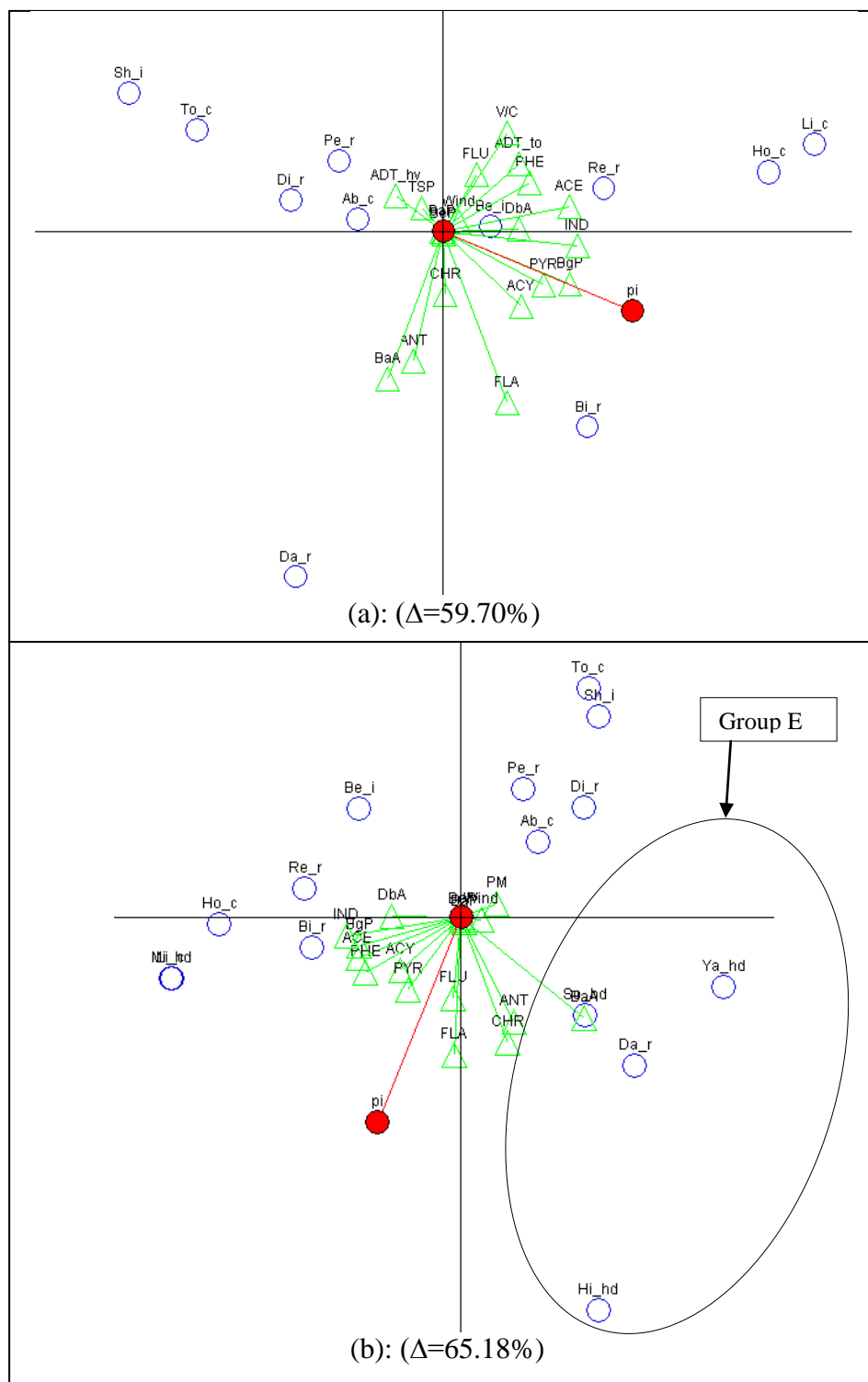


Figure 6-9: GAIA biplot of gas phase PAHs against the first two principal components for weekend sampling, (a): for “Set 3” sites, (b): for “Set 3” and “Set 1” sites

(Where i = industrial, c = commercial, r = residential, hd = sites with high anthropogenic activities, ADT_to = ADT of total vehicles, ADT_hv = ADT of heavy duty vehicles, Δ is the percentage of variance explained by the GAIA biplot)

Figure 6-9(a) shows correlation of ADT_{to}, V/C, FLU, PHE, ACE and DbA. Three of these PAHs, which are closely related with traffic, have three benzene rings and the other has five rings. As it was noted in Table 6-5 that three and four ring PAHs are present in the gas-phase, weekend traffic has contributed mainly lighter PAHs to the atmosphere. This suggests that traffic is not the main PAHs source to the atmospheric gas phase during weekends, as only four out of a total of fourteen PAHs shows correlation with traffic parameters. Therefore, other sources such as residential and industrial activities dominate over traffic sources during weekends in the generation of atmospheric gas phase PAHs. Li et al. (2003) noted that PAHs emitted from cooking make an important contribution to the atmospheric PAH concentrations.

So_{hd}, Ya_{hd} and Hi_{hd} sites generate similar PAH loads to the urban atmosphere as evident from the fact that the data points are located close to each other (Group E) in the GAIA biplot of Figure 6-9(b). These three sites are located close to high anthropogenic activities. Urban traffic is the most common anthropogenic activity at all three locations. For example, as Ya_{hd} site is located close to the Pacific Highway, traffic is the dominant PAHs source at this site. The other two sites are located at Southport Library and Highland Park. Although there is land use related activities such as industrial and commercial activities at these locations, there are no high emitting sources compared to traffic. Therefore, this once again indicates that traffic is one of the main PAH sources. This is supported by the findings of Müller et al. (1998) who noted that vehicular traffic as the main PAHs source in urban centres in Brisbane, Australia.

Subsequently, particulate phase PAHs were analysed. Firstly, “Set 1” and “Set 3” sites were analysed together without traffic data combining weekday and weekend sampling together. This was to investigate the influence of land use on atmospheric PAH concentrations. PROMETHEE 2 and GAIA were employed for this analysis and V-shape preference function was selected for the analysis. As the variables were set to their maximum in the analysis, decision axis, pi, pointed towards the most polluted site/s. The resulting biplot is shown in Figure 6-10 and PROMETHEE 2 complete rankings is given in Table A-12 of Appendix A.

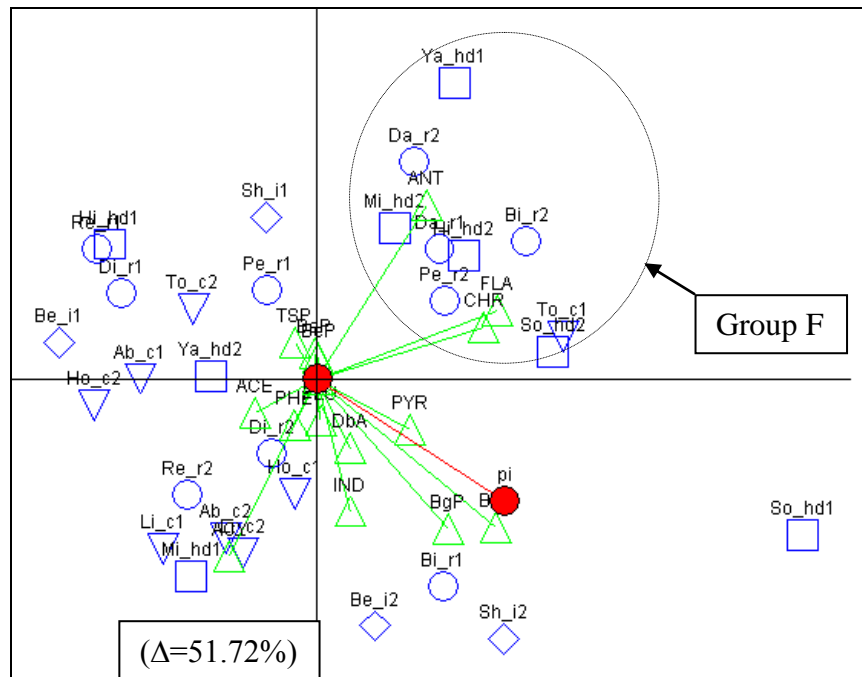


Figure 6-10: GAIA biplot of gas phase PAHs against the first two principal components for weekend sampling

(Where; i = industrial (Diamond), c = commercial (Triangle), r = residential (Circles), hd = high anthropogenic activities (Square), Δ = percentage of variance explained by the GAIA biplot, numeral 1 = weekend samples, numeral 2 = weekday samples, abbreviations used for road names in Tables 6-1 and 6-2)

Figure 6-10 shows a grouping of sites based on their land use (for example Group F). However, groups are not clearly separated. This is because there are common PAH sources in all land uses. Traffic is a common PAH source in all land uses. This suggests that atmospheric PAH concentrations are influenced by land use and traffic characteristics. Therefore, in addition to land use related activities, traffic sources contribute particulate bound PAHs to the atmosphere. A similar variation of PAHs with land use characteristics was reported by Shihua et al. (2001). However, in order to investigate the dominant sources for different PAHs, further analysis was required.

In order to identify the influence of traffic on atmospheric phase particulate bound PAHs, the data matrix for particulate phase PAHs was separated into weekday and weekend sampling and PROMETHEE 2 and GAIA analysis was carried out. Set 3” sites were analysed with the traffic variables to investigate the influence of traffic on

atmospheric PAH concentrations. “Set 1” and “Set 3” sites were analysed together without traffic data to investigate the influence of land use activities on atmospheric phase particulate bound PAH concentrations. Variables were set to their maximum in the analysis and hence the decision axis p_i pointed towards the most polluted site/s. The resulting biplot is shown in Figure 6-11. The resulting PROMETHEE 2 complete rankings are given in Tables A-13 and A-14 of Appendix A.

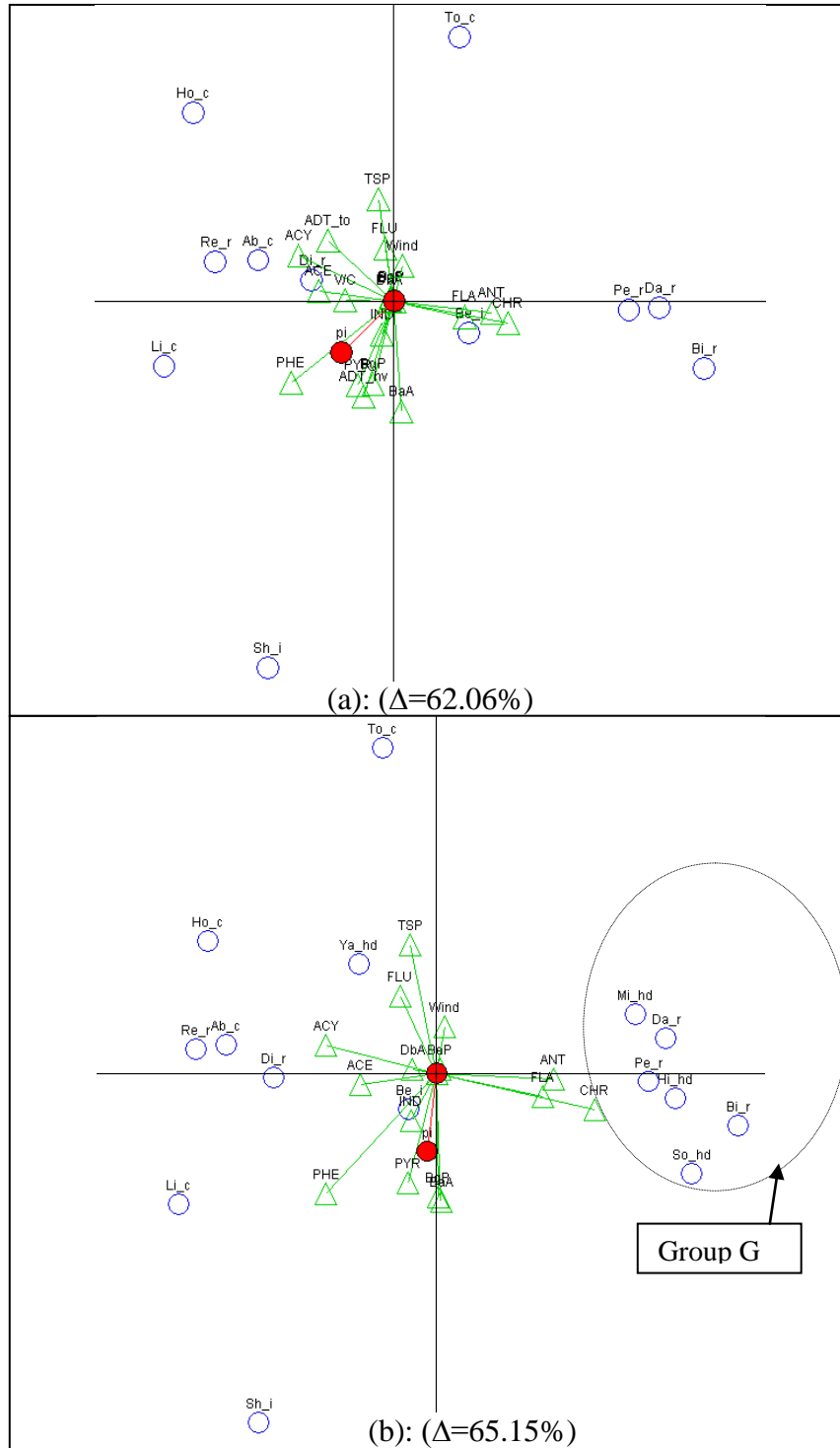


Figure 6-11: GAIA biplot of particulate phase PAHs against the first two principal components for weekday sampling, (a): for “Set 3” sites, (b): for “Set 3” and “Set 1” sites

(Where; i = industrial, c = commercial, r = residential, hd = high anthropogenic activities, Δ = percentage of variance explained by the GAIA biplot, numeral 1 = weekend samples, numeral 2 = weekday samples, abbreviations used for road names in Tables 6-1 and 6-2)

Figure 6-11(a) shows clear correlation of PHE, PYR, BgP, and BaA, IND and heavy duty traffic (ADR_hv). However, Figure 6-11(a) also illustrates that only ACE, ACY and PHE are correlated with total traffic volume (ADT_to) and traffic congestion (V/C). As most of the heavy duty traffic related PAHs have five to six benzene rings, they are generated by slow moving heavy duty traffic (Riddle et al. 2007). This is supported by the fact that heavier PAHs are associated with the particulate phase (Shimmo et al. 2004). Therefore, heavy duty traffic is a primary source of particulate phase heavier PAHs. These PAHs could also be generated not only by exhaust emissions but also by wearing of roads. As noted by Martuzevicius et al. (2011), street dust is a significant source of particulate bound PAHs to the atmosphere. Consequently, re-suspension of road deposited particles is one of the main sources of atmospheric phase PAHs.

Figure 6-11(b) shows a grouping of “Set 1” sites in the GAIA biplot (Group G). Therefore, it is expected that these sites generate similar particulate bound PAH loadings to the atmosphere. As discussed in Section 6.2, “Set 1” sites are located in close proximity to urban amenities in the Gold Coast region where intensity of anthropogenic activities is high. The most common anthropogenic activity in all these sites is vehicular traffic. Therefore, these sites contribute similar loadings of total suspended particulate matter and PAHs to the atmosphere from traffic sources.

Particulate phase PAHs collected during weekends was analysed using PROMETHEE 2 and GAIA. This was to investigate the influence of the sampling day on atmospheric PAHs concentrations. Data from “Set 3” sites were analysed initially to understand the variability of PAHs with traffic characteristics. Subsequently, “Set 1” and “Set 3” sites were analysed together to understand the variability of PAHs with different land use activities. Variables were set to their maximum for the analysis and hence decision axis pi pointed towards the most polluted site/s. The resulting biplot is shown in Figure 6-12. The resulting PROMETHEE 2 complete rankings are given in Tables A-15 and A-16 of Appendix A.

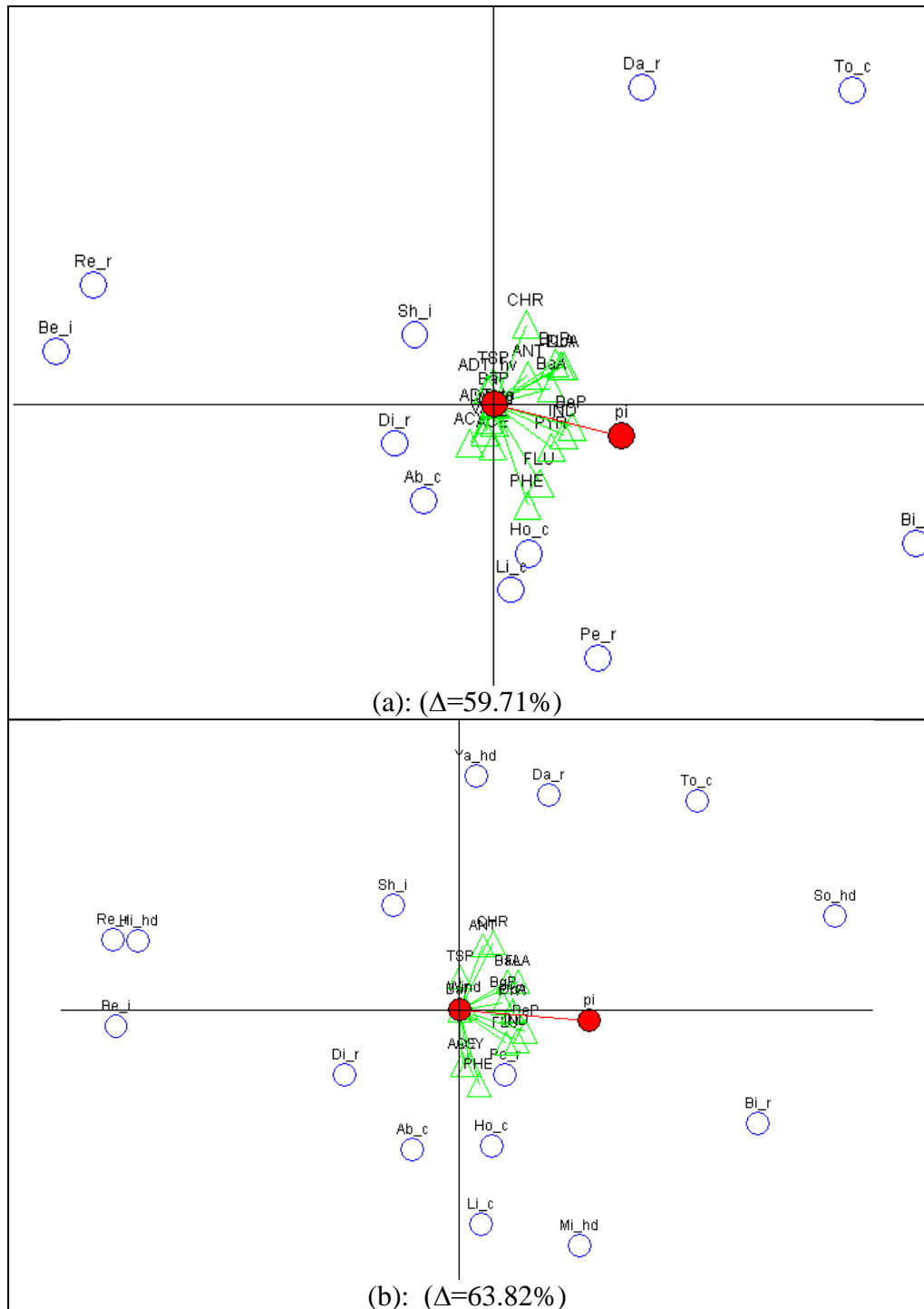


Figure 6-12: GAIA biplot of particulate phase PAHs against the first two principal components for weekend sampling, (a): for “Set 3” sites, (b): for “Set 3” and “Set 1” sites

(Where; i = industrial, c = commercial, r = residential, hd = high anthropogenic activities, Δ = percentage of variance explained by the GAIA biplot, numeral 1 = weekend samples, numeral 2 = weekday samples, abbreviations used for road names in Tables 6-1 and 6-2)

As illustrated in Figure 6-12(a), almost all the PAHs are correlated to each other but not correlated with traffic parameters. Therefore, traffic is not the dominant anthropogenic activity which generates particulate bound PAHs during weekends. This suggests that background PAHs prevail in the sampling area as traffic related emissions are at a minimum during the weekends. As the particulate bound PAHs are associated with very fine particles (aerodynamic diameter $< 1 \mu\text{m}$) (Wingfors et al. (2001), they are generated mainly with the exhaust emissions. As PAHs emissions are low during the weekends, there is not much change to the background PAH concentrations due to these low emissions. Therefore, there is no correlation between PAHs and traffic parameters and hence, background PAH concentrations prevail at all the sites.

As Figure 6-12(b) does not show any grouping of “Set 1” sites, these sites are not considered to generate similar particulate bound PAH loadings to the atmosphere during weekends. Also, traffic generated emissions are low during weekends and as particulate bound, they tend to settle quickly close to the sources of origin (Shimmo et al. 2004). Therefore, background PAH concentrations are considered to prevail in the atmosphere during weekends. This highlights the fact that PAH emissions to the atmosphere are low during the weekends and hence background concentrations prevail.

6.6 Development of predictive models

From the analysis carried out, it was found that atmospheric phase HM and PAH concentrations are influenced by total average daily traffic volume (ADT_{to}), total average heavy duty traffic volume (ADT_{hv}) and traffic congestion (V/C) and land use as discussed in Sections 6.4 and 6.5. Therefore, these influential variables needed to be included in mathematical replication equations that could be used to predict heavy metal and PAH concentrations in the atmosphere.

6.6.1 Heavy metals

Multiple linear regression analysis was carried out to develop predictive equations for the five investigated heavy metals (Zn, Pb, Mn, Cu and Cr) and total suspended

particulate matter (TSP). It was hypothesised that the variability of heavy metals and TSP could be predicted in the form of a linear equation incorporating land use and traffic parameters. A linear equation was considered, as it is the simplest possible mathematical model to investigate the relationship between several independent or predictor variables and dependent or criterion variables (Scott et al. 2007). It was assumed that Zn, Pb, Mn, Cu, Cr and TSP concentrations in the atmosphere can be expressed as a linear combination of independent variables as follows:

$$\text{Zn} = f(\text{C, I, R, ADT}_{\text{to}}, \text{V/C, ADT}_{\text{hv}}, \text{wind})$$

$$\text{Pb} = f(\text{C, I, R, ADT}_{\text{to}}, \text{V/C, ADT}_{\text{hv}}, \text{wind})$$

$$\text{Mn} = f(\text{C, I, R, ADT}_{\text{to}}, \text{V/C, ADT}_{\text{hv}}, \text{wind})$$

$$\text{Cu} = f(\text{C, I, R, ADT}_{\text{to}}, \text{V/C, ADT}_{\text{hv}}, \text{wind})$$

$$\text{Cr} = f(\text{C, I, R, ADT}_{\text{to}}, \text{V/C, ADT}_{\text{hv}}, \text{wind})$$

$$\text{TSP} = f(\text{C, I, R, ADT}_{\text{to}}, \text{V/C, ADT}_{\text{hv}}, \text{wind})$$

Where;

C, I, R = the percentage of commercial, industrial and residential land uses within 1km radius from each sampling location;

ADT_{to} = the total average daily traffic from a traffic survey carried out in 2010 as given in Table 6-2;

ADT_{hv} = the total heavy duty traffic volume determined from a traffic survey carried out in 2010 as given in Table 6-2;

V/C = the traffic congestion predicted by GCCC as given in Table 4-1; and

Wind = the average measured wind speed for the sampling day.

For this analysis, percentage of different land use types (industrial commercial and residential) within 1km radius from each sampling site was calculated by considering distribution of different land uses. Zhu et al. (2002) noted that atmospheric small particle concentrations decreased noticeably when moving away from the traffic sources. It was determined from the data given by Zhu et al. (2002), that traffic generated small particle concentrations is only 5% above the background level at 1 km distance from the source. Therefore, 1 km radius was selected as the influential region. Percentages of different land uses within 1 km radius were determined based on Gold Coast City Council (GCCC) supplied data (Dur 2011).

Since the observed air quality is significantly different for weekdays and weekends, predictive equations were developed for weekday and weekend sampling separately. For this, the data was separated into two sets depending on weekday and weekend sampling and the analysis was undertaken accordingly.

Firstly, the analysis was carried out by including all of the variables. Then, redundant variables were gradually removed in the course of the analysis including the percentage of residential land use (R) and total average daily traffic (ADT_{to}). It needs to be noted that atmospheric heavy metal concentration depends on the total traffic volume, but its influence is small compared to ADT_{hv} and V/C. In other words, increase in heavy duty traffic volume and traffic congestion contributes high pollutant loads to the atmosphere whereas increase in normal traffic volume is not that significant. Additionally, the regression model is capable of identifying dependent variables and removing the least important as per the variability of the data set. It was also found that wind is a redundant variable for some heavy metals. Only the “Set 3” sites were used for the regression analysis, as traffic data is not available for “Set 1”. However, only seven sites were used to develop each regression equation and the remaining four sites from “Set 3” were used to validate each equation for HMs. In the case of TSP, seven sites were used to develop each regression equation and the remaining three sites were used to validate each equation, as Town Centre Drive is an outlier as identified in Figure 6-2.

Validation plots are given in Figure A-17 of Appendix A. The analysis was undertaken using SigmaPlot 11.0 software (SP 2008). Table 6-8 presents the equations derived. In Table 6-8, R is the regression coefficient and POT is the power of the test (SP 2008).

Table 6-8: Equations derived for HMs for weekdays and weekends

Equations (predicts values in $\mu\text{g}/\text{m}^3$)	R	POT
$\text{Zn}(\text{wk}) = 0.0346 - (0.0228 * \text{C}) + (0.0886 * \text{I}) + (0.166 * \text{V}/\text{C}) + (0.000529 * \text{ADT_hv}(\text{wk})) - (0.00841 * \text{wind}(\text{wk}))$	0.991	1
$\text{Zn}(\text{we}) = -0.0137 + (0.0103 * \text{C}) + (0.0187 * \text{I}) + (0.0435 * \text{V}/\text{C}) + (0.000593 * \text{ADT_hv}(\text{we})) - (0.00192 * \text{wind}(\text{we}))$	0.862	0.740
$\text{Pb}(\text{wk}) = 0.0946 + (0.141 * \text{C}) - (0.000735 * \text{I}) - (0.138 * \text{V}/\text{C}) - (0.000134 * \text{ADT_hv}(\text{wk}))$	0.870	0.761
$\text{Pb}(\text{we}) = -0.0331 - (0.0481 * \text{C}) + (0.00457 * \text{I}) + (0.000820 * \text{V}/\text{C}) + (0.000359 * \text{ADT_hv}(\text{we})) + (0.00146 * \text{wind}(\text{we}))$	0.95	0.966
$\text{TSP}(\text{wk}) = 86.737 + (464.940 * \text{C}) - (120.670 * \text{I}) + (72.242 * \text{V}/\text{C}) - (0.289 * \text{ADT_hv}(\text{wk}))$	0.952	0.959
$\text{TSP}(\text{we}) = 57.659 + (25.078 * \text{C}) - (13.691 * \text{I}) - (37.003 * \text{V}/\text{C}) - (0.0470 * \text{ADT_hv}(\text{we})) + (0.0274 * \text{wind}(\text{we}))$	0.958	0.97
$\text{Cu}(\text{wk}) = -0.00943 - (0.0303 * \text{C}) - (0.00266 * \text{I}) + (0.00967 * \text{V}/\text{C}) + (0.0000582 * \text{ADT_hv}(\text{wk}))$	0.801	0.595
$\text{Mn}(\text{wk}) = -116.792 + (398.623 * \text{C}) - (39.059 * \text{I}) - (50.077 * \text{V}/\text{C}) - (0.0764 * \text{ADT_hv}(\text{wk})) + (10.089 * \text{Wind})$	0.834	0.671
$\text{Mn}(\text{we}) = 0.0179 + (0.0502 * \text{C}) + (0.0188 * \text{I}) - (0.0104 * \text{V}/\text{C}) + (0.0000469 * \text{ADT_hv}(\text{we})) - (0.00108 * \text{Wind})$	0.908	0.859
$\text{Cu}(\text{we}) = -0.00436 - (0.00931 * \text{C}) + (0.00222 * \text{I}) - (0.000627 * \text{V}/\text{C}) + (0.000105 * \text{ADT_hv}(\text{we}))$	0.971	0.989
$\text{Cr}(\text{wk}) = -0.0270 - (0.0264 * \text{C}) - (0.0168 * \text{I}) + (0.0645 * \text{V}/\text{C}) + (0.0000768 * \text{ADT_hv}(\text{wk}))$	0.823	0.645
$\text{Cr}(\text{we}) = -0.0428 - (0.0378 * \text{C}) - (0.00191 * \text{I}) + (0.0152 * \text{V}/\text{C}) + (0.000130 * \text{ADT_hv}(\text{we})) + (0.00236 * \text{wind}(\text{we}))$	0.947	0.949

(Where C = % commercial, I = % industrial, V/C = traffic congestion, ADT_hv = average daily heavy duty traffic volume, wind = average wind speed, R: regression coefficient, POT= The power of the test) SigmaPlot 11.0 recommends the minimum desired power of test as 0.800.

Rubinfeld (1998) recommend using thirty data points to develop accurate multiple regression equations with 95% accuracy to predict population. However, only seven data points were used to develop the equations given above and validated against four data points for HMs and three for TSP. Consequently, the prediction accuracy could be below what is typically recommended. Furthermore, these equations are applicable only within the limits of the data set. These limits are, ADT_hv 1 - 1503, V/C 0.14 - 1.21, C 0.01 - 0.44 %, I 0 - 0.82 % and wind speed 11 - 23 m/s as shown in Table 6-2 and Table 4-1. However, as the methodology has already been

developed, the accuracy and the range of applicability can be increased with additional data.

6.6.2 Polycyclic aromatic hydrocarbons (PAHs)

Atmospheric concentration of PAHs is influenced mainly by land use, traffic characteristics and wind speed as discussed in Section 6.5. Multiple linear regression analysis was carried out to develop predictive equations for all 14 PAHs. It was assumed that the variability of PAHs can be predicted as a linear combination of land use, traffic parameters and wind speed in the form of:

PAHs =f(C, I, R, ADT_to, V/C, ADT_hv, wind).

Similar to heavy metals, a linear equation was considered as the simplest possible mathematical model to investigate the relationship between several independent or predictor variables and dependent or criterion variables.

Predictive equations were developed for weekday and weekend sampling separately as the variation of investigated PAHs was quite different. Firstly, the analysis was carried out with all of the variables and then the redundant variables were removed from the analysis. It was found that the percentage residential land use (R) and total average daily traffic (ADT_to) are redundant variables and removed from the analysis. Although the model considers ADT_to as redundant, atmospheric phase PAH concentrations depends on the ADT_to. This is because the influence of ADT_to on PAH concentrations is small compared to ADT_hv. In addition, as ADT_hv, ADT_to and V/C are interrelated to one another, interdependent and less influential variables were removed from the model. All “Set 3” sites were used for the regression analysis. However, only seven sites were used to develop each regression equation and the remaining four sites were used to validate each equation. The analysis was undertaken using SigmaPlot 11.0 software (SP 2008). Table 6-9 and Table 6-10 presents the equations derived for weekdays and weekends respectively.

Table 6-9: Equations derived for weekday PAHs

Equations –weekdays (predicts values in ng/m ³)	R	POT
ACY (fp) = -1.769 + (4.284 * C) + (1.140 * I) + (1.412 * V/C) - (0.000786 * ADT_hv) + (0.108 * wind)	0.892	0.817
ACE (fp) = 0.384 + (3.139 * C) - (3.063 * I) + (3.187 * V/C) - (0.00187 * ADT_hv) + (0.0397 * wind)	0.999	1
FLU (fp) = 18.209 - (5.001 * C) - (8.643 * I) + (0.582 * V/C) - (0.0205 * ADT_hv) - (0.461 * wind)	0.909	0.861
ANT(fp) = -3.345 - (9.751 * C) + (1.106 * I) - (3.525 * V/C) + (0.0170 * ADT_hv) + (0.195 * wind)	0.909	0.861
PHE(fp) = 1.245 + (0.332 * C) - (1.170 * I) + (1.129 * V/C) - (0.00211 * ADT_hv) - (0.0371 * wind)	0.995	1
PYR(fp) = 4.522 - (0.361 * C) - (5.011 * I) + (0.959 * V/C) - (0.00238 * ADT_hv) - (0.0799 * wind)	0.995	1
FLA(fp) = 4.690 - (4.144 * C) - (5.564 * I) - (4.019 * V/C) + (0.00988 * ADT_hv) - (0.0405 * wind)	0.876	0.776
BaA(fp) = 3.152 - (0.419 * C) - (0.111 * I) - (0.392 * V/C) - (0.00178 * ADT_hv) - (0.102 * wind)	0.961	0.975
CHR(fp) = 1.563 + (0.200 * C) - (0.140 * I) - (1.177 * V/C) + (0.000872 * ADT_hv) - (0.0498 * wind)	0.824	0.647
BaP(fp) = 3.943 + (0.211 * C) - (2.472 * I) - (0.107 * V/C) - (0.000899 * ADT_hv) - (0.0249 * wind))	0.996	1.00
BeP(fp) = 7.159 - (1.477 * C) - (0.241 * I) + (1.984 * V/C) - (0.000862 * ADT_hv) - (0.273 * wind)	0.943	0.942
DbA(fp) = 2.638 - (0.262 * C) + (1.535 * I) + (0.384 * V/C) - (0.00161 * ADT_hv) - (0.0358 * wind)	0.998	1
BgP(fp) = 3.123 + (0.270 * C) - (1.795 * I) - (0.0649 * V/C) + (0.0000383 * ADT_hv) - (0.000497 * wind)	1	1
IND(fp) = 1.609 - (0.360 * C) + (6.945 * I) + (1.424 * V/C) + (0.00190 * ADT_hv) - (0.0801 * wind)	0.985	0.998
ACY(puf)= 0.913 - (0.450 * C) - (0.807 * I) + (2.662 * V/C) - (0.00151 * ADT_hv) - (0.0305 * wind)	0.934	0.923
ACE(puf)= -3.397 + (18.115 * C) - (6.235 * I) - (0.215 * V/C) - (0.0272 * ADT_hv) + (0.750 * wind)	0.998	1
FLU(puf)=10.946 + (19.124 * C) - (2.608 * I) - (2.274 * V/C) - (0.00261 * ADT_hv) - (0.386 * wind)	0.577	0.260
ANT(puf)= 35.125 + (16.884 * C) - (10.864 * I) - (11.132 * V/C) - (0.00992 * ADT_hv) - (1.339 * wind)	0.755	0.503
PHE(puf)= -37.301 + (49.440 * C) + (8.633 * I) - (2.723 * V/C) + (0.00203 * ADT_hv) + (1.846 * wind)	0.957	0.968
PYR(puf)=-12.862 + (31.972 * C) + (1.143 * I) - (1.255 * V/C) - (0.000436 * ADT_hv) + (0.658 * wind)	0.933	0.920
FLA(puf)=6.175 + (31.258 * C) - (6.819 * Col 68) - (9.423 * V/C) - (0.000585 * ADT_hv) + (0.0126 * wind)	0.939	0.933
BaA(puf)= 12.344 + (0.279 * C) - (5.955 * Col 75) + (0.186 * V/C) - (0.00934 * ADT_hv) - (0.443 * wind)	0.989	0.999
CHR(puf)= 3.348 + (1.164 * C) - (1.584 * I) - (2.172 * V/C) + (0.00139 * ADT_hv) - (0.117 * wind)	0.892	0.818
BaP(puf)= 8.497 - (0.576 * C) - (6.703 * I) - (0.136 * V/C) - (0.00707 * ADT_hv) - (0.134 * wind)	0.994	1.00
BeP(puf)= 8.603 - (0.431 * C) - (6.765 * I) - (0.177 * V/C) - (0.00738 * ADT_hv) - (0.132 * wind)	0.993	1
DbA(puf)=0.430 + (2.090 * C) - (0.452 * I) + (0.807 * V/C) + (0.000975 * ADT_hv) + (0.0238 * wind)	0.897	0.830
BgP(puf)=-1.514 + (5.198 * C) - (2.670 * I) + (3.420 * V/C) - (0.000212 * ADT_hv) + (0.172 * wind)	0.954	0.964
IND(puf)= 6.419 + (1.870 * C) - (1.873 * I) + (0.700 * V/C) - (0.00865 * ADT_hv) - (0.0969 * wind)	0.690	0.397

(Where C = % commercial, I = % industrial, V/C = traffic congestion, ADT_hv = average daily heavy duty traffic volume, wind = average wind speed, fp = filter paper, puf = polyurethane foam, R = regression coefficient, POT = power of the test) SigmaPlot 11.0 recommends the minimum desired power of test as 0.800.

Table 6-10: Equations derived for weekend PAHs

Equations -weekends(predicts values in ng/m ³)	R	POT
ACY(fp) = -1.337 + (1.512 * C) + (2.424 * I) + (2.491 * V/C) + (0.00261 * ADT_hv) + (0.0364 * wind)	0.989	0.999
ACE(fp) = 6.983 - (19.232 * C) - (11.417 * I) + (3.360 * V/C) - (0.0344 * Col 35) + (0.180 * wind)	0.889	0.810
FLU(fp) = 4.534 + (13.481 * C) - (2.353 * I) - (2.173 * V/C) - (0.00548 * ADT_hv) - (0.188 * wind)	0.946	0.947
ANT(fp) = 0.447 - (2.742 * C) - (0.241 * I) - (1.550 * V/C) + (0.0148 * ADT_hv) - (0.000533 * wind)	1	1
PHE(fp) = 1.981 + (2.725 * C) - (1.178 * I) + (0.210 * V/C) - (0.00387 * ADT_hv) - (0.0869 * wind)	0.893	0.819
PYR(fp) = 6.650 + (2.650 * C) - (6.099 * I) - (2.989 * V/C) - (0.0113 * ADT_hv) - (0.0885 * wind)	0.974	0.991
FLA(fp) = 3.374 - (1.007 * C) - (3.327 * I) - (1.949 * V/C) + (0.0187 * ADT_hv) - (0.0682 * wind)	0.993	1
BaA(fp) = 2.767 + (5.366 * C) + (0.326 * I) - (1.056 * Col 76) + (0.00146 * ADT_hv) - (0.189 * wind)	0.999	1
CHR(fp) = 0.0704 - (0.428 * C) + (0.0839 * I) - (0.551 * V/C) + (0.00422 * ADT_hv) - (0.00167 * wind)	0.996	1
BaP(fp) = 2.677 - (0.630 * C) - (0.277 * I) + (0.00592 * V/C) - (0.000262 * ADT_hv) + (0.0374 * wind)	0.923	0.895
BeP(fp) = 3.401 + (9.569 * C) - (0.809 * I) - (0.608 * V/C) + (0.00329 * ADT_hv) - (0.153 * wind)	0.745	0.486
DbA(fp) = 2.030 + (0.636 * C) - (0.850 * I) - (0.794 * V/C) + (0.00108 * ADT_hv) - (0.000278 * wind)	0.909	0.860
BgP(fp) = 3.088 + (0.0140 * C) - (0.0277 * I) - (0.0216 * V/C) + (0.000137 * ADT_hv) + (0.000542 * wind)	0.955	0.966
IND(fp) = 2.488 + (4.856 * C) - (0.391 * I) - (0.0759 * V/C) - (0.0000671 * ADT_hv) - (0.112 * wind)	0.565	0.248
ACY(puf) = 7.466 + (14.790 * C) - (0.260 * I) - (2.235 * V/C) - (0.00363 * ADT_hv) - (0.436 * wind)	0.831	0.663
ACE (puf) = 0.276 + (29.236 * C) - (0.714 * I) + (6.169 * V/C) + (0.00650 * ADT_hv) - (0.195 * wind)	0.968	0.984
FLU(puf) = 4.668 - (2.783 * C) - (5.645 * I) + (12.373 * V/C) - (0.0195 * ADT_hv) - (0.177 * wind)	0.995	1
ANT(puf) = -1.915 + (0.777 * C) - (2.441 * I) - (13.221 * V/C) + (0.0591 * ADT_hv) + (0.429 * wind)	0.957	0.969
PHE(puf) = 17.342 + (23.761 * C) + (9.935 * I) + (9.025 * V/C) + (0.00283 * ADT_hv) - (1.478 * wind)	0.990	1
PYR(puf) = 8.382 + (29.340 * C) + (3.177 * I) + (0.112 * V/C) + (0.0237 * ADT_hv) - (0.692 * wind)	0.954	0.964
FLA(puf) = 12.035 + (16.063 * C) + (5.547 * I) - (5.522 * V/C) + (0.0402 * ADT_hv) - (0.641 * wind)	0.943	0.941
BaA = -0.910 - (5.610 * C) - (1.798 * I) - (0.409 * V/C) + (0.00227 * ADT_hv) + (0.160 * wind)	0.973	0.990
CHR(puf) = 0.897 + (0.502 * C) + (1.073 * I) - (0.890 * V/C) + (0.0138 * ADT_hv) - (0.0899 * wind)	0.990	1
BaP(puf) = 3.080 - (0.00262 * C) + (0.0163 * I) - (0.00610 * V/C) + (0.000155 * ADT_hv) - (0.00101 * wind)	0.988	0.999
BeP(puf) = 3.139 + (0.0408 * C) + (0.0150 * I) - (0.0291 * V/C) + (0.000177 * ADT_hv) - (0.00234 * wind)	0.951	0.957
DbA(puf) = 2.615 + (1.374 * C) + (0.668 * I) + (0.909 * V/C) - (0.00150 * ADT_hv) - (0.0585 * wind)	0.991	1
BgP(puf) = 12.612 + (21.273 * C) + (7.207 * I) - (0.106 * V/C) + (0.00807 * ADT_hv) - (0.837 * wind)	0.945	0.947
IND(puf) = 6.251 + (9.468 * C) + (3.752 * I) + (0.650 * V/C) + (0.000749 * ADT_hv) - (0.401 * wind)	0.973	0.990

(Where C = % commercial, I = % industrial, V/C = traffic congestion, ADT_hv = average daily heavy duty traffic volume, wind = average wind speed, fp = filter paper, puf = polyurethane foam, R = regression coefficient, POT= power of the test) SigmaPlot 11.0 recommends the minimum desired power of test as 0.800.

As already discussed for heavy metal, there are limitations in the derived equations for PAHs as well. Firstly, the equations are applicable only within the limits of data used for derivation. These limits are already defined for HMs and TSP and they are the same for PAHs. Secondly, as only seven data points were used to develop the equations and validated with four data points, prediction accuracy could be below what is typically recommended. However, the methodology has already been developed, the accuracy and the range of applicability can be increased with additional data. Validation plots are given in Figure A-17 of Appendix A. When equations predict negative values, it needs to be considered as zero.

6.6.3 Prediction of overall air quality

In order to identify the most polluted locations in relation to the atmospheric phase, it is necessary to have a model to predict the overall air quality by combining investigated PAH and HM concentrations. This is important for the development of management strategies in relation to air quality as well as urban stormwater quality. Also, the prediction model can be used to investigate the variability of air quality under different traffic and land use scenarios.

For this analysis, a data matrix was developed by including C, I, V/C, ADT_hv, wind speed. The data matrix developed considered all possible combinations of these parameters. For example, C can take one of three values (minimum, average or maximum) and I, V/C, ADT_hv and wind speed also can take one of three values. Therefore, there are 33 different ways to arrange 5 variables in a row while each variable can take one of three values in arranging them in a row. Therefore, the number of combination in the matrix was 33 as there are five variables and three data values for each variable. The resulting data matrix is given in Table A-19 of Appendix A. In these 33 combinations, there were 7 combinations with the addition of percentage commercial and industrial land uses are greater than 1. As this is not

possible, they were removed from the analysis (indicated in italic font in Table A-19 of Appendix A). The percentage of all three land uses were calculated by considering 1 km radius around the sampling point and assuming addition of all three land uses is equal to 1 (Dur 2011).

Accordingly, 5 heavy metals in the particulate phase and 14 PAHs in the gas and particulate phases were predicted using the equations derived for all 26 (33-7) combinations for weekends and weekdays, separately. They were combined by assuming similar variation within weekdays and weekends separately. Subsequently, all the 26 combinations in the data matrix were ranked using PROMETHEE 2 complete ranking based on predicted heavy metals and PAHs. In order to understand the influence of C, I, V/C, ADT_hv and wind on the atmospheric phase HM and PAH concentrations, 26 objects were ranked as shown in Table 6-11. This was carried out by arranging 26 different combinations as per the ranking order developed based on predicted heavy metals and PAHs concentrations. This was to identify the most influential parameters on air quality.

Table 6-11: Ranking of influential parameters

C	I	V/C	ADT_hv	wind speed (m/s)	Comment
0.45	0.17	1.21	1503	23	The most polluted
0.17	0.83	1.21	1503	23	
0.01	0.83	1.21	1503	23	
0.45	0.00	1.21	1503	23	
0.17	0.17	0.52	1503	18	
0.17	0.17	0.52	1503	23	
0.01	0.00	0.14	1503	23	
0.01	0.00	0.14	1503	11	
0.17	0.17	1.21	391	18	
0.45	0.17	0.52	391	18	
0.01	0.00	0.14	391	11	
0.17	0.00	0.52	391	18	
0.17	0.17	0.52	391	18	
0.01	0.17	0.52	391	18	
0.17	0.83	0.52	391	18	
0.01	0.00	0.14	391	18	
0.17	0.17	0.14	391	18	
0.01	0.00	1.21	6	11	
0.45	0.00	0.14	6	11	
0.17	0.00	0.14	6	11	
0.01	0.00	0.52	6	11	
0.01	0.00	0.14	6	11	
0.17	0.17	0.52	6	11	
0.01	0.17	0.14	6	11	
0.17	0.17	0.52	6	18	
0.01	0.83	0.14	6	11	The least polluted

Table 6-11 shows the correlation of V/C, ADT_hv and wind with the highly polluted sites. However, as variation of wind is from 11 to 23, it is difficult to assess the influence of wind. This indicates that V/C, ADT_hv are the most influential parameters for atmospheric phase HMs and PAHs. This is an important outcome as atmospheric phase HM and PAH concentrations can be reduced by reducing traffic congestion and the volume of heavy duty traffic. Additionally, although the percentage of commercial and industrial land uses are also influential variables, they do not show any clear pattern with the sequence of highly polluted sites as evident in Table 6-11.

In order to understand the limits of variation of investigated HMs and PAHs due to all the possible combination of C, I, V/C, ADT_hv, the outcomes were summarised as shown in Table 6-12. As there are 26 predicted concentrations for each pollutant type, the minimum, average and maximum of each pollutant was calculated. This was to investigate the variation of each pollutant with the variation of influential parameters. In the case of PAHs, individual PAHs were multiplied by toxic equivalent factors defined by Li et al. (2003) and Yu et al. (2007), in order to convert them to equivalent concentration of BaP. In principle, carcinogenic potential of a given PAH can be estimated on the basis of its equivalent concentration of BaP (Li et al. 2003). BaP is one of the most toxic PAHs (Li et al. 2003). The summary Table 6-12 can be used to identify the limits of variability for heavy metals and equivalent BaP concentrations due to all possible combinations of C, I, V/C, ADT_hv and wind.

Table 6-12: Variability of HMs and PAHs

	Heavy metals					PAHs in terms of BaP (ng/m ³)	
	Zn (µg/m ³)	Pb (µg/m ³)	Cu (µg/m ³)	Mn (µg/m ³)	Cr (µg/m ³)	BaP (Particulate)	BaP (Gas)
Minimum	0.00	0.00	0.00	0.00	0.00	0.9	2.0
Average	0.33	0.12	0.03	0.07	0.07	4.8	5.6
Maximum	0.86	0.27	0.07	0.19	0.19	8.0	11.0

Table 6-11 shows that gas phase is the critical in terms of BaP equivalent toxicity compared to particulate phase PAHs. This suggests that gas phase is relatively highly polluted with toxic PAHs in the Gold Coast area. Therefore, wet deposition is the most critical in terms of toxic PAHs as gas phase PAHs mainly deposit with the wet deposition rather than dry deposition. However, as the average values of BaP equivalent toxicity PAHs are 4.8 and 5.6 (ng/m³), dry deposition can also make an important contribution to toxic PAHs.

6.7 Conclusions

The following primary conclusions were derived from the data analysis undertaken:

- Weekday TSP concentrations show positive correlation with traffic. Therefore, traffic is the main source of atmospheric phase TSP during weekdays. However, as other sources such as land uses are dominant during

weekends, the contribution of both traffic and land use related sources on atmospheric TSP is important.

- Zn has the highest concentration in the atmospheric phase during weekends as well as weekdays compared to the investigated heavy metals. It was found that traffic related emissions are the primary source of Zn to the atmosphere.
- Although the usage of leaded gasoline was stopped a decade ago, Pb was the second most detected heavy metal. This is attributed to the association of previously generated Pb with roadside soil and re-suspension to the atmosphere and the emission of Pb by traffic related abrasion products.
- Traffic is the primary gas phase PAH source, whereas traffic and land use related emissions are the main sources for particulate bound PAHs in the Gold Coast area. Atmospheric phase PAH concentrations are not highly influenced by wind at the study sites.
- Exhaust emissions is the main source of PAHs to the atmosphere, whereas all traffic related sources such as exhaust, tyre and brake wear contribute to the atmospheric phase heavy metal concentrations.
- Diesel vehicles generate three to six ring PAHs depending on the operating conditions, whereas gasoline vehicles always generate 4-5 ring PAHs.
- Weekday and weekend HM and PAH concentrations can be predicted using the equations derived. These equations can be used to identify critical areas in terms of the presence of PAHs and HMs.
- Although traffic is the main source of atmospheric PAHs and HMs, traffic congestion (V/C), and heavy duty traffic volume (ADT_{hv}) are the most appropriate traffic parameters to predict atmospheric phase HM and PAH concentrations as per the regression analysis undertaken.

Chapter 7 - Analysis of Atmospheric Deposition

7.1 Background

Vehicle generated pollutant transport pathways can be broken down to a series of sub-processes, depending on the sequence of occurrence. They are atmospheric pollutant build-up, atmospheric deposition, pollutant build-up on land surfaces and wash-off. Chapter 6 focused on the analysis of air quality in order to define atmospheric pollutant build-up. This Chapter presents the outcomes of the atmospheric deposition investigations. The outcomes of this chapter will be used for pollutant build-up analysis which is presented in the following chapter.

Atmospheric deposition is one of the key processes responsible for stormwater pollution. Atmospheric deposition can occur in the form of wet or dry deposition and provides pathways for atmospheric pollutants to contribute to stormwater pollutant loads. Both these processes primarily depend on the amounts and characteristics of pollutants present in the atmosphere (Sabin et al. 2005). Urban traffic and anthropogenic activities specific to land uses are the key factors that influence the amounts and characteristics of pollutants present in the atmosphere and hence atmospheric depositions. Furthermore, due to the time dependent nature of pollutants in the atmosphere, atmospheric depositions can also be influenced by antecedent dry days (Sabin and Schiff 2008; Luo 2001). Detailed discussion on past research in relation to atmospheric pollutants and its linkage to traffic and land use is provided in Chapter 2.

Variations of atmospheric deposition with influential parameters such as the antecedent dry period, traffic characteristics and land use have not been explicitly investigated to-date. It is important to undertake in-depth investigations in order to establish a relevant knowledge base to generate enhanced stormwater quality treatment outcomes. Despite the common understanding that atmospheric deposition is related to atmospheric pollutant concentration and the intensity of the sources of emission, definitive relationships have not yet been experimentally established.

7.2 Field investigations

7.2.1 Study sites

Field investigations relevant for this study were conducted at two sets of study sites at the Gold Coast, South East Queensland. The first set is from highly urbanised areas (referred to as “Set 1”) with a varied range of urban activities. Locations of these sites and dominant land uses are given in Table 7- 1. The second set is four typical suburban road sites (referred to as “Set 2”) with variable traffic characteristics. Locations and traffic data for the selected road sites are given in Table 7- 2. For all the sites, multiple atmospheric deposition samples were collected to reflect the variability of atmospheric deposition with the antecedent dry period. The sample collection and testing was conducted as described in Chapter 5.

Table 7-1: The selected “Set 1” sites

Site name	Land use activity
Southport Library (So)	Close proximity to an urban centre with commercial and industrial activities
Miami Depot (Mi)	Close proximity to an urban centre with residential, commercial and industrial activities
Highland Park (Hi)	Residential activities in close proximity to a major highway
Yatala (Ya)	Industrial activities in close proximity to a major highway

Southport Library (So) and Miami Depot (Mi) sites are located close to major traffic areas. Highland Park (Hi) is a typical residential suburb, but in close proximity to a major highway and other traffic generating amenities. Even though Yatala (Ya) is located in a relatively less congested industrial area, it is also in close proximity to a major highway. Further details of the study sites are available in Chapter 4.

Table 7-2: The selected “Set 2” sites

Sites with different traffic characteristics		
Site Name	Average Daily Traffic	Land use
Abraham Road (Ab)	8742	Commercial
Reserve Road (Re)	10027	Residential
Discovery Drive (Di)	10690	Residential
Beattie Road (Be)	4633	Industrial

The average annual daily traffic data given in Table 7-2 was obtained from a traffic survey carried out in 2010. These four sites were selected to represent the typical spectrum of traffic characteristics of the two study suburbs of Coomera and Helensvale. A summary of traffic data and the list of road sites considered for selection are given in Table B-1 of Appendix B.

7.2.2 Field sampling and testing

As described in Section 3.3.2 of Chapter 3, the wet and dry deposition sampling apparatus developed by Hill and Caritat (2002) was adapted for this study. Dry deposition is the sampling of atmospheric deposition collected during dry periods. Wet plus dry deposition samples are referred to as bulk deposition (Huston et al. 2009). Both, bulk and dry deposition collectors were installed at the same time immediately after a rainfall event, as the atmospheric pollutant load is minimal at this stage (Ravindra et al. 2003). One sampling head was used to collect dry deposition and the other head was used to collect bulk deposition. Dry deposition samples were collected for 3, 4, 5, 6, and 7 day antecedent dry periods from all the study sites. Bulk deposition sampling was conducted at all the sampling sites for three rainfall events.

Both, bulk and dry deposition samples were tested for a suite of water quality parameters as described in Chapter 5. The parameters were: (1) Total suspended solids (TSS) and total dissolved solids (TDS); (2) Particle size distribution (PSD); (3) Total organic carbon (TOC); and (4) Heavy metals (Zn, Cd, Cr, Cu, Mn, Ni and Pb). These water quality parameters were selected based on the detailed literature review carried out which is given in Chapter 2. Analytical test methods used and quality

control and quality assurance procedure followed are given in Chapter 5. Test results were subjected to data pre-treatment and analysis as discussed in this Chapter.

Due to the significant differences in traffic and land use characteristics, data from “Set 1” and “Set 2” sites were arranged into two separate matrices. As five sampling events were undertaken at each site (for 3, 4, 5, 6, and 7 day of antecedent dry periods) covering 4 sites with each data matrix having a maximum of 20 objects. Apart from the above mentioned chemical parameters, exploratory variables such as antecedent dry period (ADP), average daily traffic volume (ADT_{to}) and traffic congestion (V/C) were included in the “Set 2” data matrix.

7.3 Physical characteristics of atmospheric deposition

Dry deposition and bulk deposition samples were analysed separately. Each analysis focused primarily on physical and chemical characteristics of atmospheric deposition. Firstly, data analysis was undertaken to investigate the variation of atmospheric deposition with the antecedent dry period and rainfall characteristics. Secondly, extensive data analysis was conducted to determine the variability of atmospheric deposition with urban traffic and land use characteristics.

Prior to the data analysis, a description of data pre-processing techniques used is presented. Firstly, analysis was undertaken using graphical methods to understand the trends and patterns in the data set. Secondly, multivariate analytical techniques were used to understand and define the influence of traffic and land use on atmospheric deposition. Thirdly, key findings were generalised by relating them to actual field characteristics and comparing them with similar studies. Finally, important conclusions were derived based on the outcomes from the data analysis.

7.3.1 Data pre-treatment

As discussed in Chapter 4, atmospheric deposition samples were collected in the liquid matrix. Therefore, most of the results obtained from laboratory tests were in the form of concentrations (mg/L). The concentration data was pre-treated prior to the analysis. The steps adopted for pre-treatment were as follows:

1. Outliers were removed from the matrix prior to the analysis. Outliers were detected using detection tools available in Sirius 8 software (PRS 2009). As explained in the user manual, isolated objects in one or several projections of score plots are defined as potential outliers. The residual standard deviation (RSD) and leverage are checked as low RSD and high leverage indicate possible outliers (PRS 2009).
2. Concentration data was converted to total solid loads (mg) by multiplying the sample concentration by the corresponding sample volume.
3. Total solids loads were converted to solids loads per unit area (mg/m^2) based on the sampling area which was the area of the collection funnel of the sampling apparatus. The data derived also helped to compare the results with similar investigations undertaken in the past.

7.3.2 Data analysis

For the data analysis, univariate and multivariate statistical tools were used by carefully considering the type of analysis to be carried out and capabilities of the available analytical tools. For multivariate analysis, The Multi Criteria Decision method, PROMETHEE 2 (Preference Ranking Organisation Method for Enrichment Evaluation) and GAIA were used for the analysis. Detailed discussions of multivariate analytical methods are given in Section 3.4.3.

7.3.3 Dry deposition

Dry deposition is a process which involves the transport and removal of aerosol from the atmosphere and deposition on surfaces in the absence of rainfall. Though Jolliet and Hauschild (2005) proposed a conceptual model to predict atmospheric deposition, there is no widely accepted methodology available to describe the variation of atmospheric deposition with influential variables such as antecedent dry days, traffic volume and land use. The lack of robust methodology is primarily attributed to the variability of atmospheric deposition and atmospheric processes with other variables such as climatic conditions (Luo 2001).

In order to understand the influence of antecedent dry period, traffic and land use on dry deposition, the solids loads recovered from each sampling episode were plotted

against the number of antecedent dry days as presented in Figure 7-1. As evident in Figure 7-1, dry deposition varies from 50 mg/m² to 758 mg/m² depending on the land use and antecedent dry days.

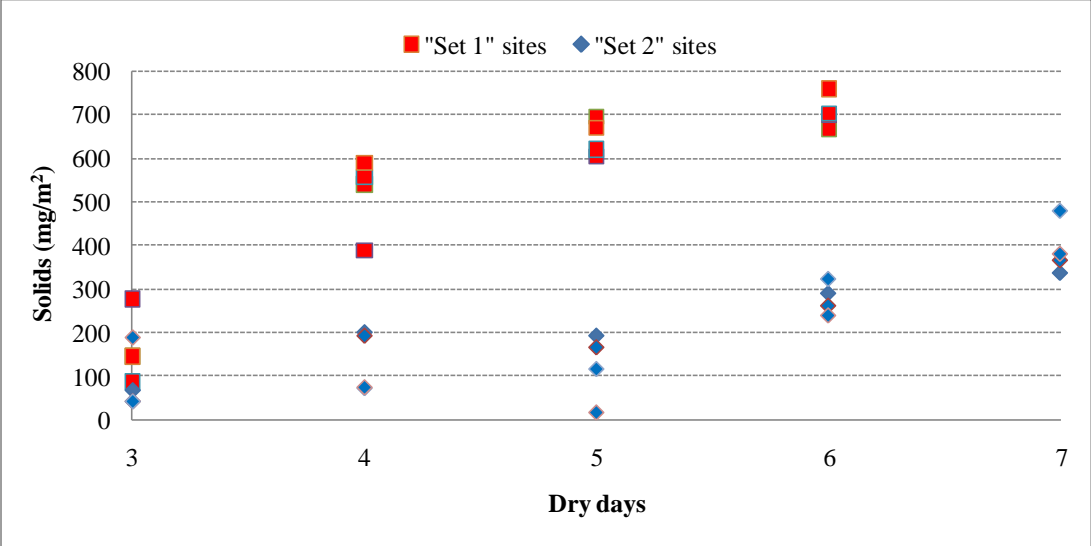


Figure 7-1: Variation of dry deposition with antecedent dry days

Distinct variations between “Set 1” and “Set 2” sites indicate that dry deposition is strongly influenced by differences in traffic and land use activities common to “Set 1” and “Set 2” sites. Dry deposition varies from about 100 mg/m² to 758 mg/m² for “Set 1” sites and from about 50 to 480 mg/m² for “Set 2” sites. As noted by Sabin et al. (2005), the dry deposition is highly influenced and often proportional to the atmospheric pollutant concentration. Based on the differences in dry deposition between “Set 1” and “Set 2” sites, it is clear that the traffic and land use activities at “Set 1” sites generate atmospheric pollutants at a significantly higher rate compared to “Set 2” sites and thereby maintain high atmospheric pollutant concentrations. Also, it was noted in Chapter 6 that atmospheric particulate matter concentrations at “Set 1” sites were high and for some sites it was as high as double of “Set 2” values.

Increase in dry deposition with antecedent dry days is postulated to be due to the increase in atmospheric pollutant concentrations (Lim et al. 2006; Sabin et al. 2005). This can be explained in three steps. Firstly, rainfall scavenges pollutants from the atmosphere. Pollutants then keep accumulating in the atmosphere during the antecedent dry period. As evident in Table 7-3, with the increase in antecedent dry

days, the dry deposition rate also increases. This suggests that the atmosphere has a finite capacity to hold pollutants. Table 7-3 was prepared for “Set 2” sites by averaging the dry deposition data collected at four sites.

Table 7-3: Comparison of metrological condition on dry deposition

Dry days	Total average dry deposition (mg/m ²)	Average dry deposition rate (mg/m ² /day)	Temp. (°C)	Relative Humidity	Wind Speed (km/hr)	Direction
3	84.40	28.13	23.09	58.11	19.15	NNE
4	134.55	33.64	19.33	77.06	13.62	N
5	122.61	24.52	17.20	85.00	8.50	WSW
6	278.03	46.34	19.13	56.89	19.89	S
7	390.16	55.74	21.88	73.34	17.21	S

Even though “Set 2” sites were selected by considering the variability in traffic, no appreciable variation in dry deposition is seen among these sites as shown in Figure 7-1. There are two possible reasons for this behaviour: (1) transport of particulates from nearby sources to these areas by natural processes such as wind; (2) rapid redistribution of traffic generated pollutants by dispersion processes. Particulates could be transported by wind to Coomera and Helensvale areas from surrounding land use related activities and traffic emissions from adjacent roads. Therefore, these processes would tend to create a uniform pollutant concentration over a large area despite differences in traffic characteristics. Although the study sites were selected by considering the variation in traffic volume, the variability in traffic is not high enough to be able to discriminate between sites on the basis of traffic volume.

As the traffic congestion is relatively higher at most of the “Set 1” sites, the traffic generated emissions are also considerably higher in those areas. These sites are located close to traffic bottlenecks such as road intersections. Consequently, the traffic speed is considerably reduced resulting in higher emissions. Therefore, it is logical to have higher dry deposition rates at “Set 1” sites as illustrated in Figure 7-1.

The data analysis revealed that dry deposition is significantly lower during one sampling event as shown in Table 7-3. Total dry deposition of 122.61 mg/m² occurred for a 5 day sampling event as shown in Table 7-3 and the lowest wind speed of 8.5 km/hr was also recorded during this sampling event. Investigations were

undertaken to assess whether there is a clear relationship between this event and climate parameters. The minimum dry deposition occurred when the wind speed was minimal. Therefore, it can be concluded that the wind plays an important role in the distribution of particulates to “Set 2” sites (Coomera and Helensvale area) from the other areas. Alphen (1999) confirmed that climate parameters can exert a strong influence on atmospheric deposition.

7.3.4 Bulk deposition

The combination of wet and dry deposition is referred to as bulk deposition in research literature (Huston et al. 2009; Durst et al. 1991). The same terminology is used in this study with the summation of the dry deposition during the dry period preceding the rain event and the wet deposition termed as bulk deposition. A preliminary data analysis revealed that there is no clear relationship between bulk deposition and antecedent dry days. Therefore, it was decided to investigate other influential parameters such as rainfall depth. Figure 7-2 shows the variation of bulk deposition with rainfall depth. Recorded rainfall values are very small for some sampling events and they appear close to the rainfall depth axis in Figure 7-2.

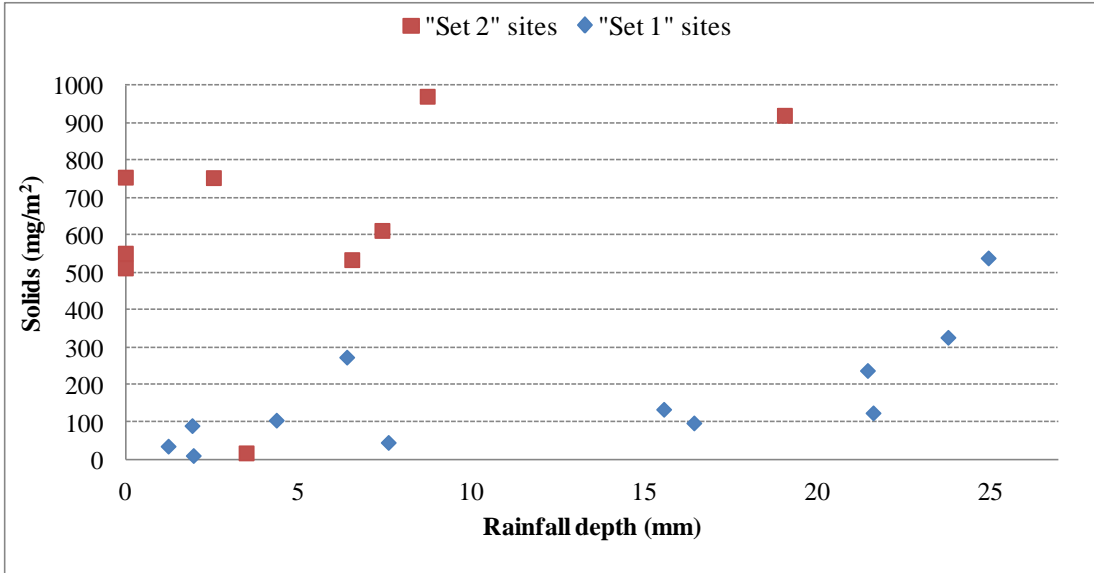


Figure 7-2: Variation of bulk deposition with rainfall depth for set 1 sites and set 2 sites

As shown in Figure 7-2, two distinct clusters for “Set 1” and “Set 2” sites can be identified. Therefore, it can be postulated that bulk deposition is dependent on the

intensity of anthropogenic activities. As “Set 1” sites have relatively poorer air quality compared to “Set 2” sites, rainfall has brought down a relatively larger amount of particulates from the atmosphere. Croft et al. (2009) found that wet deposition process is very efficient in removing atmospheric particulate matter.

As evident in Figure 7-2, bulk deposition can be considered as having an approximately linear relationship with the rainfall depth for the measured range of rainfall events. For “Set 2” sites, bulk deposition has varied from 10.6 mg/m² to around 539 mg/m² when the rainfall depth varies from about 1.2 mm to 25 mm and for “Set 1” sites, bulk deposition has varied from 17.7 mg/m² to around 971.4 mg/m² when the rainfall depth varies from about 2.5 mm to 19 mm. It is clear that small rainfall events can remove only a part of the atmospheric pollutant load. However, large rainfall events are capable of removing a considerable amount of pollutants from the atmosphere. This is attributed to the fact that smaller particulate matter can combine with rainfall droplets and come down as wet deposition (McLachlan & Sellström 2009).

7.3.5 Physical characteristics of atmospheric deposition

It is hypothesised that depending on traffic characteristics, land use and influential climate variables, atmospheric deposition can vary in terms of load as well as in physical characteristics. Consequently, analysis was undertaken to investigate the physical characteristics in the form of variations in particle size distributions.

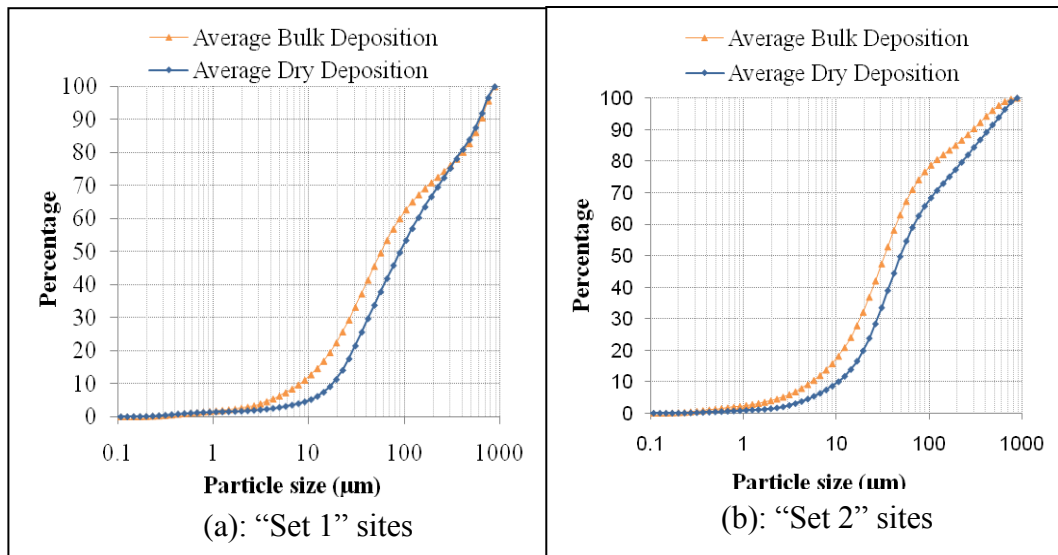


Figure 7-3: Cumulative average particle size distribution

Initially, the PSD data were combined and averaged separately for “Set 1” and “Set 2” for each set of sites as shown in Figure 7-3. As evident in Figure 7-3, bulk deposition contains a higher amount of smaller particles compared to dry deposition. Only 10% of dry deposition particles are below 10 μm , whereas around 18% of bulk deposition particles are below 10 μm . This is attributed to the ability of rainfall events to scavenge fine particles. Croft et al. (2009) found that rainfall has the ability to efficiently remove particles with diameter less than 0.2 μm .

Based on Figure 7-3, it can be noted that the separation of bulk and dry deposition particle size distribution curves starts around 1 μm diameter. In order to explain this behaviour, the maximum and minimum limits for 1% difference between bulk deposition and dry deposition for “Set 1” and “Set 2” sites was determined. These were 2.2 μm to 296.9 μm and 0.6 μm to 742.5 μm for “Set 1” and “Set 2” sites, respectively. Within these limits, bulk deposition particles are smaller than dry deposition by more than 1%. The average of 2.2 μm and 0.6 μm (1.4 μm) can be considered as the starting point of the separation.

As there is a clear separation of particle size distribution of bulk and dry deposition samples as evident in Figure 7-3, comparison of particle size distributions was undertaken for average dry and bulk deposition samples from each site for further in-depth investigations.

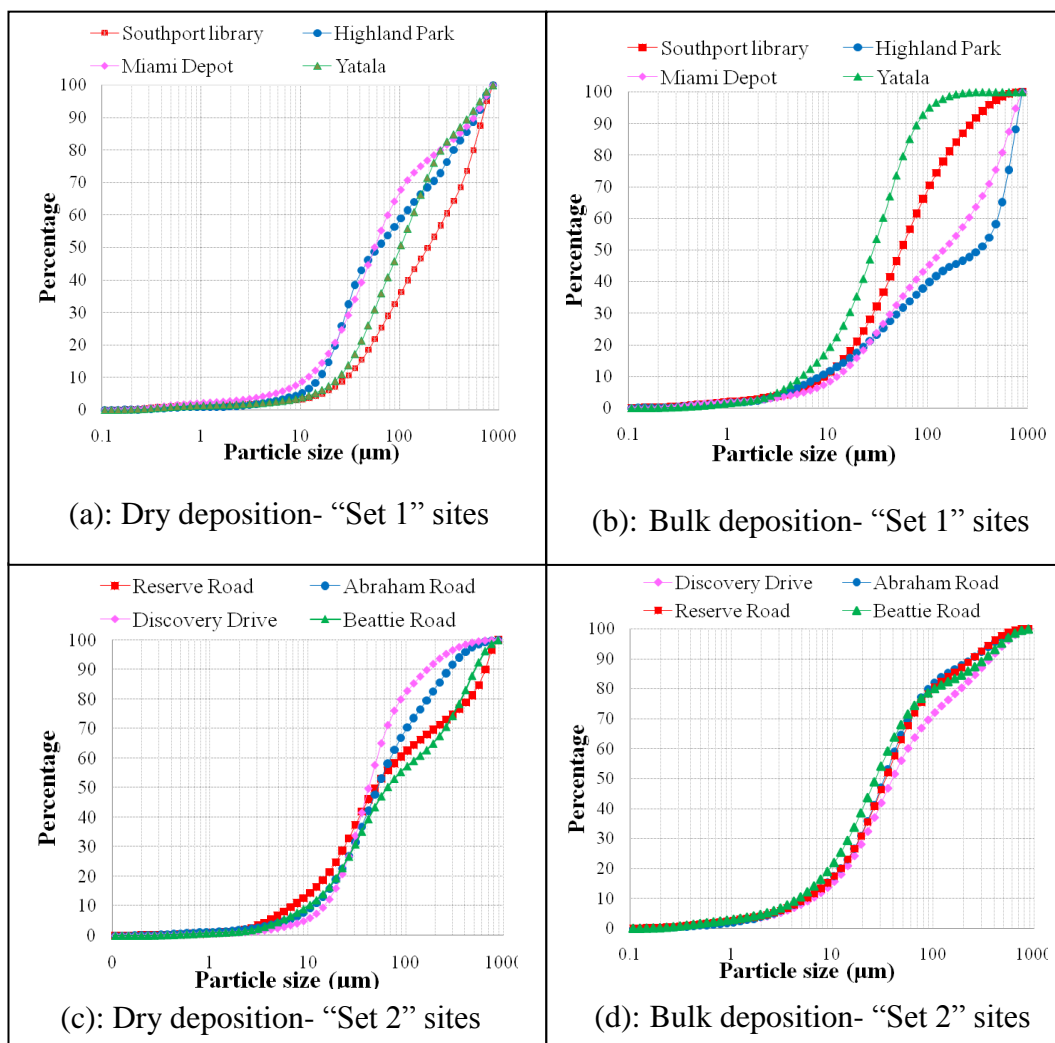


Figure 7-4: Variation of average particle size distribution for different study sites for dry and bulk deposition

It is evident from Figure 7-4, that although the sites were spatially distributed, the atmospheric depositions of finer particles (approximately $<1.4 \mu\text{m}$) are similar for all sites. This suggests that the concentration of this size range in the atmosphere is relatively uniform. In turn, this would mean that there is rapid dispersion of smaller particles from their sources of generation. Such rapid dispersion is possible when wind and buoyancy forces become dominant compared to the mass of individual particles. However, atmospheric mixing of larger particles ($>1.4 \mu\text{m}$) is not uniform as the influence of gravity become dominant (Zheng et al. 2005). Hence, larger particles would deposit within a short period of time in close proximity to their

source of origin, demonstrating a strong influence of source characteristics such as traffic and land use.

7.4 Heavy metals in atmospheric deposition

7.4.1 Analysis of heavy metals

A significant amount of particles comprising of bulk and dry depositions are generated by urban traffic sources (Sabin et al. 2005; Davis and Birch 2010). Additionally, researchers have noted that bulk and dry depositions contain high amounts of heavy metals which are regarded as a critically important group of pollutants in stormwater quality research (Huang et al. 1994; Sabin and Schiff 2008). Therefore, understanding the characteristics of heavy metals in atmospheric deposition is important. In this regard, heavy metal species, namely, Cr, Cd, Ni, Pb, Mn, Zn and Cu associated in bulk and dry deposition samples were investigated. These seven heavy metals were selected in view of their potential toxicity and association with traffic related activities. It was found from initial testing that the concentrations of PAHs in atmospheric deposition are below detection limits for most of the sites. Therefore, they were not tested.

Figure 7-5(a) gives the mass of the recovered heavy metal species from dry deposition at each site. In Figure 7-5(a), the deposition rates were calculated by dividing total mass of metal by the number of dry days and averaged over the five sampling episodes. Figure 7-5(b) shows the mass of the recovered heavy metal species from dry deposition at each site. The values were calculated similar to Figure 7-5(a).

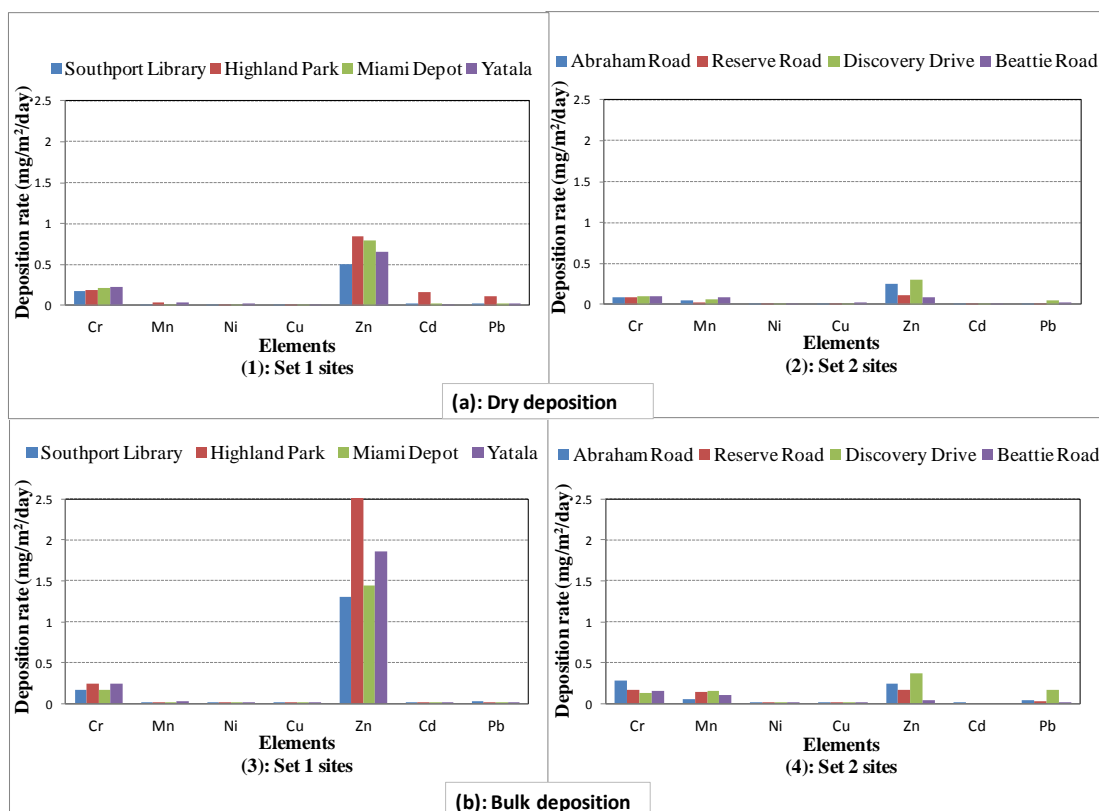


Figure 7-5: Average deposition rates of heavy metals: (a) dry deposition, (b) bulk deposition

As shown in Figure 7-5(a) and 7-5(b), in the seven heavy metals tested, Zn is the most dominant heavy metal in dry deposition followed by Cr for most of the sites. The high concentration of Zn and Cr in both bulk and dry depositions can be attributed to high concentrations of these metals in the atmospheric phase (Chester et al. 1999). It was noted in Section 6.5.1 that the atmospheric concentration of Zn was consistently higher among the investigated heavy metals. Past researchers such as Karar et al. (2006), Sansalone (1997) and Pitt (1979) have noted that vehicular traffic as one of the main sources of Zn in the atmosphere.

A Zn deposition rate which is two times higher in bulk deposition samples when compared to dry deposition as evident in Figure 7-5 suggests that wet deposition is a significant source. However, this is not necessarily the case for Cr as evident in Figure 7-5. For example, maximum Zn deposition rates for bulk and dry deposition were 2.5 and 0.85 mg/m²/day whereas maximum Cr deposition rates are 0.25 and 0.22 mg/m²/day respectively. Morsellia et al. (2003) noted that the solubility of heavy metals in wet deposition follow the order; Zn > Cd > Cu > Ni > Pb > Cr.

Therefore, wet deposition can only scavenge a relatively smaller amount of Cr from the atmospheric phase. Furthermore, Samara and Voutsas (2005) found that mean mass median aerodynamic diameter (MMMAD) of these heavy metals followed the order of Pb ($0.96 \pm 0.71 \mu\text{m}$) < Cd ($1.14 \pm 0.82 \mu\text{m}$) < Ni ($1.45 \pm 0.88 \mu\text{m}$) < Cu ($2.04 \pm 0.77 \mu\text{m}$) < Mn ($2.61 \pm 1.23 \mu\text{m}$) < Cr ($2.91 \pm 1.40 \mu\text{m}$). As Cr has the largest MMMAD, it would be expected to deposit primarily with dry deposition.

7.4.2 Influence of traffic on atmospheric deposition

As highlighted in Chapter 2, urban traffic has been recognised as one of the main sources of stormwater pollution. In turn, the characteristics of atmospheric deposition are influenced by urban traffic characteristics (Mijic et al. 2010). However, current state of knowledge does not provide a direct link between HMs in atmospheric deposition with traffic parameters such as average daily traffic (ADT_{to}) and traffic congestion (V/C). Therefore, in order to understand the possible relationships between traffic characteristics and heavy metals in atmospheric deposition, multivariate statistical analysis was undertaken. For this, PROMETHEE and GAIA analysis were conducted.

PROMETHEE is a non-parametric method, which means that in principle it is possible to compare as few as two objects (Carmody et al. 2005). GAIA is a visualisation tool based on the principal component approach. Detail discussions of the multivariate analytical methods used are given in Section 3.4.3. Although there are six different preference functions available in the PROMETHEE method, the V-shaped function was selected for all variables as this function compares values based on one threshold value (Podvezko and Podvezko 2010). This threshold value, namely, P is required to be defined for each preference function (Herngren et al. 2005).

(a) Dry deposition

In order to investigate the variation of heavy metals in atmospheric deposition with traffic, PROMETHEE 2 analysis was conducted using the dry deposition data collected at “Set 2” sites. The “Set 2” sites were used for the analysis as traffic data is available only for these sites. Secondly, PROMETHEE 2 analysis was conducted

for “Set 1” and “Set 2” sites together in order to investigate the variation of atmospheric deposition with land use. Even though the ranking of objects can be one of the key outcomes of PROMETHEE 2 analysis, ranking was not incorporated in every analysis. This is primarily due to the limited number of sites and the repetitive sampling. The GAIA biplot was used to explain the outcomes of the analysis. Ranking tables for each analysis are given in Tables B-2, B-3, B-4 and B-5 of Appendix B.

Average daily traffic measured in 2010 (ADT_{to}) and traffic congestion (V/C) were the key traffic parameters used in the analysis. Daily average wind speed (wind) data was also incorporated into the analysis (AGBOM 2010). The other variables used for the analysis were HMs (Cr, Cd, Mn, Cu, Pb, Zn and Ni) loading per unit area, Total organic carbon (TOC) loading per unit area, and antecedent dry period (ADP). As variables were set to maximum, the decision axis π_1 points towards most polluted site/s. The GAIA biplot derived is shown in Figure 7-6.

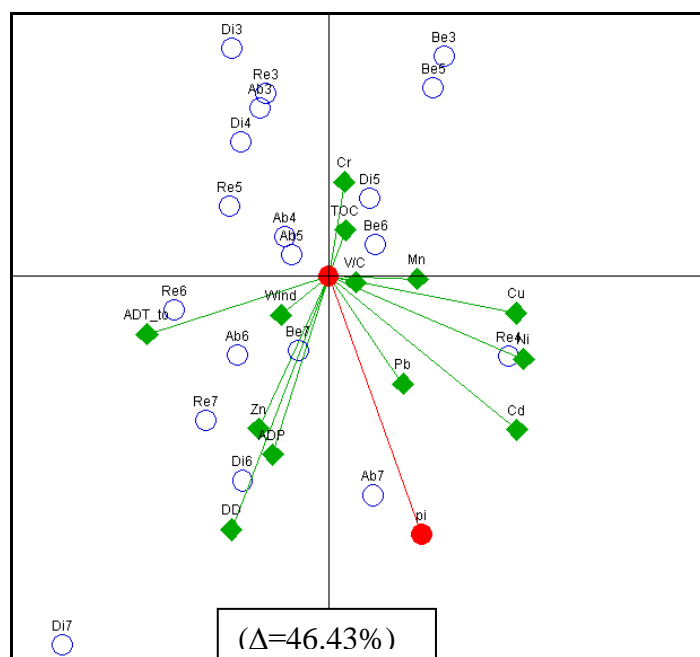


Figure 7-6: GAIA biplot of dry deposition for “Set 2” sites

(Where Δ is the percentage variance described by the GAIA Biplot, DD is the total dry deposition, numbers 3, 4, 5, 6, 7 refer to 3, 4, 5, 6, 7 ADPs)

Figure 7-6 confirms that total dry deposition solids (DD) strongly correlates with the antecedent dry period (ADP) and Zn. This confirms the strong influence of ADP on atmospheric build up and consequent dry deposition. Zn could be associated with relatively large particles as dry deposition particles are relatively larger. It is commonly accepted that wear and tear of vehicle parts are larger than exhaust particles. As exhaust particles are very small, contribution of exhaust particles to total DD mass would be lower. Availability of Zn from traffic sources can be further supported by the findings of Sternbeck et al. (2002). They noted that wear of vehicle parts is a major pathway for airborne Zn. Furthermore, Councell et al. (2004) noted that tyre wear particles as the main sources of Zn in the atmospheric phase.

As evident in Figure 7-6, even though Zn in dry deposition is correlated with average daily traffic (ADT_{to}), other heavy metals such as Mn, Cu, Ni, Pb and Cd are related to traffic congestion (V/C). As these metals show no correlation to DD, it can be argued that these are associated primarily with the finer fraction of airborne particles which does not contribute significantly to the total particulate matter. As noted by Samara and Voutsas (2005), mean mass median aerodynamic diameter (MMAD) of Cd, Mn, Cu, Pb, and Ni in the atmospheric phase is less than 2.61 μm . This suggests that except Zn and Cr, the other metals originate primarily from exhaust emissions rather than wear and tear of vehicle parts.

(b) Bulk deposition

PROMETHEE and GAIA were also employed to analyse the data matrix for bulk deposition samples collected. The same variables were used for this analysis as well. As the variables were set to their maximum in the analysis, the decision axis pointed towards the most polluted site/s. The resulting GAIA biplot is shown in Figure 7-7.

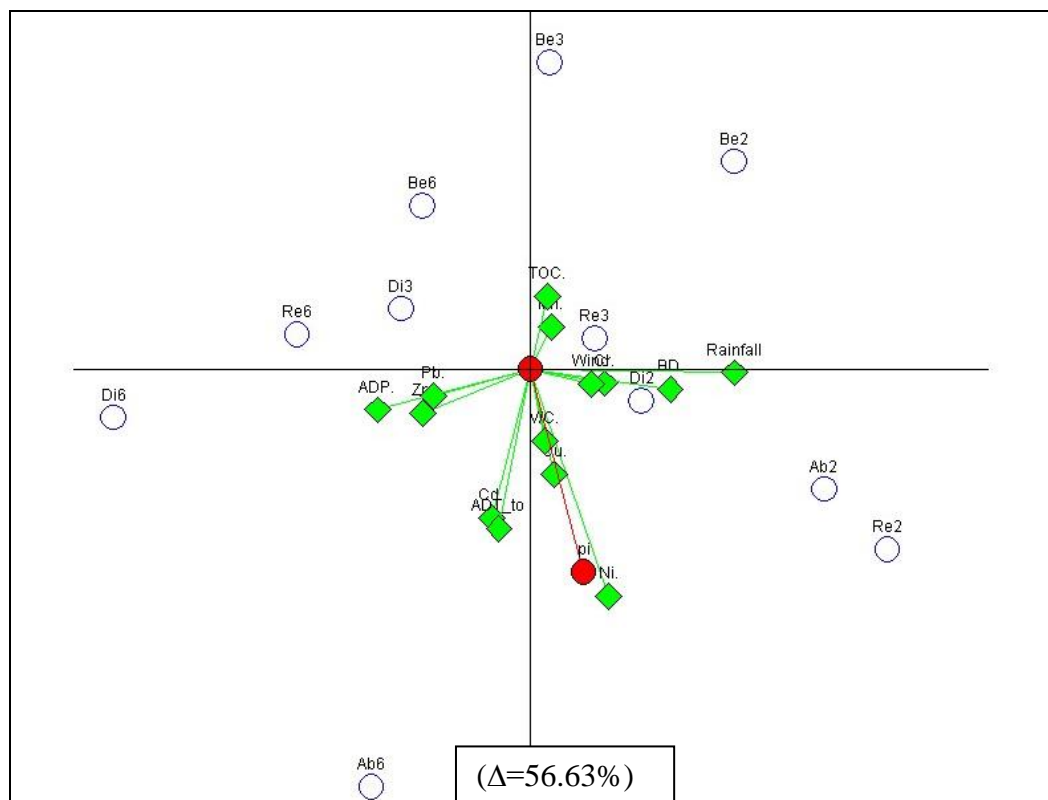


Figure 7-7: GAIA biplot of bulk deposition for “Set 2” sites

(Where Δ is the percentage variance described by the GAIA Biplot, BD=Total bulk deposition mass, numbers 2, 3 and 6 refer to 2, 3 and 6 ADPs)

Both Zn and Pb are strongly correlated to ADP and weakly correlated to ADT_to in bulk deposition as shown in Figure 7-7. This suggests that atmospheric concentration of Zn and Pb depends on the antecedent dry period and traffic is one of the sources of these two metals. This highlights the fact that Zn and Pb accumulate in the atmosphere during the dry period and deposition depends on the atmospheric concentration. However, the correlation of Pb to ADT_to in bulk deposition samples and no correlation in dry deposition samples suggest that the form of existence of Pb is different to Zn in the atmospheric phase. Pb is generated primarily in exhaust emissions, which produce fine particulates whereas Zn is an abrasion by-product. However, as the usage of leaded fuel was stopped about a decade ago, Pb is due to the re-suspension of already deposited Pb. Typically, exhaust particles are relatively fine and wet deposition is a very effective mechanism of scavenging smaller particles (Fang et al. 2004). Huston et al. (2009) noted that the majority of heavy metals in ambient air are associated with particles $<6 \mu\text{m}$. Furthermore, they noted that rain scavenges the 2–10 μm size range particles efficiently.

The correlation of Cd, Cu, Ni and V/C in Figure 7-7 suggests that these metals are generated by exhaust emissions as traffic congestion aggravates exhaust emissions. Additionally, as these heavy metals are associated with relatively smaller particles (MMMD for Cd, Cu, Ni ranges between 1.14-2.04 μ m) (Samara and Voutsas 2005), it provides further confirmation of the above conclusion. Furthermore, as wet scavenging is an efficient process of removing smaller particles, deposition of Cd, Cu, Ni can be considered to be associated with bulk deposition.

There is a close relationship between wind speed with Cr and bulk deposition (BD) in Figure 7-7. Therefore, it can be concluded that wind has a high influence on Cr in bulk deposition. This is attributed to the fact that dry deposition depends strongly on the wind speed (Fang et al. 2004) and as confirmed in Figure 7-6. As bulk deposition is a combination of dry and wet deposition, bulk deposition can also be influenced by wind speed. Cr in bulk deposition is contributed by dry deposition as Cr is associated with relatively larger particles (MMMD for Cr is 2.9 μ m). Also, wet deposition is responsible for scavenging an appreciable solids load from the atmosphere as rainfall is strongly correlated with BD in Figure 7-7.

7.4.3 Variation of atmospheric deposition with land use characteristics

(a) Dry deposition

Based on the outcomes of above analysis, it is clear that the atmospheric deposition is influenced by traffic parameters. Land use parameters may exert a similar influence where anthropogenic activities generate significant pollutant loads. In order to determine possible linkages between atmospheric deposition with land use characteristics, data matrices for “Set 1” and “Set 2” sites were combined and analysed using PROMETHEE and GAIA methods. Outcomes generated were also verified based on the findings noted in the earlier analyses for “Set 2” sites. “Set 1” sampling sites were selected to represent key land use activities within the study region as explained in Chapter 4. Even though these sites belong to different land use categories, they have similar dry deposition characteristics as previously discussed in Section 7.3.3.

Wind and antecedent dry period (ADP) were two important variables used for this analysis. The other variables used for the analysis were HMs (Cr, Cd, Mn, Cu, Pb, Zn and Ni) and total organic carbon (TOC) loading per unit area. As the variables were set to their maximum, the decision axis pi, points towards the most polluted site/s. Also, total dry deposition (DD) was incorporated into the analysis. The resulting GAIA biplot is shown in Figure 7-8.

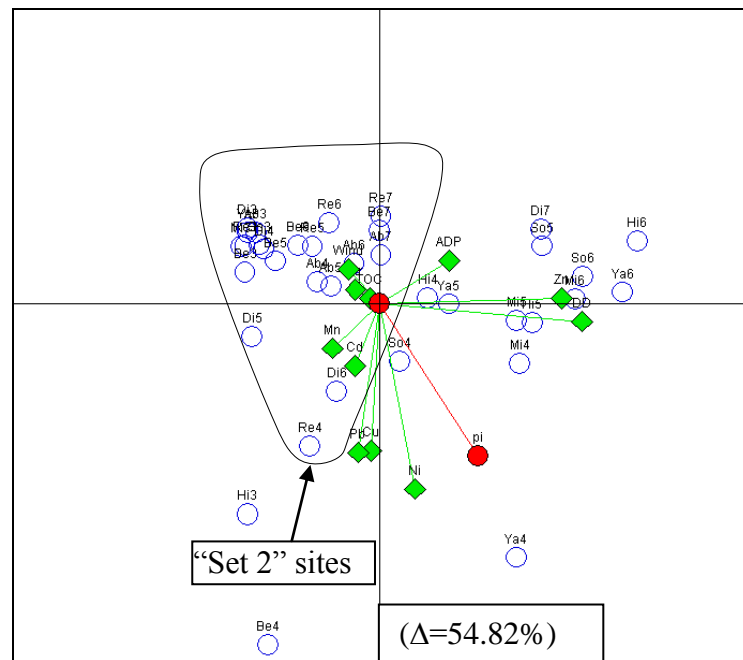


Figure 7-8: GAIA biplot of dry deposition for “Set 1” and “Set 2” sites

(Where Δ is the percentage variance described by the GAIA biplot, DD=total deposition, ADP=Antecedent dry period, numbers 3, 4, 5, 6 and 7 refer to 3, 4, 5, 6 and 7 ADPs)

Even though “Set 2” sites belong to three different land uses, namely, industrial, commercial and residential, they are grouped together as shown in Figure 7-8. There is no clear separation of these sites based on land use. Also, even though “Set 1” sites are located close to intensive anthropogenic activities, they do not show a clear grouping in Figure 7-8. However, they are pointed towards the decision axis pi indicating their highly polluted nature. This suggests that the atmospheric deposition of HMs is not directly influenced by land use but rather by proximity to high emission sources such as roadways. For example, almost all the sampling events for the Yatala site, which is close to the Pacific Motorway, are located close to the decision axis pi in Figure 7-8.

The positive correlations between Zn, TD and ADP are similar to the correlations observed in Figure 7-6 for “Set 2” sites. As noted in Section 7.4.2, the reasons for this behaviour are: (1) dry deposition particles are relatively larger and Zn is associated with relatively large particles; (2) contribution of exhaust particles to total TD mass is minimal. Therefore, the wear of vehicles parts is a major source of airborne Zn and the contribution of exhaust emissions to the Zn load is minimal. This suggests that the outcomes from the sampling study are generic and is not influenced by the location of the sampling sites.

As evident in Figure 7-8, the correlations among Cd, Pb, Mn Ni and Cu suggests that these heavy metals are generated by similar sources at both “Set 1” and “Set 2” sites. As noted in Section 7.4.2, it can be concluded that these metals are generated by exhaust emissions. An atmospheric deposition study conducted by Sharma et al. (2008) concluded that Zn deposition is governed by local anthropogenic activities, but Cu, Cd and Pb may have long distance sources. A similar argument can be built to explain the correlation of Mn, Ni, Cd, Cu and Pb in Figure 7-8. Therefore, it is hypothesised that Zn and Cr are generated by local anthropogenic activities, but other metals are generated by local sources as well as distant sources.

(b) Bulk deposition

In order to investigate the influence of land use on heavy metal deposition, bulk deposition data collected at “Set 1” and “Set 2” sites were analysed together using PROMETHEE and GAIA. Additionally, a further approach was to generalise the key findings noted earlier and to investigate the variability of bulk deposition with key land use characteristics. The same set of variables as previous was also used for this analysis. However, as actual traffic data was not available for “Set 1” sites, traffic data was not incorporated into this analysis. All variables were set to their maximum in the analysis. The resulting GAIA biplot is shown in Figure 7-9.

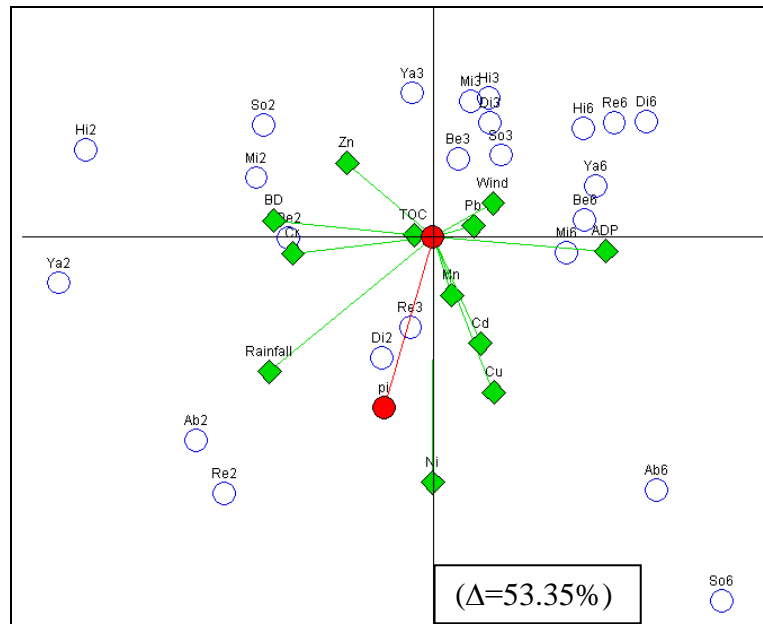


Figure 7-9: GAIA biplot of bulk deposition for “Set 1” sites

(Where Δ is the percentage variance described by the GAIA biplot, BD=Bulk deposition, ADP=Antecedent dry period, numbers 2, 3 and 6 refer to 2, 3 and 6 ADPs)

It is evident in Figure 7-9, that there is no clear grouping of sites based on land use. However, a clear separation of “Set 1” and “Set 2” sites were observed for solids in bulk deposition in Section 7.3.2. Also, not all “Set 1” sites are pointed in the direction of the decision axis π_i in Figure 7-9. Therefore, this suggests that pollutants in wet deposition are less sensitive to the source characteristics compared to dry deposition. This is attributed to the fact that wet deposition particles are smaller and hence they have the tendency to spread over a larger area in the atmosphere from the source of origin.

According to Figure 7-9, BD shows correlation with rainfall, Cr and Zn for the investigated sites. It was previously noted in Figure 7-7 that rainfall is strongly correlated with BD and Cr for “Set 2” sites. This is attributed to the fact that Zn is primarily associated with relatively larger particles ($> 2\mu\text{m}$) (Huston et al. 2009). Furthermore, the relative contribution of particulate matter with rainfall to bulk deposition is higher. Therefore, this would be the reason for the close relationship between rainfall and BD. The correlation between BD, rainfall and Cr was already explained in Section 7.4.2(b). The only difference is that Zn is also correlated with

BD, Cr, wind and rainfall. This is attributed to the fact that Zn is associated with larger particles in bulk deposition.

7.5 Ranking of sites

It was noted from the analysis carried out that atmospheric deposition depends not only on the traffic characteristics but also on the land use characteristics. Atmospheric deposition cannot be explained only in terms of traffic or land use characteristics and, an overall assessment was needed. Consequently, PROMETHEE 2 complete ranking analysis was undertaken to determine the most polluted site in terms of atmospheric deposition by combining the data sets obtained from all the sampling sites. A summary of outcomes is given in Table 7-4. Deposition rates were used for this analysis as the sampling was undertaken for different antecedent dry days. This analysis helped especially in understanding the critical sources of target pollutants to the urban atmosphere and in turn to atmospheric deposition.

According to PROMETHEE 2 complete ranking, Yatala is the most polluted site as the target pollutants have been detected in high concentration consistently at this site as shown in Table 7-4. The fact that the Yatala sampling site was located very close to the Freeway is the reason for detecting target pollutants in high concentration. Therefore, highways can be considered as one of the main sources of pollutants to the urban atmosphere including heavy metals. A similar finding has also been observed by Hitchins et al. (2000).

Table 7-4: PROMETHEE 2 complete ranking of dry deposition sampling sites

	Phi Net	Ranking	Comment
Yatala	0.2177	1	The most polluted site
Highland park	0.1597	2	
Beattie road	0.1199	3	
Miami depot	0.0205	4	
Southport library	-0.0694	5	
Discovery drive	-0.1244	6	
Abraham road	-0.1557	7	
Reserve road	-0.1684	8	The least polluted site

Chapter 6 investigated the variation of HMs and PAHs in the atmospheric phase with traffic and land use characteristics by collecting air samples. Air sampling and testing was carried out at fifteen sites including the “Set 1” and “Set 2” sites. Therefore, for seven sites, atmospheric deposition sampling was not carried out and hence was not included in this analysis. It was noted in Chapter 6 that Yatala is not the most polluted site in terms of atmospheric HMs. Town Centre Drive site was found to be the most polluted during both weekend and weekday sampling. This site does not belong to either “Set 1” or “Set 2” sites. This suggests that highways are one of the main sources of pollutants to the atmosphere.

GAIA analysis was undertaken to investigate whether “Set 1” and “Set 2” sites are clearly separated in the biplot. Also this analysis helped to identify the important HMs for each site in terms of their deposition rates. Variables considered for the analysis were; (1) heavy metal deposition rates, (2) total organic carbon deposition rates and (3) total particulate matter deposition rates (DD). Traffic data was not incorporated into the analysis as such data was not available for all the sites. Additionally, a site with a high traffic volume may not be the most polluted in terms of the investigated pollutants. The GAIA biplot is presented in Figure 7-10.

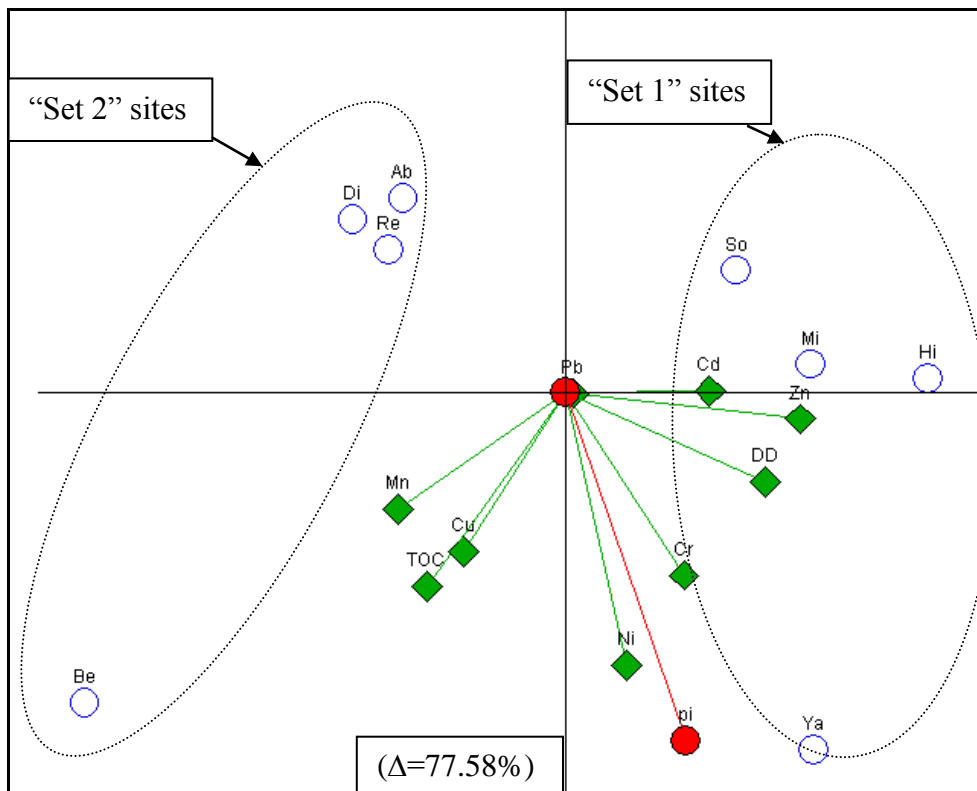


Figure 7-10: GAIA biplot of dry deposition for “Set 1” and “Set 2” sites

(Where Δ is the percentage variance described by the GAIA Biplot DD=Total particulate matter deposition)

It can be seen from the Figure 7-10 that “Set 1” sites and “Set 2” sites are clearly separated in the GAIA biplot. Once again, this confirms the fact that “Set 1” sites and “Set 2” sites have different atmospheric deposition characteristics. This is mainly due to the fact that “Set 1” sites generate much higher pollutant loads to the urban atmosphere compared to “Set 2” sites. This is due to the fact they are located close to intensive anthropogenic activities. As the difference between “Set 1” and “Set 2” sites is very significant in Figure 7-10, it can be concluded that atmospheric deposition is highly dependent on the surrounding anthropogenic activities including traffic.

As evident from the Figure 7-10, Mn, TOC and Cu point towards “Set 2” sites whereas Zn, Cr, Ni and Cd point towards “Set 1” sites. This suggests that “Set 1” sites contribute Zn, Cr, Ni and Cd with dry deposition. Furthermore, “Set 2” sites contribute primarily Mn, Cu and organic carbon in high concentration with the dry deposition. Therefore, atmospheric depositions originating from “Set 1” sites are

important in terms of stormwater pollution, as these sites generate toxic heavy metals (Zn, Cr, Ni and Cd) (Shi et al. 2010).

7.6 Conclusions

The following important conclusions were derived from the analysis of atmospheric deposition data:

- Dry atmospheric deposition strongly correlates with antecedent dry period. Therefore, atmospheric deposition can be considered as an important source of pollutants to the build-up on surfaces especially during dry periods and in turn contribute higher pollutant loads to urban stormwater runoff.
- Bulk deposition is not correlated to the antecedent dry period, but rather it is related to the rainfall depth. As solids in bulk deposition increase with the rainfall depth, wet deposition caused by high rainfall events can be a significant pollutant source to stormwater.
- Bulk deposition contains a relatively higher percentage of smaller particles (<1.4 μm) compared to dry deposition. Vehicle emissions generated particles are associated primarily with bulk deposition. Also, the influence of wind is stronger in relation to dry deposition compared to bulk deposition.
- Zn in dry deposition is mainly associated with vehicle wear and tear particles whereas Mn, Cu, Ni, Pb are mainly associated with emission exhaust particles. Therefore, wear and tear by-products of vehicles can be considered as an important source of Zn to pollutant build-up on roads.
- Zn is related to traffic volume and Cd, Cu, Ni is correlated with traffic congestion. Therefore, the reduction in traffic congestion is much more important than reducing traffic volume as Cd, Cu and Ni causes higher impacts in the receiving water environment compared to Zn.

- Pollutants in wet deposition are less sensitive to the source characteristics compared to dry deposition. This is attributed to the fact that wet deposition particles are smaller and hence they disperse over a larger area in the atmosphere from the source of origin.
- Atmospheric deposition of HMs is not directly influenced by land use but rather by proximity to high emission sources such as highways. Therefore, it is important to consider atmospheric deposition as a key pollutant source to urban stormwater in the vicinity of these types of sources.

Chapter 8 - Analysis of Pollutant Build-up Data

8.1 Background

It is commonly accepted that urban traffic is one of the primary stormwater pollutant sources (Kayhanian et al. 2007; Sartor and Boyd 1972). Due to the increase in urban traffic in future scenarios (ABS 2010), the severity of the pollutant contribution will continuously increase. Traffic generated pollutants exhibit complex processes and pathways from generation to reach receiving waters. Part of traffic generated pollutants directly deposit on road surfaces and re-suspend due to vehicular traffic (Khairy et al. 2011). Emissions from vehicles can also contribute to atmospheric pollutant load and then deposit as atmospheric deposition. Understanding these complex processes and pathways is the key for successful source control measures. In this regard, Chapter 6 and 7 concentrated on atmospheric pollutant build-up and atmospheric deposition, respectively. This Chapter focuses on analysing pollutant build-up on road surfaces. Outcomes of this Chapter will be used for the modelling of pollutant processes discussed in Chapter 9.

Road surface pollutant build-up is an important pollutant process and has been studied by many researchers (for example Egodawatta 2007; Hengren 2005; Sartor and Boyd 1972). However, there is no widely accepted definition for build-up accounting for its variability with traffic and land use characteristics (Duong and Lee 2011; Opher and Friedler 2010). This constrains the formulation and implementation of stormwater pollution control measures.

8.2 Field investigations

Build-up sampling was conducted in 11 road sites, which were located within Gold Coast, South East Queensland, as given in Table 6-2. The sites are located within Coomera and Helensvale suburbs. The selected roads belong to three types of urban land uses, namely, commercial, industrial and residential. One build-up sample was collected from each site after 7 antecedent dry days. Sample collection and testing was undertaken as described in Chapter 5.

Build-up samples were collected using a wet and dry vacuuming system as described in Section 3.3.3. The collected samples were sub-sampled into five different particle size fractions and tested as described in Section 5.5. Each sub-sample was tested for PAHs, HMs, TSS, and TOC. The total build-up sample was tested for other parameters such as PSD, EC, pH and DOC.

Average annual daily traffic data given in Table 6-2 was obtained from a traffic survey conducted in year 2010. The traffic survey was carried out using automatic traffic counters and it was conducted at all 11 road sites covering two weekdays and one weekend day. Additionally, as part of the survey, classified traffic volumes and speed data were recorded in 15 minute intervals for each direction. The 11 sites were selected based on the variability of predicted traffic data obtained from Gold Coast City Council (GCCC) as given in Table 4-1.

8.3 Analysis

Analysis was undertaken to identify relationships between traffic and land use parameters for a range of build-up pollutants and linking these relationships with processes and pathways identified in Chapter 6 and Chapter 7. After data pre-treatment, initial data analysis was conducted using univariate statistical techniques and graphical methods in order to ensure the consistency of the data set compared to a range of similar studies. Subsequently, multivariate statistical techniques were used to investigate the influence of traffic and land use activities on investigated HMs and PAHs build-up and their relationships with air quality and atmospheric deposition.

8.3.1 Pre-treatment

Build-up samples were collected in the liquid matrix as discussed in Chapter 4. Therefore, the test results were in the form of concentrations (mg/L) for most of the parameters. Prior to analysis, pre-treatment was carried out for the data obtained from the laboratory tests to remove any bias and avoid any influence resulting from different scales of measurement (Egodawatta 2007). It was noted during the data pre-treatment that data collected at one site is an outlier and was removed from the analysis. The key steps followed are given in Section 6.3.1 and 7.3.1. Additionally, total build-up solids load per each sampling area was calculated by multiplying

sample concentration by the corresponding sample volume (L). Then, the calculated solid mass was divided by the corresponding sampling area to calculate solids deposition per unit area (mg/m^2).

8.3.2 Univariate analysis

(a) Solids

Consistency of the solids build-up data was first assessed by comparing them with values given in research literature. Comparisons were also done for the other pollutant species separately. The research study found that the build-up of total solids on road surfaces varied from $0.05 \text{ g}/\text{m}^2$ to $1.1 \text{ g}/\text{m}^2$ after 7 antecedent dry days. In a similar study, Egodawatta (2007) reported a maximum build-up load from three sites varying from 3 to $6 \text{ g}/\text{m}^2$ after 21 days. Furthermore, Miguntanna et al. (2010) noted a maximum build-up solids load of $2.25 \text{ g}/\text{m}^2$ after 8 antecedent dry days. Studies by Egodawatta (2007) and Miguntanna et al. (2010) were also conducted in the Gold Coast area. The above data confirms that the solids build-up loads noted in this study are consistent with the typical build-up loads reported in previous research studies.

Traffic volume and the surrounding dominant land use have been considered as the most influential variables for pollutant build-up. Based on this, the variation of solids build-up with traffic volume in the form of average daily traffic (ADT) is plotted in Figure 8-1. The different land uses are denoted in different colours. Variation of dissolved and total solids are plotted separately as shown in Figure 8-1(a) and (b) respectively.

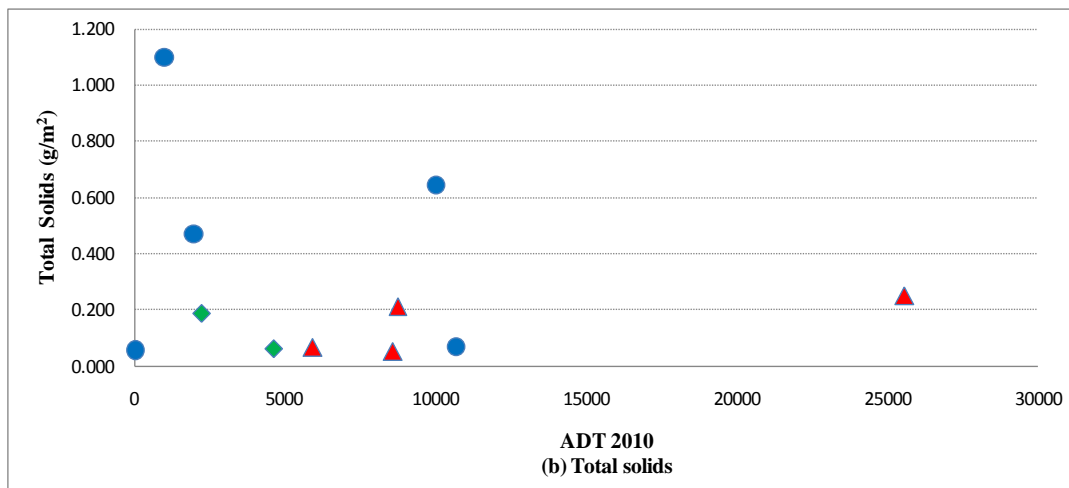
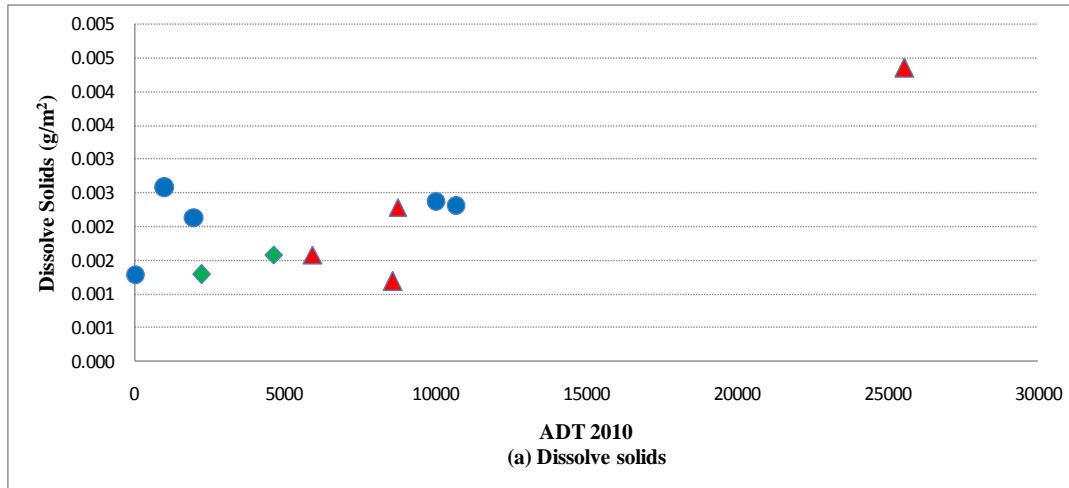


Figure 8-1: Variation solids with average daily traffic, (a): dissolve solids, (b): total solids

(Where ▲ = commercial, ● = residential and ◆ = industrial)

As evident in Figure 8-1, neither dissolved nor total solids show a clear trend with ADT or land use. This points to the complexity of build-up processes and the possible influence of a range of traffic and land use related parameters in addition to the above. Build-up is also significantly influenced by atmospheric deposition and soil inputs (Sabin et al. 2006; Hengren 2005). As noted by Opher and Friedler (2010), atmospheric deposition is a significant source of pollutants to road surface pollutant build-up which can occur as either dry deposition or wet deposition.

Furthermore, atmospheric deposition depends on the surrounding land use as noted in Chapter 6. This suggested the necessity of selecting a detailed set of traffic and land use parameters to encompass appreciable variability in characteristics for build-up analysis. The selected traffic parameters were total average daily traffic volume (ADT_{to}), total average heavy duty daily traffic volume (ADT_{hv}) and traffic congestion (V/C) and land use. Similar parameters were employed in the analyses discussed in Chapter 6 and Chapter 7 as exploratory variables. The complexity of the build-up process and the involvement of a range of parameters and processes suggested the use of multivariate analytical techniques.

For better understanding of build-up processes and its variability with traffic and land use characteristics, build-up of solids in five different particle size classes were investigated. This was to account for the differences in build-up and atmospheric deposition processes with particle size. The particle sizes classes considered were <1 µm, 1-75 µm, 75-150 µm, 150-300 µm and >300 µm as shown in Table 8-1. Additionally, the distribution of these five particle size fractions in industrial, commercial and residential land uses were also investigated. Variations of particle size distribution for different land uses are presented in Figure 8-2.

Table 8-1: Classification of particle size distribution (PSD)

Road site	Solids (volumetric percentages)				
	<1 µm	1-75 µm	75-150 µm	150- 300 µm	>300 µm
Shipper Drive (Sh _i)	3.9	46.9	13.7	13.8	21.7
Beattie Road (Be _i)	2.6	48.7	14.6	15.5	18.6
Average -Industrial	3.3	47.8	14.2	14.7	20.2
Billinghurst Crescent (Bi _r)	2.1	45.7	10.0	14.6	27.6
Dalley Park Drive (Da _r)	5.0	80.0	8.3	3.9	2.8
Discovery Drive (Di _r)	3.7	33.7	24.0	17.2	21.4
Peanba Park road (Pe _r)	2.0	34.5	15.9	18.9	28.7
Reserve Road (Re _r)	6.9	84.3	3.4	3.3	2.1
Average- Residential	3.9	55.6	12.3	11.6	16.5
Hope Island Road (Ho _c)	2.7	74.8	12.9	5.7	3.9
Lindfield Road (Li _c)	3.3	53.8	21.1	10.1	11.7
Abraham Road (Ab _c)	4.4	85.1	4.5	3.3	2.7
Town Centre Drive (To _c)	3.9	38.5	11.8	14.3	31.5
Average-Commercial	3.6	63.1	12.6	8.3	12.5

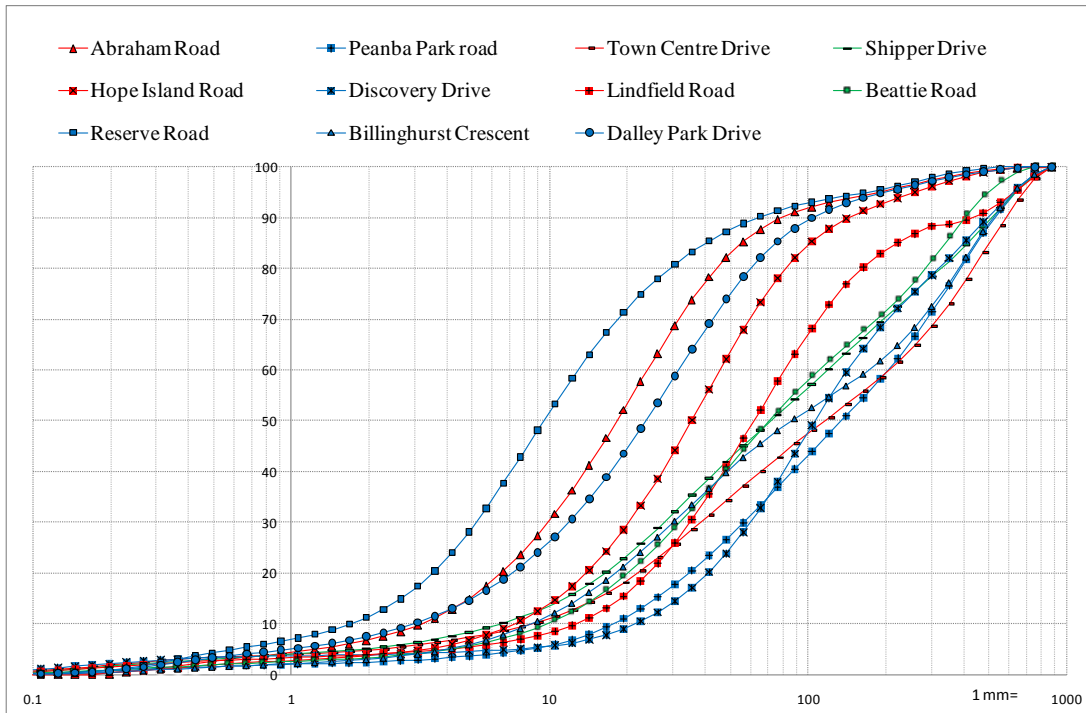


Figure 8-2: Variation of particle distribution among selected road sites

(Where, red - commercial, blue - residential and green - industrial)

Table 8-1 and Figure 8-2 show similar distribution of percentage particle size fractions for residential and commercial sites. However, industrial sites contribute comparatively lower volumetric percentage of $<1 \mu\text{m}$ and $1-75 \mu\text{m}$ particle size fractions, but higher volumetric percentage of $> 300 \mu\text{m}$ size fraction particles. This suggests that residential and commercial sites contribute relatively higher percentage of fine particles to urban road surfaces. Furthermore, according to Table 8-1, industrial, residential and commercial sites generated on average 14.2, 12.3 and 12.6 volumetric percentages of solids in the $75-150 \mu\text{m}$ size fraction. Variability in particle size suggested the need for the inclusion of a particle size distribution related parameter in further analysis. For this purpose, the coefficient of uniformity (referred to as PSD_D50) was considered suitable. The coefficient of uniformity (PSD_D50) is defined as D_{60}/D_{10} (Mbonimpa et al. 2002). D_{60} and D_{10} are the diameter corresponding to 60% and 10% passing on the cumulative grain-size distribution curve, respectively. This parameter was calculated for each sampling episode separately.

(b) Heavy metals

To ensure the consistency of heavy metals recorded in this study, the data recorded were compared with the values reported by Gunawardana (2011) as shown in Table 8-2.

Table 8-2: Heavy metals build-up on roads

HMs	Concentrations observed in this study		Adapted from Gunawardana (2011)	
	Max. (mg/m ²)	Min. (mg/m ²)	Max. (mg/m ²)	Min. (mg/m ²)
Cr	0.195	<0.001	0.478	0.394
Mn	0.482	0.035	3.661	0.037
Ni	0.491	<0.001	0.320	0.001
Cu	2.448	0.750	1.719	0.024
Zn	3.513	1.066	8.436	0.049
Cd	0.003	<0.001	0.021	<0.001
Pb	0.195	<0.001	1.912	<0.001

Values obtained by Gunawardana (2011) were selected for this comparison due to the similarities in the areas of sampling and the sampling technique used. The study reported in Gunawardana (2011) was also undertaken in the Gold Coast region, Australia using a similar wet and dry vacuuming technique as in this study. The heavy metal loads recovered by Gunawardana (2011) are in similar ranges to the values in this study as shown in Table 8-2 except for Mn and Zn. Gunawardana (2011) detected Mn and Zn in relatively high loads per unit area compared to this study. The detection of Mn and Zn in higher concentrations is attributed to differences in traffic and land use characteristics between this study and study undertaken by Gunawardana (2011). As the variation in heavy metal concentrations are mostly in very similar ranges it can be considered that the heavy metal loads detected in the current study are consistent with the typical amounts for the study region. The heavy metal concentrations for different sites are illustrated in Figure 8-3.

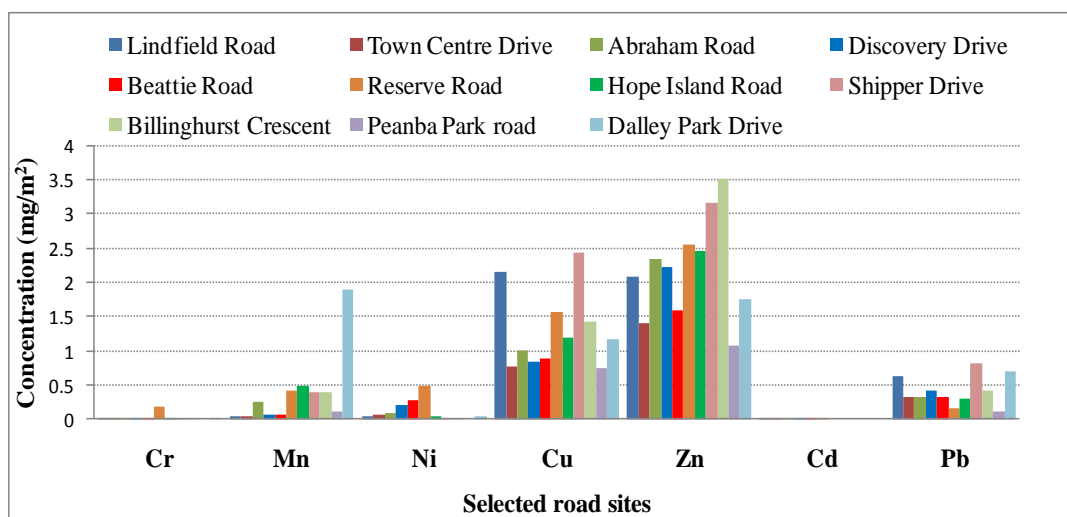


Figure 8-3: Comparison of heavy metal concentrations with particle size

As evident in Figure 8-3, Zn is the highest detected heavy metal species followed by Cu for almost all the sites, irrespective of traffic and land use characteristics. It has already been noted in Chapter 6 and 7 that Zn is the most common heavy metal in the atmospheric phase and in atmospheric deposition. This points to the appreciable contribution from atmospheric phase to build-up Zn load via atmospheric deposition. However, considering the rates of Zn deposition noted in Chapter 7, a considerable fraction of Zn is also being directly deposited on road surfaces.

(c) Polycyclic aromatic hydrocarbons (PAHs)

PAHs detected in this study were compared with the outcomes reported from a similar study conducted by Lau and Stenstrom (2005). The comparison of study outcomes are given in Table 8-3 below.

Table 8-3: PAHs build-up on roads

PAHs	Concentrations observed in this study		Adopted from Lau and Stenstrom (2005)	
	Max.(mg/m ²)	Min.(mg/m ²)	Max.(mg/m ²)	Min.(mg/m ²)
ACE	93.095	2.309	0.082	0.000
FLU	72.258	16.834	3.282	0.995
PHE	31.213	2.548	10.461	1.239
PHE	40.278	6.884	4.502	0.013
FLA	27.205	3.120	10.134	1.063
PYR	11.434	0.182	14.373	2.349
BaA	8.416	0.000	5.602	0.658
CHR	13.445	0.000	11.115	1.712

Note: Lau and Stenstrom (2005) did not investigate other priority PAHs species.

Even though ACE, FLU, PHE, PHE were detected in high concentration in the current study compared to the values reported by Lau and Stenstrom (2005), the other PAHs given in Table 8-3 are in a similar range. Detection of some PAHs in high concentrations can be due to a range of factors including the differences in field conditions and traffic volume. As the collected data are in reasonable agreement and variations can be explained, it can be considered that the data obtained for PAHs in current study are consistent.

The comparison of PAHs for different sites are presented in Figure 8-4 for the seven low molecular weight (three and four ring) and the seven heavier (four and five ring) PAHs shown in Figure 8-4(a) and (b), respectively.

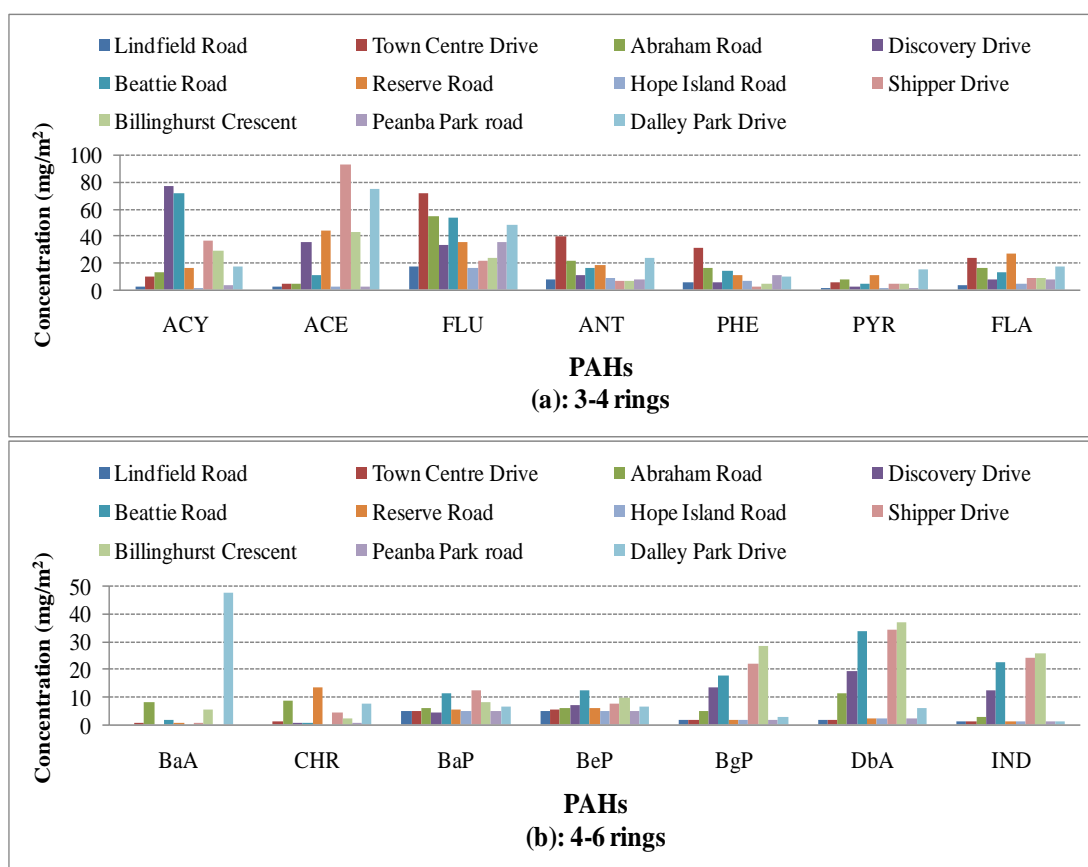


Figure 8-4: Variation PAHs in build-up for study sites

As evident in Figure 8-4, low molecular weight (three and four ring) PAHs are detected in high concentrations in the study region compared to the high molecular weight PAHs. As noted in Chapter 6, a high fraction of three and four ring PAHs in atmospheric phase originate from gasoline combustion and incomplete combustion (Singh et al. 2008; Kocbach et al. 2006). Presence of these PAHs in build-up, suggest

the presence of a strong linkage between atmospheric deposition and build-up. However, PAHs are also associated with other traffic related petroleum products such as crankcase oil and engine oils which can contribute to build-up directly. This highlighted the need for a detailed analysis to understand PAH sources and pathways.

In order to differentiate the PAHs between petrogenic and pyrogenic sources, Liu et al. (2009) noted the possibility of using diagnostic ratios of two and three ring PAHs to four and six ring PAHs. According to them, diagnostic ratios >1 relates to petrogenic sources and <1 relates to pyrogenic sources. It was found that except at Billinghamurst Crescent, all the other sites had diagnostic ratios >1 indicating the predominance of petrogenic sources. However, the presence of variable traffic related sources and the possibility of generating PAHs from land use related activities adds an extra complexity. A multivariate analytical technique was considered essential for the analysis of such a complex dataset.

8.3.3 Multivariate Analysis of Heavy Metals and Solids

Multivariate analysis was undertaken to understand the complex relationships between build-up pollutants with traffic and land use characteristics and to develop linkages between build-up with air quality and atmospheric deposition. The primary traffic parameters considered during the analysis were ADT_{to}, ADT_{hv} and V/C. In addition, coefficient of uniformity (PSD_{D50}) was also used for the analysis as noted under Figure 8-2. PROMETHEE and GAIA analytical techniques were used to undertake the analysis. Details of these methods have been described in Section 3.4.3.

(a) Solids

Firstly, PROMETHEE analysis was undertaken for the solids after separating them into five size fractions. As discussed in Chapter 5, build-up samples were analysed after separating them into five size fractions. They are $<1 \mu\text{m}$, $1-75 \mu\text{m}$, $75-150 \mu\text{m}$, $150-300 \mu\text{m}$, and $>300 \mu\text{m}$. For this, the build-up data collected from 10 sites (Set 3) were used. It was found that Hope Island road site is an outlier and removed from the analysis. V-shape preference function was selected for all the variables as it

compares values based on one threshold. As noted by Herngren et al. (2005), V-shape preference function is best suited for quantitative criteria. Figure 8-5 illustrates the GAIA biplot generated by analysing solids in the five size fractions mainly with traffic parameters. The resulting PROMETHEE 2 complete rankings are given in Table C-1 of Appendix C.

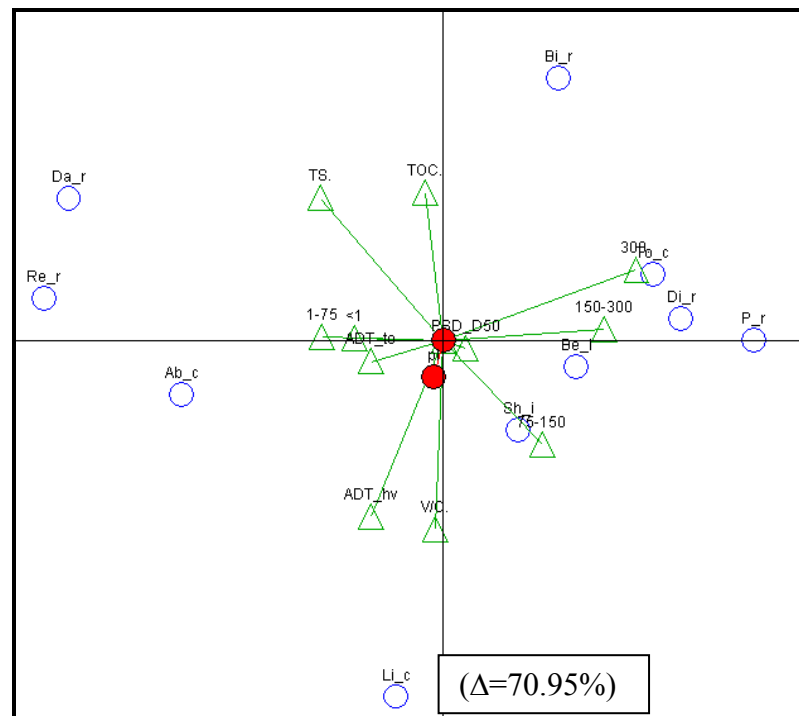


Figure 8-5: GAIA biplot of PSD based on 11sites

(Where Δ is the percentage variance described by the GAIA biplot, refer Table 8-1 for land use notations of c, i and r)

As evident from the GAIA biplot in Figure 8-5, particle size fractions of $<1 \mu\text{m}$ and $1-75 \mu\text{m}$ correlate with ADT_to. As there is no correlation of V/C with the $<1 \mu\text{m}$ and $1-75 \mu\text{m}$ particle sizes, it suggests that they are independent of traffic congestion. Additionally, Figure 8-5 shows a negative correlation of $75-150 \mu\text{m}$, $150-300 \mu\text{m}$ and $>300 \mu\text{m}$ size fractions with ADT_to. Correlation of finer particle sizes with traffic volume and negative correlation of larger particles with traffic volume suggests the possibility of the grinding of larger particles or the occurrence of re-suspension and re-distribution processes enabling the increase of $<75 \mu\text{m}$ particles. However, traffic congestion has no influence on these processes. Chapter 7 noted that traffic congestion mainly increases exhaust related emissions and they are small

in size. Such particles tend to accumulate mainly in the atmosphere rather than on road surfaces.

(b) Heavy metals

Similar PROMETHEE analysis was conducted for heavy metals to investigate the variation of HMs with traffic and land use characteristics. Data analysis was undertaken for the first three fractions separately and the last two fractions were analysed together due to similarity of outcomes. All heavy metal species tested (Cr, Cd, Mn, Cu, Pb, Zn and Ni) and the influential physical and chemical parameters such as total organic carbon (TOC), dissolved organic carbon (DOC), uniformity coefficient of particle size distribution (PSD_D50), electrical conductivity (EC) and pH were used as the primary variables in the analysis. Total average daily traffic measured in 2010 (ADT_to), total daily average heavy duty traffic (ADT_hv) and traffic congestion (V/C) were the key exploratory variables used. In order to investigate the influence of different land uses on heavy metal build-up, the study sites were identified with a letter to designate the corresponding land use.

<1 μm size fraction.

The resulting PROMETHEE 2 complete rankings are given in Tables C-2 of Appendix C.

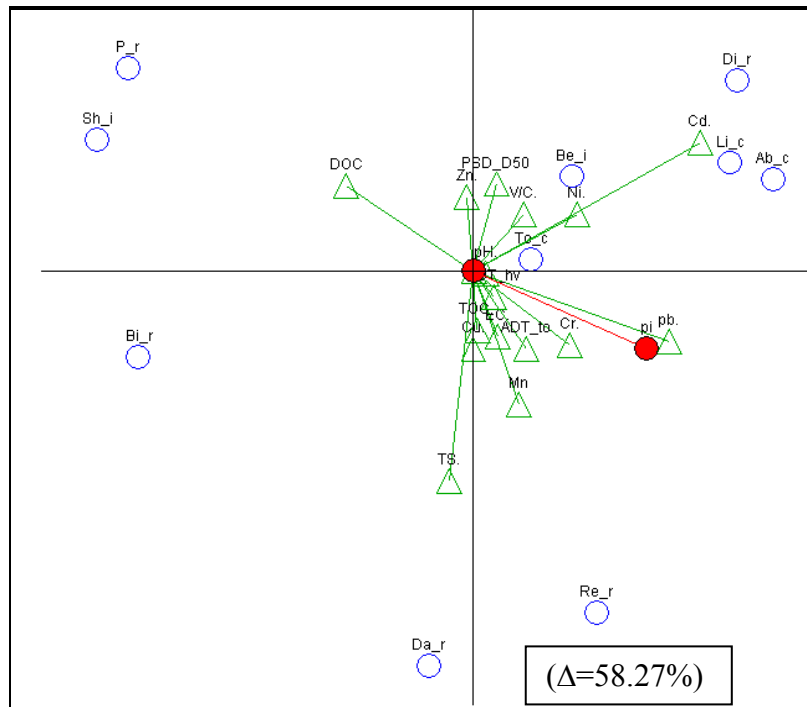


Figure 8-6: PCA biplot of HMs with the first two principal components for <math><1\mu\text{m}</math> fraction

(Where Δ is the percentage variance described by the GAIA biplot, TS=Total solids, refer Table 8-1 for land use notations of c, i and r)

Figure 8-6 shows that Ni, Cd and V/C are correlated. This means that traffic congestion influences the generation of Ni and Cd in the fine fraction ($<1\mu\text{m}$) of road surface build-up solids. It was noted in Section 6.4.1 that V/C shows strong correlation with Cd in the atmospheric phase. Furthermore, it was also noted in Chapter 7 that Ni and Cd are associated with the fine fraction of atmospheric deposition particles and they correlate with V/C. This pointed to the fact that atmospheric deposition being the primary pathway for the build-up of Ni and Cd on road surfaces. This is also supported by the fact that both V/C and ADT_hv increase exhaust emissions. Additionally, as ADT_hv shows a weak correlation with Ni and Cd, it can be postulated that heavy duty traffic generate high exhaust emissions to the atmosphere and in turn contribute to atmospheric deposition. This process could be significant, as exhaust emissions generate a high fraction of finer particles ($<1\mu\text{m}$). A similar finding was noted by Duong and Lee (2011) highlighting traffic congestion as one of the main generation processes for Ni and Cd.

Figure 8-6 also shows that TOC, TS, Cu, Mn and EC are closely correlated to ADT_{to}. As discussed in Chapter 2, traffic sources generally do not generate TOC. However, traffic sources contribute solids and Cu to urban roads. As noted by Herngren (2006) and Weng et al. (2002), in the liquid matrix with the presence of organic carbon, heavy metals can undergo organic complexation. As build-up samples were collected in a liquid matrix, heavy metals could undergo organic complexation with dissolved organic matter in the <1 μm size fraction. Therefore, this suggests that TOC, TS, Cu, Mn are present as organic complexes on road surface build-up. Furthermore, Weng et al. (2002) noted that Cu has the best ability to form organic complexes with organic matter. This means that the correlation of TOC and TS with Cu could be due to the presence of Cu in organic complexes.

Figure 8-6 does not show any grouping of sites based on the type of land use for the <1μm size fraction. This is due to the reduced involvement of land use activities in heavy metal build-up on roads for this size fraction. It was noted in Chapter 6 that traffic generated small particles disperse in the atmosphere quickly and become more uniformly distributed. This can create uniformity in build-up in the atmospheric deposition pathway. Furthermore, atmospheric heavy metal concentration is not highly influenced by land use types during weekdays due to the dominance of traffic sources. Therefore, the influence of non-traffic related activities can be overshadowed by traffic activities, although the former generated a fraction of the pollutants. Deletic and Orr (2005) noted that the concentration of heavy metals in road deposited sediments depends mainly on traffic volume.

1-75 μm size fraction.

Figure 8-7(a) illustrates the Actions in GAIA biplot and Figure 8-7(b) illustrates the Criteria for the same GAIA biplot. The resulting PROMETHEE 2 complete ranking is given in Tables C-3 of Appendix C.

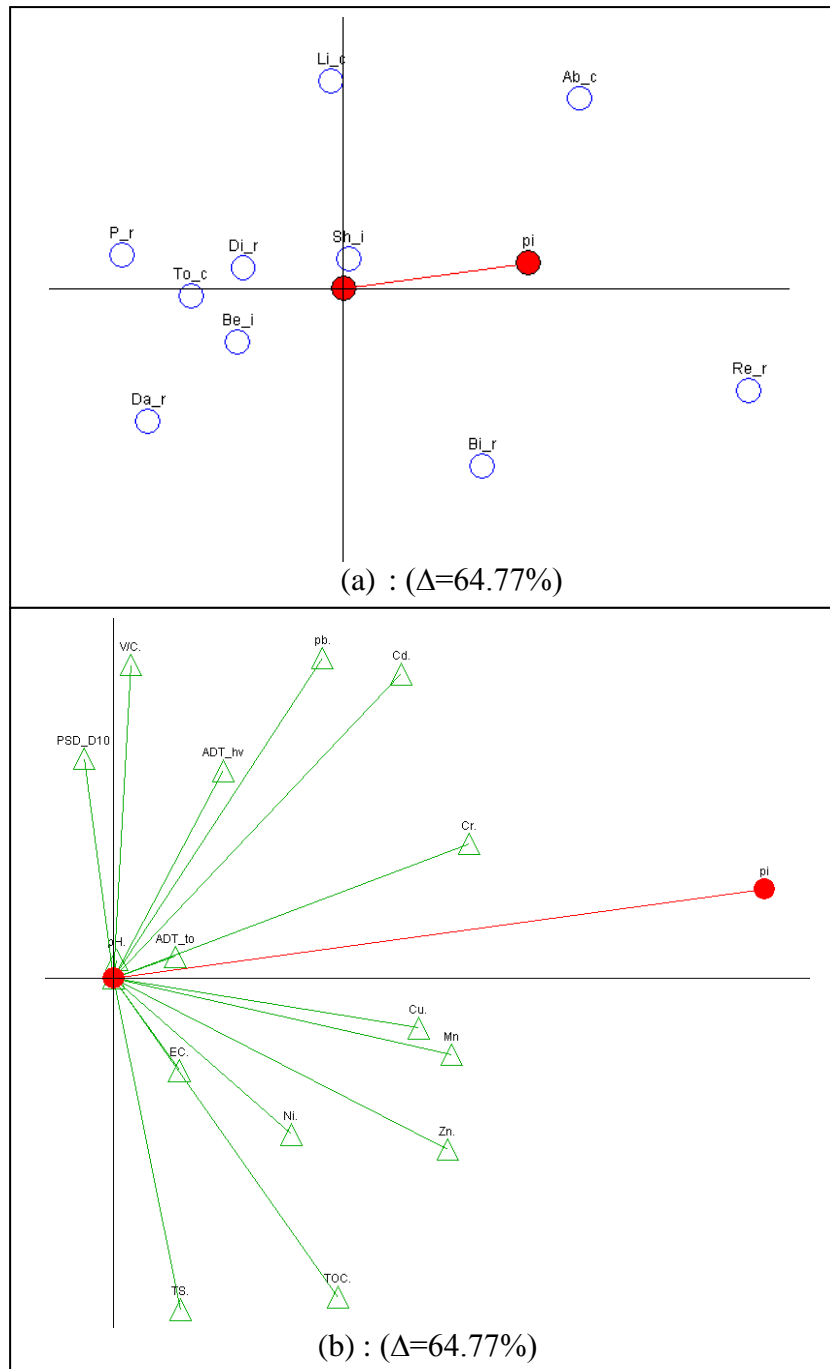


Figure 8-7: PCA biplot of HMs with the first two principal components for 1-75 μm fraction, (a): for actions, (b): for criteria

(Where Δ is the percentage variance described by the GAIA biplot, TS=Total solids, refer Table 8-1 for land use notations of c, i and r, plots (a) and (b) are in two different scales)

Figure 8-7(b) shows correlation of V/C and ADT_hv with Pb, Cd and Cr. This suggests that heavy duty traffic and effects of congestion generate Pb, Cd and Cr in

the 1-75 μm size fraction. Correlation of Pb, Cd and Cr to ADT_{hv} relates to the possibility of these metals originating from combustion related sources. Analysis in Section 7.4.2(a) linked Cd and Cr metal species to exhaust emissions. Furthermore, it was noted in Section 6.41 that ADT_{hv} is strongly correlated to Cu and Cr in the atmospheric phase. This points to the predominance of exhaust emissions as the primary contributing source of Cd and Cr and the importance of atmospheric deposition as an important pathway. As confirmation, Opher and Friedler (2010) reported the significance of exhaust emissions as a source of Cd and Cr. Section 6.3.2 identified that soil dust enriched with Pb from previous decades of leaded fuel usage as the primary source of Pb.

Figure 8-7(b) illustrates that TOC, TS and EC are correlated. This is primarily attributed to organic complexation as discussed under Figure 8-6. Figure 8-7(a) does not show any grouping of sites based on land use. This is attributed to the low involvement of land use activities, excluding traffic in heavy metal build-up on roads in the case of the 1-75 μm fraction as discussed under Figure 8-6.

75-150 μm size fraction

The resulting PROMETHEE 2 complete ranking is given in Tables C-4 of Appendix C.

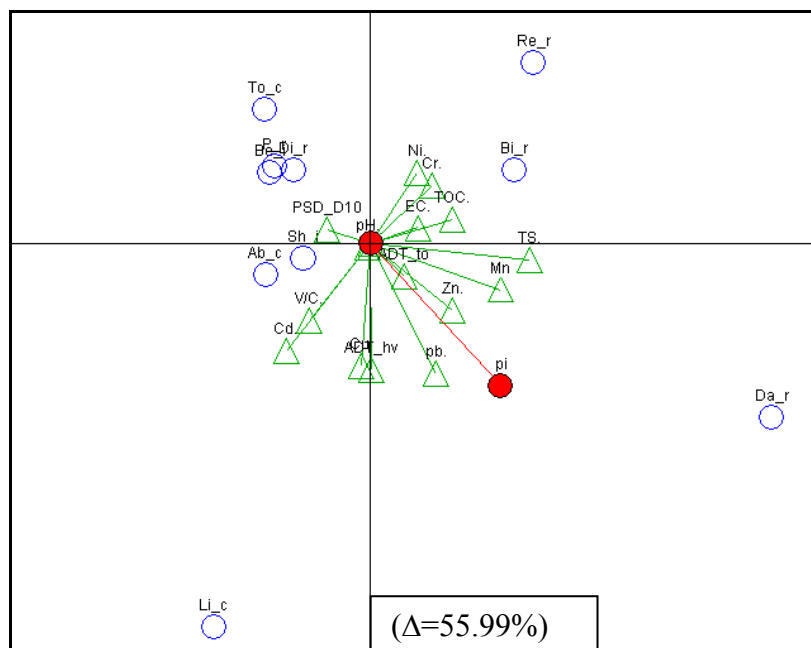


Figure 8-8: PCA biplot of HMs with the first two principal components for 75-150 μm fraction

(Where Δ is the percentage variance described by the GAIA biplot, TS=total solids, refer Table 8-1 for land use notations of c, i and r)

Figure 8-8 shows correlation of Cu, Cd, with V/C and ADT_hv and to a lesser extent with Pb. As discussed previously in relation to the 1-75 μm size fraction, these three heavy metals originate primarily from exhaust emissions. However, 75-150 μm size fraction is not the size range that combustion engines emit directly. As Morawska (2008) and Harris and Maricq (2001) noted, all diesel and gasoline exhaust particles are less than 10 μm and 1 μm , respectively. In addition, Gietl et al. (2010) noted that vehicle wear particles (brake and tyre) are less than 50 μm in size. Furthermore, Ntziachristos (2009) noted that tyre and brake wear particles are <30 μm and < 20 μm , respectively, under normal driving conditions. Therefore, these metal elements are not the direct emission products from traffic related exhaust or wear related emissions. However, Sternbeck et al. (2002) noted that Cd and Cu are primarily generated by traffic related wear and tear. Therefore, it is possible that these metal species are generated from both exhaust and traffic related wear sources and undergo further processes such as adsorption to larger particle sizes. This is further supported by the finding of Han et al. (2008) who reported that the highest concentration of Cd, Cu and Pb in 80 to 101 μm size range for road deposited sediments.

Figure 8-8 shows correlation of Zn, TOC, TS, EC, Mn and ADT_{to} in the 75-150 μm size fraction. Although exhaust and tyre wear particles are the main sources of Zn and TS on road deposited solids, they are associated mainly with $< 50\mu\text{m}$ particles size fraction (Singh 2011; Sansalone and Buchberger 1997). Therefore, soil related sources could be the primary source of Mn, Zn and TS in the 75-150 μm size fraction. However, Mn and Zn and TS correlate with ADT_{to}. Therefore, the one possibility is that traffic sources transport soil related Mn and Zn to road surfaces. Additionally, this could be due to metal complexation in the presence of organic carbons as noted by Weng et al. (2002) and Herngren (2006). Herngren (2006) also reported a weak correlation among Zn, Mn and TOC for the $<150 \mu\text{m}$ fraction in a similar study. Moreover, it was noted in Section 7.4.2(b) that TOC is related to Mn in bulk deposition samples. Therefore, bulk deposition is also an important pathway of Mn in build-up on roads.

Figure 8-8 does not show grouping of sites based on land use for the 75-150 μm size fraction in terms of heavy metals loadings. This is primarily attributed to the low involvement of land use activities, excluding traffic, in heavy metal build-up on roads in this size fraction as discussed in Figure 8-6.

150-300 μm and $>300\mu\text{m}$ size fractions

It was noted that the GAIA biplots of 150-300 μm and $>300 \mu\text{m}$ size fractions are similar. Therefore, these two fractions were analysed together. Figure 8-9(a) illustrates the Actions in GAIA biplot and Figure 8-9(b) illustrates the Criteria for the same GAIA biplot. The resulting PROMETHEE 2 complete ranking is given in Tables C-5 of Appendix C.

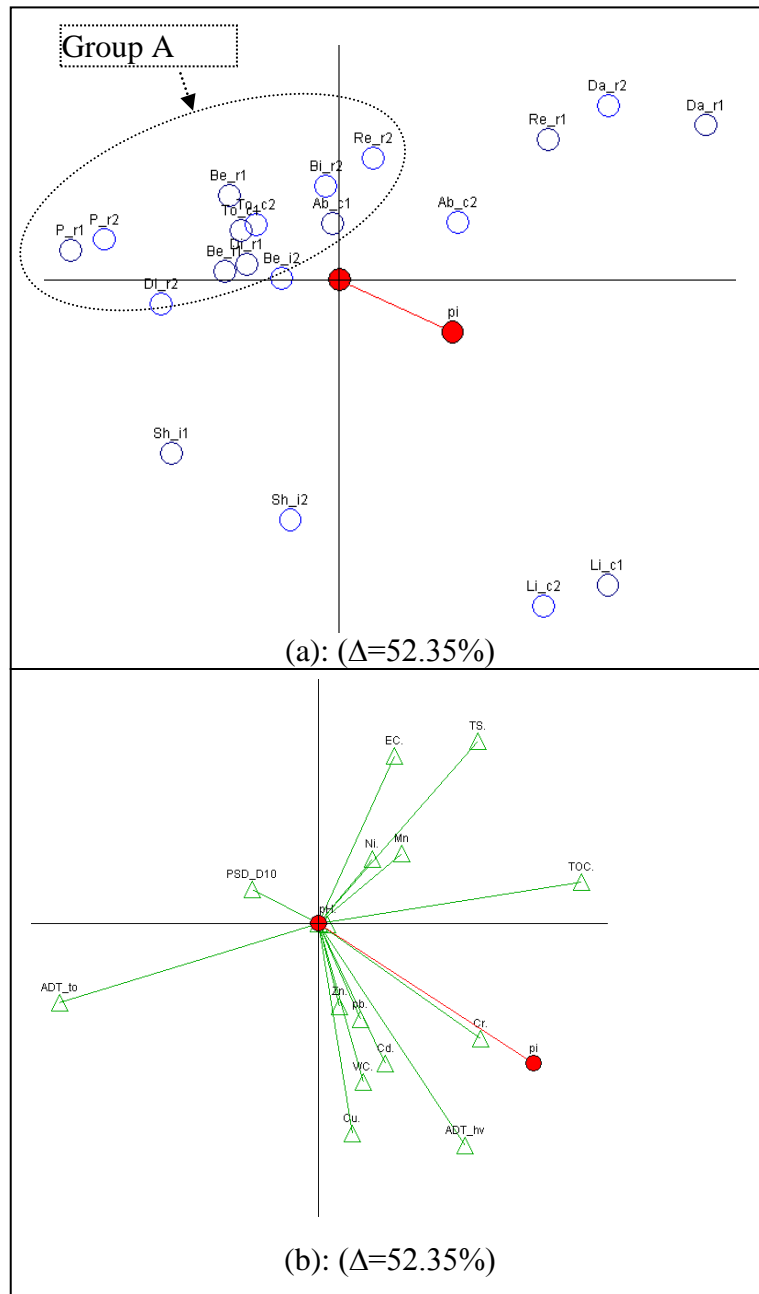


Figure 8-9: PCA biplot of HMs with the first two principal components for 150-300 μm and $>300 \mu\text{m}$ fractions, (a): for actions, (b): for criteria
 (Where Δ is the percentage variance described by the GAIA biplot, TS= total solids, refer Table 8-1 for land use notations of c, i and r, 1 = 150-300 μm , 2 = $>300 \mu\text{m}$, plots (a) and (b) are in two different scales)

Figure 8-9(b) shows correlation of Cu, Pb, Cr and Zn with V/C and ADT_hv. However, traffic related emission particles (including exhaust and brake and tyre wear) are $<50 \mu\text{m}$ as discussed in relation to Figure 8-8. Therefore, traffic sources do not directly contribute particles to the 150-300 μm and $>300 \mu\text{m}$ size fractions. This

suggests that either traffic generated smaller particles are attached to larger particles due to adsorption and/or the transport of soil particles containing Cu, Pb, Cr, Zn to roads. Furthermore, this is supported by the findings discussed in Section 6.7 regarding previously generated Pb being associated with road dust. However, Figure 8-9 shows that these elements are almost independent of total traffic volume. This is due to the fact that total traffic volume consists primarily of light duty vehicles (large number of cars) and gasoline exhaust particles are less than 1 μ m. Hence, they accumulate in the atmosphere instead of direct deposition (Maricq 2001). However, as noted by Morawska (2008), a single diesel truck can produce as much pollution as 100 cars and these particles are less than 10 μ m. They can deposit relatively quickly on roads and associate with other solids present.

Figure 8-9(b) shows the correlation of TOC, Mn, TS and EC in the 150-300 μ m size fraction. There are two main reasons for this behaviour as already explained in relation to Figure 8-8. Firstly, soil sources can contribute Mn and TS to road surfaces. Secondly, metal complexation can take place in the presence of organic carbon. This conclusion is supported by the findings of Khairy et al. (2011) who noted that Mn is generated by natural sources such as soil. Additionally, correlation of TOC, Mn, TS can be attributed to the organic complexation of Mn and TOC with soil, as organic complexation affects the solubility and mobility of heavy metals (Weng et al. 2002).

Figure 8-9(a) shows a grouping of 12 objects (Group A) which belong to commercial and residential land uses based primarily on their heavy metal loadings. Therefore, this suggests that these two land uses have generated similar heavy metal loadings which are associated with relatively larger particles (>150 μ m) on road surfaces. Additionally, as land use related activities contribute organic carbon, it can promote organic complexation of small particles which are associated heavy metals. This conclusion is supported by the finding of Hamilton et al. (1984). They noted that heavy metals in residential road sites are mainly associated with coarse particle size fractions.

HMs in all size fractions

Figure 8-10 shows the GAIA biplot of the outcomes of the PROMETHEE analysis undertaken for the data set with all the particle size fractions combined together. This was undertaken to understand the overall site characteristics in terms of heavy metal pollution. In this analysis, heavy metal concentrations were divided by the corresponding solid mass to remove any bias due to differing solids loadings. Figure 8-10(a) illustrates the Actions in GAIA biplot and Figure 8-10(b) illustrates the Criteria for the same GAIA biplot. The resulting PROMETHEE 2 complete ranking is given in Table C- 6 of Appendix C.

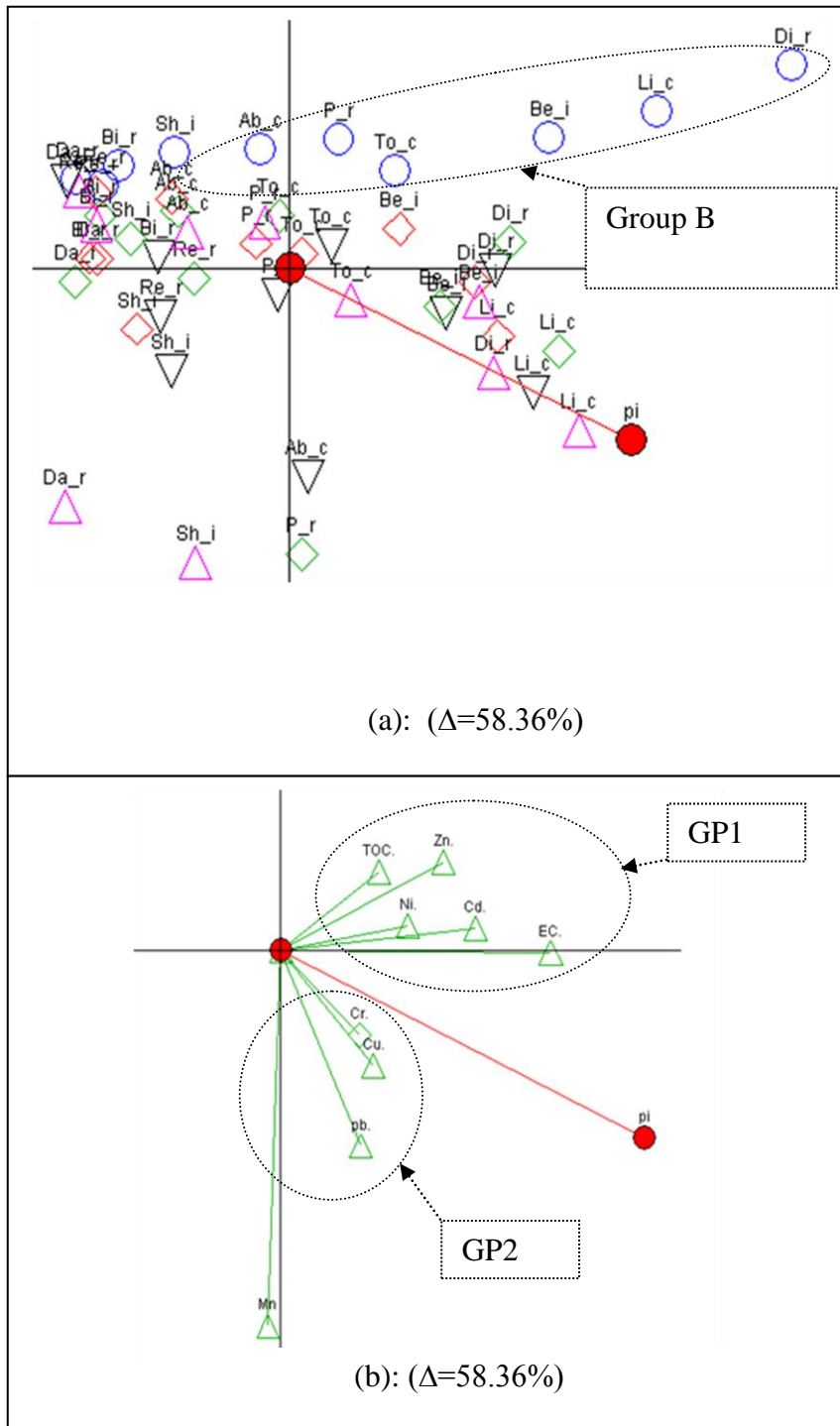


Figure 8-10: PCA biplot of HMs with the first two principal components for all size fractions, (a): for actions, (b): for criteria

(Where $\circ = <1 \mu\text{m}$ fraction, $\diamond = 75\text{-}150 \mu\text{m}$ fraction, $\nabla = 1\text{-}75 \mu\text{m}$ fraction $\diamond = 150\text{-}300 \mu\text{m}$ fraction, $\triangle = >300 \mu\text{m}$ fraction), refer Table 8-1 for land use notations of c, i and r, Δ is the percentage variance described by the GAIA biplot, plots (a) and (b) are in two different scales)

Figure 8-10(b) shows two separate groups of Zn, Ni, Cd, TOC and EC (GP1) and Cr, Cd and Pb (GP2). Zn, Ni, Cd, TOC and EC (GP1) vectors point towards Group B which is the $<1 \mu\text{m}$ size fraction. As noted in relation to Figures 8-8, all traffic generated particles including exhaust and abrasion related particles are $<50 \mu\text{m}$. Therefore, this suggests that direct traffic related emissions are the primary source of Zn, Ni, Cd and are primarily associated with the $<1 \mu\text{m}$ size fraction. This conclusion is supported by Lim et al. (2006) who noted that traffic is the main Zn source on road surfaces. However, as Cr, Cd and Pb vectors point towards the $1-75 \mu\text{m}$ and $75-150 \mu\text{m}$ size fractions, it can be concluded that, either these heavy metals are generated mainly by soil related sources as discussed in relation to Figure 8-8 or from traffic sources but attached to relatively larger particles. Additionally, these particles form organic complexes in the presence of organic carbon as noted in relation to Figure 8-8 and favourable EC will accelerate this process (Herngren 2006).

Figures 8-10(a) and (b) shows that the concentration of Mn, Pb, Cu increases with the particle size. This again confirms the conclusions derived in relation to Figure 8-7 where it was noted that smaller particles associated with Mn, Pb, Cu are attached to larger particles in the presence of organic carbon. It was noted in relation to Figure 8-9 that soil sources generate Mn in the $>150 \mu\text{m}$ particles size fraction.

8.3.4 Analysis of polycyclic aromatic hydrocarbons (PAHs)

PAHs were also analysed using the same approach as for the analysis of heavy metals. Data from only ten sites were used for the analysis. Hope Island road site was removed from the data set for this analysis due to it being considered as an outlier. The analysis was conducted for $<1 \mu\text{m}$ $1-75 \mu\text{m}$, $75-150 \mu\text{m}$, $150-300 \mu\text{m}$, and $>300 \mu\text{m}$ size fractions separately.

$<1\mu\text{m}$ size fraction

Figure 8-11(a) illustrates the Actions in GAIA biplot and Figure 8-11(b) illustrates the Criteria for the same GAIA biplot. Resulting PROMETHEE 2 complete ranking is given in Table C- 7 of Appendix C.

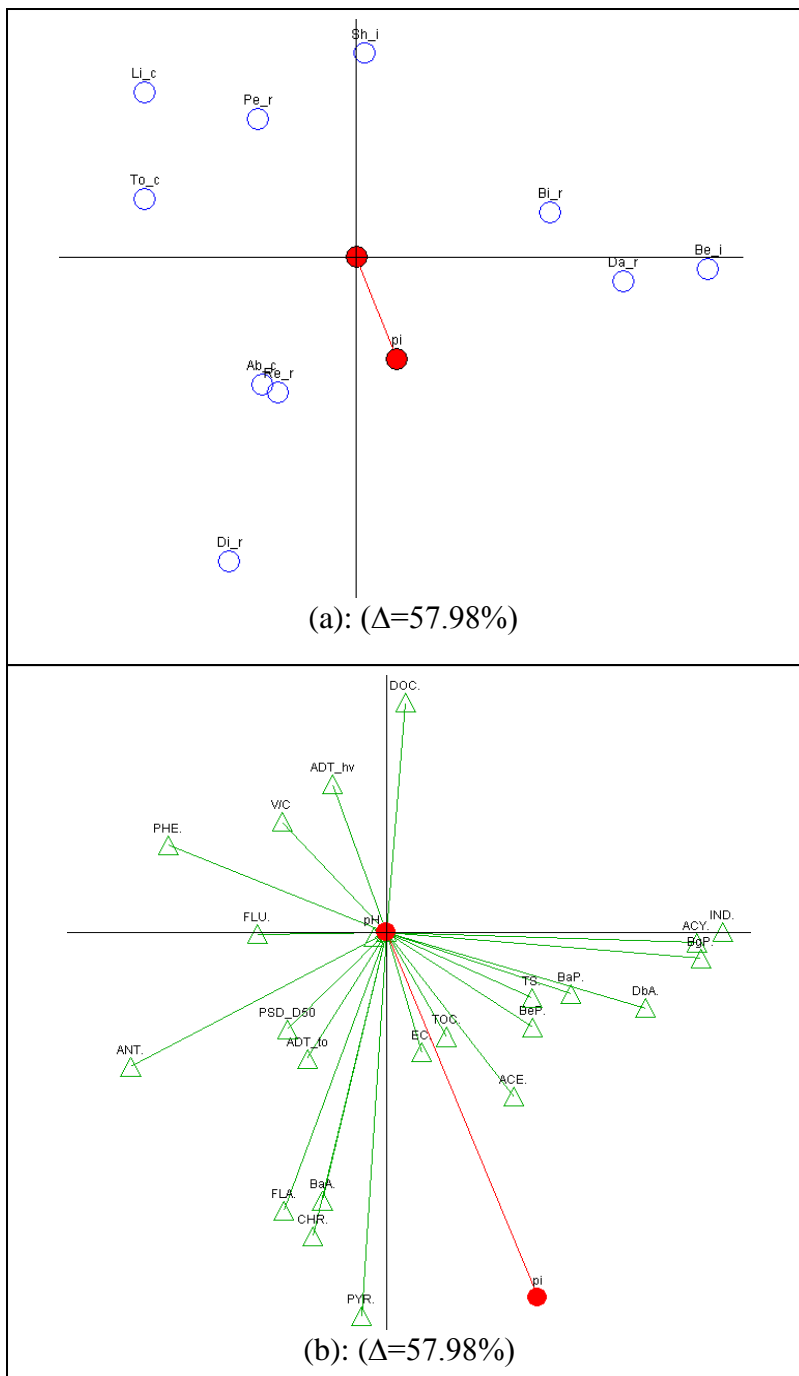


Figure 8-11: GAIA biplot of PAHs for the first two principal components for <1 μm fraction, (a): for actions, (b): for criteria

Where Δ is the percentage variance described by the GAIA biplot, TS is the total solids, refer Table 8-1 for land use notations of c, i and r, Δ is the percentage variance described by the GAIA biplot, plots (a) and (b) are in two different scales)

Figure 8-11(b) shows that FLU, ANT, FLA, CHR, BaA, PYR, PSD_D50 and pH correlate with traffic (ADT_to) in the <1 μm particle size fraction. These PAHs have

three and four benzene rings. It is likely that these PAHs are generated by incomplete combustion of fossil fuels. Incomplete combustion of fossil fuels has been recognised as the dominant PAH source (Zuo et al. 2007). Furthermore, it was noted in relation to Figure 8-8 that diesel and gasoline exhaust particles are less than 10 µm and 1 µm, respectively (Miguel et al. (1998). Therefore, it is most likely that primarily gasoline exhaust generates FLU, ANT, FLA, CHR, BaA, PYR in the <1 µm size fraction. Additionally, as noted in Section 6.5, traffic sources generate three and five ring PAHs in the atmospheric phase. Therefore, atmospheric deposition can be recognised as a pathway for these PAHs in the <1 µm particle size fraction. This is supported by the findings of Takada et al. (1990) who noted that traffic exhaust is one of the main sources of PAHs in road deposited solids and asphalt contributes only a negligible amount.

Figure 8-11(b) shows a grouping of ACE, BeP, BaP, DbA, BgP, ACY, IND, EC, TS and TOC and negatively related with V/C and ADT_hv for the <1 µm particle size fraction. Majority of these PAHs have four and six benzene rings. As noted in Chapter 6.5, four and six ring PAHs are associated with particulate matter in the atmosphere and is mainly emitting by diesel engines. Diesel engines emit four and six ring PAHs as well as three and four ring PAHs for slow and fast moving conditions, respectively, whilst gasoline engines emit three and four ring PAHs for both the cases (Riddle et al. 2007; Lee et al. 2005). Additionally, as the traffic congestion increases, increase in four and six ring PAHs can be associated with diesel exhaust. However, these PAHs do not appear to be primarily from diesel exhaust emission as V/C and ADT_hv are negatively correlated with these PAHs. As such, the main source of these PAHs is not clear. However, the overall understanding suggests that these PAHs are associated with organic carbon and particulate matter. This is supported by the finding by Herngren et al. (2010) who noted that TOC increases adsorption of PAHs with particulate matter due to organic complexation. Additionally, these PAHs have high molecular weight and very low solubility (See Table A-1 of Appendix A), and are primarily associated with particulate matter (Guo et al. 2007).

Figure 8-11(a) does not show any clear grouping of sites depending on their dominant land use. Therefore, PAHs in road deposited solids in the $<1 \mu\text{m}$ particle size fraction is not generated by other land use related activities, excluding traffic. Traffic is the most common generator of PAHs for all three land use types. However, Ab_c, Re_r and Di_r show a grouping and point in the direction of ADT_to. It was found that these three sites are located close to the Pacific highway. Therefore gasoline vehicles operating in the highway could contribute PAHs to these sites.

1-75 μm size fraction

Figure 8-12(a) illustrates the Actions in GAIA biplot and Figure 8-12(b) illustrates the Criteria for the same GAIA biplot. Resulting PROMETHEE 2 complete ranking is given in Table C- 8 of Appendix C.

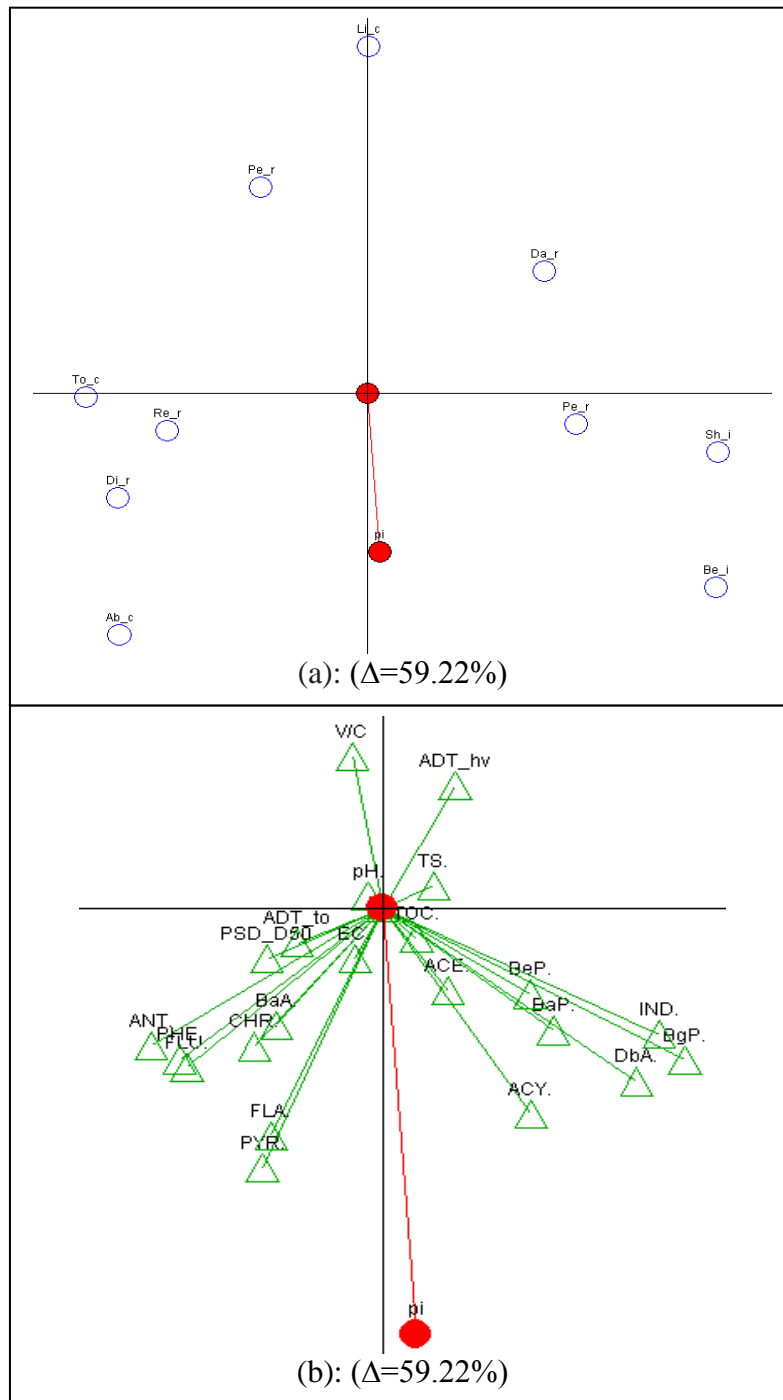


Figure 8-12: GAIA biplot of PAHs for the first two principal components for 1-75 μm fraction, (a): for actions, (b): for criteria

Where Δ is the percentage variance described by the GAIA biplot, TS is the total solids, refer Table 8-1 for land use notations of c, i and r, Δ is the percentage variance described by the GAIA biplot, plots (a) and (b) are in two different scales)

Figure 8-12(b) shows that FLU, ANT, FLA, CHR, BaA, PYR, PHE, PSD_D50 and EC correlate with traffic (ADT_to) and negatively correlate with ADT_hv and V/C

for the 1-75 μm particle size fraction. These PAHs mainly consist of three and four rings. PAHs with three and four benzene rings are generated mainly by gasoline vehicles as discussed in relation to Figure 8-11. However, gasoline exhaust particles are $<1 \mu\text{m}$ in size. This suggests that these PAHs combine with relatively larger solids particles ($> 75 \mu\text{m}$) in build-up.

Figure 8-12(b) shows correlation among ACE, BeP, BaP, DbA, BgP, ACY, IND, and TOC and no correlation with ADT_hv and V/C. These are higher molecular weight PAHs (four and six ring). As shown in Table A-1 of Appendix A and noted by Kim and Young (2009), high molecular weight PAHs have very low solubility. Therefore, they are associated primarily with particulate matter (Guo et al. 2007). Hengren (2005) and Hengren et al. (2010) noted that organic carbon play an important role in the adsorption of PAHs to solids. However, as organic matter have low specific gravity, the resulting particulates do not make a large contribution to TS load. Additionally, leakage of fuel and oil from vehicles also primarily contribute high molecular weight (HMW) PAHs. This is dependent on the age of the vehicles (Lim 2007). This suggests that leakage of fuel and oil from vehicles is one of the main PAHs sources in the 1-75 μm particle size fraction.

Figure 8-12(a) do not show any clear grouping of sites based on the land use. As noted in Figure 8-11, this suggests that PAHs in road deposited solids in the 1-75 μm particle size fraction are generated mainly from traffic related activities.

75-150 μm size fraction

Figure 8-13(a) illustrates the Actions in GAIA biplot and Figure 8-13(b) illustrates the Criteria for the same GAIA biplot. Resulting PROMETHEE 2 complete ranking is given in Table C- 9 of Appendix C.

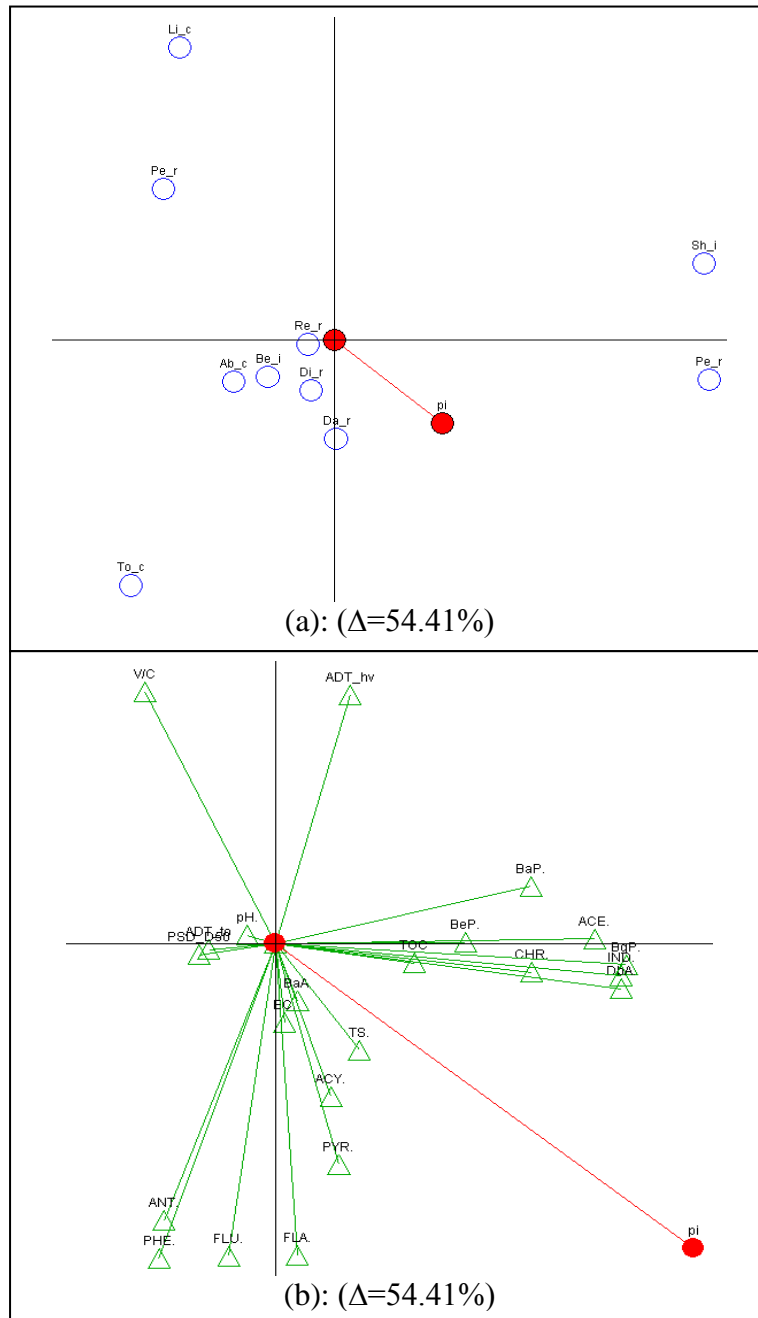


Figure 8-13: GAIA biplot of PAHs for the first two principal components for 75-150 μm fraction, (a): for actions, (b): for criteria

Where Δ is the percentage variance described by the GAIA biplot, TS is the total solids, refer Table 8-1 for land use notations of c, i and r, Δ is the percentage variance described by the GAIA biplot, plots (a) and (b) are in two different scales)

Figure 8-13(b) shows that ANT, PHE, FLU, FLA, ACY, PYR, TS, and EC are correlated and negatively correlated with V/C and ADT_hv. These PAHs have three and four rings. Also, Figure 8-13 shows that total traffic is independent of these

PAHs. These PAHs are not directly generated from exhaust emissions as exhaust particles are outside this size range as discussed in relation to Figure 8-8. This suggests that these PAHs could be attached to larger particles. However, the analysis fails to explain the negative correlation of these PAHs with V/C and ADT_hv.

Figure 8-13(b) shows a grouping of ACE, CHR, IND, BeP, Bap, BgP, DbA and TOC and negative correlation with ADT_to. As a majority of these PAHs have four and six benzene rings, their water solubility are very limited (Manoli and Samara 1999; Guo et al. 2007). Therefore, these PAHs are primarily bound to organic particles in this particle size fraction forming complexes with organic carbon in aqueous solution (Poerschmann et al. 2008; Herngren et al. 2010). This is supported by the findings of Stracquadiano and Trombini (2006) who noted that combustion processes emits both soot and particulate associated PAHs. This suggests that these PAHs are generated by traffic and associated with traffic generated soot. However, the analysis fails to explain the negative correlation of ADT_to with these PAHs.

Figure 8-13(a) does not show any clear grouping of sites depending of their dominant land use. As noted in relation to Figure 8-12, this once again suggests that PAHs in road deposited sentiments are not highly influenced by land use related activities.

150-300 μ m size fraction

Figure 8-14(a) illustrates the Actions in GAIA biplot and Figure 8-14(b) illustrates the Criteria for the same GAIA biplot. Resulting PROMETHEE 2 complete ranking is given in Table C-10 of Appendix C.

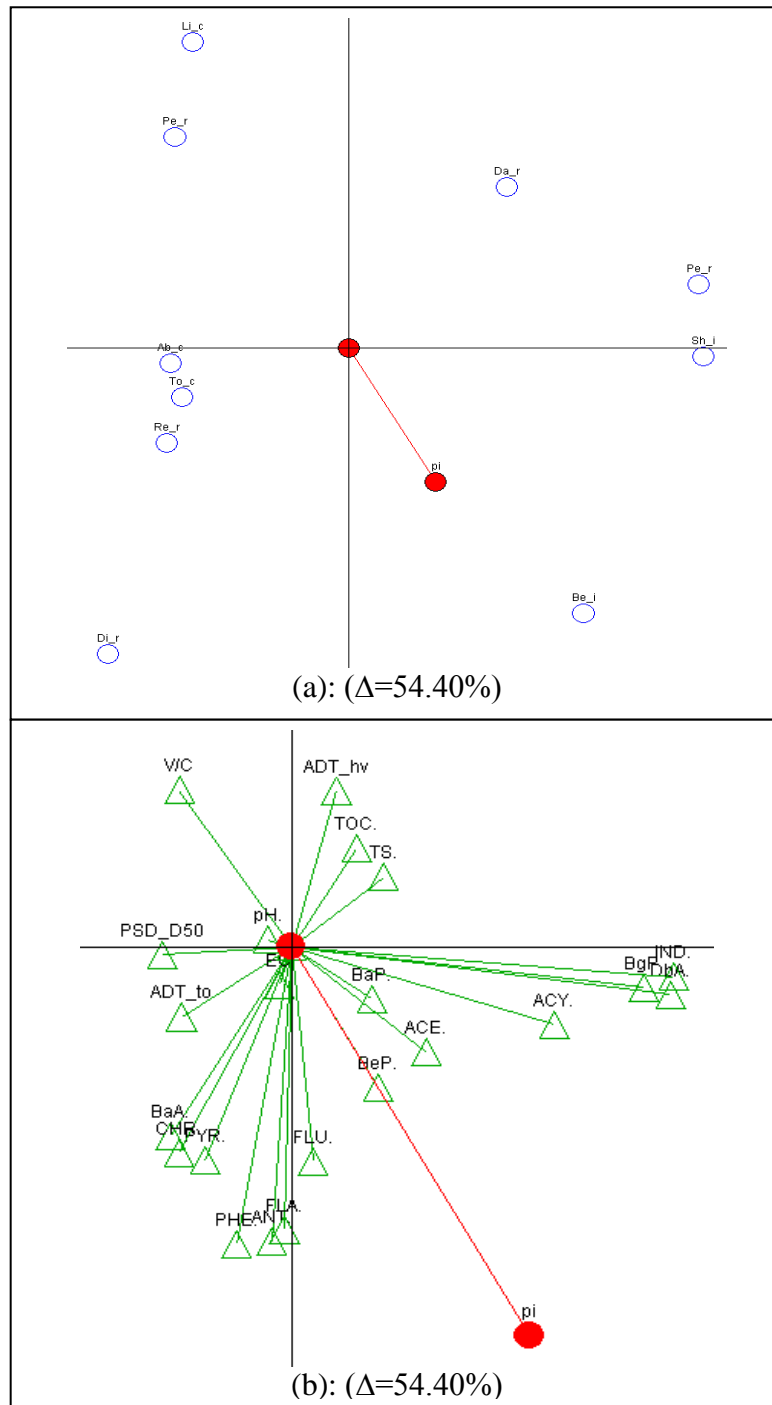


Figure 8-14: GAIA biplot of PAHs for the first two principal components for 150-300 μm fraction, (a): for actions, (b): for criteria

Where Δ is the percentage variance described by the GAIA biplot, TS is the total solids, refer Table 8-1 for land use notations of c, i and r, Δ is the percentage variance described by the GAIA biplot, plots (a) and (b) are in two different scales)

Figure 8-14(b) shows correlation of ANT, PHE, FLU, FLA, CHR, BaA, PYR, EC and ADT_to and a negative correlation with ADT_hv and V/C. These PAHs have

three and four benzene rings. Herngren (2005) noted that increase in EC of the stormwater increases the adsorption affinity of particles above 150 μm . Therefore, the correlation with EC suggests that EC promotes the attachment of PAHs to relatively larger particles. Additionally, the correlation between these PAHs and ADT_{to} could be due to the fact that ADT_{to} contributes small particle associated with metal cations which increases EC as discussed in relation to Figure 8-8. However, the analysis fails to explain the negative correction with ADT_{hv} and V/C.

Figure 8-14(b) shows that ACY, IND, BgP, DbA, BaP, BeP and ACE are correlated. Majority of these PAHs have four to six rings. As these PAHs do not correlate with TOC, organic complexation is not a dominant process in this size range. However, Karlsson and Viklander (2008) and Boonyatumanond et al. (2007) noted that leakage of oil is the main source for a range of PAHs in road runoff. Therefore, this could be the primary PAHs source in this size fraction. This mainly depends on the age of the vehicles.

Figure 8-14(a) shows no clear grouping of sites based on the land use. The same behaviour was noted for 75-150 μm particle size fraction and it was discussed in relation to Figure 8-13.

>300 μm size fraction

Figure 8-15(a) illustrates the Actions in GAIA biplot and Figure 8-15(b) illustrates the Criteria for the same GAIA biplot Resulting PROMETHEE 2 complete ranking is given in Table C- 11 of Appendix C.

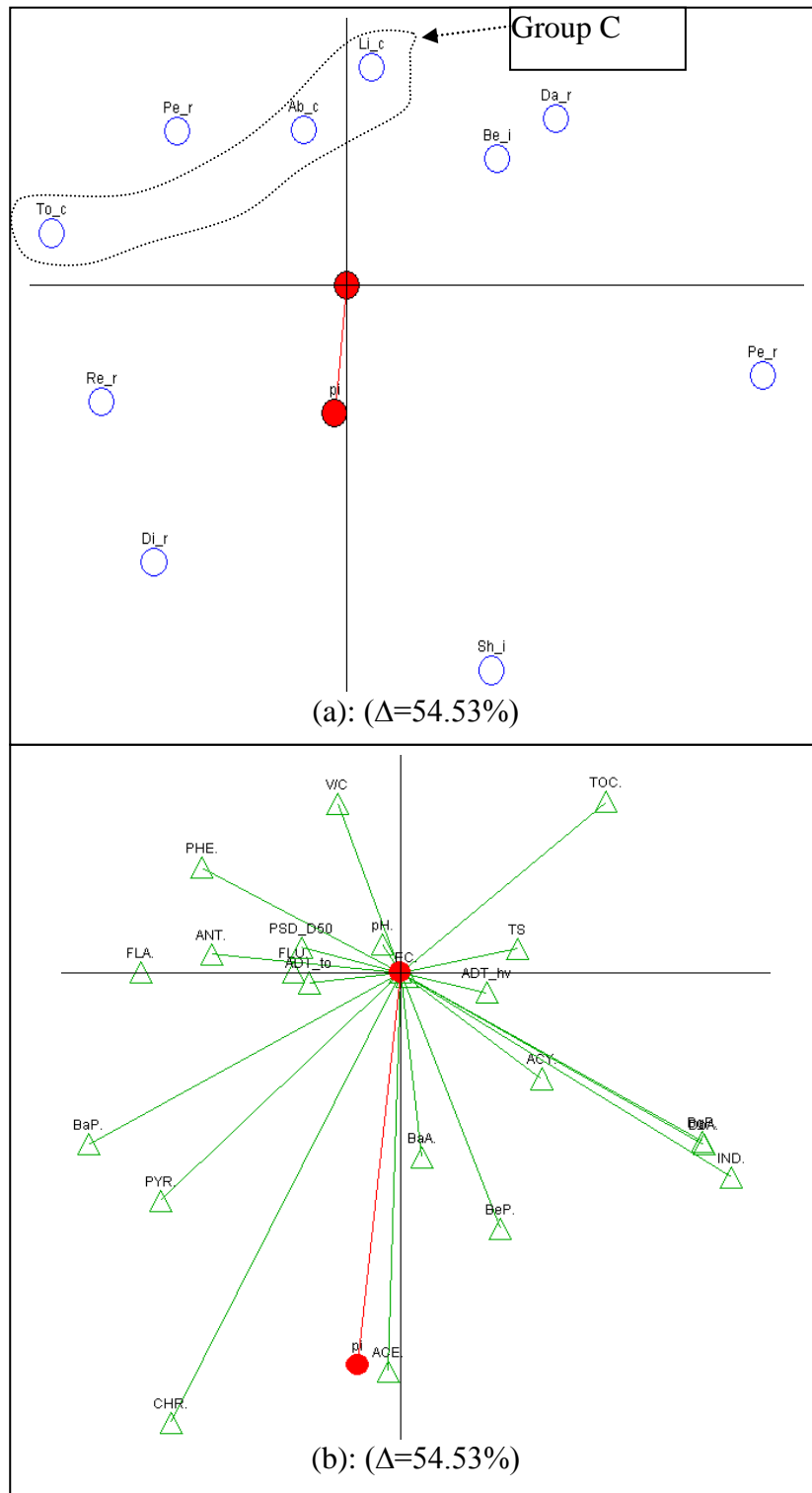


Figure 8-15: GAIA biplot of PAHs against the first two principal components for >300 μm fraction, (a): for actions, (b): for criteria

(Where Δ is the percentage variance described by the GAIA biplot, TS is the total solids, refer Table 8-1 for land use notations of c, i and r, Δ is the percentage variance described by the GAIA biplot, plots (a) and (b) are in two different scales)

Figure 8-15(b) show strong correlation of ANT, PHE, FLU, FLA, with ADT_{to} and weak correlation with V/C. However, these PAHs show negative correlation with ADT_{hv}. Most of these PAHs are relatively lighter compounds (three and four benzene rings). Gasoline vehicles mainly generate three and four benzene ring PAHs. Additionally, the negative correlation with ADT_{hv} indicates that heavy duty traffic travels slowly in these sites as slow moving heavy vehicles generate four and six ring PAHs. Therefore, this suggests that gasoline vehicles could generate these PAHs in commercial sites as these PAHs points towards commercial sites. However, as gasoline exhaust particles are <1 μm, these PAHs are not due to direct emissions. Furthermore, Boehm and Farrington (1984) and Brown and Maher (1992) have noted that the presence of low molecular weight three and four ring PAHs indicate that fuel leakage is the main source of these PAHs. Therefore, fuel leakage from vehicles could be the main source of PAHs in >300 μm size fraction. Also, these PAHs show a positive correlation with PSD_{D50}. This suggests that these PAHs are associated with solids.

Figure 8-15(b) shows correlation among ACY, IND, BgP, DbA, TS, and ADT_{hv}. Most of these PAHs are relatively heavier compounds with four and six benzene rings. As previously noted, slow moving heavy duty vehicles generates high molecular weight PAHs. This is supported by the correlation of these PAHs with ADT_{hv}. However, these PAHs are associated with larger particles and diesel exhaust particles are <10 μm. However, as these PAHs do not show correlation with TOC, organic complexation is not the relevant mechanism for binding them to larger particles. There could be other mechanisms for this size fraction.

Figure 8-15(a) shows a grouping (Group C) of commercial sites on the basis of PAHs loading. This indicates that these commercial sites generate similar PAH loadings to road surfaces. A similar observation was noted in relation to Figure 6-11(b) in Section 6.5. Therefore, this suggests that commercial sites generate PAHs to the atmospheric phase and subsequently to the ground phase. Consequently, commercial land use is an important PAHs source for > 300 μm size fraction.

PAHs in all size fractions

It was noted from the analysis carried out so far that PAHs are not uniformly associated with different build-up particle size fractions. Therefore, the behaviour of PAHs in build-up cannot be explained only with individual size fraction analysis. An overall assessment was needed and accordingly PROMETHEE analysis was undertaken for the combined size fractions. In order to remove any bias caused by differences in solids load collected from each site, PAH concentrations were divided by the corresponding total solids mass prior to analysis. Figure 8-16(a) illustrates the Actions in GAIA biplot and Figure 8-16(b) illustrates the Criteria for the same GAIA biplot. Resulting PROMETHEE 2 complete ranking is given in Table C-12 of Appendix C.

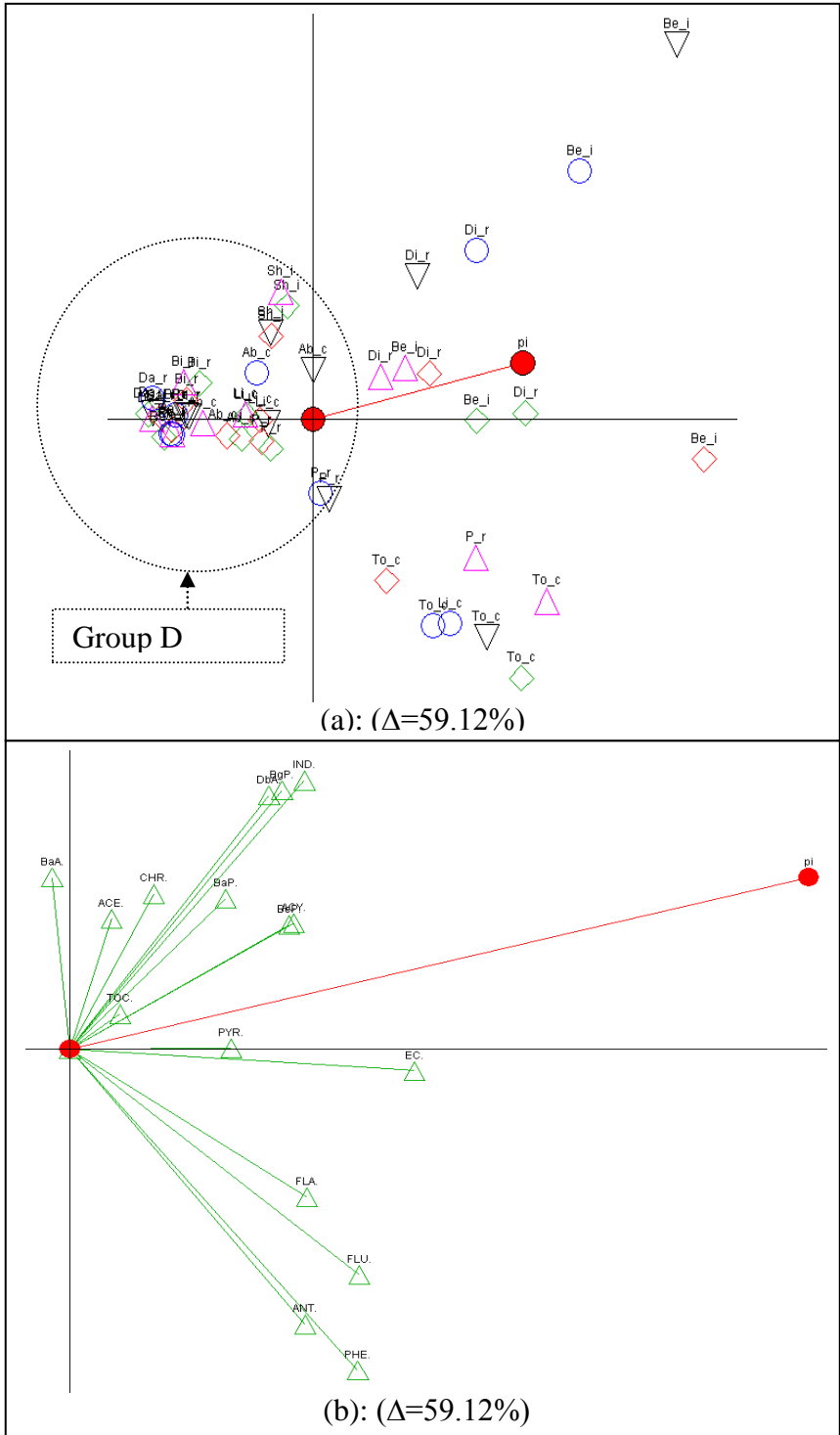


Figure 8-16: GAIA biplot of HMs against the first two principal components for all size fractions, (a): for actions, (b): for criteria

(Where $\circ = <1 \mu\text{m}$ fraction, $\nabla = 1-75 \mu\text{m}$ fraction, $\diamond = 75-150 \mu\text{m}$
 $\diamond = 150-300 \mu\text{m}$ fraction, $\triangle = >300 \mu\text{m}$ fraction, refer Table 8-1 for land use notations of c, i and r, Δ is the percentage variance described by the GAIA biplot, plots (a) and (b) are in two different scales)

Figure 8-16(b) shows correlation of IND, BgB, DbA, CHR, ACE, BaP, ACY and BeP with TOC. Except ACE and ACY, all the others are higher molecular weight PAHs. Riddle et al. (2007) noted that diesel vehicles emit four and six ring PAHs at low speeds (congested mode) and three and four ring PAHs at higher speeds. Concentrations of these PAHs are similar on a per unit solids basis. In other words, slow moving diesel vehicles generate mainly these PAHs and emissions per unit solids load is similar for all the investigated roads. Additionally, as these PAHs are related to TOC, it can be considered that they are attached to organic carbon in build-up. Furthermore, Herngren et al. (2010) noted that TOC increases adsorption of PAHs with particulate matter due to the organic complexation.

Figure 8-16(a) shows a grouping (Group D) of 31 objects irrespective of the size fractions or land use. Therefore, these size fractions are associated with similar PAH concentrations per unit solids mass. This suggests that the majority of PAHs have certain capacity to associate with different size fractions on per unit mass basis. This may be dependent of TOC concentrations, as TOC influences the association of PAHs to solids.

8.4 Traffic generated pollutant transport pathways

From the analysis carried out in Chapters 6, 7 and 8, it was found that pollutant build-up on road surfaces are influenced by the pollutants in the atmosphere and atmospheric deposition. Hence, in order to investigate the pathways of traffic generated pollutants, analysis was undertaken combining these processes together.

The PROMETHEE analysis was carried out for heavy metals by dividing their concentration by the corresponding solids mass for all three phases. V-shape preference function was used for the analysis. Variables were set to maximise so that the decision axis pi points towards the most polluted site/s in terms of heavy metals. Resulting PROMETHEE 2 complete ranking is given in Table C- 13 of Appendix C. The resulting GAIA biplot is given in Figure 8-17.

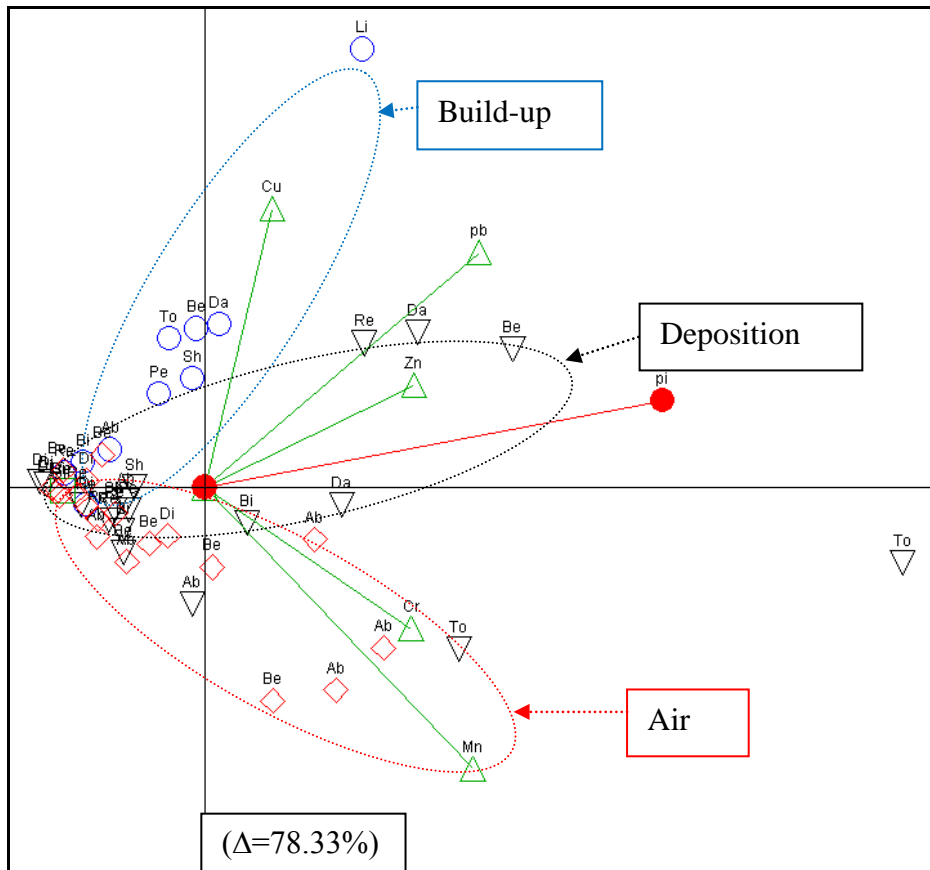


Figure 8-17: GAIA biplot of HMs for the first two principal components for all three phases

(Where \circ = build-up, \diamond = deposition, ∇ =air,

Δ is the percentage variance described by the GAIA biplot, refer Table 8-1 for land use notations of c, i and r)

Figure 8-17 shows that there are three clusters representing heavy metals, namely, “Build-up”, “Deposition” and “Air”. Also, more than 50 % of the data points in each cluster are grouped together. This suggests that heavy metals in these three phases are interdependent for more than 50% of the cases. This proves one of the hypotheses of the research study, namely, that atmospheric deposition of vehicle generated pollutants is the major source of road surface pollutant build-up. These conclusions are supported by the findings of Sabin et al. (2006) who noted that atmospheric deposition makes an important contribution to urban stormwater pollution. Furthermore, it was noted in Section 8.3.4 and Chapters 6 and 7 that heavy metals present in these three phases are generated by traffic sources and land use based sources. As noted in Chapter 6 and 7, heavy metals distribution processes depend on

natural and traffic generated wind. Therefore, distribution of data points in “Air” and “Deposition” clusters could be due to this effect.

Figure 8-17 shows that Cu, Pb and Zn points towards “Build-up” and “Deposition” clusters whereas Cr and Mn points towards the “Air” cluster. This suggests that, on per unit mass basis, air is relatively highly polluted in terms of Cr and Mn and build-up and deposition is relatively highly polluted with Cu, Pb and Zn. The main reason for this behaviour is that a high fraction of Cu, Pb and Zn are associated to solids which are in settleable form (relatively larger). Therefore, Cu, Pb and Zn associated solids are deposited on road surfaces relatively quickly.

Figure 8-17 shows correlation of Cu, Zn and Pb with build-up and atmospheric deposition. This highlights the strong linkage of these metals in atmospheric depositions and build-up.

PROMETHEE analysis was subsequently carried out for PAHs by dividing their concentration by corresponding solids mass. V-shape preference function was used for the analysis. Variables were set to maximise so that the decision axis π_1 points towards the most polluted site/s in term of PAHs. Resulting PROMETHEE 2 complete ranking is given in Table C- 14 of Appendix C. The resulting GAIA biplot is given in Figure 8-18.

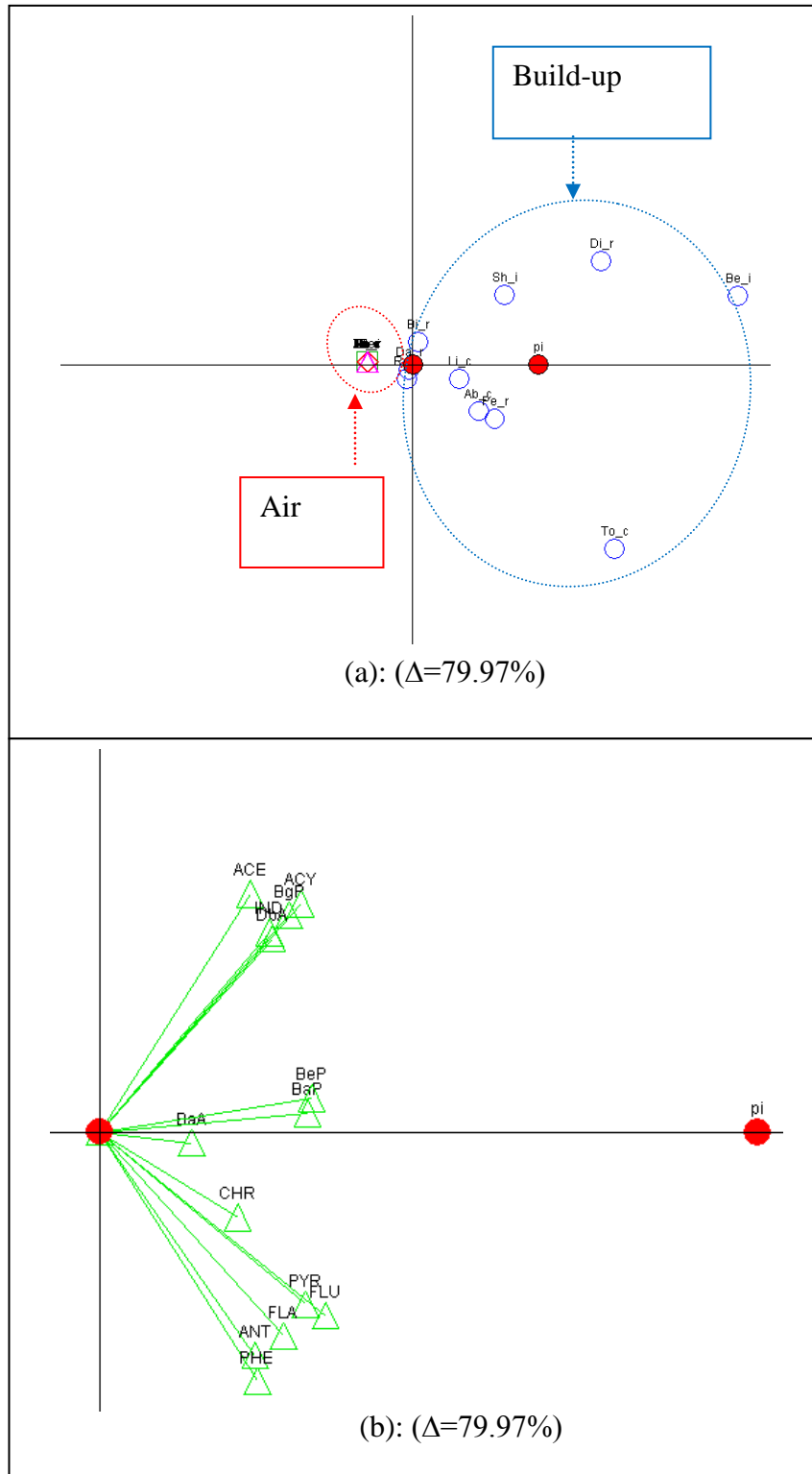


Figure 8- 18: GAIA biplot of particulate bound PAHs for the first two principal components for build-up and air, (a): for actions, (b): for criteria

(Where \circ = build-up, \diamond = air, Δ is the percentage variance described by the GAIA biplot, refer Table 8-1 for land use notations of c, i and r, plots (a) and (b) are in two different scales)

Figure 8-18 shows that PAHs in the atmosphere make a small contribution to build-up. This could be due to two main reasons. Firstly, atmospheric concentration (nanogram per m³ as shown in Table 6-5 and Table 6-6 in Chapter 6) of PAHs is very small compared to the build-up load (mg/m²) as shown in Figure 8-4. Secondly, atmospheric temperature and wind increases the dispersion of PAHs (Amodio 2009). Therefore, PAHs distribute in the atmosphere relatively quickly. As atmospheric deposition does not contribute an appreciable amount of PAHs to road surface build-up, atmospheric phase PAHs are not a significant stormwater pollutant.

8.5 Conclusions

A numbers of important conclusions were derived from the analysis of build-up data as given below:

- Neither dissolved nor total solids show a clear trend with ADT or land use activities suggesting the presence of other important sources. The main sources include traffic and land use related activities, atmospheric deposition and soil related inputs.
- Zn is the dominant heavy metal species followed by Cu for almost all the sites, irrespective of traffic and land use characteristics. Atmospheric deposition is one of the main sources of Zn in build-up.
- Traffic generated particles are primarily <50 µm. Therefore <1 µm and 1-75 µm size fractions are the most polluted in terms of traffic related direct emissions. However, traffic generated particles can be attached to larger particles (75-150 µm, 150-300 and > 300 µm) due to adsorption and organic complexation.
- Although traffic is the main heavy metal source in the investigated sites, land use related activities contribute HMs mainly in the 150-300 and >300 µm size

fractions. Therefore, heavy metal in build-up is influenced by land use related activities as well, but to a lesser extent.

- Direct traffic emitted PAHs (exhaust and wear related) are associated primarily with $<50 \mu\text{m}$ size fraction. However, leakage of oil and fuel contribute much larger particles associated with PAHs.
- Diesel vehicles generate four and six ring PAHs at low speeds and lighter PAHs at high speeds. As heavier PAHs are more toxic than lighter species, an increase in vehicle speed can minimise heavier PAH emissions.
- Although land use related activities contribute PAHs to build-up, traffic sources are more dominant. The investigated PAHs correlated only with commercial land use areas for $>300 \mu\text{m}$ size fraction.
- Heavy metals present in the atmosphere, atmospheric deposition and build-up are highly correlated on per unit solids load. Therefore, it can be concluded that heavy metal build-up on roads is highly influenced by heavy metals present in the atmosphere and atmospheric deposition.
- Atmospheric phase PAHs are not a significant source to build-up compared to road surface build-up load.

Chapter 9 - Mathematical Modelling

9.1 Background

Strategies for stormwater quality mitigation can be enhanced with accurate stormwater quality predictions. Such predictions can result from the accurate replication of state-of-the-art pollutant processes of wet and dry deposition and pollutant build-up. In this context, Chapters 6, 7 and 8 presented the knowledge created in relation to these three pollutant processes. This Chapter focuses on methodology for predicting stormwater quality for targeted pollutants (PAHs, HMs) incorporating previously derived process equations to a commonly available modelling tool.

The modelling approach presented in this Chapter is organised in a logical order in that the estimations of each targeted pollutant group (PAHs and HMs) is done at a processes level incorporating knowledge generated in Chapters 6, 7 and 8. The Chapter initially discusses model selection and the modelling approach adopted followed by model setup including schematisation of ten selected study sites. Detailed discussion of the boundary conditions used is also presented, followed by the replication of pollutant build-up and wash-off processes. The selection of appropriate mathematical equations for the replication of pollutant build-up and wash-off processes is also discussed.

9.2 Computer modelling

9.2.1 Model selection

As treatment design is commonly based on long-term pollutant characteristics (Sagona 2007), the modelling approach was formulated to estimate annual pollutant loads. Stormwater treatment objectives are commonly defined in term of annual pollutant loads (CSIRO 2006). Due to the need for accurate estimation of a range of pollutant types with varied process characteristics, a state-of-the-art modelling tool capable of simulating pollutant processes on an event-by-event basis was used.

Consequently, three commonly used stormwater quality models were extensively reviewed for their stormwater quality prediction capabilities as discussed in Section 3.5. The models reviewed were EPA SWMM, MIKE URBAN and MUSIC. It was found from the review that either EPA SWMM or MIKE URBAN is suitable for the envisaged modelling, as they are capable of modelling pollutants build-up and wash-off processes on an event-by-event basis. Consequently, EPA SWMM was selected as the most suitable model for the study. This was primarily due to its ability to incorporate user defined pollutant process equations in the modelling structure. Additionally, EPA SWMM performed better in trial simulations and giving consistent outputs.

9.2.2 Modelling approach

In typical modelling studies, model calibration and validation forms important roles. Model calibration is a process for adjusting model parameters to suit actual field conditions. However, this component was not undertaken in this study. Instead, model parameters to suit actual field conditions were determined from the outcomes of the detailed field investigations undertaken. This approach was recommended by Egodawatta (2007) noting that small-plot pollutant processes can be extrapolated to catchment scale. This approach was considered as the most appropriate for this study, as historical stormwater quality and quantity data was not available for the investigated study areas.

In this approach, fundamental knowledge generated through field investigations on air pollutants, atmospheric deposition, pollutant build-up and pollutant wash-off was used to determine model parameters. Details of the analysis of air pollutants, atmospheric deposition and pollutant build-up are discussed in Chapters 6, 7 and 8.

9.2.3 Model schematisation

As data collected from Hope Island road site was identified as an outlier in Chapter 8, it was removed from the modelling exercise. Accordingly, ten sites from the originally selected eleven study sites were considered for the modelling exercise. Existing maps and aerial photographs were used to calculate the baseline road characteristics such as road width at the study sites.

A 100 m long road section with typical road geometry and drainage characteristics was selected as the schematised model catchment for each road site. Each model catchment was divided into two sub-catchments draining to either side of the road as shown in Figures 9-1 and 9-2. Road kerb drains were modelled as a triangular open channel section with roughness equivalent to concrete. Geometric data was obtained from maps and aerial photographs provided by the Gold Coast City Council (GCCC).

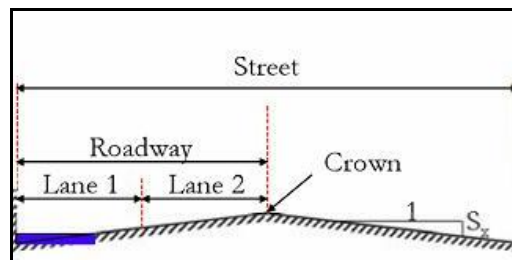


Figure 9-1: Schematisation of road cross section

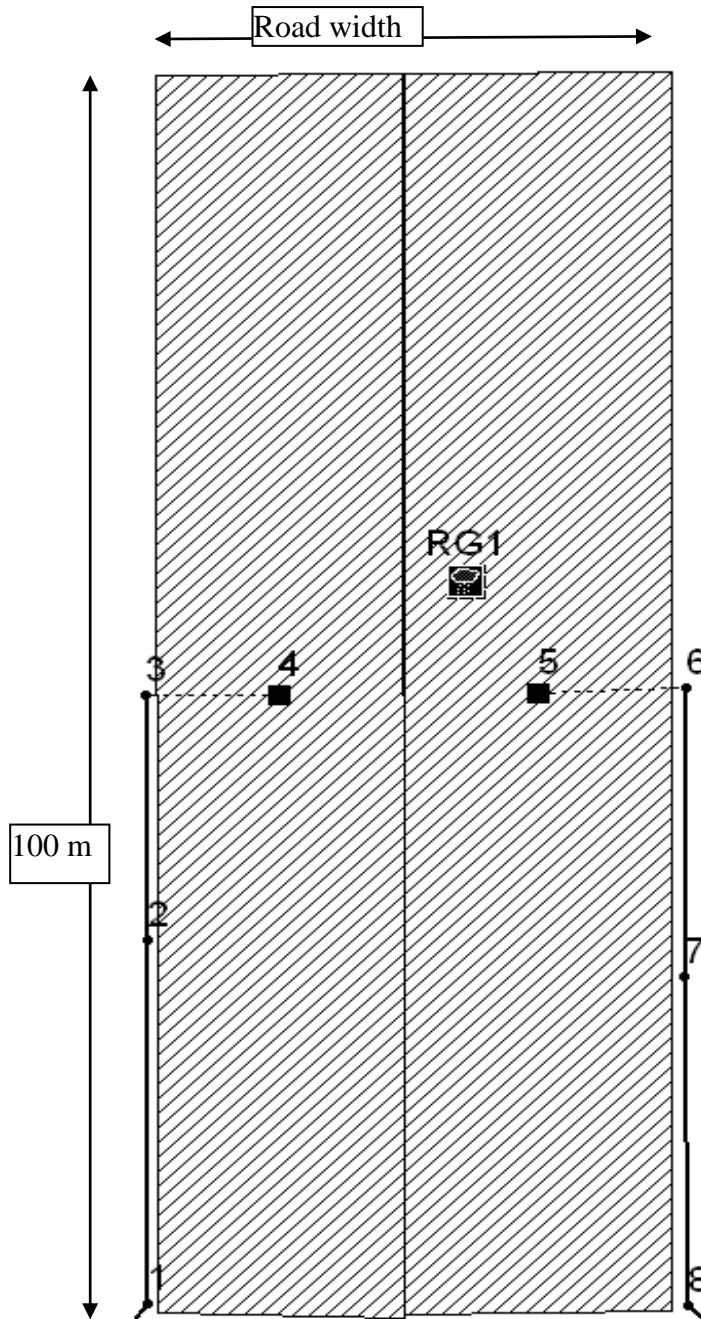


Figure 9-2: Schematisation of catchment area
(Where RG1=Rain gauge)

9.2.4 Boundary conditions

Typically, two types of boundary conditions, namely, quantity and quality boundary conditions were needed in this modelling exercise. Rainwater quality was used as the quality boundary condition and it was derived using the data obtained from the fieldwork as discussed in Chapter 7.

(a) Rainfall data

The correct selection of rainfall boundary conditions was critical for the accurate estimation of pollutant loads. The rainfall data recorded at the Gold Coast Seaway Station (Bureau of Meteorology station no: 040764) was used as the rainfall boundary conditions. Gold Coast Seaway site was selected because of its close proximity to the study sites and the availability of 6 min rainfall data (AGBOM 2011). It was decided to use a subset of rainfall data from year 2000 to 2010 period for this study. Rainfall data was obtained from the Australian Bureau of Meteorology (AGBOM 2011).

It was found that the selected model is extremely sensitive to the effects of temporal rainfall data density (USEPA 2010b). Therefore, in order to predict quantitative and qualitative parameters accurately, fine resolution rainfall data were used. As such, the data recorded at 6 min intervals was used for the modelling. In this approach, accurate estimation of both quantitative and qualitative parameters on an individual event basis was considered important in deriving annual pollutant loads.

After processing the rainfall data from years 2000 to 2010, three representative years were selected for modelling. They were the year with minimum annual rainfall depth (2001), the year with average rainfall (2004) and the year with the maximum rainfall (2010) as shown in Figure 9-3. This was to account for the variability of annual pollutant load due to the variations in annual rainfall characteristics.

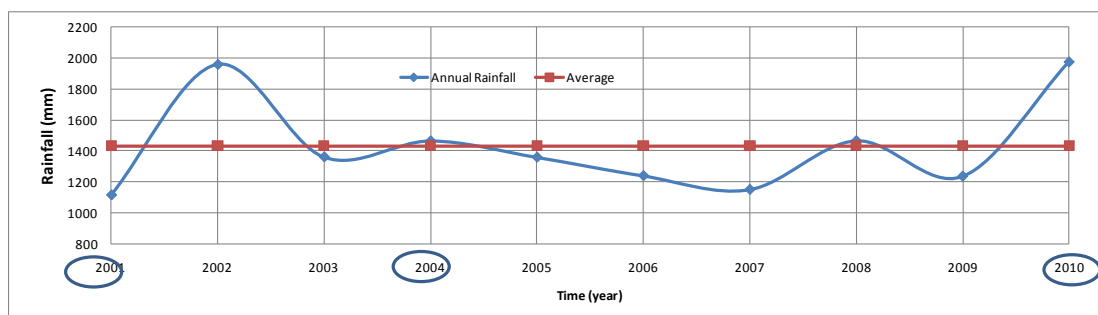


Figure 9-3: Variation of total rainfall over the last 10 years at Gold Coast Seaway

(Where ○ = indicates the selected years for modelling)

(b) Wet deposition

Atmospheric wet deposition was used as one of the quality boundary conditions in the modelling study. As noted in Section 7.3.3 of Chapter 7, a high load of stormwater pollutants were recorded in the atmospheric deposition samples close to the urban centres. Atmospheric wet deposition varies with the rainfall depth as noted in Chapter 7. However, EPA SWMM model is not capable of incorporating variations in rainfall quality with time. Therefore, average concentrations of solids and heavy metals in wet depositions were used in the study. Average values were calculated considering annual rainfall data and variations in wet depositions with rainfall depth. Use of average, instead of actual water quality may result in errors. However, these errors were considered be not significant since modelling was undertaken to estimate annual pollutant loads. Quality boundary conditions for wet deposition were used only for TSS and HMs. As the PAH concentrations in wet depositions were below detection, PAHs were not considered as part of the rainwater quality boundary conditions.

9.2.5 Replication of pollutant build-up and wash-off

The selected EPA SWMM model simulates water quality and quantity together by replicating pollutant build-up and wash-off processes on catchment surfaces. However, the appropriate replication equations needed to be selected depending on the pollutant build-up and wash-off characteristics of the catchment. The model supports power, exponential and saturated build-up replication equations and exponential, rating curve and event mean concentration wash-off replication equations (SWMM 2010a). The following Sections (a) and (b), discusses the selection of appropriate build-up and wash-off replication equations together with the determination of their coefficients.

(a) Pollutant build-up

Pollutant build-up is a dynamic process and at any given time, the process may undergo change based on the state of deposition and removal characteristics (Herngren 2005). A detailed review of literature on pollutant build-up process is given in Chapter 2 and a detailed analysis of pollutant build-up process is undertaken in Chapter 8. The analysis performed in this section was to select the most suitable

form of pollutant build-up replication equation and site-specific parameters for the selected ten road sites.

Egodawatta (2007) recommended a power function to replicate pollutant build-up on road surfaces and hence the power function given in EPA SWMM was selected (as shown in Equation 1). In Equation (1), C_1 is the upper limit of pollutant build-up on a catchment surface (USEPA 2010b). As noted by Egodawatta (2007), pollutant build-up approaches its maximum possible value after twenty one antecedent dry days. He also noted that the coefficient (C_2) is dependent on site-specific parameters such as population density and time exponent (C_3) depends only on the road surface types. For this study, C_3 was selected as 0.16 to represent a typical bitumen road surface as recommended by Egodawatta (2007). The build-up rate coefficient C_2 was determined based on actual measured seven day pollutant build-up values. The pollutant build-up curves for the selected ten roads are given in Figure 9-4. The coefficients for power functions are given in Table 9-1 for the road sites.

$$B = \text{Min} (C_1, C_2 t^{C_3}) \dots \dots \dots (1)$$

Where, B = Build-up load (kg/ha);

C_1 = Maximum possible build-up (kg/ha);

C_2 = Build-up rate constant (kg/ha);

t = Time (days);

C_3 = Time exponent; and

Min = Refers to the minimum of C_1 and $C_2 t^{C_3}$.

(Adapted from USEPA 2010b).

Table 9-1: Coefficients for power function

	Shippe Drive	Towncentre Drive	Abraham Road	Linfield Road	Beattie Road	Billinghurst Crescent	Peanba Park	Dalley Park Drive	Discivery Drive	Reserve Road
C_1 (kg/ha)	2.21	0.78	2.52	0.60	0.74	5.60	0.68	13.09	0.80	7.68
C_2 (kg/ha)	1.36	0.48	1.55	0.37	0.46	3.44	0.42	8.04	1.81	0.49
C_3	0.16	0.16	0.16	0.16	0.16	0.16	0.16	0.16	0.16	0.16

As evident in Table 9-1, the maximum build-up coefficients (C_1) obtained for Dalley Park Drive, Reserve Road and Billinghurst Crescent are significantly high compared to the values recommended for typical road surfaces (Egodawatta 2007). There were exposed soil surfaces on either side of the Billinghurst Crescent road resulting in a high build-up load. High road surface roughness at Reserve Road and Dalley Park Drive sites could be attributed to the high maximum build-up capacity at these sites.

As evident in Table 9-1, all the other sites have similar build-up coefficients (C_1) and similar to the values recommended by Egodawatta (2007).

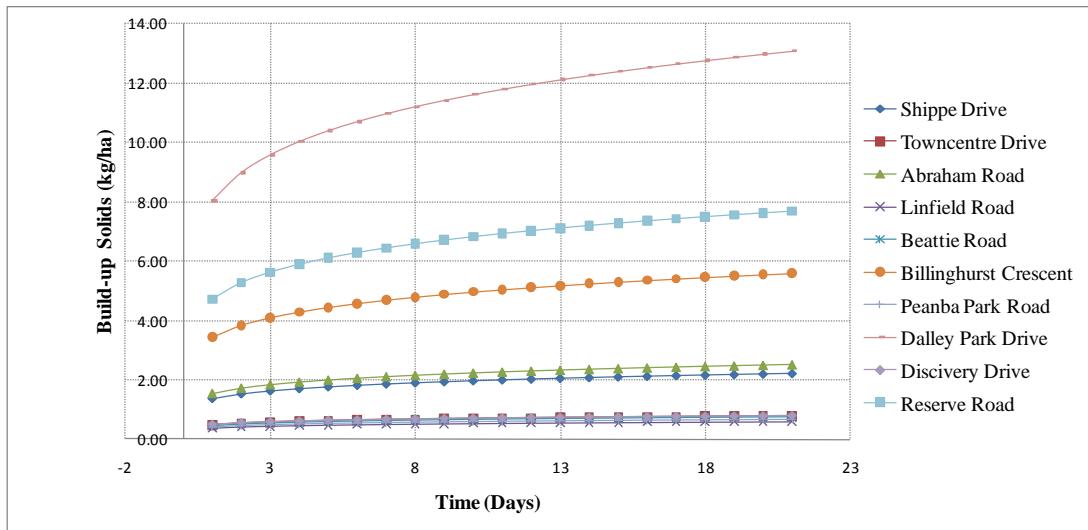


Figure 9-4: Exponential solid build-up curves

(b) Pollutant wash-off

EPA SWMM model supports different forms of mathematical replications for wash-off including exponential, rating curve and event mean concentration. In this study, wash-off data obtained from Mahbub (2011) was plotted to assess the most suitable mathematical replication equation. The method of least squares regression was applied to select the most appropriate form of mathematical replication equation and accordingly an equation format with least data scatter was selected. It was found that an exponential form of mathematical replication is the most suitable to replicate solids wash-off. Hence, it was employed in this study. The exponential wash-off function in EPA SWMM model is given below;

$$W = (D_1 q^{D_2} B) \dots \dots \dots (2)$$

Where, W = Wash-off load in units of mass per hour;

D_1 = Wash-off coefficient;

D_2 = Wash-off exponent;

q = Runoff rate per unit area (mm/hour); and

B = Pollutant build-up in mass units given in Equation (1).

(Adapted from USEPA 2010b).

Unlike pollutant build-up, the wash-off process does not depend on site-specific characteristics. Wash-off primarily depends on the build-up load and the rainfall

characteristics (Miguntanna 2009). Therefore, in order to determine the coefficients for the wash-off equation, the Equation (2) was expressed as wash-off per unit build-up (W/B) where W and B are the actual wash-off and build-up mass collected for the seven day antecedent dry period. B is the build-up mass given by Equation (1) with site specific parameters as detailed in Table 9-1. W/B is referred to as the fraction wash-off (Egodawatta 2007). The wash-off coefficient (D_1) and the wash-off exponent (D_2) were estimated by plotting fraction wash-off against duration of rainfall events as shown in Figure 9-5. Figure 9-5 was generated based on simulated rainfall events in four of the ten road study sites in the Gold Coast (Mahbub 2011). Figure 9-5 as presented was obtained after removing several data points due to inconsistencies. The coefficients D_1 and D_2 were determined from the method of least squares regression and were found to be 80.409 and -0.875, respectively.

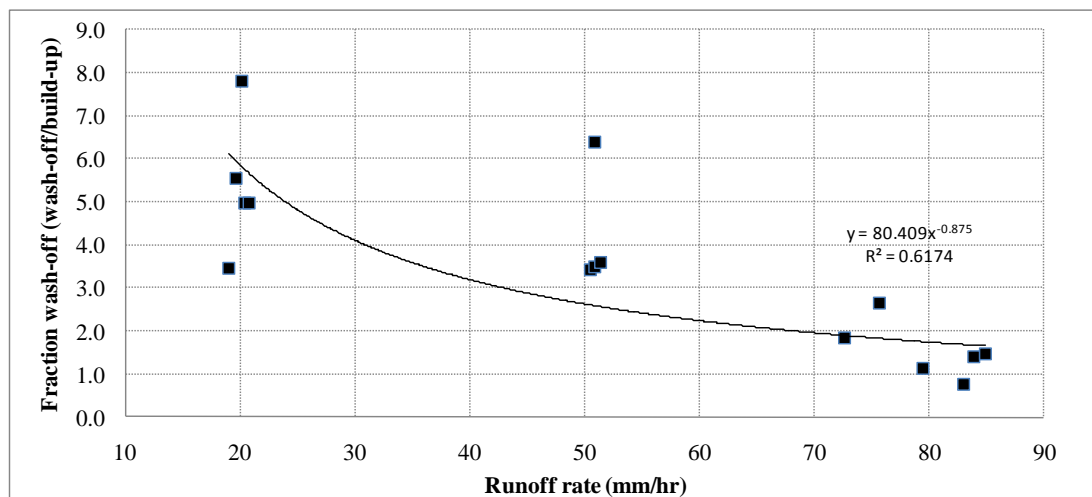


Figure 9-5: Variation of fraction wash-off with the Runoff rate for solids

(c) Heavy metals

In order to investigate the applicability of the wash-off equation in the form of Equation (2) for heavy metals, least squares regression analysis was undertaken using the data obtained for Zn, Cu, Ni, Cr, Pb, Cd and Mn. This resulted in regression coefficients less than 0.5 for all the heavy metals. Consequently, the exponential wash-off equation was not used to replicate the wash-off of these heavy metals.

The applicability of co-fraction wash-off approach was investigated for heavy metals as this is one of the recommended approaches in EPA SWMM model (USEPA 2010a). In this approach, heavy metals are modelled as a co-fraction of suspended

solids. Variation of co-fractions of HMs with duration was plotted as shown in Figure 9-6 to investigate the applicability of this approach for modelling HMs.

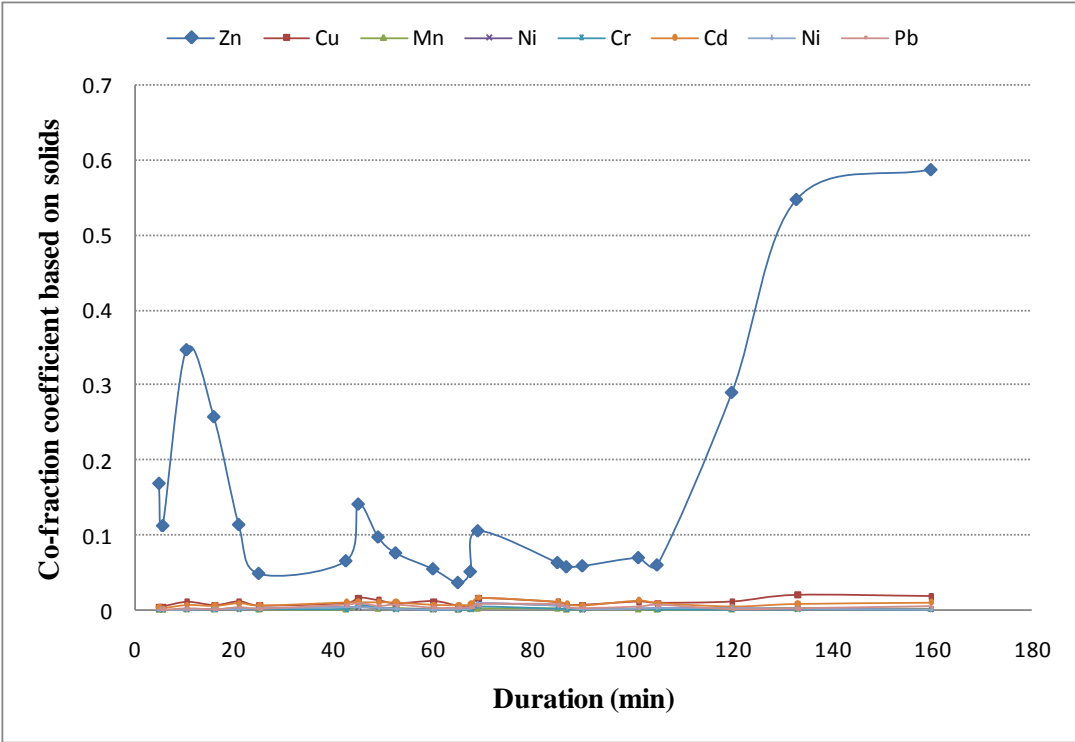


Figure 9-6: Variation of co-fractions with duration

In order to develop Figure 9-6, co-fraction of heavy metals was calculated by dividing the heavy metal concentration by the corresponding total suspended solids concentration. The resulting co-fractions were then plotted against the simulated rainfall durations. As evident in Figure 9-6, except for Zn, other heavy metals such as Cu, Mn, Ni, Pb, Cd and Cr have consistent co-fractions. Therefore, the co-fraction approach was considered suitable to model wash-off of Cu, Mn, Ni, Pb, Cd and Cr. Though the variation of Zn is high, the co-fractions approach was also used for Zn due to its reasonable consistency until the 120 min rainfall duration. As rain events with duration greater than 120 minutes is rare in occurrence, use of co-fractions for Zn was considered appropriate. Additionally, as the focus of the study was to predict annual heavy metal load, the accuracy in the co-fractions approach was considered reasonable for this study. Heavy metal co-fractions were calculated based on TSS as shown in Table 9-2. These co-fractions were used in EPA SWMM modelling to estimate annual HM loadings.

Table 9-2: Heavy metal co-fractions based on TSS

Zn	Cu	Mn	Ni	Cr	Cd	Pb
0.113	0.010	0.001	0.002	0.001	0.008	0.004

(d) PAHs

PAHs wash-off data generated by Herngren (2005) using rainfall simulation was used to determine the most suitable PAH wash-off replication equation. Outcomes from the study by Herngren (2005) were considered appropriate for the current research study due to the similarity of the study areas. Herngren (2005) also conducted his field investigations in the Gold Coast region. TSS wash-off data generated by Mahbub (2011) using rainfall simulation was used for the modelling. Coefficients for Equation (2) were already determined for solids (TSS) in Section 9.2.5 (b).

As discussed for HMs, a similar process was followed to determine wash-off coefficients for Equation (2) to simulate PAHs wash-off. Out of the 14 PAHs tested for build-up, only nine were considered for this modelling as Herngren (2005) detected only nine PAHs consistently during the investigations undertaken. However, none of these nine PAHs closely follow Equation (2) as the regression coefficients were always less than 0.5. Therefore, Equation (2) was not considered applicable to model PAHs wash-off.

Consequently, it was decided to model PAHs also as a co-fraction of suspended solids. Variation of co-fractions for PAHs with duration was plotted as shown in Figure 9-7 to investigate the applicability of this approach to model PAHs.

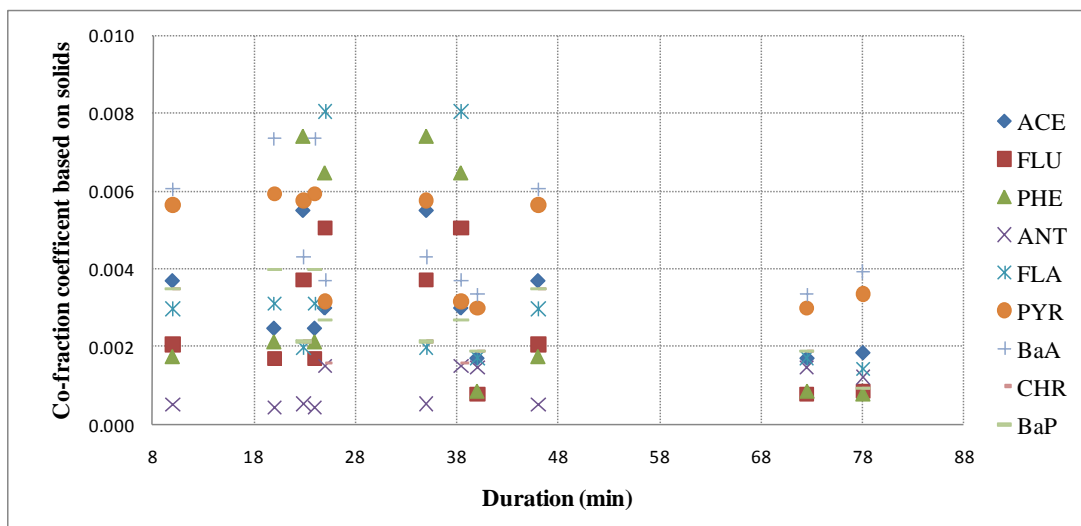


Figure 9-7: Variation of co-fractions with duration

As evident in Figure 9-7, all the investigated PAHs such as ACE, FLU, PHE, ANT, FLA, PYR, BaA, CHR and BaP have appreciably consistent co-fractions. Therefore, the co-fraction approach was considered suitable to model PAHs wash-off. Co-fractions were calculated based on suspended solids. The co-fractions of each PAH used for modelling are given in Table 9-3.

Table 9-3: Co-fraction coefficients used for modelling

ACE	FLU	PHE	ANT	FLA	PYR	BaA	CHR	BaP
0.0018	0.0012	0.0019	0.0009	0.0027	0.0027	0.0024	0.0014	0.0020

9.3 Model simulation and results

The EPA SWMM model was simulated for years 2001, 2004 and 2010 rainfall events as these correspond to the years with minimum, average and maximum annual rainfall. The results were extracted for all ten sites corresponding to these three years. Furthermore, in order to identify the most polluted sites in terms of HMs and PAHs loading, results were further analysed using PROMETHEE 2 multicriteria decision-making method. Detailed descriptions of the PROMETHEE analytical methods are given in Section 3.4.3. Annual heavy metals loading in stormwater are given in Section 9.3.1 followed by annual PAHs loading in Section 9.3.2 below.

In order to predict the annual solids load in stormwater generated by a 100 m long road segment, predictive equations were developed based on the model results for year 2001, 2004 and 2010 rainfall data. The predictive equations were developed

based on the traffic and land use characteristics. A detailed discussion on the development of predictive equations is given in Section 9.3.3 below. As heavy metals and PAHs were modelled as co-fractions of solids, prediction equations were developed only for solids.

9.3.1 Results for heavy metals

Annual heavy metal loads were calculated from the model output and a summary of results are given in Table 9-4 together with traffic data.

Table 9-4: Annual heavy metal load from 100 m long road section

Site	Notation	Year	TSS (mg)	Pb (mg)	Cr (mg)	Cd (mg)	Zn (mg)	Mn (mg)	Ni (mg)	Cu (mg)	Traffic(ADT)
Abraham road	Ab_c	2001	11167	31	26	41	699	30	14	59	8742
		2004	13167	34	33	41	734	39	15	61	
		2010	16707	42	44	47	874	51	18	71	
Beattie road	Be_i	2001	10373	23	30	19	424	36	9	33	4633
		2004	13317	29	40	21	506	48	11	39	
		2010	17858	39	54	27	665	64	15	51	
Billinghamhurst	Bi_r	2001	14781	47	28	74	1156	32	22	100	1964
		2004	17983	55	36	85	1346	42	26	115	
		2010	19688	57	44	79	1310	51	25	111	
Dalley park drive	Da_r	2001	33160	122	45	227	3295	49	59	289	997
		2004	47713	176	65	328	4765	69	86	418	
		2010	49116	176	71	321	4713	78	85	412	
Discovery drive	Di_r	2001	16404	45	39	60	1017	45	20	74	10690
		2004	20348	54	51	66	1172	59	23	82	
		2010	26977	71	68	85	1527	79	31	106	
Linfield road	Li_c	2001	19574	52	48	65	1139	56	70	95	8599
		2004	24794	64	63	75	1356	74	83	111	
		2010	30508	75	82	79	1522	95	93	123	
Peanba park road	Pe_r	2001	6774	35	19	14	298	23	6	24	30
		2004	8294	41	25	14	325	29	7	25	
		2010	10568	46	33	14	377	38	9	29	
Reserve road	Re_r	2001	19455	62	44	77	1275	51	25	108	10027
		2004	23282	77	57	80	1393	66	27	116	
		2010	27531	77	72	79	1466	84	30	120	
Shipper drive	Sh_i	2001	21254	46	38	113	1737	44	32	150	2236
		2004	28252	60	52	149	2295	59	43	198	
		2010	28277	62	60	124	2001	69	38	170	
Town centre drive	To_c	2001	10474	12	30	20	436	36	9	34	5931
		2004	13428	15	41	22	518	48	12	40	
		2010	18000	20	54	28	681	64	15	52	

Note: c - commercial, i - industrial, r - residential; ADT - average daily traffic

As evident in Table 9-4, Zn has the highest annual load followed by Cu. Additionally, annual loads of Cd and Ni are relatively small compared to the Zn load.

Consequently, PROMETHEE 2 complete ranking was undertaken to analyse the sites based on annual stormwater quality. This was to categorise the sites in terms of their annual heavy metal loadings. For this analysis, all the investigated heavy metals were considered as equal in their importance (a weighting factor of one for all heavy metals). Even though some heavy metals are more toxic than others, there is no

commonly accepted ranking framework available based on heavy metal toxicity. As the road widths were not the same, a 1 m width of each road segment was considered for the analysis. This standardisation helped to compare the HMs generated at each site.

Although the annual HMs loadings were predicted for years 2001, 2004 and 2010 rainfall data, the ranking was carried out only for HMs generated based on year 2004 rainfall. This was because year 2004 annual rainfall is close to the average rainfall observed during last 10 years for the study sites and, therefore, this is the most accurate estimation for annual pollutant load. The predicted HM loadings for years 2001 and 2010 were to understand the limits of variability. Therefore, it is logical to rank the sites based on annual HMs loadings predicted for year 2004 year rainfall.

Table 9-5: PROMETHEE 2 ranking of sites based on year 2004 HMs loading

	Phi Plus	Phi Minus	Phi Net	Ranking	Comments
Da_r	0.7589	0	0.7589	1	The most polluted site
Sh_i	0.1558	0.0689	0.0869	2	
Bi_r	0.0966	0.0855	0.0111	3	
Li_c	0.0508	0.1119	-0.0612	4	
Re_r	0.0365	0.1129	-0.0764	5	
Di_r	0.0198	0.1271	-0.1073	6	
Ab_c	0.0173	0.1303	-0.113	7	
Pe_r	0.0087	0.1572	-0.1486	8	
Be_i	0.0008	0.1727	-0.1719	9	
To_c	0.0001	0.1787	-0.1786	10	The least polluted site

(Note: Traffic data was not used for ranking)

Implementation of stormwater quality treatment practices can be prioritised as per the ranking given in Table 9-5. Highly polluted stormwater in terms of HMs are generated from Dalley Park Drive, Shipper Drive and Beattie Road. These roads are located in Commercial and Residential land uses.

9.3.2 Results for PAHs

The Annual PAH loads calculated from the model outputs are summarised in Table 9-6.

Table 9-6: Annual PAHs load from 100 m long road section

Site	Notation	Year	ACE (mg)	FLU (mg)	PHE (mg)	ANT(mg)	FLA (mg)	PYR (mg)	BaA (mg)	CHR (mg)	BaP (mg)	Traffic(AD)
Abraham road	Ab_c	2001	9.1	6.2	9.7	4.6	13.8	13.8	12.2	7.1	10.1	8742
		2004	9.1	6.0	9.7	4.5	13.7	13.7	12.2	7.0	10.2	
		2010	10.4	7.0	11.0	5.1	15.6	15.6	13.9	8.2	11.6	
Beattie road	Be_i	2001	4.0	2.7	4.2	2.0	6.3	6.3	5.6	3.1	4.5	4633
		2004	4.6	2.9	4.8	2.2	6.9	6.9	6.2	3.5	5.0	
		2010	5.8	3.7	6.2	2.8	8.7	8.7	7.8	4.5	6.5	
Billinghamurst	Bi_r	2001	16.7	11.0	17.6	8.2	24.9	24.9	22.2	12.9	18.5	1964
		2004	19.0	12.7	20.0	9.6	28.6	28.6	25.4	14.9	21.1	
		2010	17.6	11.7	18.6	8.9	26.6	26.6	23.6	13.8	19.6	
Daily park drive	Da_r	2001	50.9	34.0	53.7	25.5	76.4	76.4	67.9	39.5	56.6	997
		2004	73.7	49.1	77.8	36.9	110.6	110.6	98.2	57.3	81.8	
		2010	72.2	48.1	76.1	36.1	108.2	108.2	96.2	56.2	80.1	
Discovery drive	Di_r	2001	13.4	8.6	14.2	6.5	19.9	19.9	17.8	10.3	14.9	10690
		2004	14.7	9.8	15.6	7.4	22.1	22.1	19.7	11.3	16.5	
		2010	19.0	12.6	20.0	9.4	28.6	28.6	25.3	14.7	21.1	
Linfield road	Li_c	2001	14.2	9.5	15.0	7.1	21.6	21.6	19.1	11.1	15.8	8599
		2004	16.4	10.9	17.4	8.3	24.9	24.9	22.1	12.8	18.4	
		2010	17.5	11.5	18.5	8.7	26.4	26.4	23.5	13.4	19.4	
Peanba park road	Pe_r	2001	3.0	2.0	3.2	1.5	4.7	4.7	4.1	2.3	3.3	30
		2004	3.0	1.9	3.2	1.5	4.6	4.6	4.1	2.3	3.3	
		2010	3.1	2.0	3.3	1.5	4.7	4.7	4.2	2.4	3.5	
Reserve road	Re_r	2001	16.9	11.3	17.9	8.5	25.7	25.7	22.9	13.1	18.9	10027
		2004	17.9	11.8	18.9	8.8	26.7	26.7	23.9	13.8	19.8	
		2010	17.6	11.6	18.6	8.7	26.3	26.3	23.4	13.6	19.6	
Shipper drive	Sh_i	2001	12.5	8.3	13.2	6.3	18.8	18.8	16.7	9.8	13.9	2236
		2004	16.2	10.8	17.1	8.1	24.4	24.4	21.7	12.6	18.1	
		2010	17.8	11.8	18.7	8.7	26.5	26.5	23.7	13.8	19.8	
Town centre drive	To_c	2001	4.1	2.8	4.4	2.1	6.5	6.5	5.9	3.3	4.7	5931
		2004	4.8	3.1	5.0	2.3	7.1	7.1	6.5	3.7	5.3	
		2010	6.1	4.0	6.5	2.9	9.1	9.1	8.1	4.7	6.8	

Note: c - commercial, i - industrial, r - residential; ADT - average daily traffic

In order to identify the highly polluted sites in terms of PAHs, they were ranked using PROMETHEE 2 multicriteria decision making methods based on annual loading. As the road widths were not the same, a 1 m width of each road segment was considered for the analysis. This standardisation helped to compare HMs generated by each site. Accordingly, the values given in the Table 9-7 was divided by the corresponding road width before proceeding to PROMETHEE 2 analysis. Toxicity ranking given by Li et al. (2003) was employed for PROMETHEE 2 analysis. This helped to rank sites based on toxic PAHs loading to stormwater.

As already discussed for HMs ranking, although the annual PAH loadings were predicted for years 2001, 2004 and 2010 rainfall data, the ranking was carried out only for PAHs generated based on year 2004 rainfall. This was because year 2004 annual rainfall is close to the average rainfall observed during the last 10 years for study sites. Therefore, this was the closest estimate for annual pollutant load. The predicted PAHs loading for years 2001 and 2010 can be used to understand the limits of variability.

Table 9-7: PROMETHEE 2 ranking of sites based on year 2004 PAHs loading

	Phi Plus	Phi Minus	Phi Net	Ranking	Comments
Da_r	0.840	0.000	0.840	1	The most polluted site
Bi_r	0.098	0.082	0.016	2	
Re_r	0.084	0.086	-0.002	3	
Li_c	0.071	0.092	-0.021	4	
Sh_i	0.068	0.093	-0.025	5	
Di_r	0.057	0.104	-0.047	6	
Ab_c	0.023	0.156	-0.133	7	
To_c	0.003	0.202	-0.199	8	
Be_i	0.002	0.205	-0.203	9	
Pe_r	0.000	0.226	-0.226	10	The least polluted site

Note: (1). The ranking was based on the toxic equivalent factor defined by Li et al. (2003); (2) Traffic data was not used for ranking

Table 9-7 shows that Dalley Park Drive generates the highest PAHs loading to stormwater. As evident from Table 9-7, Dalley Park Drive, Billingham crescent and Reserve Road generate more polluted stormwater in terms of PAHs. All three sites belong to residential land use. It was also noted that top five sites are the same for both HMs and PAHs as shown in Table 9-5 and Table 9-7.

9.3.3 Development of predictive equations

The purpose of developing predictive equations is to estimate the annual pollutant load generated from roads with varying traffic and land use characteristics. In turn, total annual pollutant load generated by each road can be estimated based on traffic and land use characteristics. This is important for the implementation of appropriate stormwater treatment strategies.

Multiple linear regression analysis was carried out to develop predictive equations to estimate the annual solids load based on model outcomes generated for year 2001, 2004 and 2010 rainfall. It was assumed that the variability of solids load among different sites could be predicted as a linear combination of land use and traffic parameters. A linear combination was considered, as it is the simplest possible model to investigate the relationship between several independent or predictor variables and a dependent or criterion variable (Scott et al. 2007). It was assumed that the solids

load generated by a 100 m road section can be expressed as a linear combination of independent variables as follows:

$$\text{Solids} = f(C, I, R, \text{ADT}_{\text{to}}, V/C, \text{ADT}_{\text{hv}}) \dots \dots \dots (3)$$

Where:

- C, I, R The percentages of commercial, industrial and residential land uses within 1km radius from the each sampling sites;
- ADT_{to} The total average daily traffic volume from a traffic survey carried out in 2010;
- ADT_{hv} The total heavy-duty traffic volume determined from a traffic survey carried out in 2010; and
- V/C The traffic congestion predicted by GCCC.

Methodology for the calculation of C, I, R and traffic parameters is given in Section 6.6.1. Redundant variables in Equation (3) were gradually removed during the course of the analysis. Percentage of residential land use (R) was a redundant variable and removed from the analysis. Validation plots are given in Figure D-1 of Appendix D. The analysis was undertaken using SigmaPlot 11.0 software. Table 8 presents the summary of the developed equations.

Table 9-8: A summary of equations developed for solids

Equations	R	POT
Solids(2001)=11204.147 - (0.0700 * ADT _{to}) + (74.079 * ADT _{hv}) + (136.582 * V/C) - (52959.185 * C) - (7524.183 * I)	0.978	0.994
Solids(2004)= 14540.746 - (0.285 * ADT _{to}) + (111.716 * ADT _{hv}) + (745.376 * V/C) - (83870.577 * C) - (10027.701 * I)	0.986	0.999
Solids(2010)= 16200.682 + (0.137 * ADT _{to}) + (108.813 * ADT _{hv}) + (2138.812 * V/C) - (86809.775 * C) - (8180.689 * I)	0.979	0.995

Notes: POT is the power of test, R is the regression coefficient, SigmaPlot 11.0 recommends the minimum desired power of test as 0.800

In order to develop equations with 95% accuracy to predict the population, it is recommended to have at least 30 data points (Rubinfeld 1998). However, only seven data points were used to develop these equations and validated with three data points. Consequently, the prediction accuracy could be below what is typically

recommended. Additionally, these equations are capable of predicting solids accurately only within the limits of the data set. These limits are ADT_{to}, from 29 to 10639, ADT_{hv} from 4 to 1139, V/C from 0.14 to 1.21, C from 0.01 to 0.44, I from 0 to 0.82. Outside these limits, predictions may result in greater errors. However, the prediction accuracy of equations can be improved by including more sites (best to include at least 30 sites) and following the same modelling and regression approach to further refine these equations. Furthermore, in order to increase the applicable limits, the selected sites need to have traffic and land use characteristics with high variability.

9.4 Conclusions

The following important conclusions were derived from the mathematical modelling of traffic-generated pollutants (HMs and PAHs):

- This study was undertaken using EPA SWMM stormwater quality model, which is a physically based model. This model replicates pollutant build-up and wash-off processes using a set of well-developed replication equations. Therefore, by conducting field measurement of atmospheric deposition, build-up and wash-off on small-scale plots (2m x 1.5m), contribution of traffic-generated pollutants to urban stormwater can be estimated using the developed modelling approach.
- The sites were ranked based on the toxic equivalent factors defined for the 16 EPA priority PAHs. However, the same weighting factor of one was applied for HMs ranking as there is no commonly accepted toxicity scale for them. Stormwater improvement measures can be implemented on the basis of these rankings. PAHs ranking indicates that annual toxic PAH loads also depend on the type of the dominant land use activities. Therefore, traffic and land use related activities make a significant contribution to annual toxic PAH loads in stormwater.

- The EPA SWMM model predicted solids loads were used to develop predictive equations to estimate annual solids loads. The predictive equations can be used not only to estimate solids generation from other roads but also to identify required changes to improve the resulting stormwater quality as an urban planning tool. However, these predictive equations can only be applicable within their limits. The prediction accuracy can be below what is typically recommended due to the limited number of sampling sites used. Therefore, it is recommended that the accuracy of the equations developed should be further improved by including additional sites.
- The modelling approach developed is limited to pollutants originating from road surfaces which is one of the primary sources of pollutants to urban stormwater. The modelling approach can be further refined by incorporating the actual variation of atmospheric wet deposition with the rainfall as the EPA SWMM is open-source software.
- As heavy metals and PAHs were modelled as co-fractions of solids, prediction equations were developed only for solids. This is justifiable as solids are an indicator pollutant. However, a similar set of equations can be developed for PAHs and HMs.

Chapter 10 - Conclusions and Recommendations

10.1 Conclusions

This study primarily developed an in-depth understanding of processes and deposition pathways for traffic generated pollutants, defining linkages between pollutants in the atmospheric and ground phases. PAHs, HMs, TSP and solids were the selected traffic generated target pollutants for this study. These four groups of pollutants present in the atmosphere, atmospheric deposition and build-up were collected and analysed to understand their variability with traffic and land use related parameters. This was based on the hypothesis that a portion of traffic generated pollutants accumulate in the atmosphere and subsequently deposit on road surfaces whilst the remainder directly deposits on road surfaces. The ‘real world’ application of knowledge generated was demonstrated through mathematical modelling of solids in urban stormwater accounting for the variability in traffic and land use characteristics.

Data required for the definition of pollutant processes and transport pathways was generated by undertaking in-depth field investigations covering targeted traffic and other land use generated pollutants in the atmosphere, atmospheric deposition and build-up on roads. The investigations were undertaken at selected road sites in the Gold Coast region. Field investigations were undertaken at fifteen sites for air sampling, eight sites for atmospheric deposition sampling and eleven sites for road surface build-up sampling. Multiple samples were collected from sites to allow for the variability of a range of influential parameters.

Data analysis was undertaken for atmospheric, wet and dry deposition and build-up samples separately using univariate and multivariate techniques. In-depth understanding of processes and transport pathways were developed for target pollutants and linkages among these processes were then developed. Practical application of the knowledge generated was demonstrated by developing a stormwater quality modelling approach. Important outcomes generated from the

analysis of pollutant processes in the different phases and the modelling exercise are discussed below.

10.1.1 Atmosphere pollutant build-up

Due to the involvement of many air pollutant sources such as exhaust, abrasion, soil inputs and land use related inputs and underlying processes such as re-suspension, the air quality demonstrated a complex variability with influential parameters. Therefore, it was difficult to develop a single generic model for air quality to allow for all the sources. In order to resolve this complexity, analysis of air quality was undertaken for weekdays and weekends separately. Key outcomes generated from this analysis were:

- Weekday TSP concentrations show positive correlation with traffic. Therefore, traffic is the main source of atmospheric phase TSP during weekdays. However, when traffic volume reduces, other sources such as land use related activities become dominant during weekends. This suggests the importance of both traffic and land use related sources on atmospheric TSP.
- Traffic exhaust emissions is the primary gas phase PAH source, whereas traffic exhaust emissions and land use related emissions contribute to particulate bound PAH loads in the atmosphere.
- Traffic related sources such as exhaust, tyre and brake wear contribute to atmospheric phase heavy metal loads. Linkages between different heavy metals and traffic sources vary.
- High traffic volume leads to the increase in abrasion products and re-suspended particulate pollutants in the atmosphere whereas effects of traffic congestion leads to the increase in exhaust related particles in the atmosphere. Heavy duty traffic was identified as the most critical source in generating high pollutant contributions to the atmospheric phase.

- Traffic congestion (V/C) and heavy duty traffic volume (ADT_hv) are the most influential traffic variables for the prediction of atmospheric phase HM and PAH loads.

Mathematical equations to quantify key pollutants were developed using regression analysis. A set of equations were developed for PAHs, HMs and TSP in atmospheric phase. As particulate matter was considered as the indicator pollutant, the equations were developed only for TSP and examples are given below.

$$\text{TSP (we)} = 57.659 + (25.078 * C) - (13.691 * I) - (37.003 * V/C) - [0.0470 * \text{ADT_hv (we)}] + [0.0274 * \text{wind (we)}] \dots\dots\dots(1)$$

$$\text{TSP (wk)} = 86.737 + (464.940 * C) - (120.670 * I) + (72.242 * V/C) - [0.289 * \text{ADT_hv(wk)}] \dots\dots\dots(2)$$

Where:

C, I = the percentage of commercial, industrial and residential land uses within 1km radius from each sampling location

ADT_hv = the total heavy duty traffic volume determined from a traffic survey carried out in 2010

V/C = the traffic congestion predicted by GCCC

Wind = the average measured wind speed for the sampling day

We = weekend

Wk = weekday

A complete list of the equations developed and their applicability are discussed in Section 6.6.

10.1.2 Atmospheric pollutant deposition

Atmospheric deposition is primarily influenced by the corresponding air quality. Consequently, atmospheric deposition showed indirect linkages with identified traffic variables and antecedent dry period. Analysis of atmospheric deposition was primarily undertaken to identify the linkages between atmospheric pollutants and

ground phase pollutant build-up. The following key conclusions were derived from the analysis:

- Atmospheric deposition is an important pathway for pollutant builds up on road surfaces. The rate of dry deposition of solids was found to be in the range of 28.13 and 55.74 mg/m²/day for the study sites and showed strong correlation with the antecedent dry period.
- Bulk deposition showed no correlation with the antecedent dry period, whilst showing strong correlation to the rainfall depth.
- Bulk deposition contains a relatively higher percentage of finer particles (<1.4 µm) compared to dry deposition. Traffic generated pollutants are strongly associated with bulk deposition. Dry deposition is strongly influenced by wind speed whereas the influence of wind is not significant for wet deposition.
- Pollutant loads in wet deposition are less sensitive to the traffic and land use characteristics compared to dry deposition. This is due to the easy dispersion of smaller particles over a larger area in the atmosphere from the source of origin. It is these particles that are primarily scavenged by wet deposition.
- Atmospheric deposition of HMs is directly influenced by proximity to high emission sources such as highways. Therefore, it is important to consider atmospheric deposition as a key source to urban stormwater in the vicinity of high emission of sources such as highways.

10.1.3 Pollutant build-up

Pollutant build-up of HMs and PAHs on road surfaces was analysed for five particle size fractions (<1 µm, 1-75 µm, 75-150 µm, 150-300 µm and >300 µm) individually. This was to facilitate the identification of key sources and pathways. Following conclusions were made from the analysis undertaken:

- Analysis of build-up samples revealed that neither the soluble fraction nor total solids show a clear trend with ADT or land use related activities,

suggesting the presence of other important sources and variables. As identified, the main sources include traffic and land use related activities, atmospheric deposition and soil related inputs.

- Particle size fraction $<75 \mu\text{m}$ is the most polluted in terms of traffic related direct emissions. This is due to the high contributions of traffic related sources such as exhaust emissions and abrasion related emissions. Except for the leakage of fuel and lubricants, traffic generated particles can be considered as fine. However, the fraction of these small particles creates bonds with larger particles due to various processes such as organic complexation.
- Land use related activities contribute HMs mainly in the 150-300 and $>300 \mu\text{m}$ size fractions. Contribution of land use related activities to heavy metal loads in build-up is minor compared to traffic related sources. This validates one of the primary hypothesis of the study, namely, that urban stormwater quality is directly influenced by traffic and land use characteristics.
- Heavy metals present in the atmosphere, atmospheric deposition and build-up are highly interrelated. This confirms the fact that atmosphere deposition is an important pathway for heavy metals in urban stormwater. This conclusion validates one of the primary hypothesis of the study, namely, that atmospheric deposition of traffic related pollutants is a major source of road surface build-up in relation to HMs.
- Although land use related activities contribute PAHs to build-up, traffic sources are the more dominant. As the investigated PAHs correlated only with commercial land use for $> 300 \mu\text{m}$ size fractions, the influence of land use is not as significant as traffic contributions.
- Atmospheric phase PAHs were found to be not a significant source to PAHs in build-up on road surfaces. Hence, atmospheric deposition can be considered not an important PAHs source in urban stormwater.

10.1.4 Mathematical modelling

Mathematical modelling was undertaken to validate the hypothesis for the study, namely, that traffic generated pollutants in urban stormwater can be predicted based on traffic and land use characteristics. This demonstrates the practical application of the knowledge created by this research study.

Mathematical equations were developed to predict stormwater quality based on traffic and land use characteristic through multiple linear regression. The equations can predict annual pollutant loads generated by roads based on traffic and land use characteristics. These equations can play an important role in treatment design and as a planning tool to identify the most suitable locations as pollutant loads can be predicted for known traffic and land use characteristics. The equation developed for predicting solids is given below. More details are given in Section 9.3.3.

$$\text{Solids (2004)} = 14540.746 - (0.285 * \text{ADT_to}) + (111.716 * \text{ADT_hv}) + (745.376 * \text{V/C}) - (83870.577 * \text{C}) - (10027.701 * \text{I}) \dots \dots \dots (3)$$

Where:

ADT_to = the total average daily traffic from a traffic survey carried out in 2010
2004 = based on year 2004 rainfall recorded at the Gold Coast Seaway Station (Bureau of Meteorology station no: 040764).

For equation (3), the independent variables and limits of applicability are the same as for equation (1) and (2). These predictive equations were developed for the Gold Coast region. However, they are applicable to other areas where there are no high pollutant emitting industries or construction and demolition activities. Following are the important points in relation to the mathematical modelling approach developed:

- Traffic and other land use generated stormwater pollutants can be estimated by knowing the traffic and land use characteristics. The equations can be used not only as a stormwater quality estimation tool, but also as an urban planning tool. Also, this approach does not require calibration and

verification. Hence, the modelling is simplified as historical data is not required.

- The equations can be extended to predict the traffic generated pollutants in urban stormwater quality for future scenarios by the combined use of changing traffic, land use and changed rainfall patterns.
- It is recommended that further validation and improvements to the accuracy of prediction equations is undertaken by including data from further study sites.

10.1.5 Practical applications of knowledge generated

Traffic generated pollutants such as heavy metals and polycyclic aromatic hydrocarbons threaten the ecosystem health of urban waterways. A key component in the sustainability of urban environments is the protection and management of water resources in both current and future scenarios. The extent to which pollutants enter urban water systems in the future is likely to change as a result of future traffic growth and urban form changes.

The outcomes generated in this study define direct linkages between traffic and land use related factors and, air quality, pollutants deposited on road surfaces and stormwater quality for future scenarios. The defined linkages can be utilised in urban and transport planning for achieving sustainable outcomes. Consequently, outcomes from this study will contribute to the development of adaptation measures for stormwater management strategies such as treatment devices to minimise the adverse impacts on urban receiving waters.

In this research study, traffic characteristics such as traffic congestion and volume of heavy duty traffic were identified as the most influential. Their degree of influence on air quality, atmospheric deposition and stormwater quality was also identified. This knowledge can be applicable in urban and transport planning in order to ensure that traffic characteristics are optimised to achieve environmental sustainability.

Exposure health assessments for heavy metals and PAHs can be carried out using the measured atmospheric concentration of HMs and PAHs by linking these concentrations to traffic and land use parameters and weekday and weekends variations. In turn, resulting environmental and inhalation risks can be assessed for these pollutants during weekdays and weekends. Furthermore, the air quality prediction model developed can be applied to generate hazard and risk mapping for air using geographical information systems (GIS). These maps can be used to assess health vulnerability due to traffic generated atmospheric PAH and HM emissions.

10.2 Recommendations for further research

This research study has contributed new knowledge in relation to the estimation of traffic and land use related pollutants in urban stormwater based on urban traffic and land used characteristics. It developed fundamental knowledge in relation to stormwater pollutant transport pathways and application of this knowledge was demonstrated through mathematical modelling. As part of this research investigation, a number of areas were identified for further investigation. These include:

- Further investigation of the spatial distribution of atmospheric deposition and air pollutants by undertaking air and deposition sampling at different distances from critical sources such as highways.
- Validation of the pollutant transport pathways developed for volatile organic compounds and total petroleum hydrocarbons as they are also primarily generated by traffic sources.
- Undertaking air sampling using a “High Volume Cascade Impactor” to determine PM-10, PM-2.5, PM-0.1 and ultrafine particle size fractions in the atmosphere to further refine the distribution and pathways of traffic generated TSP from air to ground deposition.

- Detailed investigation of the organic complexation process in relation to atmospheric build-up and road surface wash-off to identify the significance of this process in relation to these two phases.
- Development of sustainability level assessment tools based on traffic and land use related emissions by using measured PAHs and HMs concentrations and developed predictive equations.
- Development of decision support systems to plan sustainable transport systems for the future. In this regards, the data generated and the predictive equations developed in this research can be used as baseline knowledge.

References

1. AATSE. (1997). Urban Air Pollution in Australia, Australian Academy of Technological Sciences and Engineering, Ian McLennan House, 197 Royal Parade, Parkville VIC 3052.
2. ABS. (2008a). Australian Bureau of Statistics (Report No. 1379.0.55.001), National Regional Profile, Gold Coast 2002 to 2006, Canberra, Australia.
3. ABS. (2008b). Motor Vehicle Census Australia, Australian Bureau of Statistic.
4. ABS. (2010). Motor Vehicle Census, Australia, Australian Bureau of Statistics- <http://www.abs.gov.au/ausstats/abs@.nsf/mf/9309.0#>.
5. AGBOM. (2010). Climate Data Online, 040764, Gold Coast Seaway, <http://reg.bom.gov.au/climate/data/index.shtml>, Australian Government Bureau of Meteorology.
6. AGBOM. (2011). Six minutes rainfall data at Gold Coast seaway station, Australian Government Bureau of Meteorology- <http://ftp.bom.gov.au/anon2/home/nsw/Data/jg/>.
7. Alphen, V. M. (1999). Atmospheric heavy metal deposition plumes adjacent to a primary lead-zinc smelter. *The Science of The Total Environment*, 236(1-3), 119-134.
8. Amodio, M., Caselli, M., Gennaro, G., and Tutino, M. (2009). Particulate PAHs in two urban areas of Southern Italy: Impact of the sources, meteorological and background conditions on air quality. *Environmental Research*, 109, 812–820.
9. Anderson, J. M. (1996). Potential for water recycling in Australia: expanding our horizons. *Desalination*, 106, 151-156.
10. APHA. (2004). Standard methods for the examination of water & wastewater, Washington DC, American Public Health Association.
11. AS/NZS. (1998). Australian New Zealand Standards, Water quality Sampling, Part 1: Guideline of the Design of Sampling Programmes, Sampling Techniques and the Preservations and Handling of Samples.
12. Ashley, R. M., Wotherspoon, D. J. J., Coghlan, B.P., and McGregor, I. (1992). The erosion and movement of sediments associated pollutants in combined sewers. *Water Science Technology*, 23(8),101-114.
13. Ayoko, G. A., Bornire, J. J., Abdulkadir, S. S., Olurinola, P. F., Ehinmidu, J. O., Kokot, S., Yiasel, S. (2003). A multicriteria ranking of organotin (IV) compounds with fungicidal properties, 17.

14. Ayoko, G. A., Singh, K., Balerea, S., and Kokot, S. (2007). Exploratory multivariate modeling and prediction of the physico-chemical properties of surface water and groundwater. *Journal of Hydrology*, 336(1-2), 115-124.
15. Azimi, S., Rocher, V., Garnaud, S., Varrault, G., and Thevenot, D.R. (2005). Decrease of atmospheric deposition of heavy metals in an urban area from 1994 to 2002 (Paris, France). *Chemosphere*, 61, 645–651.
16. Ball, J. E., Jenks, R., and Aubourg, D. (1998). An assessment of the availability of pollutant constituents. *The Science of the Total Environment*, 209, 243-254.
17. Barco, J., Papiri, S., and Stenstrom, M. K. (2008). First flush in a combined sewer system. *Chemosphere*, 71(5), 827-833.
18. Balestrini, R., and Tagliaferri, A., 2001. Atmospheric deposition and canopy exchange processes in alpine forest ecosystems (northern Italy). *Atmospheric Environment*, 35(36), 6421-6433.
19. Barrett, M. E., Zube R. D., Colling, E. R., Malina, J., Charbeneau, R. J., and Ward, G. H., (1995). A Review and Evaluation of Literature Pertaining to the Quality and Control of Pollination from Highway Runoff and construction, Centre for Research in Water Resources, Bureau of Engineering Research, The University of Texas at Austin.
20. Barrios, A. (2000). Urbanisation and Water Quality. American Farmland Trust's Center for Agriculture in the Environment, CAE Working Paper Series, DeKalb, Ill.
21. Barry, M. E., McAlister, A. B., Weber, T. R., Abal, E., and Scott, N. (2004). Impacts of stormwater runoff from roads in South East Queensland. Proceedings of the 2004 International Conference on Water Sensitive Urban Design, Adelaide, Australia, 21-25.
22. Beman, J. M., Arrigo, K. R., and Matson, P. A. (2005). Agricultural Runoff Fuels Large Phytoplankton Blooms in Vulnerable Areas of the Ocean. *Nature*, 434, 211-214.
23. Berko, D. H. N. (1999). Technical Report No. 2: Polycyclic aromatic hydrocarbons (PAHs) in Australia. Perth, Western Australia: Department of Environmental Protection, 1-55.
24. Bhargava, A. R. N., Khanna, S. K., and Bhargava, B. S. (2004) Exposure risk to carcinogenic PAHs in indoor-air during biomass combustion whilst cooking in rural India, *Atmospheric Environment*, 38, 4761-4767.

25. Boddy, J. W. D., Smalley, R.J., Dixon, N.S., Tate, J.E. and Tomlin, A.S. (2005). The spatial variability in concentrations of a traffic-related pollutant in two street canyons in York, UK -Part I: The influence of background winds. *Atmospheric Environment*.
26. Boehm, P. D., and Farrington, J. W. (1984). Aspects of the polycyclic aromatic hydrocarbon geochemistry of recent sediments in the Georges Bank region. *Environmental Science and Technology*, 18, 840-845.
27. Boyd, G., and Gardner, N. (1990). Urban stormwater: An overview for municipalities. *Public Works*, 39-42.
28. Brachtl, M. V., Durant, J. L., Perez, C. P., Oviedo, J., Sempertegui, F., Naumova, E. N., and Griffiths, J. K. (2009). Spatial and temporal variations and mobile source emissions of polycyclic aromatic hydrocarbons in Quito, Ecuador. *Environmental Pollution*, 157(2), 528-536.
29. Brcic, I., and Skender, L. (2003). Determination of benzene, toluene, ethylbenzene, and xylenes in urine by purge and trap gas chromatography, Institute for Medical Research and Occupational Health, Zagreb, Croatia, 26, 1225–1229.
30. Brinkmann, W. L. F., and Schaften, J. W. (1985). Urban Stormwater pollutants: Sources and Loading, *GeoJournal*, 11(3), 277-283.
31. Brodie, I., and Young, F. (2006). Stormwater particle characteristics of five different urban surfaces. *Proceedings of the 7th International Conference on Urban Drainage Modelling in conjunction with 4th International Conference on Water Sensitive Urban Design 2006*, Melbourne, Australia, 237-244.
32. Brook, J. R., Dann, T. F., and Burnett, R. T. (1997). The relationship among TSP, PM10, PM2.5, and inorganic constituents of atmospheric particulate matter at multiple Canadian locations. *Air Waste Management Association*, 47, 2-19.
33. Brown, G., and Maher, W. (1992). The occurrence, distribution, and sources of polycyclic aromatic hydrocarbons in the sediments of the Georges River estuary, Australia. *Organic Geochemistry*, 18, 657-668.
34. Brown, P., Jefcoat, I. A., Parrish, D., Gill, S., and Graham, E. (2000a). Evaluation of the adsorptive capacity of peanut hull pellets for heavy metals in solution. *Advance Environmental Research*, 4, 19-29.
35. Brown, P. A., Gill, S. A., and Allen, S. J. (2000b). Metal removal from wastewater using peat. *Water Research*, 16, 3907-3916.
36. Carmody, O., Kristóf, J., Frost, R. L., Makó, E., Klopogge, J. T., and Kokot, S. (2005). A spectroscopic study of mechanochemically activated kaolinite with the aid of chemometrics. *Journal of Colloid and Interface Science*, 287(1), 43-56.

37. Carter, W. P. L. (2007). Detail Mechanism for the gas-phase Atmospheric reactions of organic compounds. State-wide Air Pollutant Research Centre, University of California, Riverside, USA, 24A,(3), 481-508.
38. Chang, Y. M., Chou, C. M., Su, K. T., and Tseng, C. H. (2005). Effectiveness of Street Sweeping and Washing for Controlling Ambient TSP. *Atmospheric Environment*, 39, 1891-1902.
39. Chester, R., Nimmo, M., and Preston, M. R. (1999). The trace metal chemistry of atmospheric dry deposition samples collected at Cap Ferrat: a coastal site in the Western Mediterranean. *Marine Chemistry*, 68(1-2), 15-30.
40. Chow, J. C., Watson, J. G., Lowenthal, D. H., and Countess, R. J. (1996). Sources and Chemistry of PM10 aerosol in Santa Barbara County, CA. *Atmospheric Environment*, 30(9), 1489-1499.
41. Chu, C. C., Fang, G. C., Chen, J. C., and Yang, I. L. (2008) Dry deposition study by using dry deposition plate and water surface sampler in Shalu, central Taiwan, *Environ Monit Assess*, 146, 441-451.
42. Chui, T. (1981). Highway Runoff in the State of Washington: Model Validation and Statistical Analysis. Master's thesis. University of Washington, Seattle, Washington.
43. Cohen, D. D., Gulson, B. L., Davis, J. M., Stelcer, E., Garton, D., Hawas, O., and Taylor, A., (2005). Fine-particle Mn and other metals linked to the introduction of MMT into gasoline in Sydney, Australia: Results of a natural experiment. *Atmospheric Environment*, 39(36), 6885-6896.
44. Colvile, R. N., Hutchinson, E. J., Mindell, J. S., and Warren, R. F. (2001). The Transport Sector as a Source of Air Pollution. *Atmospheric Environment*, 35(9), 1537-1565.
45. Cook, B. (2008). Gold Coast Rapid Transit concept design and impact management plan air quality technical report, GHD Pty Ltd Brisbane, Australia, 7.
46. Councell, T. B., Duckenfield, K.U., Landa, E. R., and Callender, E. (2004). Tire-Wear Particles as a Source of Zinc to the Environment. *Environmental science and technology*, 38, 4206-4214.
47. Croft, B., Lohmann, U., Martin, R. V., Stier, P., Wurzler, S., Feichter, J., et al. (2009). Aerosol size-dependent below-cloud scavenging by rain and snow in the ECHAM5-HAM. *Atmospheric Chemistry and Physics*, 9, 4653-4675.
48. CSIRO. (1999). Review of Storm Models, Integrated Water Management Group, Land and water Technical Report Canberra, ACT Australia.

49. CSIRO. (2006). Urban Stormwater: Best Practice Environmental Management Guidelines. Collingwood VIC 3066, Australia: 15.
50. CSIRO. (2007). The impact of climate change on extreme rainfall and coastal sea levels over south-east Queensland, Part 2: A High-Resolution Modelling Study of the Effect of Climate Change on the Intensity of Extreme Rainfall Events, prepared for Gold Coast City Council.
51. Davis, B., and Birch, G. (2010a). Comparison of heavy metal loads in stormwater runoff from major and minor urban roads using pollutant yield rating curves. *Environmental Pollution*, 158(8), 2541-2545.
52. Davis, B., and Birch, G. (2010b). Spatial Distribution of Bulk Atmospheric Deposition of Heavy Metals in Metropolitan Sydney, Australia. *Water, Air, and Soil Pollution*, 1-16.
53. Davis, A. P., M. Shokouhian, and Ni, S. (2001). Loading estimates of lead, copper, cadmium, and Zinc in urban runoff from specific sources. *Chemosphere*, 44(5), 997-1009.
54. Deletic, A., Maksimovic, C., Loughreit, F., and Butler, D. (1998). Modelling the Management of Street Surface Sediments in Urban Runoff. In *Proceedings of the Conference on Innovative Technologies in Urban Storm Drainage*, Lyon, France.
55. Deletic, A. (1998). The first flush load of urban surface runoff. *Water Research*, 32(8), 2462-2470.
56. Deletic, A., and Orr, D., W. (2005). Pollution Build-up on Road Surfaces, *Journal of Environmental Engineering*, 131(1), 49-59
57. Delfino, R. J. (2002). Epidemiological Evidence for Asthma and Exposure to Air Toxics: Linkages between Occupational, Indoor, and Community Air Pollution Research. 110, 573-589.
58. Delleur, J. W. (1982). Introduction to urban hydrology and stormwater management. In *Urban Stormwater Hydrology*, Washington D.C., American Geophysical Union, 1-34.
59. DHI. (2007). DHI Software product catalogue, Danish Hydraulic Institute-Water and Environment, Denmark.
60. DL. (2000a). Decision Lab, version 1.01.0388, Visual Decision Inc. <http://www.visualdecision.com>
61. DL. (2000b). Getting Started Guide, Decision Lab 2000, Montreal, QC, Canada, 1999-2003.

62. Drewry, J. J., Newham, L. T. H., Greene, R. S. B, Jakeman, A. J., and Croke, B. F. W. (2006). A review of nitrogen and phosphorus export to waterways: context for catchment modelling. *Marine and Freshwater Research Canberra, ACT 0200, Australia*, 57, 757-774.
63. Duong, T. T. T., and Lee, B.-K. (2011). Determining contamination level of heavy metals in road dust from busy traffic areas with different characteristics. *Journal of Environmental Management*, 92(3), 554-562.
64. Durst, A. R., Davison, W., Toth, K., Rotherp, J. E., Peden, M. E., and Griepink, B. (1991). Analysis of wet deposition (Acid Rains): Determination of the major ionic constituents by iron chromatography. *Pure and Applied Chemistry* 63(6), 907-915.
65. ECOTECH. (2005). User manual Edition 2.0, PUF/XAD Sampler Version, ECOTECH Environmental monitoring, Head Office, 12 Apollo Court, Blackburn, Australia.
66. Egodawatta, P., and Goonetilleke, A. (2008a). Modelling Pollutant Build-up and Wash-off in Urban Road and Roof surfaces. *Proceedings of the 31st Hydrology and Water Resources Symposium and the 4th International Conference on Water Resources and Environment Research, Engineers Australia*.
67. Egodawatta, P., and Goonetilleke, A. (2008b). Understanding urban road surface pollutant wash-off and underlying physical processes using simulated rainfall, *Water Science and Technology*, 57(8), 1241-1246.
68. Egodawatta, P., (2007). Translation of small-plot scale pollutant build-up and wash off measurements to urban catchment scale. Queensland University of Technology, Brisbane. PhD Thesis.
69. Elliott, A.H, and Trowsdale, S.A. (2007). a review of models for low impact urban stormwater drainage, *Environmental Modelling and Software*, 22, 394-405.
70. EPASGV, (1999). Measurement of Motor Vehicle Pollutants and Fleet Average Emission Factors in Melbourne, Environmental Protection Authority State Government of Victoria.
71. Esen, F., Tasdemir, Y., and Vardar, N. (2008). Atmospheric concentrations of PAHs, their possible sources and gas-to-particle partitioning at a residential site of Bursa, Turkey. *Atmospheric Research*, 88(3-4), 243-255.
72. Espinasse, B., Picolet, G., and Chouraqui, E. (1997). Negotiation support systems: A multi-criteria and multi-agent approach. *European Journal of Operational Research*, 103(2), 389-409.

73. Express, E. (2005). HotBlock™ Digestion System Operation and Instruction Manual, Environmental Express, 490 Wando Park Blvd., Mt. Pleasant, South Carolina 29464.
74. Faiz, A., and Sturm, P. J. (2002). New Directions: Air pollution and road traffic in developing countries, *Atmospheric Environment*, 34, 4745-4746.
75. Fang, G.-C., Wu, Y.-S., Huang, S.-H., and Rau, J.-Y. (2004). Dry deposition (downward, upward) concentration study of particulates and heavy metals during daytime, nighttime period at the traffic sampling site of Sha-Lu. *Taiwan Chemosphere*, 56(6), 509-518.
76. Fenger, J. (1999). Urban air quality, *Atmospheric Environment*, 33, 4877-4900.
77. Fine, P. M., Shen, S., and Sioutas, C. (2004). Inferring the sources of fine and ultrafine particulate matter at downwind receptor sites in the Los Angeles basin using multiple continuous measurements. *Aerosol Science and Technology*, 38, 182-195.
78. Fon, T. Y. W., Ozaki Noriatsu, O. and Hiroshi, S. (2007). Polycyclic Aromatic Hydrocarbons (PAHs) in the Aerosol of Higashi Hiroshima, Japan: Pollution Scenario and Source Identification. *Water Air Soil Pollution*, 182, 235–243.
79. Fraser, M. P., Yue, Z. W., and Buzcu, B. (2003). Source apportionment of fine particulate matter in Houston, TX, using organic molecular markers. *Atmospheric Environment*, 37(15), 2117–2123.
80. Galindo, N., Varea, M., Gil-Moltó, J., Yubero, E., and Nicolás, J. (2010). The Influence of Meteorology on Particulate Matter Concentrations at an Urban Mediterranean Location. *Water, Air, & Atmosphere; Soil Pollution*, 1-8.
81. Garcia, R., and Millan, E. (1998). Assessment of Cd, Pb and Zn contamination in roadside soils and grasses from Gipuzkoa (Spain). *Chemosphere*, 37(8), 1615-1625.
82. Garivait, H., Polprasert, C., Yoshizumi, K., and Reutergardh, L. B. (2001) Airborne Polycyclic Aromatic Hydrocarbons (PAH) in Bangkok Urban Air: Part II. Level and Distribution, *Polycyclic Aromatic Compounds*, 18(3), 325-350.
83. GCCC-WEB. (2010). Gold Coast City Council's web page - www.goldcoast.qld.gov.au.
84. Gertler, A. W., Gillies, J. A., and Pierson, W. P. (2000). An Assessment of the mobile source contribution to PM10 and PM2.5 in the United States. *Water, Air, and Soil Pollution*, 123(1), 203-214

85. Ghafouri, M., Swain, E.C. (2005). Spatial Analysis of Urban Stormwater Quality. *Journal of Spatial Hydrology*, 5(1), 33-46.
86. Ghose, M. K., Paul, R., and Banerjee, R. K. (2005). Assessment of the status of urban air pollution and its impact on human health in the city of Kolkata, Department of Civil Engineering, Bengal Engineering College, Kolkata, India, *Environmental Monitoring and Assessment*. 108, 151-167.
87. Gietl, J. K., Lawrence, R., Thorpe, A. J., and Harrison, R. M. (2010). Identification of brake wear particles and derivation of a quantitative tracer for brake dust at a major road. *Atmospheric Environment*, 44(2), 141-146.
88. Gnecco, I., Berretta, C., Lanza, L. G., and La Barbera, P. (2005). Storm water pollution in the urban environment of Genoa, Italy. *Atmospheric Research*, 77(1-4), 60-73
89. Goonetilleke, A., Thomas, E., Ginn, S., and Gilbert, D. (2005). Understanding the role of land use in urban stormwater quality management. *Journal of Environmental Management*, 74(1), 31-42.
90. Goonetilleke, A., and Thomas, E. (2003). Water Quality Impacts of Urbanisation-Evaluation of Current Research. Energy & Resource Management Research Program, Centre of Built Environment and Engineering Research, Queensland University of Technology.
91. Gulson, B., Cohen, D., Davis, J., Stelcer, E., Garton, D., Hawas, O., and Taylor, A. (2006). Fine-particle Mn and other metals linked to the introduction of MMT into gasoline in Sydney, Australia: Results of a natural experiment. *Chinese Journal of Geochemistry*, 25(0), 62-63.
92. Hall, K. J., and Anderson, B. C. (1988). Toxicity and Chemical Composition of Urban Stormwater Runoff. *Canadian Journal of Civil Engineering*, 15(1), 96-106.
93. Hamilton, R. S., Revitt, D. M., and Warren, R. S. (1984). Levels and physico-chemical associations of Cd, Cu, Pb, and Zn in road sediments. *The Science of the Total Environment*, 33, 59-74.
94. Han, B., Bai, Z., Guo, G., Wang, F., Li, F., Liu, Q., Ji, Y., Li, X., and Hu, Y. (2009). Characterization of PM10 fraction of road dust for polycyclic aromatic hydrocarbons (PAHs) from Anshan, China. *Journal of Hazardous Materials*, 170(2-3), 934-940.
95. Han, B., Bai, Z., Guo, G., Wang, F., Li, F., Liu, Q., Ji, Y., Li, X., and Hu, Y. (2009). Characterization of PM10 fraction of road dust for polycyclic aromatic hydrocarbons (PAHs) from Anshan, China. *Journal of Hazardous Materials*, 170(2-3), 934-940.
96. Harris, D. C. (2007). *Quantitative Chemical Analysis (7th edition)*, Printed in the United Estate of America.

97. Harris, S. J., and Maricq, M. M. (2001). Signature size distributions for diesel and gasoline engine exhaust particulate matter. *Journal of Aerosol Science*, 32(6), 749-764.
98. Hergren, L. (2005). Build-up and wash-off process kinetics of PAHs and heavy metals on paved surfaces using simulated rainfall. PhD thesis, School of Urban Development, Queensland University of Technology, GPO Box 2434, Brisbane QLD 4001, Australia.
99. Hergren, L., Goonetilleke, A., and Ayoko, G. A. (2005a). Understanding heavy metal and suspended solids relationships in urban stormwater using simulated rainfall. *Journal of Environmental Management*, 76(2), 149-158.
100. Hergren, L., Goonetilleke, A., and Ayoko, G. A. (2006). Analysis of heavy metals in road-deposited sediments. *Analytica Chimica Acta*, 571(2), 270-278.
101. Hill, L. J., and Caritat, P. D. (2002). A method of bulk sampling wet and dry atmospheric deposition for trace element analysis, Regolith and Landscapes in Eastern Australia, 54-57.
102. Hitchins, J., Morawska, L., Wolff, R., and Gilbert, D. (2000). Concentrations of submicrometre particles from vehicle emissions near a major road. *Atmospheric Environment*, 34(1), 51-59.
103. Hong, H., S., Yin, H., L., Wang, X. H., and Ye, C., X. (2007). Seasonal variation of PM10-bound PAHs in the atmosphere of Xiamen, China. *Atmospheric Research*, 85, 429-441.
104. Hoshiko, T., Yamamoto, K., Nakajima, F., and Prueksasit, T. (2011). Time-series analysis of polycyclic aromatic hydrocarbons and vehicle exhaust in roadside air environment in Bangkok, Thailand. *Procedia Environmental Sciences*, 4, 87-94.
105. Huang, X., Olmez, I., Aras, N. K., and Gordon, G. E. (1994). Emissions of trace elements from motor vehicles: Potential marker elements and source composition profile. *Atmospheric Environment*, 28(8), 1385-1391.
106. Huber, C. W. (1986). Deterministic Modelling of Urban Runoff Quality'. *Urban Runoff Pollution*, Springer-Verlag, Berlin, Heidelberg, 10, 167-241.
107. Huston, R., Chan, Y. C., Gardner, T., Shaw, G., and Chapman, H. (2009). Characterisation of atmospheric deposition as a source of contaminants in urban rainwater tanks. *Water Research*, 43(6), 1630-1640.
108. Imhof, J. G., and Annable, W. K. (1993). Developing an ecosystem context for the management of water and water systems. In *New Techniques for Modelling the Management of Stormwater Quality Impacts*, Proceedings of the Stormwater and Water Quality Management Modelling Conference, 29-53.

109. IPCC. (2007). Climate Change 2007: Synthesis Report. Contribution of Working Groups I, II and III to the Fourth Assessment Report of the Intergovernmental Panel on Climate Change Core Writing Team, Pachauri, R. K and Reisinger, A.(eds.). IPCC, Geneva, Switzerland, 104.
110. Janssen, C. R., Heijerick, D. G., De Schamphelaere, K.A.C., and Allen, H. A. (2003). Environmental risk assessment of metals: tools for incorporating bioavailability. *Environment International*, 28(8), 793-800.
111. Japar, S. M. (1995). Motor vehicles and particle air pollution: an overview. In: *Particulate Matter: Health and Regulatory Issues. Proceedings of an International Specialty Conference*, Pittsburgh PA, Air and Waste Management Association, 49, 577-598.
112. Johansson, C., Norman, M., and Burman, L. (2009). Road traffic emission factors for heavy metals. *Atmospheric Environment*, 43(31), 4681-4688.
113. Jolliet, O., and Hauschild, M. (2005). Modelling the influence of intermittent rain event on the long-term fate and the transport of organic air pollutant, *Environment Science Technology*, 39, 4513-4522.
114. Kaarle, K. (2007). Road dust from pavement wear and traction sanding MONOGRAPHS of the Boreal Environment. Research MONOGRAPHS of the Boreal Environment Research, Finnish Environment Institute, Finland.
115. Kalaiarasan, M., Balasubramanian, R., Cheong, K.W.D., and Tham, K.W. (2009). Traffic-generated airborne particles in naturally ventilated multi-storey residential buildings of Singapore: Vertical distribution and potential health risks. Division of Environmental Science and Engineering, Faculty of Engineering, National University of Singapore.
116. Kalantari, A., Bina, B., Taleby M., and Loloee, M. (2006) The Relationship between Polycyclic Aromatic Hydrocarbons and Heavy Metals, *Journal of health science*, 6(1), 14-17.
117. Karar, K., Gupta, A., Kumar, A., and Biswas, A. (2006). Characterization and Identification of the Sources of Chromium, Zinc, Lead, Cadmium, Nickel, Manganese and Iron in PM10 Particulates at the Two Sites of Kolkata, India. *Environmental Monitoring and Assessment*, 120(1), 347-360.
118. Karr, J. R. (1991). Biological Integrity: A long neglected aspect of water resources management. *Ecological Applications*, 1, 66-84.
119. Kayhanian, M., Suverkropp, C., Ruby, A., and Tsay, K. (2007). Characterization and prediction of highway runoff constituent event mean concentration. *Journal of Environmental Management*, 85(2), 279-295.

120. Keller, H. R., Massart, D. L., and Brans, J. P. (1991). Multicriteria decision making: A case study. *Chemometrics and Intelligent Laboratory Systems*, 11(2), 175-189.
121. Kemp, K. (2002). Trends and sources for heavy metals in urban atmosphere. *Nuclear Instruments and Methods in Physics Research Section B: Beam Interactions with Materials and Atoms*, 189(1-4), 227-232.
122. Khalil, W. A.-S., Goonetilleke, A., Kokot, S. E., and Carroll, S. (2004). Use of chemometrics methods and multicriteria decision-making for site selection for sustainable on-site sewage effluent disposal. *Analytica Chimica Acta*, 506(1), 41-56.
123. Kishida, M., Imamura, K., Takenaka, N., Maeda, Y., Viet, P., and Bandow, H. (2008). Concentrations of Atmospheric Polycyclic Aromatic Hydrocarbons in Particulate Matter and the Gaseous Phase at Roadside Sites in Hanoi, Vietnam. *Bulletin of Environmental Contamination and Toxicology*, 81(2), 174-179.
124. Klein, L. A., Lang, M., and Kirschner, S. L. (1974). Sources of Metals in New York City Wastewater. *J. Water Poll Control Federation*, 46(12), 2653-2662.
125. Kokot, S., Grigg, M., Panayiotou, H., and Phuong, T. D. (1998). Data Interpretation by some Common Chemometrics Methods. *Electroanalysis*, 10(16), 1081-1088.
126. Kucklick, J. R., Sivertsen, S. K., Sanders, M., and Scott, G. I. (1997). Factors influencing polycyclic aromatic hydrocarbon distributions in South Carolina estuarine sediments. *Journal of Experimental Marine Biology and Ecology*, 213, 13-29.
127. Kunzli, N., Kaiser, R., Medina, S., Studnicka, M., Chanel, O., Filliger, P., Herry, M., Horak, F., Puybonnieux-Texier, V., Quenel, P., Schneider, J., Seethaler, R., Vergnaud, J. C., and Sommer, H. (2000). Public-health impact of outdoor and traffic-related air pollution: A European Assessment', 356, 795-801.
128. Latimer, J. S., Hoffman, E. J., and Quinn, J. G. (1990). Sources of petroleum hydrocarbons in urban runoff. *Water Air Soil Pollution*, 52, 1-21.
129. Lee, W.-J., Wang, Y.-F., Lin, T.-C., Chen, Y.-Y., Lin, W.-C., Ku, C.-C., and Cheng, J.-T. (1995). PAH characteristics in the ambient air of traffic-source. *Science of the Total Environment*, 159(2-3), 185-200.
130. Li, C.-T., Lin, Y.-C., Lee, W.-J., and Tsai, P.-J. (2003). Emission of Polycyclic Aromatic Hydrocarbons and Their Carcinogenic Potencies from Cooking Sources to the Urban Atmosphere. *Environmental Health Perspectives*, 111(4), 483-487.

131. Lim, M. C. H., Ayoko, G., Morawska, L. (2005) Characterization of elemental and polycyclic aromatic hydrocarbon compositions of urban air in Brisbane, *Atmospheric Environment Journal*, 39(3), 463-476.
132. Lim, M. C. H., Ayoko, G. A., Morawska, L., Ristovski, Z., Jayaratne, R., and Kokot, S. (2006). A comparative study of the elemental composition of the exhaust emissions of cars powered by liquefied petroleum gas and unleaded petrol. *Atmospheric Environment*, 40(17), 3111-3122.
133. Lim, M. C. H. (2007). Chemical and Physical Characterisation of Aerosol from the exhaust emission of motor vehicles international Laboratory for Air Quality and Health, School of Physical and Chemical Sciences, Queensland University of Technology, Brisbane, Australia. PhD Thesis
134. Lim, J.-H., Sabin, L. D., Schiff, K. C., and Stolzenbach, K. D. (2006). Concentration, size distribution, and dry deposition rate of particle-associated metals in the Los Angeles region. *Atmospheric Environment*, 40(40), 7810-7823.
135. Lockie, T. (2007) Catchment modelling using SWMM, Hydraulic Analysis Limited, New Zealand.
136. Lonati, G., and Giugliano, M. (2006). Size distribution of atmospheric particulate matter at traffic exposed sites in the urban area of Milan (Italy). *Atmospheric Environment*, 40(Supplement 2), 264-274.
137. Luo, W. (2001). Wet-deposition fluxes of soluble chemical species and the elements in insoluble materials. *Atmospheric Environment*, 35(16), 2963-2967.
138. Mage, D., Ozolins, G., Guntis, P., Webster, A., Orthofer, R., Vandeweerd, V. and Gwynne, M. (1996). Urban air pollution in megacities of the world'. *Atmos. Environ.*, 30(2), 681-686.
139. Mahbub, S. M. P. B. (2009). Impact of Urban Traffic and Climate Change on Water Quality from Road Runoff, Queensland University of Technology, Brisbane. Confirmation of PhD Candidature Report
140. Mahbub, S. M. P. B. (2011). Impact of Urban Traffic and Climate Change on Water Quality from Road Runoff. Queensland University of Technology - Thesis, Brisbane, Australia.
141. Maher, B. A., Moore, C., and Matzka, J. (2008). Spatial variation in vehicle-derived metal pollution identified by magnetic and elemental analysis of roadside tree leaves *Atmospheric Environment*, 42, 364–373.
142. Mahmud, R., Inoue, N., and Sen, R. (2007). Assessment of Irrigation water quality by using principal component analysis in an arsenic affected area of Bangladesh. *Journal of Soil and Nature*, 1 (2), 8-17.

143. Marsalek, J., Rochfort, Q., Brownlee, B., Mayer, T., and Servos, M. (1999). An exploratory study of urban runoff toxicity. *Water Science Technology*, 39(12), 33-39.
144. Martuzevicius, D., Kliucininkas, L., Prasauskas, T., Krugly, E., Kauneliene, V., and Strandberg, B. (2011). Resuspension of particulate matter and PAHs from street dust. *Atmospheric Environment*, 45(2), 310-317.
145. Massart, D. L., Vandeginste, B. G. M., Buydens, L. M. C., John, S. D., Lewi, P. J., and Smeyers-Verbeke, J. (1997). *Handbook of Chemometrics and Qualimetrics: Part A*.
146. McGaughey, G. R., Desai, N. R., Allena, D. T., Seilab, R. L., Lonnemanc, W. A., Fraserd, M. P., Harley, R. A., Pollackf, A. K., Ivyg, J. M., and Priceg, J. H. (2004). Analysis of motor vehicle emissions in a Houston tunnel during the Texas Air Quality Study. US Environmental Protection Agency, Research Triangle Park, NC 27711, USA, *Atmospheric Environment*, 38, 3363-3372.
147. McLachlan, M. S., and Sellström, U. (2009). Precipitation scavenging of particle-bound contaminants - A case study of PCDD/Fs. *Atmospheric Environment*, 43(38), 6084-6090.
148. Melaku, S., Morris, V., Raghavan, D., and Hosten, C. (2008). Seasonal variation of heavy metals in ambient air and precipitation at a single site in Washington, DC. *Environmental Pollution*, 155, 88-98.
149. Barrett, M. E., Zube R. D., Colling, E. R., Malina, J., Charbeneau, R. J., and Ward, G.H., (1995) A Review and Evaluation of Literature Pertaining to the Quality and Control of Pollution from Highway Runoff and construction, Centre for Research in Water Resources, Bureau of Engineering Research, The University of Texas at Austin.
150. Miguel, A. H., Kirchstetter, T. W., Harley, R. A., and Hering, S. V. (1998). On-Road Emissions of Particulate Polycyclic Aromatic Hydrocarbons and Black Carbon from Gasoline and Diesel Vehicles. *Environmental Science & Technology*, 32(4), 450-455.
151. Miguntanna, N. P. (2009). Nutrients build-up and wash-off processes in urban land uses. Queensland University of Technology – PhD Thesis, Brisbane, Australia.
152. Mijic, Z., Stojic, A., Perisic, M., Rajsic, S., Tasic, M., Radenkovic, M., et al. (2010). Seasonal variability and source apportionment of metals in the atmospheric deposition in Belgrade. *Atmospheric Environment*, 44(30), 3630-3637.

153. Mogo, S., Cachorro, V. E. and de Frutos, A. M. (2006). Morphological, chemical and optical absorbing characterization of aerosols in the urban atmosphere of Valladolid. *Atmospheric Chemistry and Physics Discussion*, 5, 3921–3957.
154. Morawska, L. (2008). *Environmental Aerosol Physics*. Brisbane, Australia: Review of the diesel emission and impacts on air quality in urban areas, Queensland University of Technology.
155. Moreno, T., Querol, X., Alastuey, A., Garcia do Santos, S., Fernandez Patier, R., Artinano, B., and Gibbons, W. (2006). PM source apportionment and trace metallic aerosol affinities during atmospheric pollution episodes: a case study from Puertollano, Spain. *Journal of Environmental Monitoring*, 8(10), 1060-1068.
156. Morselli, L., Olivieri, P., Brusori, B., and Passarini, F. (2003) Soluble and insoluble fractions of heavy metals in wet and dry atmospheric depositions in Bologna, Italy, *Environmental pollution*, 124(3), 457-469.
157. Motallebi, N., Tran, H., Croes, B. E., and Larsen, L. C. (2003). Day-of-Week Patterns of Particulate Matter and Its Chemical Components at Selected Sites in California. *Air & Waste Management Association*, 53, 876-888.
158. Muendo, M., Hanai, Y., Kameda, Y. and Masunaga, S. (2006). Polycyclic Aromatic Hydrocarbons in Urban Air: Concentration Levels, Patterns, and Source Analysis in Nairobi, Kenya. *Environmental Forensics*, 7, 147–157.
159. Müller, J. F., Hawker, D. W., and Connell, D. W. (1998). Polycyclic aromatic hydrocarbons in the atmospheric environment of Brisbane, Australia. *Chemosphere*, 37(7), 1369-1383.
160. MUSIC. (2005). User manual Version 3.0, MUSIC Development Team Cooperative Research Center CRC for Catchment Hydrology, Australia.
161. MUSIC. (2009). User manual Version 4.0, MUSIC Development Team Cooperative Research Center CRC for Catchment Hydrology, Australia.
162. NAC. (1985). *Oil in the Sea: Inputs, Fates, and Effects*, National Academy of Science, National Academy Press, 622.
163. Nam, J. J., Song, B. H., Eom, K. C., Lee, S. H., and Smith, A. (2003). Distribution of polycyclic aromatic hydrocarbons (PAHs) in agricultural soils in South Korea. *Chemosphere*, 50(10), 1281-1289.
164. Negrel, P., and Roy, S. (2002). Investigating the sources of the labile fraction in sediments from silicate-drained rocks using trace elements, and strontium and lead isotopes. *The Science of the Total Environment*, 298, 163-181.
165. Novotny, V., and Chesters, G. (1981). *Handbook of Nonpoint Pollution: Sources and Management*. Van Nostrand Reinhold, New York, U.S.A.

166. Novotny, V., and Olem, H. (1994). *Water Quality-Prevention, Identification, and Management of Diffuse Pollution*. Van Nostrand Reinhold, New York, U.S.A.
167. NRDC. (1999). *Handbook for the Operation, Maintenance and Management of Stormwater Systems*. Natural Resources Defence Council, Watershed Management Institute, 4-6.
168. Ntziachristos, L., and Boulter, P. (2009). Road vehicle tyre and brake wear Road surface wear EMEP/EEA emission inventory guidebook 2009.
169. Obropta, C. C., and Kardos, J. S. (2007). Review of Urban Stormwater Quality Models: Deterministic, Stochastic and Hybrid Approaches, *Journal of American Water Resources Association*, 43(6), 1508-1523.
170. Okonkwo, J. O., Awofolu, O. R., Moja, S. J., Forbes, P. C. B., and Senwo, Z. N. (2006) Total Petroleum Hydrocarbons and Trace Metals in Street Dusts from Tshwane Metropolitan Area, South Africa, *Journal of Environmental Science and Health, Part A*, 41(12), 2789 - 2798.
171. Onder, S., and Dursun, S. (2006). Air borne heavy metal pollution of Cedrus libani (A. Rich.) in the city centre of Konya (Turkey). *Atmospheric Environment*, 40, 1122–1133.
172. Ong, S. T., Ayoko, G. A., Kokot, S., and Morawska, L. (2007). Polycyclic aromatic hydrocarbons in house dust samples: Source identification and apportionment. Paper presented at the 14th International IUAPPA World Congress-<http://eprints.qut.edu.au/9930/>.
173. Opher, T., and Friedler, E. (2010). Factors affecting highway runoff quality. *Urban Water Journal*, 7(3), 155 - 172.
174. Ötvös, E., Pázmándi, T., and Tuba, Z. (2003). First national survey of atmospheric heavy metal deposition in Hungary by the analysis of mosses. *The Science of The Total Environment*, 309(1-3), 151-160.
175. Pagano, P., De Zaiacomo, T., Scarcella, E., Bruni, S., and Calamosca, M. (1996). Mutagenic Activity of Total and Particle-Sized Fractions of Urban Particulate Matter. *Environmental Science & Technology*, 30(12), 3512-3516.
176. Patel, M. M., Chillrud, S. N., Correa, J. C., Feinberg, M., Hazi, Y., Deepti, K. C., Prakash, S., Ross, J. M., Levy, D., and Kinney, P. L. (2009). Spatial and temporal variations in traffic-related particulate matter at New York City high schools. *Atmospheric Environment*, 43(32), 4975-4981.
177. Pavoni, J. L. (1977). *Handbook of Water Quality Management Planning*. Van Nostrand Rainhold Co., New York.

178. Pekey, B., Karakas, D., and Ayberk, S. (2007). Atmospheric deposition of polycyclic aromatic hydrocarbons to Izmit Bay, Turkey, 67.
179. Peltonen, K., and Kuljukka, T. (1995). Air sampling and analysis of polycyclic aromatic hydrocarbons. *Journal of Chromatography A*, 710(1), 93-108.
180. Petrovic, M., Kastelan-Macan, M., and Horvat, A. J. M. (1999). Interactive sorption of metal ions and humic acids onto mineral particles. *Water Air Soil Pollution*, 111(1), 41-56.
181. Pitt, R. (1979). Demonstration of Nonpoint Pollution Abatement Through Improved Street Cleaning Practices: U.S. Environmental Protection Agency. Cincinnati, OH, 600(2), 79-161.
182. Pitt, R., and Lalor, M. (2000) The Role of Pollution Prevention in Stormwater Management, Stormwater and Urban Water Systems Modeling, The University of Alabama at Birmingham Birmingham, AL, USA 35294.
183. Pitt, R., Bannerman, R., Clark, S., and Williamson, D. (2004a). Sources of pollutants in urban areas (Part 2) Recent Sheet flow Monitoring. Effective Modeling of Urban Water Systems, (Eds.) Monograph, 13, 485-506.
184. Pitt, R., Derek Williamson, D., Voorhees, J., and Clark, S. (2004b). Review of Historical Street Dust and Dirt Accumulation and Wash off Data. Computational Hydraulics Institute, Canada.
185. Pitt, R., Bannerman, R., Clark, S., and Williamson, D. (2005). Sources of pollutants in urban areas (Part 1)-Older Monitoring Projects. Effective Modeling of Urban Water Systems, Monograph, 1-20.
186. Podvezko, V., and Podvezko, A. (2010). Dependence of multi-criteria evaluation result on choice of preference functions and their parameters. *Technological and Economic Development of Economy*, 16(1), 143 - 158.
187. Pohjola, M. A., Kousa, A., Kukkonen, J., Harkonen, J., Karppinen, A., Aarnio, P., and Koskentalo, T. (2002). The Spatial and Temporal Variation of Measured Urban PM10 and PM2.5 in the Helsinki Metropolitan Area. *Water Air and Soil Pollution Focus*, , 2(5), 189-201
188. Pope, C. A., Burnett, R. T., Thun, M. J., Calle, E. E., Krewski, D., and Ito, K. (2002). Lung cancer, cardiopulmonary mortality, and long-term exposure to fine particulate air pollution. *Journal of the American Medical Association*, 287(9), 1132-1141.
189. Preciado, H. F., and Li, L.Y. (2006). Evaluation of Metal Loadings and Bioavailability in Air, Water and Soil along Two Highways of British Columbia, Canada, *Water, Air, Soil Pollution*, 172(1), 81-108

190. PRS. (2009). Pattern Recognition Systems, Sirius User Manual, Bergen High-Technology Centre.
191. Querol, X., Alastuey, A., Ruiz, C.R., Artinano, B., Hansson, H. C., Harrison, R. M., Buringh, E., Brink, T. H. M., Lutz, M., Bruckmann, P., Straehl, P., and Schneider, J. (2004). Speciation and origin of M10 and PM2.5 in selected European cities. *Atmospheric Environment*, 38, 6547-6555.
192. RAGODEH, (2005) Climate Change Risk and Vulnerability, Report to the Australian Greenhouse Office, Department of the Environment and Heritage.
193. Ravindra, K., Bencs, L., Wauters, E., Hoog, J. D., Deutsch, F., Roekens, E., Bleux, N., Berghmans, P., and Grieken, R. V. (2006). Seasonal and site-specific variation in vapour and aerosol phase PAHs over Flanders (Belgium) and their relation with anthropogenic activities, *Atmospheric Environment Journal* 40(4), 771-785.
194. Ravindra, K., Mor, S., Ameen, Kamyotra, J. S., and Kaushik, C. P. (2003). Variation in spatial pattern of criteria air pollutants before and during initial rain of monsoon, *Environmental Monitoring and Assessment*, 87(2), 145-153.
195. Riddle, S. G., Jakober, C. A., Robert, M. A., Cahill, T. M., Charles, M. J., and Kleeman, M. J. (2007). Large PAHs detected in fine particulate matter emitted from light-duty gasoline vehicles. *Atmospheric Environment*, 41(38), 8658-8668.
196. Rocher, V., Azimi, S., Gasperi, J., Beuvin, L., Mulle, M., Moilleron, R., and Chebbo, G. (2004). Hydrocarbons and metals in atmospheric deposition and roof runoff in central Paris, *Water, Air, and Soil Pollution*, 159(1), 67-86.
197. Roesner, L. A. (1999). Urban runoff pollution-summary thoughts-the state-of-practice today and for the 21st century. *Water Science Technology*, 39(12), 353-360.
198. Rubinfeld, D. L. (1998). Reference Guide on Multiple Regression, University of California, Berkeley.
199. Sabin, L. D., Lim, J. H., Stolzenbach, K. D., and Schiff, K. C. (2005). Contribution of trace metals from atmospheric deposition to stormwater runoff in a small impervious urban catchment, *Water Research*, 39(16), 3929-3937.
200. Sabin, L. D., Lim, H. J., Venezia, T. M., Winer, A. M., Schiff, K. C., and Stolzenbach, K. D. (2006). Dry deposition and resuspension of particle-associated metals near a freeway in Los Angeles. *Atmospheric Environment*, 40(39), 7528-7538.
201. Sabin, L. D., and Schiff, K. C. (2008). Dry atmospheric deposition rates of metals along a coastal transect in southern California. *Atmospheric Environment*, 42(27), 6606-6613.

202. Sadler, R., and Connell, D. (2003). Analytical Methods for the Determination of Total Petroleum Hydrocarbons in Soil, Proceeding of the Fifth National Workshop on the Assessment of site Contamination.
203. Sagona, F., Dobson, D., and Miller, M. (2007). Stormwater Treatment Field Demonstration and Evaluation. Paper presented at the the 2007 Georgia Water Resources Conference, University of Georgia.
204. Samara, C., and Voutsas, D. (2005). Size distribution of airborne particulate matter and associated heavy metals in the roadside environment. *Chemosphere*, 59(8), 1197-1206.
205. Sanger, D. M., Holland, A. F., and Scott, G. I. (1999). Tidal Creek and Salt Marsh Sediments in South Carolina Coastal Estuaries. Distribution of Trace Metals. *Archives of Environmental Contamination and Toxicology*, 37(4), 445-457.
206. Sansalone, J. J., and Buchberger, S. G. (1997). Partitioning and First-Flush of Metals and Solids in Highway Runoff. *Journal of Environmental Engineering* 123(2), 134-143.
207. Sartor, J. D., Boyd, G. G., and Agardy, F. J. (1974). Water Pollution Aspects of Street surface Contaminants. *Journal of Water Pollution Control Federation*, 46(3), 458-467.
208. Sartor, J. D. a. B., G. B. (1972). Water Pollution Aspects of Street Surface Contaminants. USEPA, EPA-R2-72-081, US Environmental Protection Agency, Washington, DC, USA.
209. Schauer, J. J., Hildermann, L. M., Mazurek, M. A., Cass, G. R. and Simoneit, B. R. T. (1996). Source apportionment of airborne particulate matter using organic compounds as tracers. *Atmospheric Environment Urban Water*, 3837-3855.
210. Schirmer, K., Dixon, D. G., Greenberg, B. M., and Bols, N. C. (1998). Ability of 16 priority PAHs to be directly cytotoxic to a cell line from the rainbow trout gill, *Toxicology*, 127(1-3), 129-141.
211. Scott, D. J., Russell, K., and Scheffer, J. (2007). Multi-Variable Relationships in a Batch Annealing Process. Statistics Department, The University of Auckland. Auckland, New Zealand.
212. Senyah, H. A. (2005). Comparing Nitrogen and Phosphorous trends in two watersheds: the case of the urban Cuyahoga and Agricultural Maumee Rivers, Master of Arts Thesis, Department of Geography.
213. Shaheen, D. G. (1975). Contributions of Urban Roadway Usage to Water Pollution. 600/2-75-004: U.S. Environmental Protection Agency. Washington, D.C.

214. Shannon, J. D., and Voldner, E. C. (1982) Estimation of wet and dry deposition of pollutant sulfur in eastern Canada as a function of major source regions, *Water air and soil pollution*, 18(1), 101-104.
215. Sharma, A. R., Kharol, S. K., and Badarinath, K. V. S. (2010). Influence of vehicular traffic on urban air quality - A case study of Hyderabad, India. *Transportation Research Part D: Transport and Environment*, 15(3), 154-159.
216. Sharma, R., Agrawal, M., and Marshall, F. (2008). Atmospheric deposition of heavy metals (Cu, Zn, Cd and Pb) in Varanasi City, India. *Environmental Monitoring and Assessment*, 142(1), 269-278.
217. Sheoran, A.S., and Sheoran, V. (2006). Heavy metal removal mechanism of acid mine drainage in wetlands: A critical review, *Minerals Engineering*, 19(2), 105-116.
218. Shi, G., Chen, Z., Bi, C., Li, Y., Teng, J., Wang, L., and Xu, L. (2010). Comprehensive assessment of toxic metals in urban and suburban street deposited sediments (SDSs) in the biggest metropolitan area of China. *Environmental Pollution*, 158(3), 694-703.
219. Shihua, Q., Jun, Y., Gan, Z., Jiamo, F., Guoying, S., Zhishi, W., Tong, S., Tang, U., and Yunshun, M. (2001). Distribution of Polycyclic Aromatic Hydrocarbons in Aerosols and Dustfall in Macao. *Environmental Monitoring and Assessment*, 72(2), 115-127.
220. Shimmo, M., Saarnio, K., Aalto, P., Hartonen, K., Hyötyläinen, T., Kulmala, M., Riekkola, M.-L. (2004). Particle Size Distribution and Gas-Particle Partition of Polycyclic Aromatic Hydrocarbons in Helsinki Urban Area. *Journal of Atmospheric Chemistry*, 47(3), 223-241.
221. Shlens, J. (2003). A Tutorial on Principal Component Analysis, Derivation, Discussion and Singular Value Decomposition (Version 1).
222. Shuster, W. D., Bonta, J., Thurston, H., Warnemuende, E., and Smith, D. R. (2005). Impacts of impervious surface on watershed hydrology. A review. *Urban Water Journal*, 2(4), 263 - 275.
223. SigmaPlot. (2008). *Statistic User Guide Version 11.0*, Systat Software Inc.(SSI), headquartered in San Jose, California.
224. Singh, K., Malik, A., Kumar, R., Saxena, P., and Sinha, S. (2008). Receptor modeling for source apportionment of polycyclic aromatic hydrocarbons in urban atmosphere. *Environmental Monitoring and Assessment*, 136(1), 183-196.

225. Soclo, H. H., Affokpon, A., Sagbo, A., Thomson, S., Budzinski, H., Garrigues, P., Matsuzawa, S., and Rababah, A. (2002). Urban runoff contribution to surface sediment accumulation for polycyclic aromatic hydrocarbons in the Cotonou Lagoon, Benin. *Polycyclic Aromatic Compounds*, 22(2), 111 - 128.
226. Solomon, G. M., and Balmes, J. R. (2003). Health effects of diesel exhaust. *Clinics in Occupational and Environmental Medicine*, 3, 207-219.
227. Sorensen, J. (1994). Polycyclic aromatic hydrocarbons (PAHs): Comparison of ambient air concentrations of vehicular exhaust and local emissions from roofing asphalt/tar operations. Research Proposal BIOL 381/2-A Biology of Pollutants.
228. Stayner, L., Dankovic, D., Smith, R., and Steenland, K. (1998). Predicted lung cancer risk among miners exposed to diesel exhaust particles. *American Journal of Industrial Medicine*, 34(3), 207-219.
229. Stein, E. D., Tiefenthaler, L. L, and Schiff, K. (2006) Watershed-Based Sources of polycyclic aromatic hydrocarbons in Urban Stormwater, *Environmental Toxicology and Chemistry*, 25(2), 373-385.
230. Sternbeck, J., Sjödin, A. Å., and Andréasson, K. (2002). Metal emissions from road traffic and the influence of resuspension--results from two tunnel studies. *Atmospheric Environment*, 36(30), 4735-4744.
231. Stracquadanio, M., and Trombini, C. (2006). Particulate Matter, Gas phase and Particle-bound Polycyclic Aromatic Hydrocarbons in an Urban Environment Heavily Impacted by Vehicular Traffic (Bologna, Italy). *Annali di Chimica*, 96, 463-478.
232. Sullivan, J. B., and Krieger, G. R. (2001). *Clinical environmental health and toxic exposures* (2nd ed.). Philadelphia: Lippincott Williams and Wilkins.
233. Takada, H., Onda, T., Harada, M. and Ogura, N. (1991). Distribution and sources of polycyclic aromatic hydrocarbons PAHs.in street dust from the Tokyo metropolitan area. *Science Total Environment*, 107, 45-69.
234. Tasdemir, Y., and Esen, F. (2007). Urban air PAHs: Concentrations, temporal changes and gas/particle partitioning at a traffic site in Turkey. *Atmospheric Research*, 84(1), 1-12.
235. Thorpe, A., and Harrison, R. M. (2008). Sources and properties of non-exhaust particulate matter from road traffic: A review. *Science of the Total Environment*, 400(1-3), 270-282.
236. Tippayawong, N., Pengchai, P. and Lee, L. (2006). Characterization of ambient aerosols in Northern Thailand and their probable sources. *International Journal of Environmental Science and Technology*, 3, 359-369.

237. Topalián, M. L., Castañé, P. M., Rovedatti, M. G., and Salibián, A. (1999). Principal Component Analysis of Dissolved Heavy Metals in Water of the Reconquista River (Buenos Aires, Argentina). *Bulletin of Environmental Contamination and Toxicology*, 63(4), 484-490.
238. Tranmer, M., and Elliot, M. (2008). *Multiple Linear Regression: Cathie Marsh Centre for Census and Survey Research*.
239. Truc, V. T. Q., and Oanh, K. N. T. (2007). Roadside BTEX and other gaseous air pollutants in relation to emission sources. *Atmospheric Environment*, 41(36), 7685-7697.
240. Tsihrintzis, V. A., and Hermid, R. (1997). Modeling and Management of Urban Stormwater Runoff Quality: A Review. Department of Civil and Environmental Engineering and Drinking Water Research Centre, Florida International University, *Water Resources Management*, 11(2), 136-164.
241. USEPA. (1977). Control of re-entrained dust from paved streets. U.S. Environmental Protection Agency - Rep. 907/9-77-007, Kansas City.
242. USEPA. (1989). Determination of Benzo(a)pyrene[B(a)P] and other Polynuclear Aromatic Hydrocarbons (PAHs) in indoor air.
243. USEPA. (1991b). Determination of Trace Elements in Water and Wasters by Inductively Coupled Plasma-Mass Spectrometry-Method 200.8. U.S. Environmental Protection Agency, OHIO 45268.
244. USEPA. (1999). Compendium of Methods for the Determination of Toxic Organic Compounds in Ambient Air, Second Edition, U.S. Environmental Protection Agency Cincinnati, OH 45268.
245. USEPA. (2010a). User manual Version 5.0, SWMM Water Supply and Water Resources Division, U.S. Environmental Protection Agency.
246. USEPA. (2010b). Application manual Version 5.0, SWMM Water Supply and Water Resources Division, U.S. Environmental Protection Agency.
247. USEPA. (2004). User manual Version 5.0, SWMM Water Supply and Water Resources Division, U.S. Environmental Protection Agency.
248. USEPA. (1991a). Polynuclear Aromatic Hydrocarbons - Method 610. U.S. Environmental Protection Agency, OH.
249. USEPA. (1994). Determination of Trace Elements in Water and Wasters by Inductively Coupled Plasma-Mass Spectrometry-Method 200.8. U.S. Environmental Protection Agency, OHIO 45268.
250. USEPA. (1997). Nonpoint Source Pollution: The Nation's Largest Water Quality Problem. U.S. Environmental Protection Agency.

251. USEPA. (2007). *Fundamentals of Urban Runoff Management: Technical and Institutional Issues*. U.S. Environmental Protection Agency.
252. Usman, A. R. A. (2008). The relative adsorption selectivities of Pb, Cu, Zn, Cd and Ni by soils developed on shale in New Valley, Egypt. *Geoderma*, 144(1-2), 334-343.
253. Metre, V. P. C., Mahler, B. J., and Furlong, E. T. (2000). Urban sprawl leaves its PAH signature. *Environmental Science and Technology*, 34(19), 4064-4070.
254. Vaze, J., and Chiew, F. H. S. (2002). Experimental study of pollutant accumulation on an urban road surface. *Urban Water*, 4(4), 379-389.
255. Velasco, E., Siegmann, P., and Siegmann, H. C. (2004). Exploratory study of particle-bound polycyclic aromatic hydrocarbons in different environments of Mexico City. *Atmospheric Environment*, 38(29), 4957-4968.
256. Violante, F. S., Barbieri, A., Curti, S., Sanguinetti, G., Graziosi, F., and Mattioli, S. (2006). Urban atmospheric pollution: Personal exposure versus fixed monitoring station measurements. *Chemosphere*, 64(10), 1722-1729.
257. Voutsas, D., and Samara, C. (2002). Labile and bioaccessible fractions of heavy metals in the airborne particulate matter from urban and industrial areas. *Atmospheric Environment*, 36(22), 3583-3590.
258. Warren, N., Allan, I. J., Carter, J. E., House, W. A., and Parker, A. (2003). Pesticides and other micro-organic contaminants in freshwater sedimentary environments-a review. *Applied Geochemistry*, 18(2), 159-194.
259. Watson, J. G., Fujita, E. M., Chow, J. C., and Zielinska, B. (1998). Northern Front range air quality study final report and supplemental volumes. DRI Document No. 6580-685-8750.1F2, Desert Research Institute, USA
260. WDT. (2007). *Untreated Highway Runoff in Western Washington*. Washington Department of Transportation, Olympia.
261. Wei, B., Jiang, F., Li, X., and Mu, S. (2009). Spatial distribution and contamination assessment of heavy metals in urban road dusts from Urumqi, NW China. *Microchemical Journal*, 93(2), 147-152.
262. Wey, M.-Y., Chao, C.-Y., Wei, M.-C., Yu, L.-J., and Liu, Z.-S. (2000). The influence of heavy metals on partitioning of PAHs during incineration. *Journal of Hazardous Materials*, 77(1-3), 77-87.
263. Wingfors, H., Sjödin, Å., Haglund, P., and Brorström-Lundén, E. (2001). Characterisation and determination of profiles of polycyclic aromatic hydrocarbons in a traffic tunnel in Gothenburg, Sweden. *Atmospheric Environment*, 35(36), 6361-6369.

264. Wong, T., Breen, P., and Lloyd, S. (2000). Water Sensitive Road Design - Design Options for Improving Stormwater Quality of Road Runoff, Technical Report.
265. Wu, S. P., Tao, S., and Liu, W. X. (2006). Particle size distributions of polycyclic aromatic hydrocarbons in rural and urban atmosphere of Tianjin, China. *Chemosphere*, 62(3), 357-367.
266. Xia, L., and Gao, Y. (2011). Characterization of trace elements in PM_{2.5} aerosols in the vicinity of highways in northeast New Jersey in the U.S. east coast. *Atmospheric Pollution Research*, 2, 34-44.
267. Yu Ya-juan, G. H.-C., Wang Zhen, Jiang Yu-mei, Liu Yong, Huang Kai. (2007). An Integrated Risk Assessment and Intercity Comparison Model of PAHs in Ambient Air of Six Metropolitans in China.
268. Zhang, K. M. and Wexler, A. S. (2004). Evolution of particle number distribution near roadways-Part I Analysis of aerosol dynamics and its implications for engine emission measurement. *Atmospheric Environment*, 38(38), 6643-6653.
269. Zheng, M., Guo, Z., Fang, M., Rahn, K. A., and Kester, D. R. (2005). Dry and wet deposition of elements in Hong Kong. *Marine Chemistry*, 97(1-2), 124-139.
270. Zuo, Q., Duan, Y. H., Yang, Y., Wang, X. J., and Tao, S. (2007). Source apportionment of polycyclic aromatic hydrocarbons in surface soil in Tianjin, China. *Environmental Pollution*, 147(2), 303-310.
271. Zhu, Y., Hinds, W. C., Kim, S., Shen, S., and Sioutas, C. (2002). Study of ultrafine particles near a major highway with heavy-duty diesel traffic. *Atmospheric Environment*, 36(27), 4323-4335.

Appendix A - Supporting Data for Air sample Analysis

Table A- 1: Priority PAHs as listed by USEPA (adapted from Herngren 2005 and USEPA 1999)

PAHs compound	Benzene rings	Molecular Weight	Solubility (mg/L)	K _{ow}
Acenaphthene (ACE)	3	154	3.4	21000
Acenaphthylene (ACY)	3	152	3.93	12000
Flourene (FLU)	3	166	1.9	15000
Anthracene (ANT)	3	178	0.05-0.07	28000
Phenanthrene (PHE)	3	178	1.0-1.3	29000
Fluoranthene (FLA)	4	202	0.26	340000
Benzo[a]anthracene (BaA)	4	228	0.01	4x10 ⁵
Benzo[e] pyrene (BeP)	5	252	-	7x10 ⁶
Chrysene (CHR)	4	228	0.002	4x10 ⁵
Pyrene (PYR)	4	202	0.14	2x10 ⁵
Benzo[a]pyrene (BaP)	5	252	0.0038	106
Dibenzo[a,h]anthracene (DbA)	5	287	0.0005	106
Benzo[ghi]perylene (BgP)	6	276	0.00026	107
Indeno[1,2,3-cd]pyrene (IND)	6	276	-	5x10 ⁷

K_{ow} is an octanol/water partition coefficient

Table A- 2: PROMETHEE 2 ranking of heavy metals for weekday sampling at “Set 3” sites

Site ID	Phi Plus	Phi	Phi Net	Ranking
Li_c	0.2782	0.076	0.2022	1
To_c	0.2785	0.093	0.1855	2
Sh_i	0.2549	0.1217	0.1332	3
Ho_c	0.1828	0.1178	0.065	4
Ab_C	0.1171	0.1232	-0.0062	5
Re_r	0.0956	0.1285	-0.0328	6
Pe_r	0.1112	0.1775	-0.0663	7
Da_r	0.0748	0.147	-0.0721	8
Bi_r	0.0681	0.1551	-0.087	9
Di_r	0.0486	0.2026	-0.154	10
Be_i	0.026	0.1934	-0.1674	11

Table A- 3: PROMETHEE 2 ranking of heavy metals for weekday sampling at “Set 1” and “Set 3” sites

Site ID	Phi Plus	Phi Minus	Phi Net	Ranking
To_c	0.4132	0.0537	0.3595	1
So_hd	0.3898	0.0488	0.341	2
Li_c	0.2922	0.082	0.2102	3
Sh_i	0.2575	0.0897	0.1678	4
Mi_hd	0.1304	0.089	0.0414	5
Hi_hd	0.0953	0.1092	-0.0139	6
Ab_C	0.1168	0.1536	-0.0368	7
Bi_r	0.0754	0.125	-0.0497	8
Da_r	0.0693	0.1388	-0.0695	9
Ho_c	0.0908	0.1736	-0.0828	10
Pe_r	0.089	0.1961	-0.107	11
Re_r	0.0508	0.1805	-0.1297	12
Ya_hd	0.0462	0.1869	-0.1406	13
Be_i	0.0127	0.235	-0.2224	14
Di_r	0.0108	0.2784	-0.2676	15

Table A- 4: PROMETHEE 2 ranking of heavy metals for weekend at “Set 3” sites:

Site ID	Phi Plus	Phi Minus	Phi Net	Ranking
To_c	0.3781	0.0828	0.2954	1
Li_c	0.2841	0.094	0.19	2
Da_r	0.2483	0.1083	0.14	3
Re_r	0.2027	0.0998	0.1029	4
Sh_i	0.1324	0.1626	-0.0301	5
Pe_r	0.1141	0.1547	-0.0406	6
Ho_c	0.1229	0.167	-0.0441	7
Ab_C	0.0926	0.156	-0.0634	8
Di_r	0.0402	0.2139	-0.1738	9
Bi_r	0.0325	0.2132	-0.1807	10
Be_i	0.0202	0.2159	-0.1957	11

Table A- 5: PROMETHEE 2 ranking of heavy metals for weekend sampling at “Set 1” and “Set 3” sites

Site ID	Phi Plus	Phi Minus	Phi Net	Ranking
To_c	0.3682	0.0551	0.3131	1
So_hd	0.34	0.0582	0.2819	2
Li_c	0.2591	0.0837	0.1754	3
Sh_i	0.2264	0.1107	0.1157	4
Mi_hd	0.1794	0.076	0.1034	5
Da_r	0.0795	0.1248	-0.0453	6
Hi_hd	0.0844	0.1327	-0.0482	7
Bi_r	0.0723	0.1227	-0.0504	8
Di_r	0.0924	0.1477	-0.0553	9
Ho_c	0.0974	0.1551	-0.0577	10
Pe_r	0.108	0.1672	-0.0593	11
Re_r	0.0736	0.1635	-0.0898	12
Ab_C	0.0595	0.1704	-0.1109	13
Ya_hd	0.0235	0.2261	-0.2026	14
Be_i	0.0051	0.275	-0.2699	15

Table A- 6: PROMETHEE 2 ranking of heavy metals for weekend and weekday at “Set 3” sites

Site ID	Phi Plus	Phi Minus	Phi Net	Ranking
Li_c1	0.4964	0.0331	0.4633	1
Li_c2	0.4054	0.0323	0.373	2
Sh_i2	0.3978	0.0765	0.3213	3
Ho_c2	0.1476	0.1059	0.0418	4
Be_i1	0.1322	0.1191	0.0131	5
Di_r2	0.088	0.1048	-0.0168	6
Da_r1	0.1102	0.1283	-0.0181	7
Ho_c1	0.0989	0.1216	-0.0227	8
Da_r2	0.0897	0.1178	-0.0281	9
Pe_r2	0.0979	0.127	-0.0291	10
Re_r2	0.0822	0.1157	-0.0336	11
Ab_c2	0.0566	0.1245	-0.0679	12
To_c1	0.0646	0.137	-0.0724	13
To_c2	0.0553	0.1292	-0.0739	14
Pe_r1	0.0607	0.1427	-0.0821	15
Bi_r2	0.0551	0.1415	-0.0863	16
Ab_C1	0.0521	0.1387	-0.0866	17
Sh_i1	0.0544	0.1502	-0.0958	18
Di_r1	0.0381	0.146	-0.1079	19
Re_r1	0.0341	0.1455	-0.1114	20
Be_i2	0.0232	0.1485	-0.1253	21
Bi_r1	0.019	0.1735	-0.1545	22

Table A- 7: PROMETHEE 2 ranking of atmospheric gas phase PAHs at “Set 3” sites

Site ID	Phi Plus	Phi Minus	Phi Net	Ranking
Ho_c2	0.2377	0.0474	0.1903	1
Li_c1	0.196	0.0578	0.1383	2
Ho_c1	0.1621	0.0588	0.1033	3
Re_r2	0.1553	0.0572	0.0981	4
To_c2	0.1775	0.091	0.0865	5
Di_r2	0.1679	0.0902	0.0777	6
Li_c2	0.1466	0.0777	0.0689	7
Re_r1	0.1141	0.0724	0.0417	8
Pe_r2	0.1237	0.0973	0.0264	9
Sh_i2	0.1355	0.1109	0.0246	10
Bi_r1	0.1203	0.0984	0.022	11
Bi_r2	0.1195	0.1159	0.0036	12
Da_r1	0.0999	0.1138	-0.0139	13
Ab_c2	0.0743	0.1033	-0.0291	14
Ab_c1	0.0709	0.1055	-0.0346	15
Be_i1	0.0595	0.1115	-0.0519	16
Pe_r1	0.0598	0.123	-0.0632	17
Di_r1	0.0514	0.1296	-0.0782	18
Da_r2	0.0313	0.1498	-0.1185	19
Sh_i1	0.0352	0.1702	-0.135	20
To_c1	0.0149	0.1779	-0.163	21
Be_i2	0.0211	0.2151	-0.194	22

Table A- 8: PROMETHEE 2 ranking of gas phase PAHs for weekdays sampling at “Set 1” sites

Site ID	Phi Plus	Phi Minus	Phi Net	Ranking
Ho_c	0.2513	0.0847	0.1666	1
Re_r	0.1624	0.0968	0.0656	2
To_c	0.1764	0.117	0.0594	3
Ab_C	0.1515	0.0943	0.0572	4
Di_r	0.1659	0.1261	0.0397	5
Li_c	0.1556	0.1165	0.0391	6
Pe_r	0.1444	0.1312	0.0133	7
Sh_i	0.1359	0.1444	-0.0085	8
Bi_r	0.1388	0.152	-0.0132	9
Da_r	0.0352	0.1988	-0.1636	10
Be_i	0.0162	0.2719	-0.2557	11

Table A- 9: PROMETHEE 2 ranking of gas phase PAHs for weekdays sampling at “Set 1” and “Set 3” sites

Site ID	Phi Plus	Phi Minus	Phi Net	Ranking
So_hd	0.2527	0.1018	0.1508	1
Ho_c	0.2298	0.097	0.1328	2
To_c	0.2017	0.1116	0.0901	3
Ab_C	0.1533	0.1043	0.049	4
Ya_hd	0.1565	0.1116	0.0448	5
Re_r	0.1561	0.1117	0.0445	6
Di_r	0.180	0.1366	0.0434	7
Pe_r	0.1351	0.1088	0.0262	8
Bi_r	0.1363	0.1243	0.0119	9
Mi_hd	0.1204	0.1238	-0.0034	10
Li_c	0.1297	0.1336	-0.004	11
Sh_i	0.108	0.152	-0.044	12
Hi_hd	0.0744	0.1671	-0.0927	13
Da_r	0.0304	0.1976	-0.1673	14
Be_i	0.0143	0.2965	-0.2822	15

Table A- 10: PROMETHEE 2 ranking of gas phase PAHs for weekend at “Set 1” sites

Site ID	Phi Plus	Phi Minus	Phi Net	Ranking
Li_c	0.2241	0.0525	0.1716	1
Ho_c	0.1912	0.0487	0.1424	2
Re_r	0.14	0.0618	0.0783	3
Bi_r	0.1425	0.0916	0.0509	4
Da_r	0.1484	0.1147	0.0337	5
Ab_c	0.0882	0.1085	-0.0202	6
Be_i	0.0745	0.1111	-0.0365	7
Pe_r	0.0689	0.1315	-0.0626	8
Di_r	0.0663	0.1348	-0.0685	9
Sh_i	0.0646	0.1839	-0.1192	10
To_c	0.0225	0.1923	-0.1698	11

Table A- 11: PROMETHEE 2 ranking of gas phase PAHs for weekend at “Set 1” and “Set 3” sites

Site ID	Phi Plus	Phi Minus	Phi Net	Ranking
Hi_hd	0.2907	0.0765	0.2141	1
Li_c	0.1984	0.081	0.1174	2
Mi_hd	0.1914	0.075	0.1163	3
Ho_c	0.1584	0.0729	0.0855	4
Bi_r	0.1584	0.0916	0.0668	5
Re_r	0.1387	0.0808	0.0578	6
So_hd	0.1605	0.1126	0.0479	7
Da_r	0.1489	0.1055	0.0434	8
Ya_hd	0.1213	0.1622	-0.0409	9
Be_i	0.0835	0.1284	-0.045	10
Ab_c	0.0661	0.1474	-0.0813	11
Di_r	0.0591	0.1555	-0.0964	12
Pe_r	0.0427	0.1619	-0.1192	13
To_c	0.0294	0.2099	-0.1805	14
Sh_i	0.0263	0.2122	-0.1859	15

Table A- 12: PROMETHEE 2 ranking of gas phase PAHs at “Set 3” sites

	Phi Plus	Phi Minus	Phi Net	Ranking
Sh_i2	0.1742	0.0855	0.0887	1
Li_c2	0.1404	0.0699	0.0705	2
Re_r2	0.1205	0.0666	0.0539	3
Ho_c2	0.1351	0.0856	0.0495	4
Ab_c2	0.1139	0.0687	0.0452	5
To_c1	0.1254	0.0895	0.0359	6
Pe_r1	0.1389	0.1044	0.0345	7
Li_c1	0.1201	0.0917	0.0284	8
Ho_c1	0.1081	0.0807	0.0273	9
Bi_r1	0.1148	0.0947	0.0201	10
Di_r2	0.0964	0.0779	0.0185	11
To_c2	0.1257	0.1122	0.0135	12
Pe_r2	0.1036	0.0905	0.0132	13
Bi_r2	0.101	0.1013	-0.0003	14
Be_i2	0.1211	0.1436	-0.0225	15
Da_r2	0.0852	0.1093	-0.0241	16
Da_r1	0.0752	0.1104	-0.0352	17
Ab_c1	0.0621	0.1009	-0.0388	18
Sh_i1	0.0687	0.1211	-0.0524	19
Di_r1	0.0723	0.1266	-0.0543	20
Re_r1	0.0269	0.1573	-0.1304	21
Be_i1	0.0233	0.1642	-0.1409	22

Table A- 13: PROMETHEE 2 ranking of particulate phase PAHs for weekdays at “Set 3” sites

Site ID	Phi Plus	Phi Minus	Phi Net	Ranking
Sh_i	0.2194	0.1185	0.1009	1
Li_c	0.1769	0.1015	0.0754	2
Re_r	0.1369	0.0992	0.0377	3
Ho_c	0.1484	0.1256	0.0228	4
Ab_c	0.1172	0.1037	0.0135	5
Bi_r	0.1368	0.1478	-0.011	6
Di_r	0.1058	0.1185	-0.0127	7
Pe_r	0.1238	0.1428	-0.019	8
Da_r	0.1094	0.1628	-0.0534	9
To_c	0.1218	0.1791	-0.0573	10
Be_i	0.117	0.2139	-0.0969	11

Table A- 14: PROMETHEE 2 ranking of particulate phase PAHs for weekdays at “Set 1” and “Set 3” sites

Site ID	Phi Plus	Phi Minus	Phi Net	Ranking
Sh_i	0.2131	0.1165	0.0966	1
Li_c	0.1687	0.1132	0.0555	2
So_hd	0.1417	0.1015	0.0403	3
Bi_r	0.1353	0.1041	0.0312	4
Re_r	0.1355	0.1053	0.0303	5
Ab_c	0.1232	0.1081	0.0151	6
Pe_r	0.1148	0.1037	0.0111	7
Di_r	0.1171	0.1142	0.0029	8
Ho_c	0.1251	0.1364	-0.0113	9
Mi_hd	0.1080	0.1200	-0.012	10
Da_r	0.1091	0.1289	-0.0198	11
Hi_hd	0.1006	0.1216	-0.021	12
To_c	0.1403	0.1665	-0.0262	13
Be_i	0.1332	0.2142	-0.0811	14
Ya_hd	0.0465	0.158	-0.1115	15

Table A- 15: PROMETHEE 2 ranking of particulate phase PAHs for weekends sampling at “Set 3” sites

Site ID	Phi Plus	Phi Minus	Phi Net	Ranking
Bi_r	0.4345	0.166	0.2685	1
To_c	0.4401	0.1845	0.2556	2
Ho_c	0.3583	0.2226	0.1357	3
Pe_r	0.3353	0.2455	0.0898	4
Li_c	0.3377	0.2495	0.0882	5
Da_r	0.3139	0.2694	0.0446	6
Ab_c	0.2838	0.2539	0.03	7
Sh_i	0.265	0.3016	-0.0365	8
Di_r	0.2328	0.3008	-0.068	9
Re_r	0.0547	0.4524	-0.3977	10
Be_i	0.0549	0.465	-0.4102	11

Table A- 16: PROMETHEE 2 ranking of particulate phase PAHs for weekends sampling at “Set 1” and “Set 3”

Site ID	Phi Plus	Phi Minus	Phi Net	Ranking
So_hd	0.6129	0.1274	0.4855	1
Bi_r	0.4962	0.1726	0.3236	2
To_c	0.4886	0.211	0.2777	3
Mi_hd	0.4105	0.2323	0.1782	4
Pe_r	0.3639	0.2785	0.0855	5
Ho_c	0.3577	0.2764	0.0813	6
Da_r	0.3555	0.2955	0.06	7
Ya_hd	0.3654	0.3115	0.0539	8
Li_c	0.3288	0.2969	0.0319	9
Ab_c	0.321	0.3005	0.0205	10
Sh_i	0.2568	0.3444	-0.0876	11
Di_r	0.2451	0.3492	-0.1041	12
Be_i	0.0547	0.5156	-0.4609	13
Hi_hd	0.035	0.5002	-0.4652	14
Re_r	0.036	0.5163	-0.4802	15

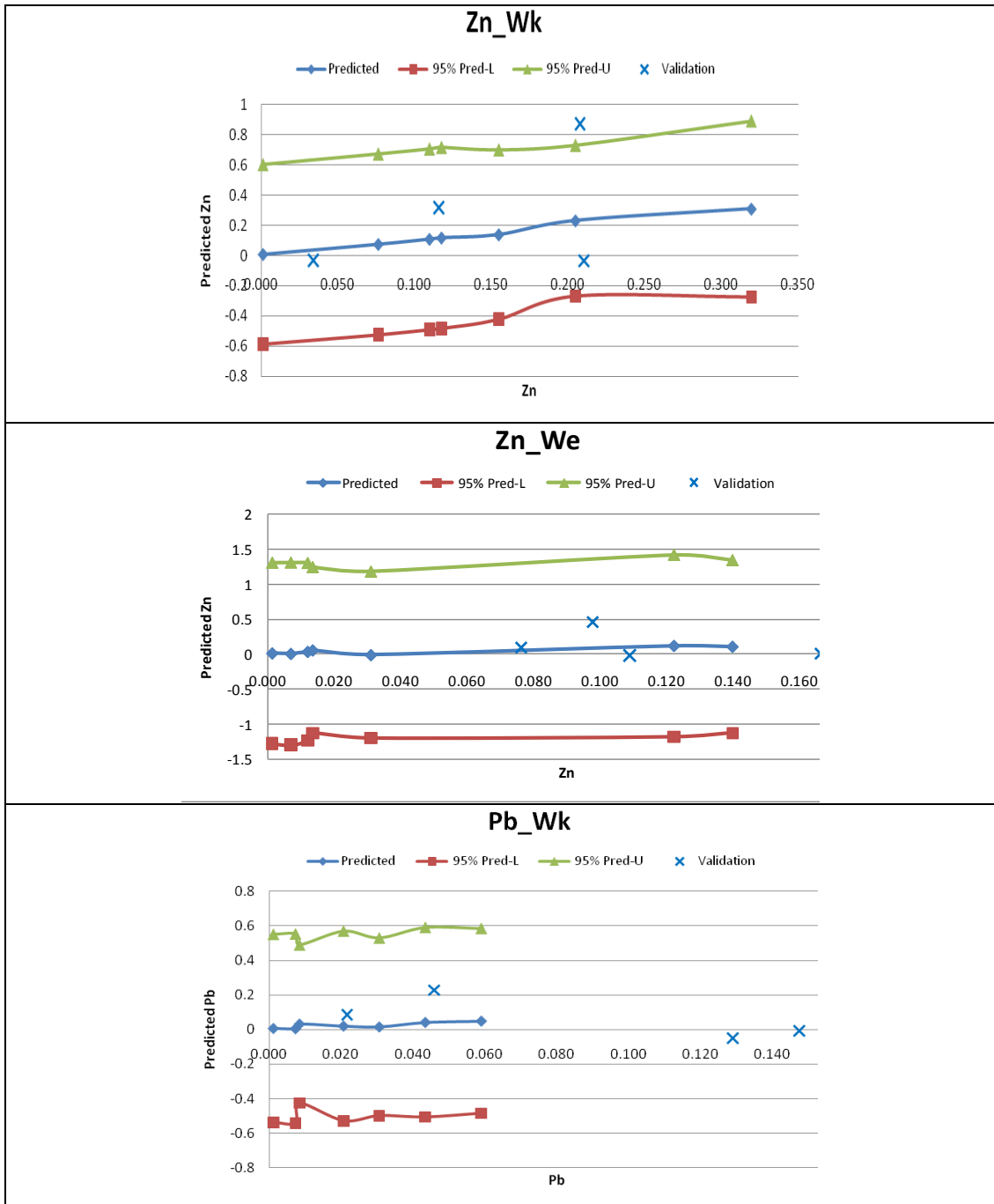


Figure A- 17: Summary of selected validation plots
 (Where We= Weekday, Wk=Weekend)

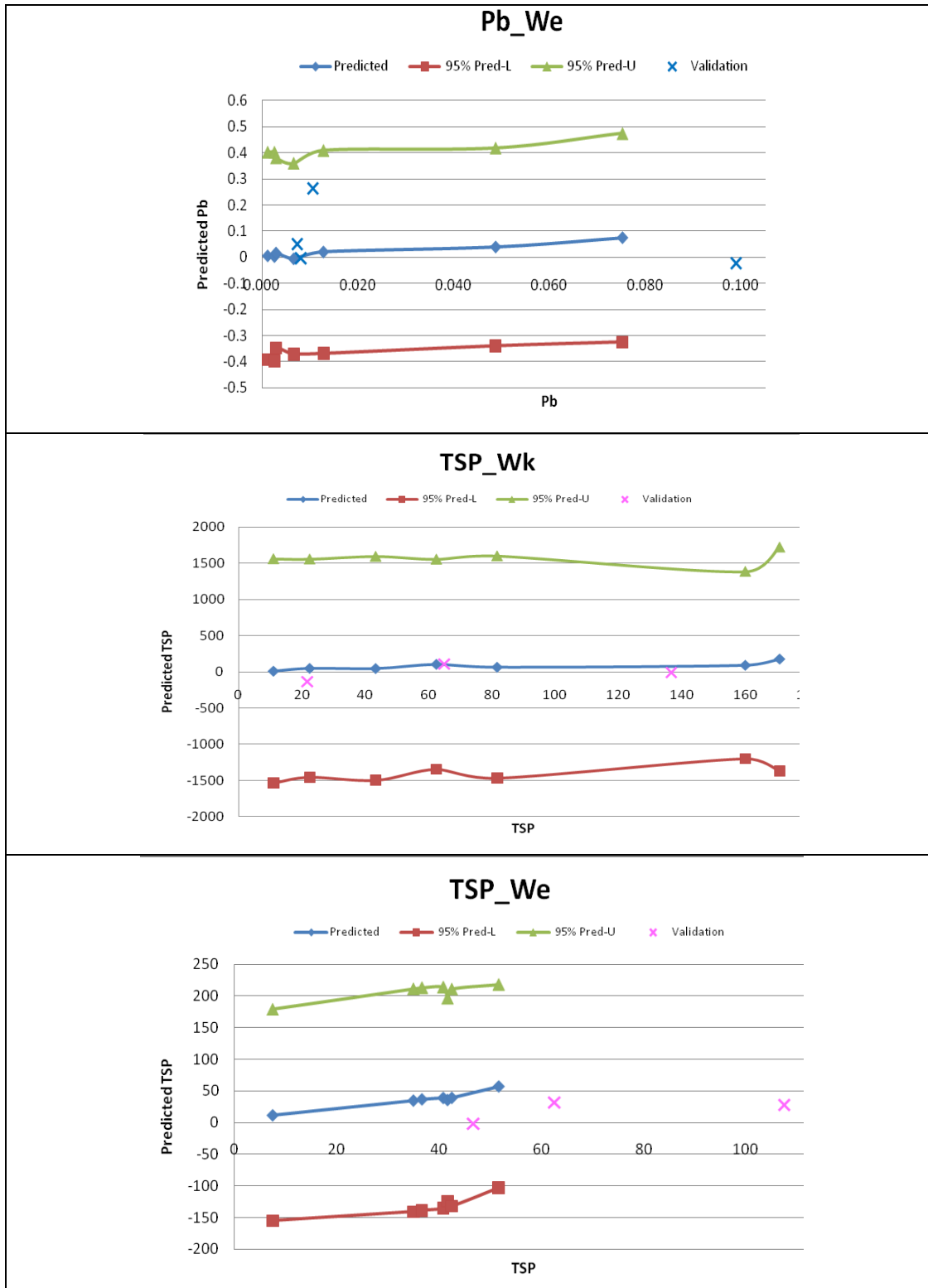


Figure A- 17: Summary of selected validation plots-continued
 (Where We= Weekday, Wk=Weekend)

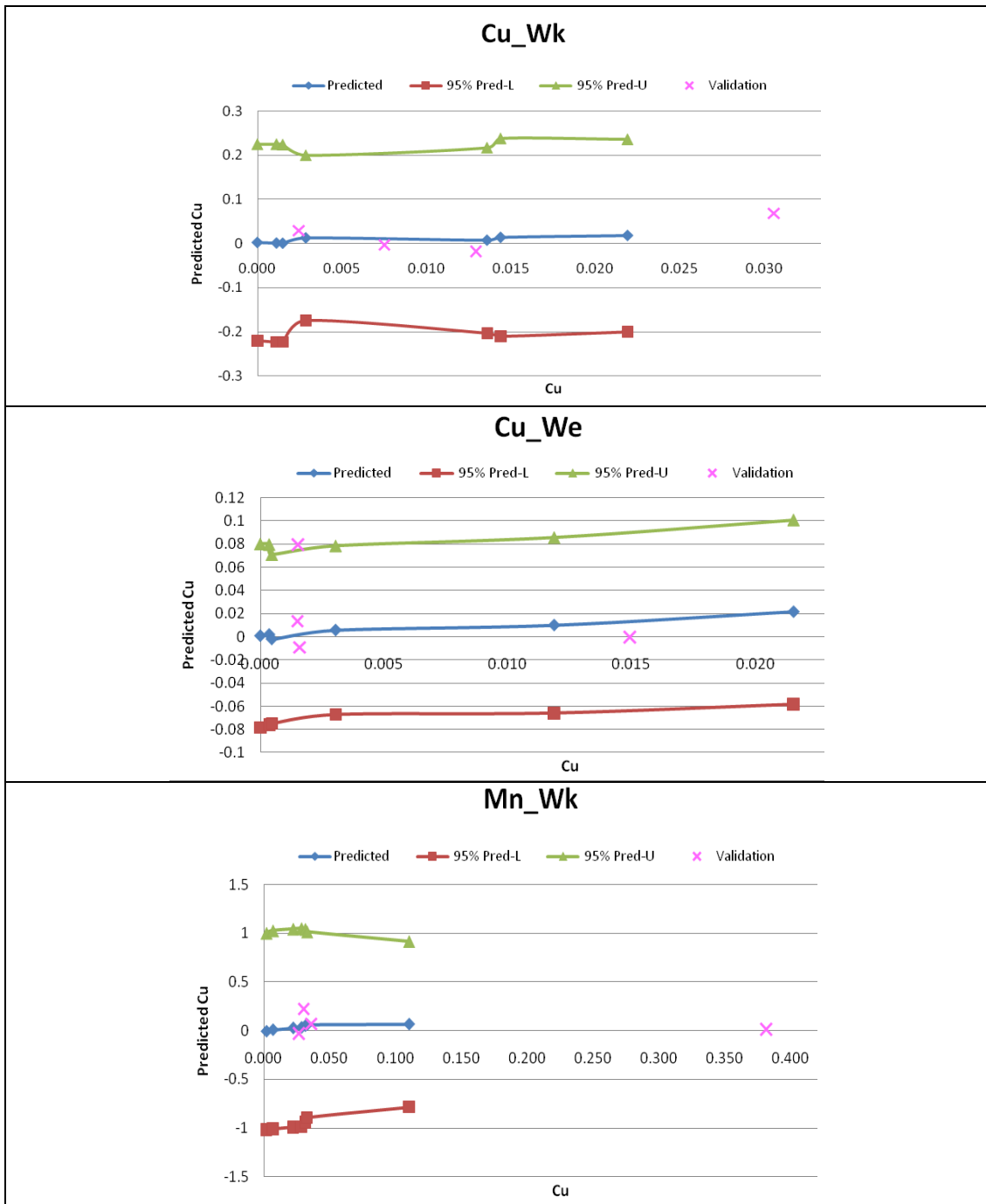


Figure A-17: Summary of selected validation plots-continued

(Where We= Weekday, Wk=Weekend)

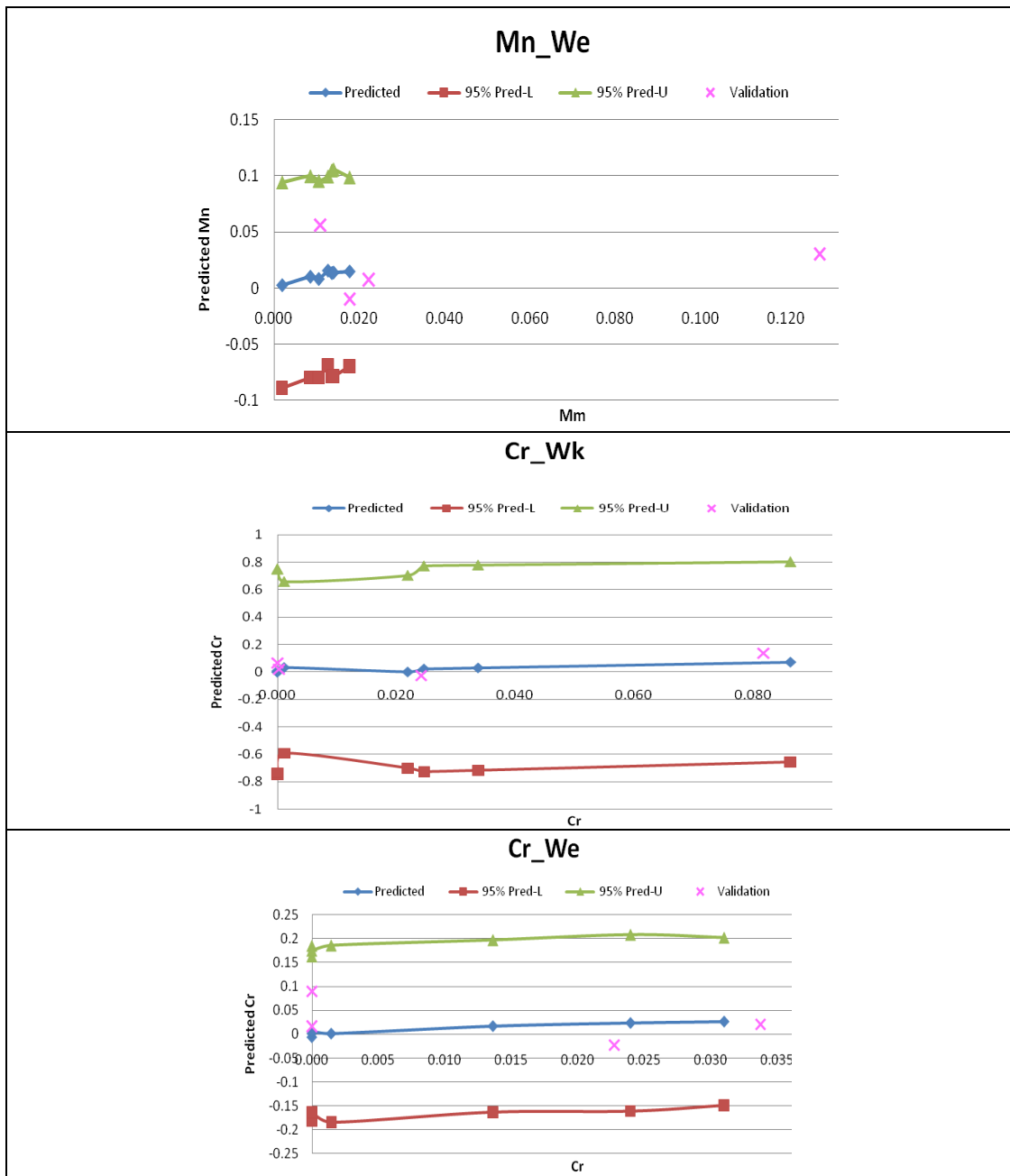


Figure A-17: Summary of selected validation plots-continued

(Where We= Weekday, Wk=Weekend)

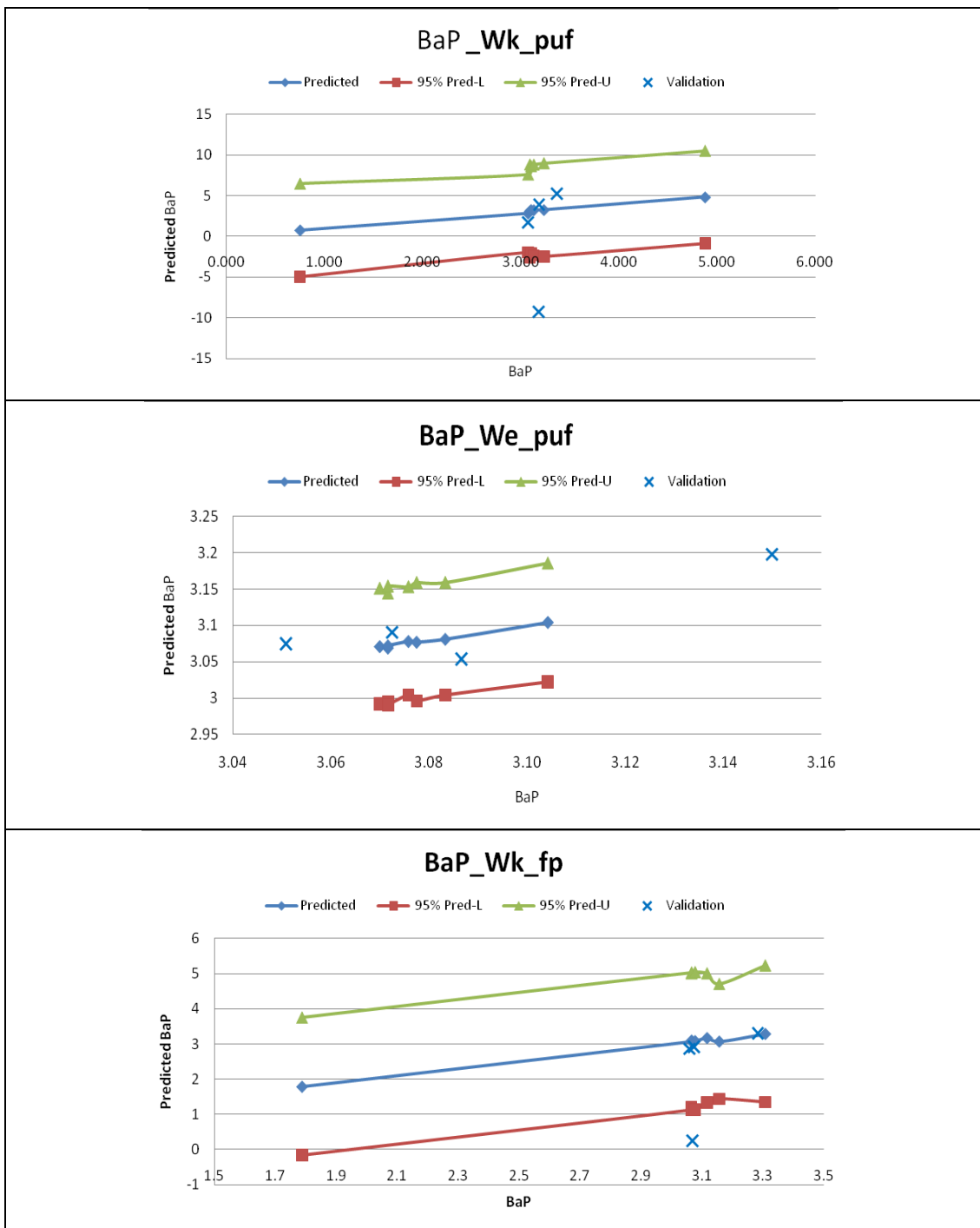


Figure A-17: Summary of selected validation plots for PAHs-continued

(Where We = Weekday, Wk = Weekend, puf = polyurethane foam, fp= particulate phase)

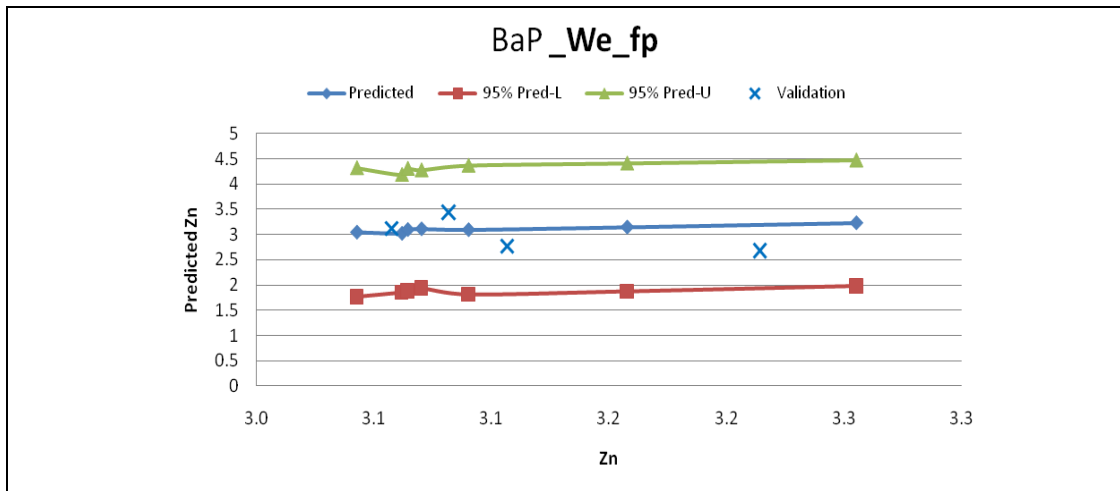


Figure A-17: Summary of selected validation plots for PAHs-continued
 (Where We = Weekday, Wk = Weekend, puf = polyurethane foam, fp= particulate phase)

Table A-17: Data matrix generated to predict air quality

Row No.	C	I	V/C	ADT_hv	Wind speed (m/s)	(C+I)
1	0.01	0.00	0.14	6	11.00	0.01
2	0.17	0.17	0.52	391	18.00	0.34
3	0.45	0.83	1.21	1503	23.00	1.28
4	0.17	0.00	0.14	6	11.00	0.17
5	0.45	0.17	0.52	391	18.00	0.62
6	0.01	0.83	1.21	1503	23.00	0.84
7	0.45	0.00	0.14	6	11.00	0.45
8	0.01	0.17	0.52	391	18.00	0.18
9	0.17	0.83	1.21	1503	23.00	1.00
10	0.01	0.17	0.14	6	11.00	0.18
11	0.17	0.83	0.52	391	18.00	1.00
12	0.45	0.00	1.21	1503	23.00	0.45
13	0.01	0.83	0.14	6	11.00	0.84
14	0.17	0.00	0.52	391	18.00	0.17
15	0.45	0.17	1.21	1503	23.00	0.62
16	0.01	0.00	0.52	6	11.00	0.01
17	0.17	0.17	1.21	391	18.00	0.34
18	0.45	0.83	0.14	1503	23.00	1.28
19	0.01	0.00	1.21	6	11.00	0.01
20	0.17	0.17	0.14	391	18.00	0.34
21	0.45	0.83	0.52	1503	23.00	1.28
22	0.01	0.00	0.14	391	11.00	0.01
23	0.17	0.17	0.52	1503	18.00	0.34
24	0.45	0.83	1.21	6	23.00	1.28
25	0.01	0.00	0.14	1503	11.00	0.01
26	0.17	0.17	0.52	6	18.00	0.34
27	0.45	0.83	1.21	391	23.00	1.28
28	0.01	0.00	0.14	391	18.00	0.01
29	0.17	0.17	0.52	1503	23.00	0.34
30	0.45	0.83	1.21	6	11.00	1.28
31	0.01	0.00	0.14	1503	23.00	0.01
32	0.17	0.17	0.52	6	11.00	0.34
33	0.45	0.83	1.21	391	18.00	1.28

Appendix B - Supporting Data for Atmospheric Deposition Analysis

Table B- 1: Traffic Data (from Gold Coast City Council)

No	SITE NAME	PREDICTED DAILY 2011	PREDICTED V/C 2011
1	Abraham Road	8149	0.57
2	Reserve Road	8144	0.61
3	Peanba Park road	6420	0.76
4	Billinghurst Cres	628	0.14
5	Beattie Road	3822	0.39
6	Shipper Drive	2501	0.39
7	Hope Island Road	26506	0.64
8	Lindfield Road	14091	1.21
9	Town Centre Drive	9860	0.31
10	Dalley Park Drive	2888	0.26
11	Discovery Drive	6856	0.46

Table B- 2: PROMETHEE 2 complete ranking of dry deposition sampling sites for the analysis given in Figure 7-6.

Site	Notation	Phi		Phi Net	Ranking
		Phi Plus	Minus		
Abrahm-7	Ab7	0.2139	0.0462	0.1678	1
Beattie Rd-4	Be4	0.2803	0.1205	0.1598	2
Discovery-7	Di7	0.1896	0.0907	0.0988	3
Discovery-6	Di6	0.165	0.072	0.0931	4
Reserve-4	Re4	0.1514	0.0851	0.0663	5
Reserve-7	Re7	0.1306	0.0669	0.0637	6
Abrahm-6	Ab6	0.0989	0.0681	0.0308	7
Beattie Rd-3	Be3	0.1483	0.1397	0.0085	8
Discovery-5	Di5	0.1136	0.1206	-0.007	9
Reserve-6	Re6	0.0718	0.0862	-0.0144	10
Beattie Rd-6	Be6	0.0858	0.1133	-0.0275	11
Abrahm-4	Ab4	0.0625	0.0975	-0.035	12
Discovery-3	Di3	0.0884	0.1253	-0.0369	13
Reserve-3	Re3	0.0639	0.1146	-0.0507	14
Abrahm-5	Ab5	0.0607	0.1134	-0.0527	15
Beattie Rd-7	Be7	0.0734	0.1301	-0.0567	16
Abrahm-3	Ab3	0.0474	0.1239	-0.0765	17
Discovery-4	Di4	0.0434	0.123	-0.0796	18
Reserve-5	Re5	0.036	0.1345	-0.0985	19
Beattie Rd-5	Be5	0.0263	0.1794	-0.1531	20

Note: Numbers given in notations are for antecedent dry days before sampling

Table B- 3: PROMETHEE 2 complete ranking of dry deposition sampling sites for the analysis given in Figure 7-7

		Phi		Phi Net	Ranking
		Phi Plus	Minus		
Reserve-2	Re2	0.2103	0.0863	0.124	1
Abrahm-6	Ab6	0.2319	0.1104	0.1215	2
Abrahm-2	Ab2	0.1929	0.0911	0.1017	3
Reserve-3	Re3	0.1718	0.087	0.0848	4
Discovery-6	Di6	0.1844	0.1411	0.0433	5
Discovery-2	Di2	0.1372	0.1065	0.0307	6
Reserve-6	Re6	0.075	0.1547	-0.0798	7
Discovery-3	Di3	0.0597	0.1588	-0.0991	8
Beattie Rd-3	Be3	0.0934	0.1981	-0.1047	9
Beattie Rd-6	Be6	0.0701	0.1759	-0.1058	10
Beattie Rd-2	Be2	0.0734	0.1899	-0.1166	11

Note: Numbers given in notations are for antecedent dry days before sampling

Table B- 4: PROMETHEE 2 complete ranking of dry deposition sampling sites for the analysis given in Figure 7-8

		Phi		Phi Net	Ranking
		Phi Plus	Minus		
Yatala-4	Ya4	0.2253	0.0527	0.1726	1
Highland park-3	Hi3	0.2449	0.0817	0.1632	2
Beattie Rd-4	Be4	0.2253	0.0954	0.1299	3
Yatala-6	Ya6	0.165	0.0459	0.1191	4
Highland park-6	Hi6	0.1544	0.0599	0.0945	5
Miami-6	Mi6	0.1377	0.0498	0.0879	6
Southport-6	So6	0.1352	0.0517	0.0835	7
Discovery-6	Di6	0.1488	0.0671	0.0817	8
Discovery-7	Di7	0.129	0.0674	0.0616	9
Miami-4	Mi4	0.1266	0.0662	0.0604	10
Abrahm-7	Ab7	0.1181	0.0671	0.0511	11
Beattie Rd-3	Be3	0.1489	0.1058	0.0431	12
Highland park-5	Hi5	0.1034	0.0782	0.0253	13
Miami-5	Mi5	0.0955	0.0795	0.0159	14
Reserve-4	Re4	0.1036	0.0981	0.0055	15
Yatala-3	Ya3	0.118	0.1147	0.0032	16
Beattie Rd-6	Be6	0.088	0.0866	0.0014	17
Abrahm-6	Ab6	0.0711	0.0743	-0.0032	18
Southport-4	So4	0.0802	0.0876	-0.0074	19
Yatala-5	Ya5	0.0748	0.089	-0.0142	20
Discovery-5	Di5	0.1065	0.124	-0.0175	21
Beattie Rd-7	Be7	0.0663	0.0854	-0.0191	22
Southport-5	So5	0.0827	0.1034	-0.0207	23
Reserve-7	Re7	0.065	0.0902	-0.0252	24
Highland park-4	Hi4	0.0632	0.0901	-0.0269	25
Reserve-6	Re6	0.0532	0.0936	-0.0404	26
Abrahm-4	Ab4	0.0363	0.1065	-0.0702	27
Miami-3	Mi3	0.0511	0.1331	-0.0819	28
Southport-3	So3	0.0455	0.1314	-0.0859	29
Abrahm-5	Ab5	0.0331	0.1223	-0.0892	30
Reserve-3	Re3	0.0289	0.1326	-0.1037	31
Discovery-3	Di3	0.0309	0.1385	-0.1076	32
Discovery-4	Di4	0.0183	0.1315	-0.1132	33
Abrahm-3	Ab3	0.0225	0.1365	-0.1139	34
Reserve-5	Re5	0.0145	0.1438	-0.1293	35
Beattie Rd-5	Be5	0.0201	0.1505	-0.1304	36

Note: Numbers given in notations are for antecedent dry days before sampling

Table B- 5: PROMETHEE 2 complete ranking of dry deposition sampling sites for the analysis given in Figure 7-9

		Phi Plus	Phi Minus	Phi Net	Ranking
Southport-6	So6	0.2653	0.0966	0.1686	1
Highland park-2	Hi2	0.2386	0.0944	0.1442	2
Yatala-2	Ya2	0.2238	0.0962	0.1275	3
Reserve-3	Re3	0.1701	0.0918	0.0782	4
Abrahm-6	Ab6	0.174	0.0983	0.0757	5
Reserve-2	Re2	0.1718	0.0988	0.073	6
Abrahm-2	Ab2	0.1627	0.1025	0.0602	7
Yatala-6	Ya6	0.1327	0.1045	0.0282	8
Discovery-6	Di6	0.1437	0.1273	0.0164	9
Miami deport-6	Mi6	0.1108	0.1084	0.0025	10
Discovery-2	Di2	0.1226	0.1264	-0.0038	11
Miami deport-2	Mi2	0.1093	0.1155	-0.0062	12
Beattie Rd-3	Be3	0.1091	0.121	-0.0118	13
Beattie Rd-6	Be6	0.0966	0.1141	-0.0175	14
Southport-2	So2	0.1007	0.1253	-0.0245	15
Highland park-6	Hi6	0.0847	0.1192	-0.0346	16
Yatala-3	Ya3	0.0734	0.1155	-0.0421	17
Beattie Rd-2	Be2	0.0758	0.1448	-0.0691	18
Reserve-6	Re6	0.0549	0.142	-0.0871	19
Discovery-3	Di3	0.0354	0.1406	-0.1051	20
Southport-3	So3	0.0361	0.1449	-0.1088	21
Miami deport-3	Mi3	0.0333	0.155	-0.1216	22
Highland park-3	Hi3	0.0282	0.1707	-0.1425	23

Note: Numbers given in notations are for antecedent dry days before sampling

Appendix C - Supporting Data for Build up Analysis

Table C- 1: PROMETHEE 2 ranking of solids for “Set 3” sites ($\Delta=70.95\%$)

Site	Phi Plus	Phi Minus	Phi Net	Ranking
Li_c	0.2166	0.1272	0.0894	1
Di_r	0.165	0.1287	0.0363	2
Bi_r	0.1708	0.1504	0.0204	3
Da_r	0.1873	0.1704	0.0169	4
Re_r	0.1958	0.1818	0.014	5
P_r	0.1649	0.153	0.0119	6
Sh_i	0.1241	0.1313	-0.0072	7
Ab_c	0.1465	0.1874	-0.0409	8
To_c	0.1079	0.1579	-0.0499	9
Be_i	0.0804	0.1712	-0.0908	10

Table C- 2: PROMETHEE 2 ranking of heavy metals for <1 μm fraction for “Set 3” sites ($\Delta=58.27\%$)

Size Fractions	Phi Plus	Phi Minus	Phi Net	Ranking	Comments
Li_c<1	0.2122	0.0902	0.122	1	The most polluted
Re_r<1	0.217	0.1081	0.1088	2	
Di_r<1	0.1942	0.0948	0.0994	3	
Ab_c<1	0.1785	0.09	0.0885	4	
Da_r<1	0.1701	0.1235	0.0467	5	
Be_i<1	0.0935	0.1403	-0.0468	6	
Sh_i<1	0.1054	0.1865	-0.0811	7	
Bi_r<1	0.0942	0.1768	-0.0826	8	
To_c<1	0.0711	0.1595	-0.0883	9	
P_r<1	0.0657	0.2322	-0.1665	10	The least polluted

Table C- 3: PROMETHEE 2 ranking of heavy metals for 1-75 μm fraction for “Set 3” sites ($\Delta=64.77\%$)

Size Fractions	Phi Plus	Phi Minus	Phi Net	Ranking	Comments
Re_r1-75	0.4063	0.0426	0.3637	1	The most polluted
Ab_c1-75	0.3023	0.0626	0.2397	2	
Bi_r1-75	0.1972	0.1268	0.0705	3	
Li_c1-75	0.1737	0.1368	0.0368	4	
Sh_i1-75	0.1137	0.1445	-0.0308	5	
Di_r1-75	0.0778	0.1724	-0.0946	6	
Be_i1-75	0.0799	0.1918	-0.1119	7	
Da_r1-75	0.1043	0.2183	-0.114	8	
To_c1-75	0.0333	0.2029	-0.1697	9	
P_r1-75	0.0465	0.2361	-0.1896	10	The least polluted

Table C- 4: PROMETHEE 2 ranking of heavy metals for 75-150 µm fraction for “Set 3” sites ($\Delta=55.99\%$)

Size Fractions	Phi Plus	Phi Minus	Phi Net	Ranking	Comments
Li_c150-300	0.127	0.0531	0.0738	1	The most polluted
Da_r150-300	0.1185	0.0544	0.0641	2	
Li_c300	0.1133	0.0636	0.0497	3	
Ab_c300	0.0877	0.0464	0.0413	4	
Re_r150-300	0.0953	0.0551	0.0402	5	
Di_r150-300	0.0755	0.0439	0.0315	6	
Da_r300	0.1046	0.076	0.0286	7	
Sh_i300	0.0917	0.0814	0.0103	8	
Ab_c150-300	0.0605	0.0587	0.0019	9	
Sh_i150-300	0.0677	0.0764	-0.0087	10	
Di_r300	0.0555	0.0739	-0.0184	11	
Be_i300	0.0511	0.0711	-0.0199	12	
Bi_r300	0.0546	0.0753	-0.0207	13	
Bi_r150-300	0.0471	0.0715	-0.0244	14	
Be_i150-300	0.0398	0.0723	-0.0326	15	
P_r300	0.0472	0.0857	-0.0385	16	
Re_r300	0.0465	0.0855	-0.0391	17	
P_r150-300	0.0475	0.0865	-0.0391	18	
To_c300	0.0319	0.0799	-0.048	19	
To_c150-300	0.0271	0.0794	-0.0523	20	The least polluted

Table C- 5: PROMETHEE 2 ranking of heavy metals for 150-300, >300 µm fraction for “Set 3” sites ($\Delta=52.35\%$)

Size Fractions	Phi Plus	Phi Minus	Phi Net	Ranking	Comments
Li_c150-300	0.127	0.0531	0.0738	1	The most polluted
Da_r150-300	0.1185	0.0544	0.0641	2	
Li_c300	0.1133	0.0636	0.0497	3	
Ab_c300	0.0877	0.0464	0.0413	4	
Re_r150-300	0.0953	0.0551	0.0402	5	
Di_r150-300	0.0755	0.0439	0.0315	6	
Da_r300	0.1046	0.076	0.0286	7	
Sh_i300	0.0917	0.0814	0.0103	8	
Ab_c150-300	0.0605	0.0587	0.0019	9	
Sh_i150-300	0.0677	0.0764	-0.0087	10	
Di_r300	0.0555	0.0739	-0.0184	11	
Be_i300	0.0511	0.0711	-0.0199	12	
Bi_r300	0.0546	0.0753	-0.0207	13	
Bi_r150-300	0.0471	0.0715	-0.0244	14	
Be_i150-300	0.0398	0.0723	-0.0326	15	
P_r300	0.0472	0.0857	-0.0385	16	
Re_r300	0.0465	0.0855	-0.0391	17	
P_r150-300	0.0475	0.0865	-0.0391	18	
To_c300	0.0319	0.0799	-0.048	19	
To_c150-300	0.0271	0.0794	-0.0523	20	The least polluted

Table C-6 PROMETHEE 2 complete ranking of PAHs for all size fractions for “Set 3” sites ($\Delta=58.36\%$)

Size Fractions	Phi Plus	Phi Minus	Phi Net	Ranking	
Di_r<1	0.3858	0.041	0.3449	1	The most polluted
Li_c300	0.3002	0.0418	0.2584	2	
Li_c<1	0.2836	0.0547	0.2288	3	
Li_c1-75	0.2613	0.0352	0.2261	4	
Li_c75-150	0.2677	0.0455	0.2222	5	
Li_c150-300	0.2352	0.0483	0.1869	6	
Be_i<1	0.1997	0.0551	0.1446	7	
Be_i1-75	0.1966	0.0612	0.1354	8	
Di_r75-150	0.1828	0.0477	0.1351	9	
Di_r300	0.2008	0.0662	0.1347	10	
Be_i300	0.1907	0.0598	0.131	11	
Di_r1-75	0.1757	0.0472	0.1285	12	
Di_r150-300	0.1595	0.0535	0.1059	13	
Be_i75-150	0.166	0.0617	0.1043	14	
Ab_c1-75	0.1635	0.0694	0.0941	15	
P_r75-150	0.17	0.0782	0.0919	16	
Sh_i300	0.1458	0.1035	0.0423	17	
To_c300	0.1198	0.0803	0.0395	18	
Be_i150-300	0.1094	0.0721	0.0373	19	
To_c<1	0.1065	0.0761	0.0304	20	
To_c1-75	0.0892	0.0752	0.014	21	
P_r<1	0.0863	0.1012	-0.0149	22	
P_r1-75	0.0762	0.0922	-0.0159	23	
To_c150-300	0.0719	0.089	-0.0171	24	
Re_r75-150	0.1237	0.1442	-0.0205	25	
Sh_i1-75	0.0776	0.1056	-0.0279	26	
Ab_c<1	0.0622	0.1115	-0.0493	27	
Re_r1-75	0.0637	0.1142	-0.0505	28	
To_c75-150	0.0499	0.1028	-0.0529	29	
Bi_r1-75	0.061	0.1216	-0.0606	30	
P_r150-300	0.0445	0.1092	-0.0647	31	
P_r300	0.0497	0.1148	-0.0651	32	
Da_r300	0.0822	0.1545	-0.0723	33	
Sh_i150-300	0.0421	0.1297	-0.0877	34	
Ab_c300	0.0332	0.1249	-0.0918	35	
Sh_i<1	0.0332	0.1388	-0.1056	36	
Ab_c75-150	0.0226	0.1335	-0.1109	37	
Da_r150-300	0.0352	0.1492	-0.1139	38	
Ab_c150-300	0.02	0.1406	-0.1206	39	
Sh_i75-150	0.0183	0.1406	-0.1222	40	
Bi_r<1	0.0142	0.1544	-0.1402	41	
Da_r75-150	0.0177	0.1588	-0.1411	42	
Bi_r150-300	0.0123	0.1573	-0.1449	43	
Bi_r75-150	0.0083	0.1552	-0.1469	44	
Bi_r300	0.0083	0.1596	-0.1513	45	
Re_r<1	0.0073	0.1605	-0.1533	46	
Re_r150-300	0.0065	0.1678	-0.1613	47	
Da_r<1	0.0024	0.1758	-0.1733	48	
Re_r300	0.0011	0.1773	-0.1762	49	
Da_r1-75	0.0007	0.1839	-0.1832	50	The least polluted

Table C- 7: PROMETHEE 2 ranking of heavy metals for <1 µm fraction for “Set 3” sites ($\Delta=57.98\%$)

Size Fractions	Phi Plus	Phi Minus	Phi Net	Ranking	Comments
Ab_c <1	0.1589	0.1204	0.0385	5	The most polluted
Be_i <1	0.2289	0.1316	0.0972	1	
Bi_r <1	0.1348	0.1467	-0.0119	6	
Da_r <1	0.209	0.1169	0.0921	2	
Di_r <1	0.2099	0.1179	0.092	3	
Li_c <1	0.14	0.1532	-0.0132	7	
Pe_r <1	0.0592	0.1938	-0.1346	9	
Re_r <1	0.167	0.1144	0.0526	4	
Sh_i <1	0.0694	0.2187	-0.1493	10	
To_c <1	0.1062	0.1698	-0.0635	8	The least polluted

Table C- 8: PROMETHEE 2 ranking of heavy metals for 1-75 µm fraction for “Set 3” sites ($\Delta=59.22\%$)

Size Fractions	Phi Plus	Phi Minus	Phi Net	Ranking	Comments
Ab_c 1-75	0.2613	0.0975	0.1638	1	The most polluted
Be_i 1-75	0.2301	0.135	0.0951	2	
Re_r 1-75	0.2104	0.1273	0.0831	3	
Sh_i 1-75	0.1971	0.1354	0.0616	4	
Di_r 1-75	0.1897	0.139	0.0507	5	
Bi_r 1-75	0.1639	0.1443	0.0196	6	
Da_r 1-75	0.1324	0.1716	-0.0392	7	
To_c 1-75	0.1144	0.1856	-0.0712	8	
Li_c 1-75	0.0749	0.2475	-0.1726	9	
Pe_r 1-75	0.0434	0.2345	-0.191	10	The least polluted

Table C- 9: PROMETHEE 2 ranking of heavy metals for 75-150 µm fraction for “Set 3” sites ($\Delta=54.41\%$)

Size Fractions	Phi Plus	Phi Minus	Phi Net	Ranking	Comments
Bi_r 75-150	0.2825	0.0993	0.1832	1	The most polluted
Sh_i 75-150	0.2557	0.1155	0.1402	2	
Da_r 75-150	0.1887	0.1321	0.0566	3	
Di_r 75-150	0.1809	0.1389	0.042	4	
Re_r 75-150	0.1527	0.1314	0.0213	5	
Ab_c 75-150	0.1457	0.1296	0.0161	6	
To_c 75-150	0.1574	0.1675	-0.0102	7	
Be_i 75-150	0.1027	0.1927	-0.0901	8	
Li_c 75-150	0.0805	0.2398	-0.1593	9	
Pe_r 75-150	0.04	0.2399	-0.1999	10	The least polluted

Table C- 10: PROMETHEE 2 ranking of heavy metals for 150-300 µm fraction for “Set 3” sites ($\Delta=54.40\%$)

Size Fractions	Phi Plus	Phi Minus	Phi Net	Ranking	Comments
Be_i150-300	0.2472	0.1069	0.1404	1	The most polluted
Di_r150-300	0.228	0.1122	0.1158	2	
Sh_i150-300	0.2278	0.1121	0.1156	3	
Re_r150-300	0.1652	0.1205	0.0447	4	
Da_r150-300	0.1745	0.1524	0.0221	5	
Bi_r150-300	0.1591	0.1461	0.013	6	
Ab_c150-300	0.1125	0.1266	-0.0141	7	
To_c150-300	0.0693	0.171	-0.1017	8	
Li_c150-300	0.0768	0.2166	-0.1398	9	
Pe_r150-300	0.0325	0.2285	-0.1961	10	The least polluted

Table C- 11: PROMETHEE 2 ranking of heavy metals for >300 µm fraction for “Set 3” sites ($\Delta=54.53\%$)

Size Fractions	Phi Plus	Phi Minus	Phi Net	Ranking	Comments
Sh_i>300	0.252	0.1105	0.1415	1	The most polluted
Re_r>300	0.1881	0.1245	0.0636	2	
Di_r>300	0.1943	0.1396	0.0547	3	
Bi_r>300	0.2162	0.166	0.0502	4	
To_c>300	0.1835	0.1508	0.0326	5	
Ab_c>300	0.1277	0.1409	-0.0132	6	
Pe_r>300	0.1299	0.1689	-0.039	7	
Da_r>300	0.1342	0.1855	-0.0513	8	
Li_c>300	0.0979	0.2103	-0.1124	9	
Be_i>300	0.0737	0.2005	-0.1268	10	The least polluted

Table c-12: PROMETHEE 2 complete ranking of build-up PAHs in all size fractions ($\Delta=59.12\%$)

Size Fractions	Phi Plus	Phi Minus	Phi Net	Ranking	
Be_i1-75	0.4969	0.0327	0.4642	1	The most polluted
Be_i150-300	0.3728	0.0483	0.3245	2	
Be_i<1	0.3414	0.0504	0.291	3	
Di_r<1	0.3015	0.0558	0.2457	4	
To_c>300	0.3084	0.0659	0.2424	5	
Di_r75-150	0.2279	0.0638	0.1641	6	
To_c75-150	0.2284	0.0748	0.1536	7	
P_r>300	0.2089	0.0689	0.1401	8	
To_c1-75	0.2052	0.0683	0.1369	9	
Di_r1-75	0.1935	0.0724	0.1211	10	
Be_i75-150	0.1973	0.0844	0.1129	11	
Li_c<1	0.1774	0.0801	0.0973	12	
Ab_c1-75	0.1797	0.0871	0.0926	13	
Di_r150-300	0.1536	0.0847	0.0689	14	
To_c<1	0.1512	0.0858	0.0654	15	
Be_i>300	0.1392	0.0882	0.051	16	
To_c150-300	0.1153	0.0943	0.021	17	
Di_r>300	0.1194	0.1027	0.0167	18	
Sh_i>300	0.1235	0.1082	0.0153	19	
Sh_i75-150	0.1149	0.1056	0.0093	20	
Ab_c<1	0.1088	0.1064	0.0024	21	
P_r1-75	0.0832	0.0963	-0.0131	22	
P_r<1	0.0777	0.0982	-0.0206	23	
Sh_i150-300	0.0891	0.1127	-0.0236	24	
Sh_i1-75	0.0861	0.1105	-0.0244	25	
Li_c1-75	0.06	0.1159	-0.0559	26	
Ab_c75-150	0.056	0.1213	-0.0653	27	
P_r75-150	0.0466	0.116	-0.0694	28	
Li_c150-300	0.0491	0.1196	-0.0704	29	
Ab_c150-300	0.0448	0.1273	-0.0825	30	
P_r150-300	0.0394	0.1224	-0.083	31	
Li_c75-150	0.0399	0.1279	-0.088	32	
Ab_c>300	0.0473	0.137	-0.0897	33	
Li_c>300	0.0388	0.1291	-0.0903	34	
Bi_r75-150	0.039	0.136	-0.097	35	
Re_r1-75	0.0432	0.144	-0.1008	36	
Da_r<1	0.0448	0.1587	-0.1139	37	
Bi_r1-75	0.03	0.1451	-0.115	38	
Bi_r>300	0.0357	0.1523	-0.1166	39	
Da_r150-300	0.0357	0.1537	-0.118	40	
Da_r1-75	0.0338	0.1617	-0.128	41	
Bi_r150-300	0.0212	0.1532	-0.132	42	
Bi_r<1	0.0175	0.1519	-0.1345	43	
Re_r150-300	0.0201	0.1575	-0.1374	44	
Re_r<1	0.0172	0.1547	-0.1375	45	
Re_r>300	0.0184	0.1582	-0.1398	46	
Da_r75-150	0.0269	0.1676	-0.1408	47	
Da_r>300	0.0204	0.1665	-0.146	48	
Sh_i<1	0.0118	0.1606	-0.1488	49	
Re_r75-150	0.0092	0.1635	-0.1543	50	The least polluted

Table c-13: PROMETHEE 2 complete ranking of build-up HMs in all three phases ($\Delta=78.33\%$)

(Where a= air,b=build-up,d=deposition, we=weekend, wk=weekday)

	Phi Plus	Phi Minus	Phi Net	Ranking	Comments
Pe_wk_a	0.7096	0.0062	0.7035	1	The most polluted
To_wk_a	0.6203	0.0064	0.6139	2	
Li_b	0.3281	0.0665	0.2615	3	
Be_wk_a	0.2925	0.052	0.2405	4	
To_we_a	0.2307	0.052	0.1787	5	
Da_we_a	0.2178	0.049	0.1687	6	
Ab_6_d	0.2281	0.0596	0.1686	7	
Da_wk_a	0.1562	0.0537	0.1026	8	
Re_wk_a	0.1733	0.0761	0.0973	9	
Ab_5_d	0.1414	0.0627	0.0787	10	
Ab_3_d	0.155	0.0764	0.0787	11	
Da_b	0.1249	0.0801	0.0448	12	
Be_5_d	0.1228	0.0878	0.035	13	
Be_b	0.1158	0.0831	0.0326	14	
Bi_wk_a	0.0958	0.0695	0.0263	15	
Sh_b	0.1008	0.0795	0.0212	16	
Be_3_d	0.1254	0.1049	0.0204	17	
To_b	0.0934	0.0931	0.0003	18	
Pe_b	0.0853	0.0879	-0.0026	19	
Di_3_d	0.0756	0.0998	-0.0242	20	
Ab_wk_a	0.0673	0.0947	-0.0274	21	
Be_4_d	0.0437	0.0971	-0.0534	22	
Sh_we_a	0.0328	0.1009	-0.0681	23	
Ab_b	0.0333	0.1051	-0.0718	24	
Pe_we_a	0.029	0.1028	-0.0737	25	
Ab_4_d	0.0341	0.109	-0.0748	26	
Re_3_d	0.037	0.1125	-0.0755	27	
Ab_we_a	0.0287	0.1058	-0.0771	28	
Bi_we_a	0.0253	0.1078	-0.0825	29	
Be_we_a	0.0282	0.111	-0.0827	30	
Sh_wk_a	0.0207	0.1085	-0.0878	31	
Re_we_a	0.0205	0.1088	-0.0883	32	
Re_7_d	0.0161	0.1134	-0.0973	33	
Be_6_d	0.0211	0.1184	-0.0973	34	
Bi_b	0.0173	0.1174	-0.1001	35	
Ab_7_d	0.0168	0.1175	-0.1007	36	
Di_4_d	0.0134	0.1191	-0.1057	37	
Re_4_d	0.0116	0.1174	-0.1058	38	
Di_b	0.0123	0.1192	-0.107	39	
Li_wk_a	0.0092	0.1208	-0.1116	40	
Re_5_d	0.0086	0.1214	-0.1128	41	
Re_b	0.0099	0.1264	-0.1166	42	
Be_7_d	0.0102	0.1328	-0.1226	43	
Re_6_d	0.0045	0.1304	-0.126	44	
Di_6_d	0.0042	0.1328	-0.1286	45	
Di_5_d	0.0064	0.1351	-0.1287	46	
Di_7_d	0.0041	0.1387	-0.1345	47	
Di_we_a	0.0006	0.1422	-0.1416	48	
Di_wk_a	0.0001	0.1465	-0.1464	49	The least polluted

Table c-14: PROMETHEE 2 complete ranking of build-up HMs in all three phases ($\Delta=79.97\%$)

(Where a1= gas phase PAHs in air, a2 = particulate phase PAHs in air, b = build-up, we = weekend, wk = weekday)

	Phi Plus	Phi Minus	Phi Net	Ranking	Comments
Be_b	0.6704	0.0125	0.6578	1	The most polluted
To_b	0.4383	0.0329	0.4054	2	
Di_b	0.4088	0.0285	0.3803	3	
Sh_b	0.2476	0.0464	0.2012	4	
Ab_b	0.2274	0.0505	0.1769	5	
Pe_b	0.2007	0.0464	0.1543	6	
Li_b	0.1411	0.059	0.082	7	
Da_b	0.1031	0.0743	0.0289	8	
Bi_b	0.0901	0.0698	0.0202	9	
Re_b	0.068	0.0735	-0.0055	10	
Li_we_a2	0.0004	0.0954	-0.095	11	
Be_wk_a2	0.0003	0.0955	-0.0951	12	
Be_7_d	0.0003	0.0955	-0.0952	13	
Sh_wk_a2	0.0003	0.0955	-0.0952	13	
Di_wk_a2	0.0002	0.0955	-0.0954	14	
Da_we_a2	0.0001	0.0956	-0.0955	15	
Bi_we_a2	0.0001	0.0956	-0.0955	16	
Re_6_d	0.0001	0.0956	-0.0956	17	
Di_we_a2	0.0001	0.0956	-0.0956	18	
Bi_wk_a2	0.0001	0.0956	-0.0956	19	
Pe_we_a2	0.0001	0.0956	-0.0956	20	
Sh_we_a2	0	0.0957	-0.0956	21	
Li_wk_a2	0	0.0957	-0.0956	22	
Ab_we_a2	0	0.0957	-0.0956	23	
To_we_a2	0	0.0957	-0.0956	24	
Da_wk_a2	0	0.0957	-0.0957	25	
Be_we_a2	0	0.0957	-0.0957	26	
Pe_wk_a2	0	0.0957	-0.0957	27	
Ab_wk_a2	0	0.0957	-0.0957	28	
Re_we_a2	0	0.0957	-0.0957	29	
Re_wk_a2	0	0.0958	-0.0957	30	
To_wk_a2	0	0.0958	-0.0957	30	The least polluted

Appendix D - Validation Plots

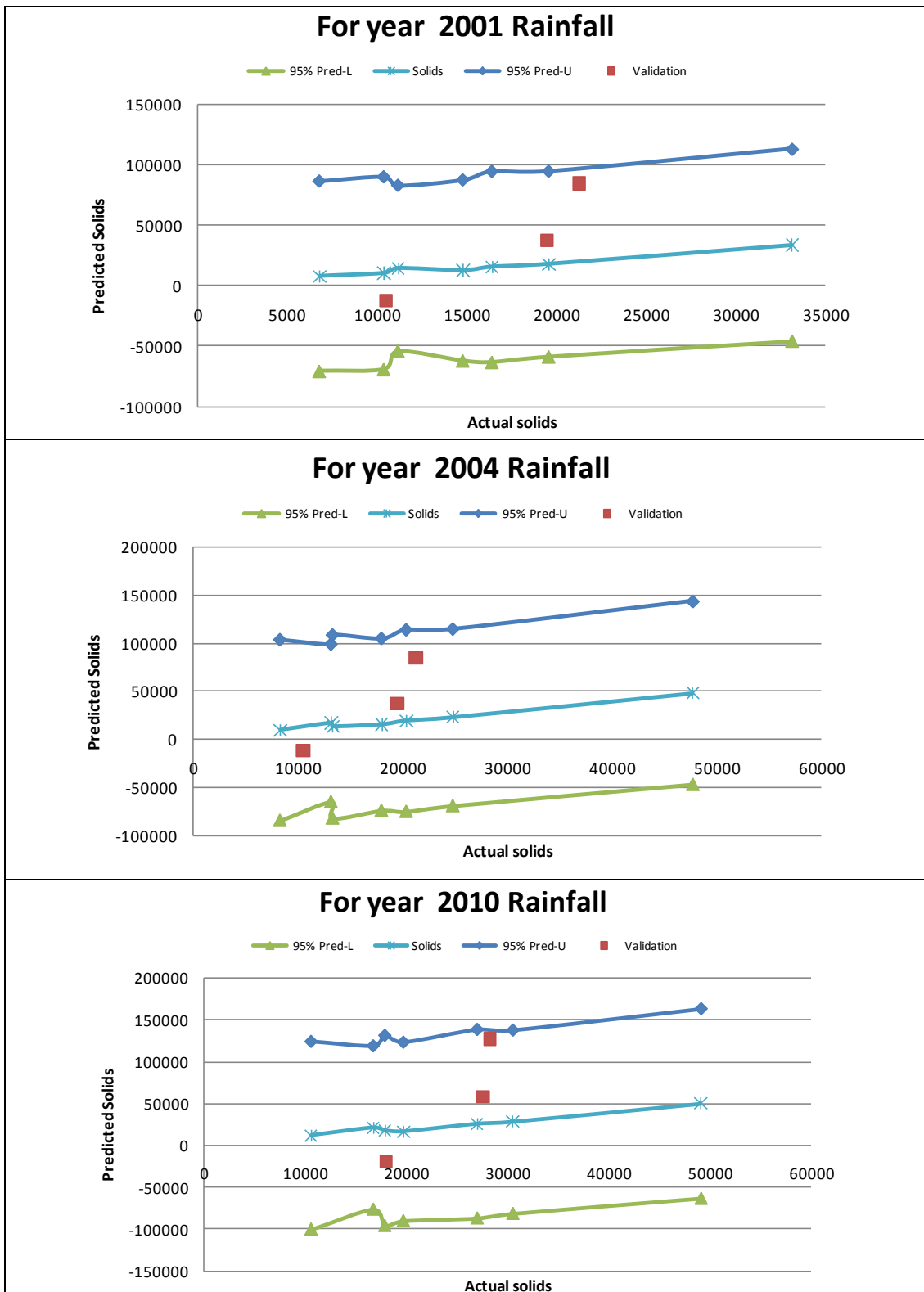


Figure D- 1: Validation plots